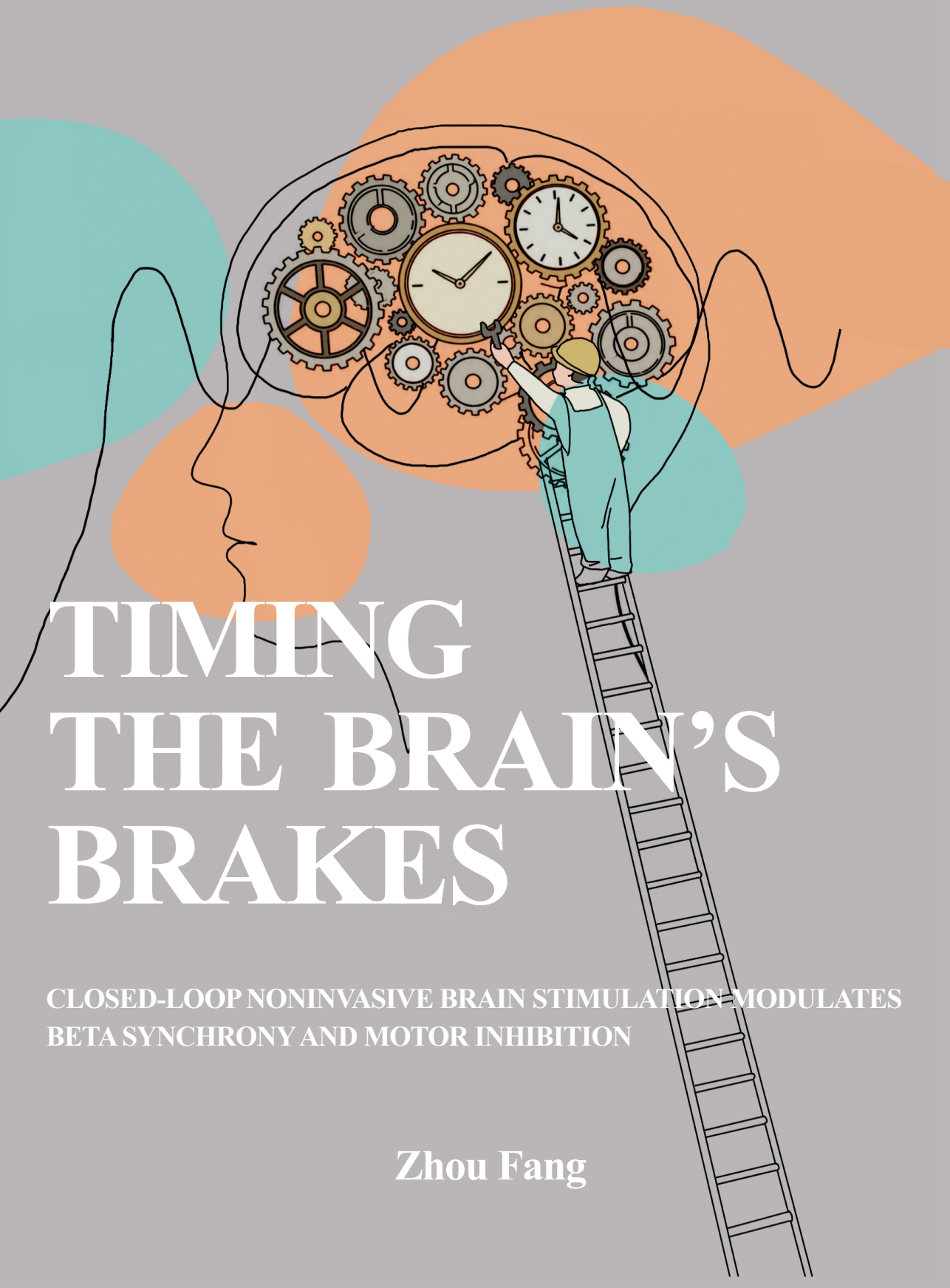


TIMING THE BRAIN'S BRAKES

CLOSED-LOOP NONINVASIVE BRAIN STIMULATION MODULATES BETA SYNCHRONY AND MOTOR INHIBITION

Zhou Fang

Propositions accompanying the PhD thesis

Timing the Brain's Brakes: Closed-Loop Noninvasive Brain Stimulation Modulates Beta Synchrony and Motor Inhibition

Zhou Fang, 3 February 2026

Propositions directly derived from this dissertation

1. The effectiveness of stopping an action depends on the instantaneous phase of ongoing beta oscillations at the moment inhibitory control is engaged.
2. A stable phase relationship characterizes successful inhibitory control.
3. When inhibition fails, the beta phase associated with maximal inhibitory efficacy shifts systematically under rhythmic external drive.
4. In-phase and anti-phase transcranial alternating current stimulation (tACS) exert opposite causal effects on inhibitory performance by respectively reinforcing and disrupting oscillatory beta synchrony.
5. In closed-loop beta stimulation, stimulation duration determines whether anti-phase input produces net desynchronization or adaptive re-entrainment.
6. Phase-dependent closed-loop neuromodulation requires an explicit systems-level approach in which signal acquisition, real-time processing, phase estimation and prediction, stimulation control, and performance validation are treated as a single integrated control system.

Propositions related to the broader scientific field

7. Effective neural control is achieved by maintaining precise temporal coordination under uncertainty.
8. Phase-precession-like dynamics can be induced by tACS, specifically when neural circuits are in an error-prone state, suggesting that learning-related processes gate the impact of neuromodulation.
9. Precise alignment of stimulation to the ongoing oscillatory phase enables temporally specific modulation of neural excitability and inter-regional communication.

Societal and translational proposition

10. Phase-dependent closed-loop brain stimulation paves the way for the clinical translation of noninvasive neuromodulation in disorders characterized by pathological neural synchrony.

The author's propositions

11. Modulation of brain function requires interventions that respect the timing, state, and intrinsic goals of ongoing neural dynamics.
12. Success reflects alignment with the existing structure, whereas failure reveals an adaptive system attempting to reconstruct.

- Zhou Fang

Doctoral thesis

TIMING THE BRAIN'S BRAKES: CLOSED-LOOP NONINVASIVE BRAIN STIMULATION MODULATES BETA SYNCHRONY AND MOTOR INHIBITION

Zhou Fang

2026

TIMING THE BRAIN'S BRAKES: CLOSED-LOOP NONINVASIVE BRAIN STIMULATION MODULATES BETA SYNCHRONY AND MOTOR INHIBITION

Dissertation

To obtain the degree of Doctor at Maastricht University,
on the authority of the Rector Magnificus, Prof. Dr. Jan Smits,
in accordance with the decision of the Board of Deans,
to be defended in public
on 29th of June, 2026, at 16:00

by

Zhou Fang

Promotor
Prof. Dr. Alexander T. Sack

Copromotor
Dr. Inge Leunissen

Assessment Committee
Prof. Dr. Peter de Weerd (chair)
Prof. Dr. Sonja Kotz
Dr. Mark Janssen
Dr. Miles Wischnewski





DOCTORAL THESIS, MAASTRICHT UNIVERSITY
© Zhou Fang, Maastricht 2026

Cover: Zhou Fang
Production: Fang 2026
ISBN: 978-94-6534-493-5

Contents

1 General introduction 1
- 1.1 An introduction to motor inhibition . . . 2
- 1.2 The rhythm of neural communication: oscillations and oscillatory phase . . . 6
- 1.3 Pathological beta activity in Parkinson's . . . 14
- 1.4 Fine-tuning motor inhibition with non-invasive brain stimulation . . . 17
- 1.5 Outline of this thesis . . . 29

2 The phase of tACS-entrained pre-SMA beta oscillations modulates motor inhibition 53
- 2.1 Introduction . . . 55
- 2.2 Methods . . . 57
- 2.3 Results . . . 66
- 2.4 Discussion . . . 74
- 2.5 Conclusion . . . 78
- 2.6 Supplementary information . . . 90

3 TACS induces state-dependent shifts in inhibitory phase preference consistent with phase precession 97
- 3.1 Introduction . . . 99
- 3.2 Methods . . . 100
- 3.3 Results . . . 106
- 3.4 Discussion . . . 111
- 3.5 Conclusion . . . 115
- 3.6 Supplementary information . . . 121

4 Closed-loop anti-phase tACS over preSMA reduced oscillatory beta synchronization and modulated motor inhibition performance 127
- 4.1 Introduction . . . 129

4.2 Methods . . . 131
4.3 Results . . . 146
4.4 Discussion . . . 156
4.5 Conclusion . . . 161
4.6 Supplementary information . . . 172

5 Anti-phase closed-loop tACS disrupts cortico-muscular coherence during isometric contraction 181
5.1 Introduction . . . 182
5.2 Methods . . . 185
5.3 Results . . . 194
5.4 Discussion . . . 201
5.5 Conclusion . . . 206
5.6 Supplementary information . . . 215

6 Online EEG phase tracking for adaptive tACS: practical engineering and methodological considerations 221
6.1 Introduction . . . 223
6.2 A guide for successfully implementing a phase-dependent closed-loop tACS system . . . 225
6.3 Future Directions and Emerging Trends . . . 240

7 General discussion 265
7.1 Summary of the main findings . . . 266
7.2 Beta oscillations and inhibitory control . . . 268
7.3 tACS interacts with the brain state . . . 273
7.4 A novel tACS strategy for adaptive modulation: EEG-guided phase-dependent closed-loop tACS . . . 278
7.5 Considerations and limitations . . . 286

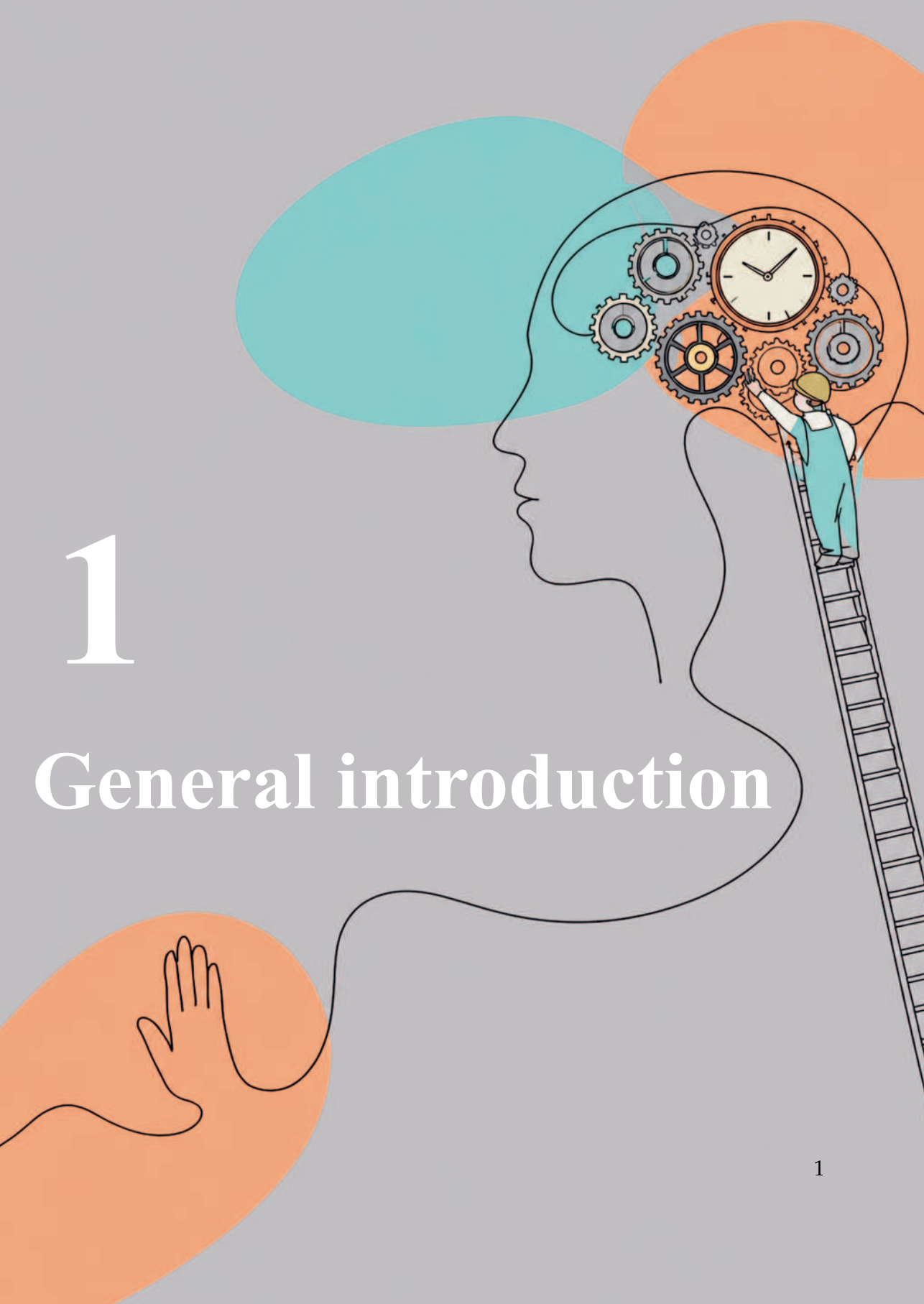
Valorisation 305

Summary 309

Samenvatting 315

About the author 321

Acknowledgments 323



1

General introduction

1.1 An introduction to motor inhibition

Every day, your brain must decide not only what to do, but also what not to do. You step toward the crosswalk and then freeze when a car suddenly accelerates through its signal. You begin to reach for your phone during a meeting and then stop yourself. In each case, your brain actively sends a cancellation command to override an action plan that is already in motion.

Depending on behavioral demands, the brain engages in two primary forms of motor inhibition: reactive and proactive. Reactive inhibition serves as an emergency response, cancelling an ongoing action in response to an external cue. Such as immediately freeze to avoid the oncoming car. Proactive inhibition arises when we anticipate that stopping might be required. Imagine you are driving through a congested street; you may keep your foot poised above the brake pedal and slow your movements in preparation for the possibility of having to stop. These two types of inhibition work together, providing a flexible braking system capable of both anticipation and rapid cancellation. When this inhibitory system breaks down, its consequences become evident. For example, in Parkinson's disease (PD), excessive tonic inhibitory influence on voluntary movement contributes to bradykinesia and rigidity. In the remainder of this dissertation, we focus on reactive motor inhibition and will simply refer to it as motor inhibition.

1.1.1 Measuring inhibition

Quantifying behavior that consists of not doing something is inherently challenging. Early research utilized a Go/No-Go task, where participants learned a simple binary rule, pressing a button when they saw a 'Go' sign and remaining still for a 'No-Go' sign. This paradigm was effective for measuring the brain's ability to identify a 'stop' sign, but it failed to capture the dynamic of action cancellation. This limitation led to the development of the Stop-Signal Task. This paradigm is designed to first lure the brain into action mode, then require a fast

response to withdraw a movement. In a typical session, the participants are engaged in a rapid-response game. For example, they might be asked to respond to an arrow pointing left or right, or to press a button to stop a constantly filling bar at a specific target. For the majority of trials (usually about 70%), the stimuli presented are constant and require participants to press the button immediately. This repetitive rhythm is designed to build up a strong, habitual prepotent response. However, the task introduces a critical trap on the remaining 30% of trials: a 'Stop Signal', such as an arrow turning red or a fill bar stopping before reaching the target line, appearing a few milliseconds after the initial stimulus. This signal acts as an emergency brake, commanding the participant to cancel the movement they have already started to prepare.

To quantify the ability of the inhibition, an independent horse race model was proposed by Logan and Cowan in 1984: a Go process, which is triggered by the initial stimulus and drives the action toward execution, and a Stop process, which is triggered later by the stop signal and attempts to cancel the action, race against each other toward completion. The outcome of a stop-signal trial is determined by which of these two processes finishes first: if the Stop process wins the race, the action is successfully cancelled, but if the Go process wins, the participant executes the response and fails to stop. This framework assumes that the go and stop processes operate independently and that participants do not deliberately slow down to improve stopping success [1, 2]. The central latent variable, the stop-signal reaction time (SSRT), indexes the completion time of the unobservable stop process, as indicated in Figure 1.1. In essence, the SSRT represents the time the brain takes to generate and successfully execute the internal cancellation command. Modern research uses non-parametric integration methods on the distribution of Go trial reaction times to derive this covert SSRT metric [2].

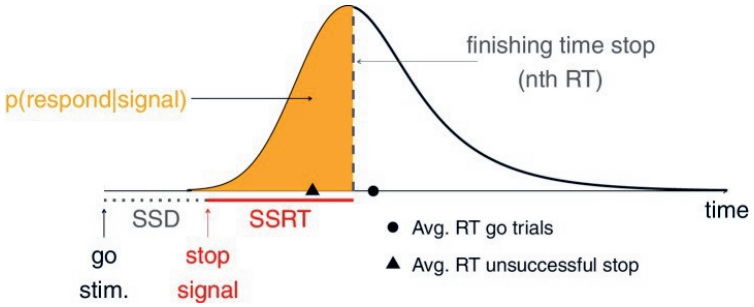


Figure 1.1: **Stop-Signal Race Model Illustration [2].** SSD = stop-signal delay; RT = reaction time; SSRT = stop-signal reaction time.

1.1.2 Under the hood: basal ganglia network

Motor inhibition relies on a finely tuned dialogue between the cortex and deeper brain structures called the basal ganglia. The basal ganglia act as a decision hub, helping the cortex determine which motor commands should proceed and which should be suppressed. This control is achieved via three main circuits, often referred to as the direct, indirect, and hyperdirect pathways [3, 4, 5, 6, 7, 8, 9] (Figure 1.2).

The direct pathway acts as a 'go' route. When the cortex initiates an action plan, it stimulates the striatum (the input station of the basal ganglia). Neurons in the striatum expressing D1 dopamine receptors then send inhibitory signals to the GPi. Because the GPi's normal job is to silence the thalamus, inhibiting the GPi effectively "inhibits the inhibitor." This process, known as disinhibition, releases the thalamus from its restraints, allowing it to excite the motor cortex and execute the movement.

Running in parallel is the indirect pathway, which functions as a 'no-go' or 'slow-down' route. Here, cortical input excites a different population of neurons in the striatum (targeting D2 receptors), sending inhibitory signals to the Globus Pallidus Externus (GPe), and subsequently activates the Subthalamic Nucleus (STN). STN then boosts the activity of the Gpi, ultimately increasing inhibitory output to the thalamus.

The hyperdirect pathway acts like an 'emergency brake', activating when a sudden stop is required. In this circuit, the cortex directly sends an excitatory signal to the STN, which then excites the GPi, eliciting the "brakes" signals on the thalamus globally. This process operates at speed,

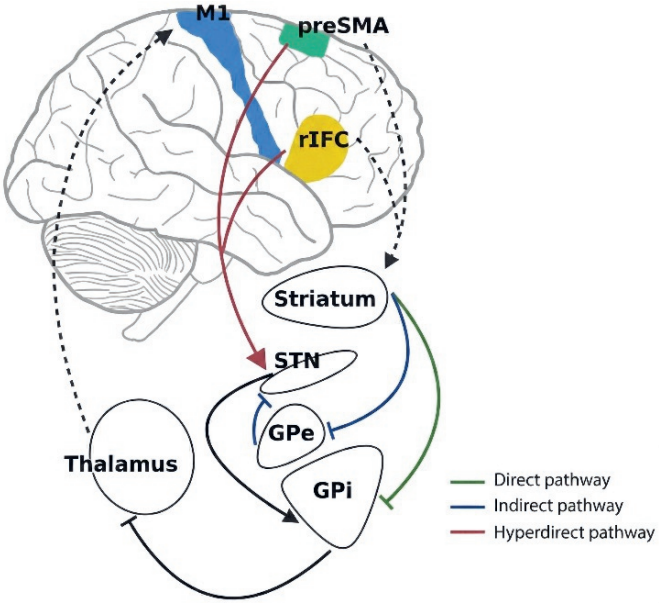


Figure 1.2: **The key structures of the cortico-basal-ganglia network.** M1 = motor area; preSMA = pre-supplementary motor area; rIFC = right inferior frontal cortex; STN = subthalamic nucleus; GPe = globus pallidus externus; GPi = globus pallidus internus. Green lines indicate the direct pathway; blue lines indicate the indirect pathway; red lines indicate the hyperdirect pathway. Pointed arrowheads (→) denote excitatory connections, while flat arrowheads (⊣) denote inhibitory connections. Dashed lines represent thalamo-cortical feedback loops.

1.1.3 When the 'brake' regulation breaks down: Parkinson's disease

The delicate balance between the direct, indirect, and hyperdirect pathways is maintained by dopamine. This neurotransmitter, produced in the substantia nigra pars compacta (SNc), functions as a modulator that facilitates the direct pathway via D1 receptors and suppresses the indirect pathway via D2 receptors. Parkinson's disease (PD) is fundamentally characterized by the progressive degeneration of these dopaminergic neurons. With the depletion of dopamine, the basal ganglia gearbox malfunctions. Without the facilitating influence on D1 receptors, the direct pathway becomes underactive, making it difficult to initiate movement. Simultaneously, the loss of inhibition on D2 receptors causes the indirect pathway to become hyperactive. The net result is a pathological increase in inhibitory output from the GPi to the thalamus. The brain is effectively trapped in a "brake-on" state. Clinically, this manifests as rigidity and bradykinesia (slowness of movement). Furthermore, while the hyperdirect pathway is critical for stopping, its relationship with the other pathways is altered in PD, contributing to a paradox where patients may struggle to initiate movement yet also face impairments in the ability to rapidly inhibit prepotent responses when required.

1.2 The rhythm of neural communication: oscillations and oscillatory phase

Through brain networks, brain oscillations act as the vehicles for information transformation. Oscillations are created from large populations of neurons firing in rhythmic patterns. These oscillations, first discovered by early electroencephalography (EEG) recordings, span frequencies from slow delta ($<$4 Hz) to fast gamma ($>$80 Hz) [10]. Rather than just noise, these rhythms facilitate communication between distant brain regions, ensuring that the correct messages are sent to the right place at the precise moment they are needed.

Neural oscillations can be characterized by amplitude and phase (Figure 1.3). Amplitude refers to the magnitude or 'power' of the oscillation, which generally reflects the size of the neuronal population engaged and the degree of their synchronization [11]. The oscillatory phase describes the specific position within the rhythmic cycle at a given moment, ranging from the peak of depolarization (high excitability) to the trough of hyperpolarization (low excitability) [12]. Phase, therefore, provides the precise temporal structure for neural spiking, determining when a neuron is firing relative to the population rhythm [13].

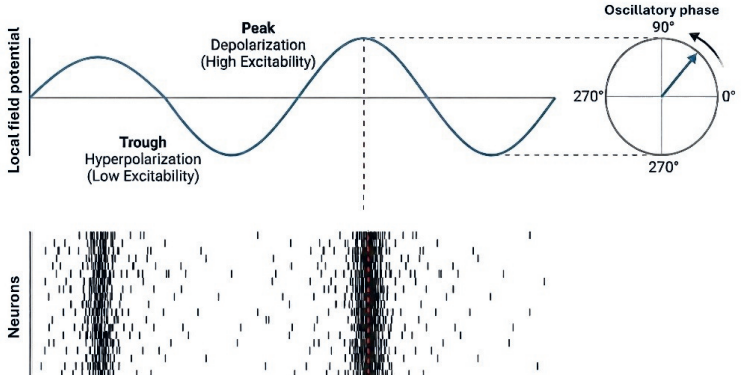


Figure 1.3: **Illustration of neuronal population firing by oscillatory phase and amplitude.** The top panel illustrates the time course of the local field potential, where the phase dictates the excitability state. Peaks correspond to the depolarization phase (high excitability), while the troughs correspond to hyperpolarization (low excitability). The bottom plot displays the spiking activity of the population of neurons.

The functional importance of neuron oscillatory phase is central to theories of long-range neural integration, consistent with the "communication through Coherence" (CTC) hypothesis (Figure 1.4). CTC proposes that effective transfer of information between distant neuronal groups depends on their oscillations being phase-locked, or coherent [14, 15]. By aligning their temporal windows of high excitability, synchronized brain regions open a transient channel for effective communication;

an input volley from a sending group will only effectively activate a receiving group if it arrives during B's excitable phase [14, 15]. Conversely, inputs arriving during the inhibitory phase of the cycle are effectively shunted, meaning that dynamic changes in phase synchronization serve as a mechanism to flexibly gate information flow across cortical networks [16, 17].

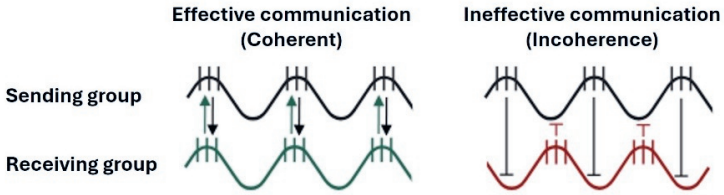


Figure 1.4: **Schematic illustration of the communication through coherence (CTC) hypothesis [14].** Left panel: Coherent oscillations allow inputs to arrive during the receiver's excitable phase, resulting in successful communication. Right panel: Incoherent or phase-shifted oscillations cause inputs to arrive during the receiver's inhibitory phase, resulting in failed communication and signal gating.

Electroencephalography (EEG) provides a non-invasive method with high temporal resolution that enables quantification of both the amplitude and instantaneous phase of cortical oscillations, thereby supporting precise characterization of their dynamics [18]. By transforming EEG time series into time-frequency representations, researchers can track rapid fluctuations in oscillatory power and phase across time and frequency bands [19]. Such approaches are particularly well-suited for testing temporally links between neural rhythms and function, revealing how moment-to-moment changes in oscillatory amplitude and phase relate to cognition and behavior on the relevant time scale of neural computation.

1.2.1 Beta oscillations: a vehicle for the 'brake' signal

Neuroscientists noticed that when people prepare to move, a distinct rhythm over the motor cortex around 13–30 Hz briefly dips before the movement and rebounds immediately after. This pattern, first captured in scalp EEG and MEG recordings [20], became recognized as the brain's "brake" signal. As found by Pfurtscheller and Silva, before and during the execution of a motor task, the neuronal populations firing in beta rhythms within the basal ganglia desynchronize, termed as movement-related beta desynchronization (MRBD). Once the movement ceases, beta oscillations transiently rebound to exceed resting amplitude, characterized by the post-movement beta rebound (PMBR).

Subsequent intracranial recordings substantially refined this picture by demonstrating that beta oscillations are a network phenomenon spanning both cortical and subcortical nodes. In patients implanted with deep-brain stimulators within the subthalamic nucleus, beta comes in brief bursts and covaries with periods of successful stopping and response suppression [21, 22, 23]. Crucially, simultaneous recordings combining STN LFPs with EEG or MEG show robust beta coherence between the STN and motor cortical regions, including primary motor cortex and supplementary motor area, both at rest and during movement. These coherent interactions are modulated by dopaminergic state and behavioral context [24, 25, 26, 27, 28].

Furthermore, beta oscillations within this network are often top-down organized, as evidenced by directed connectivity analyses: frequency-resolved Granger causality and related measures consistently show that cortical beta activity, particularly from preSMA, precedes and predicts beta activity in the STN, consistent with propagation via the hyperdirect pathways [25, 29, 30].

Finally, a broader literature demonstrates that beta modulations are not merely binary markers of inhibition but scale continuously with movement kinematics and task demands: larger or more demanding actions tend to elicit stronger MRBD and a more pronounced PMBR,

with systematic dependencies on force and speed [31, 32, 33]. Moreover, the amplitude, timing, and possibly functional role of these beta modulations change across the lifespan, aligning with age-related differences in motor vigor and control [34, 35, 36, 37].

Causal evidence emerged from studies applying rhythmic stimulation in the beta frequency range over the preSMA, a cortical entry point of the hyperdirect pathway. Such stimulation, particularly transcranial alternating current stimulation (tACS), is thought to interact with ongoing cortical dynamics by entraining and, as a result, amplifying endogenous beta activity and its associated network. Under this condition, movement became slower and weaker [38, 39]. These studies support the view that beta oscillations are not merely a readout of motor state but can actively mediate motor inhibition.

1.2.2 Beta phase: temporal scaffold for motor control

Timing the movement: phase-dependency in the motor system

The principle that the oscillatory phase structures information flow extends beyond long-range network coupling to shaping moment-to-moment behavioral performance. If neuronal excitability fluctuates rhythmically, then the effectiveness of incoming inputs and consequently the probability of generating an action should depend on their timing relative to ongoing oscillations. Numerous studies provided compelling evidence that our motor system operates through precise temporal coordination rather than static levels of activation.

Empirically testing this principle requires a method that can probe neural excitability with high temporal precision. Investigation on fluctuations in motor excitability therefore, often relies on Transcranial Magnetic Stimulation (TMS) induced Motor-Evoked Potential (MEP). TMS is a non-invasive technique that uses a coil to generate a magnetic field that induces a brief electric current in the brain. When a single TMS pulse is applied over the primary motor cortex (M1), it activates

the corticospinal neurons, sending a volley of signals down the spinal cord to a target muscle in the hand. This signal is recorded by electromyography as the MEP, which serves as a precise, real-time probe of motor excitability.

Classic work demonstrated that the size of the MEP depends on the phase of ongoing beta oscillations at the moment of stimulation. Initial studies observed that cortical excitability peaks during the rising phase of the beta cycle [40, 41], pointing to a universal temporal window facilitating the transmission of motor information. However, this pattern was complicated by other diverging evidence. Keil et al. [42] found that excitability could be maximized at both the peak and the trough of the oscillation . Similar phase-dependent effects were also seen in slightly slower mu rhythms (8–14 Hz), where stimulation during the trough or rising phases produced stronger responses than at the peak [43]. More recent studies have supplemented this map. Works from Miller et al. [44] and Wischnewski et al. [45] indicate that excitability generally increases on the falling flank of the beta wave and decreases near its peak. Hussain et al. [46] further demonstrated that motor commands are preferentially released within a specific window between beta $120°$ and $140°$. Figure 1.5 summarizes the optimal phase demonstrated in the studies using C3 as the target location.

While the modulation of cortical responsiveness follows a broadly consistent sinusoidal pattern across individuals, analyses at the single-subject level reveal that the specific beta phase that maximizes responsiveness is unique to each individual [47]. This individualized "phase fingerprint" offers a principled explanation for conflicting findings in earlier studies, as optimal phase windows may vary due to anatomical differences such as variability in cortical folding and source orientation [47]. More recent experiments refined this picture further: when TMS pulses are timed to a participant's own optimal beta phase, the resulting cortical responses are not only larger in amplitude but also occur earlier and with reduced temporal variability [48].

This phase-dependency appears to reflect a broader gating mechanism

that couples the cortex with deep brain structures. Recordings from the STN show that neural spikes are phase-locked to the 270° phase of frontal beta oscillations [49] and inhibitory signals in the motor cortex become strongest around the trough of the beta oscillations [50]. Taken together, these results indicate that beta oscillations impose a rhythmic structure on motor excitability across distributed nodes of the motor system. The functional consequence is consistent: beta oscillations flexibly gate cortical-subcortical pathways, ensuring that motor commands are released only during brief, phase-specific windows when the system is permissive.

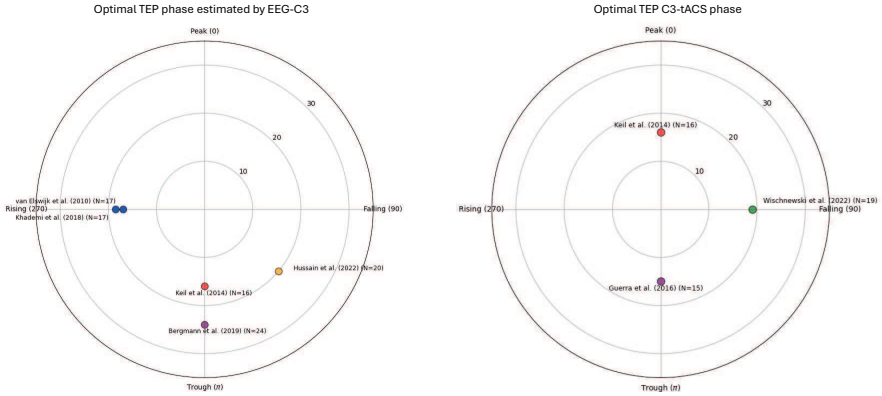


Figure 1.5: **Polar distribution of optimal beta phases at C3 for motor excitability across eight studies.** The left panel includes studies utilizing spontaneous EEG recorded from the C3 electrode; the right panel includes studies employing transcranial alternating current stimulation (tACS) at C3 to entrain the cortical oscillatory phase. Radius = Sample Size N.

Phase dependency beyond the motor system

Similar phase-dependent modulations extend beyond the motor system and beta band. In the sensory systems, for example, whether a faint stimulus is detected or missed can depend on the phase of ongoing alpha (8–12 Hz) or theta (4–8 Hz) oscillations at the moment

the stimulus appears [51, 52, 53, 54]. Synchronizing oscillations across different sensory regions enhances multisensory perception, improving the brain's ability to combine sights and sounds accurately [55, 56, 57]. In the attention domain, fluctuations in performance have been linked to rhythmic changes in cortical excitability tied to theta and alpha phases [58, 59]. Similarly, in memory research, the theta phase organizes higher-frequency activity so that information encoding and retrieval occur at distinct times within the same oscillatory cycle [60, 61, 62, 63].

A unifying picture emerges: the timing of neural oscillations determines when different parts of the brain can effectively communicate. By aligning their phases, neural networks synchronize their activity to exchange information efficiently and flexibly. Note that goal-directed behavior depends on both cognitive control and motor execution. For example, studies have shown that neurons in the prefrontal cortex synchronize their firing with hippocampal theta oscillations during tasks requiring working memory and decision-making. The strength of this phase-locking correlates with both accuracy and reaction time [64, 65, 66, 67, 68, 69]. EEG studies have further confirmed that increased theta-phase alignment between prefrontal, hippocampal, and motor regions occurs during response inhibition and task switching [70, 71, 72]. Collectively, these results support the view that the oscillatory phase provides a temporal framework that gates when information can be transmitted and integrated, thereby supporting adaptive cognitive and motor functions.

The phenomenon of phase precession

Cognitive and motor information linked to specific oscillatory phases are not always static. Scientists have found that the regarding phase could shift progressively under certain conditions, known as phase precession. This phenomenon was originally discovered in the hippocampus of rodents navigating through the space [73]. As an animal

moved along a familiar path, individual hippocampal neurons fired progressively earlier in the theta rhythm. Similar patterns have been observed in other brain regions, including the ventral striatum [74] and frontal cortex [65]. More recent evidence extends phase precession to humans, where hippocampal neurons show comparable phase shifts during memory-guided navigation [75, 76]. A related form of phase precession has also been observed in the motor cortex, where tACS leads to a progressive shift in the phase of motor cortical excitability [77].

Mechanistically, such precession was proposed to arise from the interaction of multiple oscillators within neural networks or from asymmetric synaptic inputs that bias membrane potentials toward earlier phases [78, 79]. Functionally, the neuron "fires ahead of the beat" allows the brain to compress time and encode sequences more compactly, thus supporting learning and predictive control [78, 79, 80, 81].

1.3 Pathological beta activity in Parkinson's

As discussed in section 1.2, the degeneration of dopaminergic neurons in the substantia nigra leads to an excessive 'brake' on the motor system in Parkinson's Disease. Within the framework outlined above, where beta oscillations regulate the balance between motor stability and change, this dopaminergic loss biases the system toward excessive stabilization, effectively imposing a persistent "brake" on movement.

Seminal work by Brown and Hammond demonstrated that, in the dopamine-depleted state, neurons within the cortico-basal ganglia-thalamic loop lose their independence and become excessively synchronized in the beta frequency band [82, 83]. Rather than occurring in transient, task-relevant bursts, beta activity in PD becomes abnormally sustained and spatially widespread. This pathological hypersynchrony limits the flexibility of the motor network, reducing its ability to transiently suppress beta activity when movement initiation or scaling is required.

Functionally, elevated beta synchrony interferes with the effective transmission of "go" signals from motor cortical areas through the basal ganglia to downstream brainstem and spinal motor circuits. As a result, motor commands are delayed, weakened, or incompletely released, a mechanism widely recognized as a key physiological substrate of bradykinesia and rigidity [84, 85, 23]. Clinical studies correlating local field potentials (LFPs) with motor scores consistently show that as beta power increases, the velocity of movement decreases [86, 87, 88].

This pattern is consistent with the view that Parkinsonian motor symptoms arise not from beta oscillations per se, but from their pathological persistence and loss of temporal specificity. In this state, beta no longer serves as a flexible, phase-dependent control signal, but instead enforces a rigid motor regime that impairs voluntary movement.

1.3.1 Current therapies and their limitations

Dopaminergic medication, such as apomorphine or Levodopa, are able to replenish dopamine levels. Early electrophysiological studies revealed that the administration of these agents leads to a significant suppression of beta oscillations in the STN, which coincides with the improvement of motor symptoms [89]. For most patients, starting the medication feels like a miracle, where symptoms seem to disappear. But as the disease progresses, the brain loses its ability to store and smooth out the dopamine delivered by the pill. This leads to a roller-coaster effect known as "on-off" fluctuations, where a patient might be mobile and fluid one moment, but freeze up entirely the moment the medication wears off. In addition, its long-term side effects such as dyskinesias (i.e. involuntary, writhing movements), puts doctors in a difficult bind: the side effects can be just as debilitating as the stiffness of Parkinson's itself.

Given the physiological limitations of chemical therapy, researchers sought a more direct method to stabilize the motor circuit. When surgeons use high-frequency electricity in the subthalamic nucleus, the

symptoms vanish almost instantly [90, 91]. This method, deep-brain stimulation (DBS), could act as the electronic override, suppressing beta and ameliorating symptoms. For years, the mechanism of DBS was unclear, but the likely hypothesis has been demonstrated that this high-frequency input (typically 130 Hz) on the subthalamic nucleus forces neurons to decouple from their pathological resonance, disrupting the beta hypersynchronous communication that paralyzes the patient.

While DBS offers a robust mechanistic override for the pathological beta oscillations discussed previously, it remains an invasive intervention with significant limitations. Implanting a foreign hardware directly into the brain requires stereotactic neurosurgery, which introduces non-trivial risks of complications, such as intracranial hemorrhage, infection, and seizures. Furthermore, the presence of implanted hardware creates a lifelong dependency on device maintenance, with patients inevitably facing additional surgeries for battery replacements. Importantly, a substantial proportion of patients are not eligible for DBS due to advanced age, medical frailty, or comorbid conditions that increase surgical risk, thereby limiting the general applicability of this approach.

1.3.2 The idea of restoring the unbalanced beta

One lesson we have learned from the clinical impact of DBS is that beta can be a causal modulator of PD's symptoms, so that if we can find a way to break this rhythm, we can restore movement. But can we do it without drilling into the brain?

As we know, the basal ganglia are in constant conversation with the cortex of the brain. Beta rhythms deep in the brain are often locked in with similar rhythms in the cortical area [27, 25]. Crucially, Litvak et al. [25] and Hirschmann et al. [26, 27] demonstrate that the cortex predominantly drives the STN through the oscillations in the beta frequency band. Granger causality analyses confirm this top-down directionality, revealing that oscillatory changes in the cortex precede and likely

entrain activity in the basal ganglia [30]. This top-down influence provides a compelling rationale for non-invasive therapeutic strategies. If the pathological beta rhythm in the STN is maintained or modulated by cortical drive, then targeting the cortical nodes (rIFG/preSMA) offers a potential entry point to regulate the entire circuit without the need for surgical penetration.

Motivated by this insight, Non-Invasive Brain Stimulation (NIBS) emerges as a therapeutic tool for motor disorder intervention. Among NIBS techniques, tACS is of particular interest because it can interact with ongoing neural oscillations in a frequency- and phase-specific manner. By targeting the abnormal beta synchrony that characterizes Parkinson's disease, tACS provides a principled means of engaging pathologically synchronized networks non-invasively. This dissertation focuses on leveraging tACS to probe and modulate beta-mediated motor control, a theme that will be developed in detail in the following chapters.

1.4 Fine-tuning motor inhibition with non-invasive brain stimulation

A good candidate for non-invasive cortical stimulation to normalize oscillatory activity is transcranial alternating current stimulation (tACS) [92, 93]. tACS delivers oscillating current through scalp electrodes, modulating neuronal membrane potentials and biasing spike timing. As a result, ongoing brain rhythms would be aligned with the external alternating current, consistent with entrainment [94, 95, 92], as indicated by Figure 1.6. tACS is safe, portable, and relatively inexpensive, making it attractive for both research and clinical use [96, 97, 98].

The functional role of tACS includes its investigative and modulatory features. First, the phase-alignment nature of tACS entrainment allows it to probe the spontaneous phase of ongoing brain oscillations. Researchers can align the experimental cue to a specific phase of tACS

applied over the regarding cortex, to investigate the causal role of neural oscillatory phase on behavioral outcome [99]. This is particularly valuable as it overcomes the difficulty of determining the ongoing phase by EEG/EMG, which often requires substantial amounts of trials for the post-hoc analysis and only provides correlation evidence.

The more common application of tACS is its direct modulation on cognitive and motor performance. For example, stimulating the motor cortex with tACS at the individual's mu-rhythm frequency has been shown to modulate motor learning and movement speed [100]. Similarly, prefrontal tACS at theta or gamma frequencies has been repeatedly linked to changes in working memory capacity [101, 102], attention, and creative problem-solving [103]. The following parts will focus on the effects of beta tACS on motor inhibition.

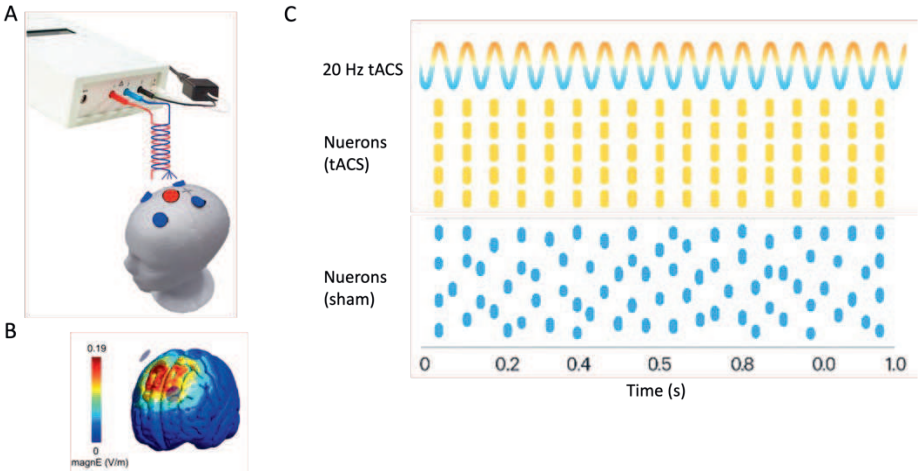


Figure 1.6: **Conceptual overview of transcranial alternating current stimulation (tACS) entraining neuron spiking.** (A) Schematic of a 4x1 tACS system delivering oscillatory current through preSMA [104]. (B) Simulated electric field with a 4x1 setup. (C) Conceptual illustration of neuronal activity with intrinsic firing rate of 20 Hz under sham (blue) and 20 Hz tACS (orange) stimulation. When stimulation is applied with the same frequency, neuronal spikes become aligned to the external electric field.

1.4.1 How beta tACS affects motor control

Human studies indicate that when tACS is applied at beta range over motor areas such as the primary motor cortex (M1), preSMA, or rIFG, movement initiation tends to slow, and response velocity decreases, consistent with enhanced motor inhibition [38, 39, 104, 105]. Conversely, stimulation frequency around the gamma range has the opposite effect, facilitating faster or more forceful movement [104]. Furthermore, beta phase-aligned TMS/tACS shows phase-dependent MEP, as we reviewed in the previous section. Collectively, these results converge on the interpretation that beta tACS over rIFG/preSMA/M1 biases the hyperdirect pathway toward global motor suppression. (See Table 1.1 for a summary of tACS effects on motor inhibition in humans.)

Despite these promising findings, conventional tACS still faces major challenges. First, responses vary widely across individuals [111, 112]. Factors include anatomical variability (skull thickness, electrode montage) [113], baseline oscillatory power/frequency [114], brain-state fluctuations [115], and non-linear network dynamics [116].

A deeper limitation arises from the nature of tACS entrainment itself. Prolonged rhythmic stimulation tends to stabilize existing oscillations rather than disrupt them [117]. In disorders like PD, where pathological beta synchrony needs to be broken rather than reinforced, such stabilization may be counterproductive. To effectively desynchronize pathological beta activity, stimulation would need to adapt in real time, delivering anti-phase perturbations precisely aligned to the instantaneous phase of ongoing neural activity. This insight is driving the development of closed-loop, phase-adaptive stimulation systems, which sense the brain's rhythms and respond dynamically.

1.4.2 Personalized stimulation

To overcome the high inter-individual variability inherent in conventional 'one-size-fits-all' tACS protocols, the field is moving toward personalized stimulation parameters. Offline parameter optimization

Table 1.1: **Summary of conventional tACS effects on motor inhibition in humans**

Study	N	Task	tACS freq.	Target	Timing	Main result on motor inhibition
Feurra et al. [106]	10	TMS–MEP indexing	5–40 Hz	M1	Online	20 Hz increased corticospinal excitability.
Joundi et al. [39]	18	Isometric force tracking	20 Hz and 70 Hz	M1	Online	70 Hz improved acceleration, 20 Hz impaired.
Leunissen et al. [104]	36	Anticipatory SST	20 Hz and 70 Hz	preSMA	Online	20 Hz tACS enhanced inhibition on directly following trials; 70 Hz tACS had opposite effect.
Lyzhko et al. [107]	20	Go/NoGo + EEG	20 Hz and 6 Hz	preSMA or rIFG	Offline (pre-task)	No behavioral change; 20 Hz tACS over rIFG increased theta power.
Moisa et al. [108]	20	Rapid visuomotor task	20 Hz and 70 Hz	M1	Online	20 Hz tended to slow movement speed/force; 70 Hz improved.
Pogosyan et al. [38]	14	Visuomotor tracking/force	20 Hz and 5 Hz	Contralateral M1	Online	20 Hz-tACS slowed movement.
Rjosk et al. [109]	19	TMS–MEP indexing	20 Hz	Left M1	Offline	No immediate change in excitability or inter-hemispheric inhibition
Wach et al. [110]	18	Fast finger tapping	10 Hz and 20 Hz	M1	Online	20 Hz slowed tapping; 10 Hz increased movement variability

involves tailoring frequency, amplitude, and timing based on pre-acquired neuroimaging or electrophysiological data. This offline approach aims to maximize the interaction between the exogenous electric field and the endogenous network dynamics.

Frequency-tuned tACS is normally designed to match individual intrinsic frequencies, boosting neural entrainment and modulating cognition. Computational and in-vivo studies have demonstrated that entrainment strength peaks when stimulation frequency matches the intrinsic oscillation frequency and that the locking range broadens with increasing intensity, while small deviations in frequency or insufficient field strengths can move stimulation outside the entrainment zone [95, 118, 119, 93], as shown in Figure 1.7. Human studies using tACS with the frequency of each participant's intrinsic rhythm consistently enhance oscillatory power, interregional synchrony, and performance in memory, perception, and attention tasks than fixed-frequency protocols [120, 121, 122]. Current recommendations emphasize mapping individual Arnold tongues and using adaptive, closed-loop tACS to sustain resonance within the entrainment zone [123].

Based on the Arnold tongue principle, entrainment strength scales with the forcing amplitude and widens the frequency range that locks to stimulation. Amplitude-dependent modulation of tACS entrainment has been demonstrated in non-human primates by Johnson et al. [124]. In humans, resting-state EEG studies report that nominal currents with 2 mA could generally produce larger effects at the group level than using 1 mA [125]. Furthermore, computational head modeling, such as finite element models (FEM), derived from individual structural MRIs, can simulate the current flow through the specific tissues of an individual's head, allowing researchers to optimize the electrode montage to maximize the field at the target region. Besides, FEM also allows for individualized dosing, where the input current is adjusted to ensure that the target region receives a standardized voltage [126, 127]. Additional studies confirmed that brain state could constrain amplitude efficacy: when endogenous alpha power is already high, additional

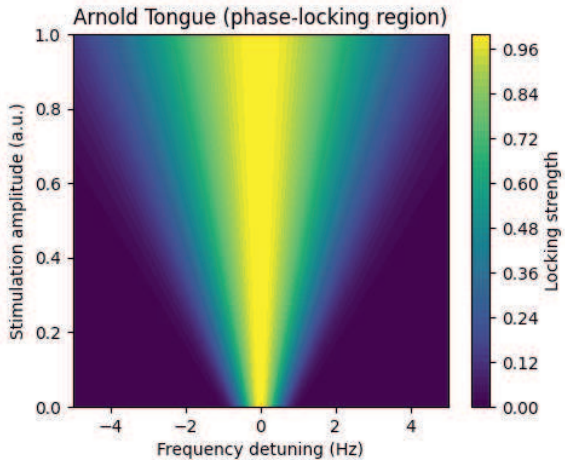


Figure 1.7: Schematic depiction of the Arnold tongue. The x-axis represents the frequency detuning between stimulation and intrinsic oscillation, while the y-axis shows stimulation amplitude. The color bar represents the phase-locking between an external oscillatory input, indicating the entrainment strength.

increases with the same current are limited, whereas low-power states permit stronger amplitude-dependent boosts [128].

Finally, optimizing the duration of the stimulation is crucial for the transient entrainment and lasting neuroplastic changes. Evidence indicates that short-duration tACS (typically under 5 minutes) is sufficient to entrain neural oscillations during the stimulation block (online effects) but rarely produces lasting after-effects. While longer durations (typically 10–20 minutes) are required to induce Spike-Timing-Dependent Plasticity (STDP) or Long-Term Potentiation (LTP)-like effects that persist after the current is turned off [129, 130].

1.4.3 Closing the loop: interacting with brain rhythm phase in real-time

The timing of stimulation relative to the brain's internal rhythms is found to be critical. For example, tACS timed to slow-wave sleep up-states reduces retroactive interference in memory [131], and EEG-triggered bursts of individualized-alpha tACS have shown feasibility and target engagement in major depression [132]. Adjacent work with EEG-triggered TMS shows state dependence boosts effect sizes and reduces variability of the motor evoked potential [133]. Together, stimulation that respects the brain's ongoing dynamics can enhance therapeutic impact. In the rest of this chapter, we will focus specifically on phase-dependent closed-loop tACS.

Phase-dependent tACS

Phase-dependent stimulation is one of the most promising approaches: it leverages the precise timing of stimulation delivery relative to the phase of endogenous neural oscillations. In contrast, conventional open-loop tACS often delivers stimulation without reference to the instantaneous phase and therefore tends to reinforce oscillatory synchrony when applied continuously over time [134]. Such reinforcement poses fundamental limitations for applications in disorders such as Parkinson's disease, where pathological beta activity within cortico–basal ganglia circuits is already excessive. In such cases, closed-loop tACS offers an approach that allows anti-phase stimulation, delivering stimulation with the opposite phase to the ongoing rhythms and attenuating them through phase cancellation [135].

In movement disorders, real-time tracking of tremor phase enables anti-phase tACS that reduces tremor amplitude in Parkinsonian and dystonic tremor [136, 137, 138]. In working memory, alpha-locked tACS during retention perturbs both alpha dynamics and performance [139]; and more recent implementations that jointly tune phase and

individual alpha frequency, such as closed-loop amplitude-modulate-tACS, reliably modulate electrophysiology and behavior in healthy adults [140]. (See Table 1.2 for a concise summary.)

Table 1.2: **Summary of published real-time phase-dependent stimulation studies applying non-invasive or invasive methods**

Study	Target	System	Task	N	Outcome
Brittain et al. [136]	M1	Tremor phase-tACS	Parkinsonian rest tremor	15	Anti-phase tACS reduced tremor amplitude
Nieuwhof et al. [138]	M1	Tremor phase-tACS	Dystonic tremor	17-18	Anti-phase tACS suppressed non-jerky dystonic tremor
Chen et al. [139]	Pz-Oz	Pz alpha phase-tACS	Working memory task	49	Anti-phase tACS perturbed alpha and altered retention performance
Haslacher et al. [140]	Oz-Cz	Pz alpha phase-CLAM-tACS	Working memory task	44-46	Phase-tuned tACS modulated alpha power and working memory behavior
Zarubin et al. [141]	Oz-Pz	Alpha phase-tACS	In-phase short tACS burst	20	Brief phase-matched bursts transiently modulated alpha amplitude
Mansouri et al. [142]	F3-F4	Alpha phase-tPCS	Subcortical network task	20	No effects on EEG and performance

tACS = transcranial alternating current stimulation; CLAM-tACS = closed-loop amplitude- and phase-modulated tACS; tPCS = transcranial pulsed current stimulation; TMS = transcranial magnetic stimulation; EEG = electroencephalography; EMG = electromyography; M1 = primary motor cortex; WM = working memory.

Implementing this approach requires a closed-loop neuromodulation framework consisting of four main stages: (1) Brain representations recording and assessment using techniques like fMRI, fNIRs, and M/EEG; (2) Phase estimation; (3) application of stimulation; and (4) a closed-loop system where the process is repeated for continuous adjustment based on real-time responses [112].

Phase estimation protocols

Precise real-time phase prediction is crucial for a closed-loop stimulation system, accounting for unavoidable system delays and filtering artifacts. Several strategies have been developed to forecast the instantaneous phase of an oscillatory neural signal.

Frequency domain-based sinusoid extrapolation A straightforward approach emerges as frequency domain decomposition, where the EEG signal is first band-pass filtered to isolate the frequency band of interest. A Fast Fourier Transform (FFT) [142] or wavelet method [143] is then computed over a short past window to estimate the dominant oscillation's frequency and phase. Assuming relative stationarity of the oscillation within this brief horizon, the algorithm extrapolates a sinusoidal waveform forward in time to predict the future phase.

Autoregressive (AR) time-series forecasting A more flexible yet computationally demanding alternative is the autoregressive (AR) time-series forecasting approach. This method models the EEG signal as a linear combination of its past samples, allowing for short-term extrapolation of the waveform into the future [144, 145]. The predicted segment then would be used to estimate the instantaneous phase (e.g., with Hilbert), enabling anticipation of when the target phase will occur. AR models generally outperform FFT methods when oscillations are stationary over the prediction horizon, capturing deviations from pure sinusoidal shapes. However, the method's accuracy depends critically on model order, window length, and signal-to-noise ratio (SNR).

Adaptive AR or LMS-based AR algorithms were developed for longer prediction horizons, in which model parameters are continuously updated in real time with learning rules such as the least-mean-square (LMS) algorithm [146, 147]. This adaptivity allows the model to track slow drifts in oscillatory frequency or amplitude, improving phase prediction accuracy under dynamic conditions.

Educated temporal prediction (ETP) A peak-interval prediction, Educated Temporal Prediction (ETP), uses a training or calibration phase to characterize the distribution of inter-peak intervals (IPI) of the target oscillation under resting conditions. During real-time operation, the system detects each oscillatory peak or trough and projects the next expected cycle using the learned IPI statistics, thereby estimating the future time point at which the desired phase will occur. An ETP approach is recommended when the baseline data are in a low-SNR environment [148].

Phase-locked loop (PLL) approach Instead of post-hoc filtering and phase extraction, the causal oscillator or phase-locked loop (PLL) approach uses a dynamic oscillator model that continuously locks onto the incoming signal's phase and frequency [149]. The internal phase of the modelled oscillator serves as the real-time estimate of the signal's phase. Such a causal technique achieves rapid tracking without non-causal operations like the Hilbert transform. This approach is suitable when system latency is constrained and computational efficiency is critical; therefore normally used for hardware embedded phase detection.

Machine learning based methods Machine learning based methods employ supervised learning techniques, such as convolutional or recurrent neural networks, to learn mappings between raw or pre-processed EEG data and future oscillatory phase [150, 151, 152]. Machine-learning models can capture non-linear and multi-component patterns in EEG data, offering potentially higher precision and generalizability across subjects. However, their performance depends on the availability of representative training data, and they must be computationally lightweight to satisfy real-time latency constraints.

Hybrid and optimized multi-layer filtering (MLOF) algorithms Rodriguez Rivero and Ditterich [153] described an adaptive closed-loop

phase-prediction method that integrated onset/offset detection of oscillatory activity with dynamic prediction of the next phase event. These hybrid techniques often employ cascaded filtering, feature extraction, and regression or classification layers to estimate phase with improved robustness. While implementation details vary, hybrid approaches generally provide a balance between computational efficiency and adaptive performance, making them attractive candidates for real-time EEG-based neurostimulation.

In summary, each phase-prediction method offers specific advantages and trade-offs. A comparative summary of the principal EEG phase-prediction algorithms and their characteristic features is presented in Table 1.3. The choice of algorithm ultimately depends on the characteristics of the target oscillation, available computational resources, and the latency constraints of the stimulation hardware.

The future of closed-loop tACS

Phase-locked closed-loop tACS represents a key step in the revolution of adaptive interventions. Advances in real-time phase prediction, wearable hardware, computational modeling, and machine learning enable precise interaction with the specific temporal structure of neural oscillations.

The clinical promise of this approach lies in its capability to bidirectionally modulate neural dynamics by precisely targeting pathological rhythms. Such precision enables desynchronization of maladaptive oscillations in Parkinson's disease, restoration of impaired cross-frequency coupling in Alzheimer's disease, and normalization of network asymmetries in affective or psychotic disorders. Yet, progress toward clinical adoption requires overcoming key challenges: miniaturizing hardware for portable home use, reducing algorithmic latency for accurate phase locking, and establishing biomarkers of optimal target engagement across heterogeneous pathologies. Early clinical trials indicate that closed-loop phase-locked tACS can yield symptom relief with lower

Table 1.3: **Comparative Summary of EEG Phase-Prediction Algorithms for Closed-Loop Neurostimulation**

Algorithm	Computation load	Adaptivity to non-stationarity	Adaptivity to latency range	Advantage	Limitations
FFT-based sinusoid extrapolation	Very low	Low	Small (past window ∼300ms)	Good when oscillation strong and stable	Poor when frequency drift/multi-component signal
AR	Moderate	Moderate	Past window + AR fit time	Good for short forecasting horizons; many published closed-loop EEG-TMS use	Sensitive to model order/parameters; higher compute
Adaptive AR / LMS-AR	Moderate to high	Higher	Similar to AR but longer horizon possible	Better at tracking frequency drift	Requires adaptation tuning; higher compute
ETP	Low	Low-moderate	Very small buffer + simple extrapolation	Robust, efficient; Shirinpour et al. found ∼70% accuracy in real-time EEG-TMS experiment	Requires training phase; less adaptivity
Causal Oscillator / PLL	Low-medium	Moderate	Very low latency	Suitable for hardware/embedded real-time estimates	Less widely employed in EEG closed-loop stimulation studies; tuning needed
Machine Learning	Potentially high	High	Depends on architecture	Potential highest accuracy; lowest variance vs AR/ETP	Needs training data; generalisability and latency tradeoffs
Hybrid / Optimised Filters	Medium	Variable	Medium	Good compromise between ease and performance (e.g., Rivero et al)	Implementation complexity; may still require tuning

Comparison of major algorithmic families used for real-time estimation and prediction of EEG oscillatory phase in closed-loop, phase-locked neurostimulation systems. EEG = electroencephalography; FFT = Fast Fourier Transform; AR = autoregressive model; LMS = least mean square; ETP = Educated Temporal Prediction; PLL = phase-locked loop; EPN = EEG Phase Prediction Network; MLOF = multi-layer optimized filter; SNR = signal-to-noise ratio.

intensities and shorter durations than conventional stimulation, indicating superior neural efficiency and safety. As computational models and neurophysiological insights converge, the next decade is likely to see emerging phase-informed neuromodulation strategies in precision network therapeutics.

The work presented in the dissertation represents the mechanistic validation of such a trajectory. By tracking beta-phase codes in motor inhibition from mere observation to causal, closed-loop control, we have now shown that phase-specific modulation of a single cortical site can bidirectionally influence human motor behavior. Our work proves that more than merely being able to observe brain rhythms, we can interact with them in real time. As this field matures, full translational potential will require deep collaboration between neuroscientists, engineers, clinicians, and patients, placing this technology front and center in future precision network therapeutics.

1.5 Outline of this thesis

1.5.1 Rationale and roadmap

Across this thesis, I asked whether the temporal code carried by the beta phase is mechanistically relevant for human motor inhibition and whether deliberately aligning or opposing that code allows causal control of behavior and corticospinal coupling. The four empirical chapters form a deliberate progression. Chapter 2 establishes that inhibitory efficacy depends on the instantaneous beta phase at which the stop process is engaged. Chapter 3 shows that this phase code is not rigid but can progress in a task-dependent and outcome-dependent manner under rhythmic drive. Chapter 4 translates these insights into a real-time closed-loop design, demonstrating that anti-phase stimulation disrupts beta and impairs stopping, while in-phase stimulation stabilizes ongoing motor output. Chapter 5 closes the loop at the efferent interface by showing that the duration of stimulation interacts with phase to bidirectionally modulate cortico-muscular coherence without altering

force output. The final chapter brings together the engineering and methodological requirements for phase-dependent closed-loop tACS, so that it can be implemented reproducibly and positioned for clinical translation. Together, these studies advance a coherent framework in which beta phase gates motor suppression and can be shaped in real time for mechanistic tests and therapeutic strategies.

1.5.2 From phase dependence to phase plasticity

Chapter 2 shows that the timing of the stop signal relative to the beta cycle matters for behavior. Stop signals that coincide with the trough of the stimulation-entrained beta rhythm yield better inhibition, whereas signals near the peak yield poorer inhibition. This pattern is consistent with the communication through coherence account in which afferent input is most effective when it lands in a window of high postsynaptic excitability set by the ongoing phase. Thus, the beta cycle provides a repeating inhibitory scaffold that can be exploited or countered depending on task demands.

Chapter 3 examines whether the privileged phase is static or adaptive. During successful stops, the optimal inhibitory phase is stable and produces a clear sinusoidal modulation of stopping efficacy. During failed stops, the phase associated with the strongest attempt to inhibit shifts progressively across the session, consistent with phase precession. The absence of precession in a control experiment without stimulation argues that precession reflects an interaction between rhythmic drive and an error-prone inhibitory state rather than a generic drift. These findings link a classic temporal coding motif to human cognitive control and indicate that phase codes can retime under external forcing and behavioral contingencies.

1.5.3 From observation to causal control

Chapter 4 implements an electroencephalography-guided closed-loop system that delivers stimulation at a desired phase of the ongoing beta

rhythm over preSMA during the stop signal task. Anti-phase stimulation, timed one hundred eighty degrees from the instantaneous cortical beta, reduces beta power after stimulation and slows the covert stopping process. In-phase stimulation has the opposite signature on ongoing motor output, reducing the peak force rate in go trials and decreasing variability of response timing. These double dissociations support a destructive interference account for anti-phase stimulation and a stabilizing entrainment account for in-phase stimulation. Importantly, they show that the beta phase code is not only descriptive but also actionable for causal perturbation.

1.5.4 Boundary conditions at the corticospinal interface

Chapter 5 tests how stimulation duration interacts with phase to shape post-stimulation corticospinal coupling during sustained isometric force. Brief anti-phase trains of one to two seconds suppress corticomuscular coherence in the beta band relative to prolonged anti-phase, in-phase, and sham, whereas in-phase stimulation increases coherence with stronger effects at longer duration. Local beta power, resting beta, and force metrics remain unchanged. These results indicate that the efficacy of desynchronization depends on both phase and duration. Short anti-phase pulses disrupt coupling before network entrainment can accumulate, while longer in-phase trains promote coupling consistent with resonant stabilization.

1.5.5 Engineering and clinical roadmap

The final chapter of this dissertation synthesizes the practical challenges and lessons learned from implementing a phase-dependent closed-loop system and insights from previous studies in the field, and provides a mechanistically informed guideline for reproducible closed-loop installation. This work highlights that achieving a reliable phase-dependent control requires rigorous engineering, including timing control, quantified end-to-end latency and jitter, artifact handling, and causal phase

estimation, alongside benchmarks for target engagement. Finally, this chapter delineates a potential clinical pathway for a phase-dependent system, combined with continued methodological advancement.

1.5.6 An integrative mechanistic model

1. Beta phase gates the probability that afferent control signals will suppress motor output. Through aligned input favors successful cancellation, peak aligned input does not.
2. Rhythmic drive can bias this gate and, under error-prone states, induce a progressive advance of the preferred phase, consistent with phase precession through interference between intrinsic and driven oscillators.
3. Real-time alignment of stimulation with the endogenous phase allows directional control. In phase stimulation reinforces the intrinsic rhythm and stabilizes ongoing motor states. Anti-phase stimulation produces destructive interference that weakens beta-mediated coupling and impairs stopping.
4. The time constant of the network matters. Desynchronization is maximized by short anti-phase trains that end before entrainment builds up, whereas coherence enhancement is maximized by longer in-phase trains that allow accumulation.

References

[1] Gordon D. Logan, William B. Cowan, and Kenneth A. Davis. "On the ability to inhibit simple and choice reaction time responses: A model and a method." In: *Journal of Experimental Psychology: Human Perception and Performance* 10.2 (1984), pp. 276–291. DOI: 10.1037/0096-1523.10.2.276.

[2] Frederick Verbruggen et al. “A consensus guide to capturing the ability to inhibit actions and impulsive behaviors in the stop-signal task”. In: *eLife* 8 (Apr. 2019). DOI: 10.7554/elife.46323.

[3] A Nambu et al. “Dual somatotopical representations in the primate subthalamic nucleus: evidence for ordered but reversed body-map transformations from the primary motor cortex and the supplementary motor area”. In: *The Journal of Neuroscience* 16.8 (Apr. 1996), pp. 2671–2683. DOI: 10.1523/jneurosci.16-08-02671.1996.

[4] Atsushi Nambu et al. “Excitatory Cortical Inputs to Pallidal Neurons Via the Subthalamic Nucleus in the Monkey”. In: *Journal of Neurophysiology* 84.1 (July 2000), pp. 289–300. DOI: 10.1152/jn.2000.84.1.289.

[5] Atsushi Nambu, Hironobu Tokuno, and Masahiko Takada. “Functional significance of the cortico-subthalamo-pallidal ’hyperdirect’ pathway”. In: *Neuroscience Research* 43.2 (June 2002), pp. 111–117. DOI: 10.1016/s0168-0102(02)00027-5.

[6] Adam R. Aron and Russell A. Poldrack. “Cortical and Subcortical Contributions to Stop Signal Response Inhibition: Role of the Subthalamic Nucleus”. In: *The Journal of Neuroscience* 26.9 (Mar. 2006), pp. 2424–2433. DOI: 10.1523/jneurosci.4682-05.2006.

[7] Adam R. Aron et al. “Triangulating a Cognitive Control Network Using Diffusion-Weighted Magnetic Resonance Imaging (MRI) and Functional MRI”. In: *The Journal of Neuroscience* 27.14 (Apr. 2007), pp. 3743–3752. DOI: 10.1523/jneurosci.0519-07.2007.

[8] Sara Jahfari et al. “Effective Connectivity Reveals Important Roles for Both the Hyperdirect (Fronto-Subthalamic) and the Indirect (Fronto-Striatal-Pallidal) Fronto-Basal Ganglia Pathways during Response Inhibition”. In: *The Journal of Neuroscience* 31.18

(May 2011), pp. 6891–6899. DOI: 10.1523/jneurosci.5253-10.2011.

[9] Witney Chen et al. "Prefrontal-Subthalamic Hyperdirect Pathway Modulates Movement Inhibition in Humans". In: *Neuron* 106.4 (May 2020), 579–588.e3. DOI: 10.1016/j.neuron.2020.02.012.

[10] Gyorgy Buzsaki and Andreas Draguhn. "Neuronal oscillations in cortical networks". In: *Science* 304.5679 (2004), pp. 1926–1929. DOI: 10.1126/science.1099745.

[11] György Buzsáki, Costas A. Anastassiou, and Christof Koch. "The origin of extracellular fields and currents — EEG, ECoG, LFP and spikes". In: *Nature Reviews Neuroscience* 13.6 (May 2012), pp. 407–420. DOI: 10.1038/nrn3241.

[12] Mike X Cohen. *Analyzing Neural Time Series Data: Theory and Practice*. The MIT Press, Jan. 2014. DOI: 10.7551/mitpress/9609.001.0001.

[13] Joshua Jacobs et al. "Brain Oscillations Control Timing of Single-Neuron Activity in Humans". In: *The Journal of Neuroscience* 27.14 (Apr. 2007), pp. 3839–3844. DOI: 10.1523/jneurosci.4636-06.2007.

[14] Pascal Fries. "A mechanism for cognitive dynamics: neuronal communication through neuronal coherence". In: *Trends in Cognitive Sciences* 9.10 (2005), pp. 474–480. DOI: https://doi.org/10.1016/j.tics.2005.08.011.

[15] Pascal Fries. "Rhythms for Cognition: Communication through Coherence". In: *Neuron* 88.1 (2015), pp. 220–235. DOI: https://doi.org/10.1016/j.neuron.2015.09.034.

[16] Thilo Womelsdorf et al. "Modulation of Neuronal Interactions Through Neuronal Synchronization". In: *Science* 316.5831 (June 2007), pp. 1609–1612. DOI: 10.1126/science.1139597.

[17] Andreas K. Engel, Pascal Fries, and Wolf Singer. “Dynamic predictions: Oscillations and synchrony in top–down processing”. In: *Nature Reviews Neuroscience* 2.10 (Oct. 2001), pp. 704–716. DOI: 10.1038/35094565.

[18] Andrea Biasiucci, Benedetta Franceschiello, and Micah M. Murray. “Electroencephalography”. In: *Current Biology* 29.3 (Feb. 2019), R80–R85. DOI: 10.1016/j.cub.2018.11.052.

[19] Marco Marino and Dante Mantini. “Human brain imaging with high-density electroencephalography: Techniques and applications”. In: *The Journal of Physiology* 604.2 (Aug. 2024), pp. 783–812. DOI: 10.1113/jp286639.

[20] G. Pfurtscheller and F.H. Lopes da Silva. “Event-related EEG/MEG synchronization and desynchronization: basic principles”. In: *Clinical Neurophysiology* 110.11 (Nov. 1999), pp. 1842–1857. DOI: 10.1016/s1388-2457(99)00141-8.

[21] Andrea A. Kühn et al. “Event-related beta desynchronization in human subthalamic nucleus correlates with motor performance”. In: *Brain* 127.4 (Apr. 2004), pp. 735–746. DOI: 10.1093/brain/awh106.

[22] Nicole Swann et al. “Intracranial EEG Reveals a Time- and Frequency-Specific Role for the Right Inferior Frontal Gyrus and Primary Motor Cortex in Stopping Initiated Responses”. In: *The Journal of Neuroscience* 29.40 (Oct. 2009), pp. 12675–12685. DOI: 10.1523/jneurosci.3359-09.2009.

[23] Nicola J. Ray et al. “The role of the subthalamic nucleus in response inhibition: Evidence from local field potential recordings in the human subthalamic nucleus”. In: *NeuroImage* 60.1 (Mar. 2012), pp. 271–278. DOI: 10.1016/j.neuroimage.2011.12.035.

[24] J. F. Marsden et al. “Subthalamic nucleus, sensorimotor cortex and muscle interrelationships in Parkinson’s disease”. In: *Brain* 124.2 (Feb. 2001), pp. 378–388. DOI: 10.1093/brain/124.2.378.

[25] Vladimir Litvak et al. “Resting oscillatory cortico-subthalamic connectivity in patients with Parkinson’s disease”. In: *Brain* 134.2 (Dec. 2010), pp. 359–374. DOI: 10.1093/brain/awq332.

[26] J. Hirschmann et al. “Distinct oscillatory STN-cortical loops revealed by simultaneous MEG and local field potential recordings in patients with Parkinson’s disease”. In: *NeuroImage* 55.3 (Apr. 2011), pp. 1159–1168. DOI: 10.1016/j.neuroimage.2010.11.063.

[27] J. Hirschmann et al. “Differential modulation of STN-cortical and cortico-muscular coherence by movement and levodopa in Parkinson’s disease”. In: *NeuroImage* 68 (Mar. 2013), pp. 203–213. DOI: 10.1016/j.neuroimage.2012.11.036.

[28] Ashwini Oswal et al. “Deep brain stimulation modulates synchrony within spatially and spectrally distinct resting state networks in Parkinson’s disease”. In: *Brain* 139.5 (Mar. 2016), pp. 1482–1496. DOI: https://doi.org/10.1093/brain/aww048.

[29] Kenji Kato et al. “Bilateral coherence between motor cortices and subthalamic nuclei in patients with Parkinson’s disease”. In: *Clinical Neurophysiology* 126.10 (Oct. 2015), pp. 1941–1950. DOI: 10.1016/j.clinph.2014.12.007.

[30] Ashwini Oswal et al. “Neural signatures of hyperdirect pathway activity in Parkinson’s disease”. In: *Nature Communications* 12.1 (Aug. 2021). DOI: 10.1038/s41467-021-25366-0.

[31] Michael T. Jurkiewicz et al. “Post-movement beta rebound is generated in motor cortex: Evidence from neuromagnetic recordings”. In: *NeuroImage* 32.3 (Sept. 2006), pp. 1281–1289. DOI: 10.1016/j.neuroimage.2006.06.005.

[32] W. Gaetz et al. “Neuromagnetic imaging of movement-related cortical oscillations in children and adults: Age predicts post-movement beta rebound”. In: *NeuroImage* 51.2 (June 2010), pp. 792–807. DOI: 10.1016/j.neuroimage.2010.01.077.

[33] Xiangzi Zhang et al. “Postmovement Beta Synchronization Induced by Speed Effects on IHI from the Ipsilateral to Contralateral Motor Cortex”. In: *eneuro* 12.3 (Mar. 2025), ENEURO.0370–24.2025. DOI: 10.1523/eneuro.0370-24.2025.

[34] Adam Fry et al. “Modulation of post-movement beta rebound by contraction force and rate of force development: Modulation of PMBR by force & amp; RFD”. In: *Human Brain Mapping* 37.7 (Apr. 2016), pp. 2493–2511. DOI: 10.1002/hbm.23189.

[35] Elizabeth Heinrichs-Graham et al. “The functional role of post-movement beta oscillations in motor termination”. In: *Brain Structure and Function* 222.7 (Mar. 2017), pp. 3075–3086. DOI: 10.1007/s00429-017-1387-1.

[36] Jaime Peter et al. “Movement-related beta ERD and ERS abnormalities in neuropsychiatric disorders”. In: *Frontiers in Neuroscience* 16 (Nov. 2022). DOI: 10.3389/fnins.2022.1045715.

[37] Lyam M. Bailey and Timothy Bardouille. “Demonstrating the need for long inter-stimulus intervals when studying the post-movement beta rebound following a simple button press”. In: *Frontiers in Neuroscience* 19 (Apr. 2025). DOI: 10.3389/fnins.2025.1547916.

[38] Alek Pogosyan et al. “Boosting Cortical Activity at Beta-Band Frequencies Slows Movement in Humans”. In: *Current Biology* 19.19 (Oct. 2009), pp. 1637–1641. DOI: 10.1016/j.cub.2009.07.074.

[39] Raed A. Joundi et al. “Driving Oscillatory Activity in the Human Cortex Enhances Motor Performance”. In: *Current Biology* 22.5 (Mar. 2012), pp. 403–407. DOI: 10.1016/j.cub.2012.01.024.

[40] Gijs van Elswijk et al. “Corticospinal Beta-Band Synchronization Entails Rhythmic Gain Modulation”. In: *The Journal of Neuroscience* 30.12 (Mar. 2010), pp. 4481–4488. DOI: 10.1523/jneurosci.2794-09.2010.

[41] Fatemeh Khademi, Vladimir Royter, and Alireza Gharabaghi. "Distinct Beta-band Oscillatory Circuits Underlie Corticospinal Gain Modulation". In: *Cerebral Cortex* 28.4 (Feb. 2018), pp. 1502–1515. DOI: https://doi.org/10.1093/cercor/bhy016.

[42] Julian Keil et al. "Prestimulus Beta Power and Phase Synchrony Influence the Sound-Induced Flash Illusion". In: *Cerebral Cortex* 24.5 (Jan. 2013), pp. 1278–1288. DOI: 10.1093/cercor/bhs409.

[43] Til Ole Bergmann et al. "Pulsed Facilitation of Corticospinal Excitability by the Sensorimotor mu-Alpha Rhythm". In: *The Journal of Neuroscience* 39.50 (Nov. 2019), pp. 10034–10043. DOI: 10.1523/jneurosci.1730-19.2019.

[44] Kai J. Miller et al. "Human Motor Cortical Activity Is Selectively Phase-Entrained on Underlying Rhythms". In: *PLoS Computational Biology* 8.9 (Sept. 2012). Ed. by Tim Behrens, e1002655. DOI: 10.1371/journal.pcbi.1002655.

[45] Miles Wischnewski et al. "The phase of sensorimotor mu and beta oscillations has the opposite effect on corticospinal excitability". In: *Brain Stimulation* 15.5 (2022), pp. 1093–1100. DOI: https://doi.org/10.1016/j.brs.2022.08.005.

[46] Sara J Hussain et al. "Voluntary Motor Command Release Coincides with Restricted Sensorimotor Beta Rhythm Phases". In: *The Journal of Neuroscience* 42.29 (June 2022), pp. 5771–5781. DOI: 10.1523/jneurosci.1495-21.2022.

[47] Lukas Schilberg et al. "Phase of beta-frequency tACS over primary motor cortex modulates corticospinal excitability". In: *Cortex* 103 (2018), pp. 142–152. DOI: 10.1016/j.cortex.2018.03.001.

[48] Flavie Torrecillos et al. "Motor Cortex Inputs at the Optimum Phase of Beta Cortical Oscillations Undergo More Rapid and Less Variable Corticospinal Propagation". In: *Journal of Neuroscience* 40.2 (2020), pp. 369–381. DOI: https://doi.org/10.1523/JNEUROSCI.1953-19.2019.

[49] Hayriye Cagnan et al. “Temporal evolution of beta bursts in the parkinsonian cortical and basal ganglia network”. In: *Proceedings of the National Academy of Sciences* 116.32 (2019), pp. 16095–16104. DOI: https://doi.org/10.1073/pnas.1819975116.

[50] Andrea Guerra et al. “Phase Dependency of the Human Primary Motor Cortex and Cholinergic Inhibition Cancelation During Beta tACS”. In: *Cerebral Cortex* 26.10 (Sept. 2016), pp. 3977–3990. DOI: https://doi.org/10.1093/cercor/bhw245.

[51] N. A. Busch, J. Dubois, and R. VanRullen. “The Phase of Ongoing EEG Oscillations Predicts Visual Perception”. In: *Journal of Neuroscience* 29.24 (June 2009), pp. 7869–7876. DOI: 10.1523/jneurosci.0113-09.2009.

[52] Kyle E. Mathewson et al. “To See or Not to See: Prestimulus Alpha Phase Predicts Visual Awareness”. In: *The Journal of Neuroscience* 29.9 (Mar. 2009), pp. 2725–2732. DOI: 10.1523/jneurosci.3963-08.2009.

[53] Kyle E. Mathewson et al. “Pulsed Out of Awareness: EEG Alpha Oscillations Represent a Pulsed-Inhibition of Ongoing Cortical Processing”. In: *Frontiers in Psychology* 2 (2011). DOI: 10.3389/fpsyg.2011.00099.

[54] Florian H. Kasten and Christoph S. Herrmann. “The hidden state-dependency of transcranial alternating current stimulation (tACS)”. In: *bioRxiv* (2020). DOI: https://doi.org/10.1101/2020.12.23.423984.

[55] Jeremy D. Thorne et al. “Cross-Modal Phase Reset Predicts Auditory Task Performance in Humans”. In: *The Journal of Neuroscience* 31.10 (Mar. 2011), pp. 3853–3861. DOI: 10.1523/jneurosci.6176-10.2011.

[56] Jeremy D. Thorne and Stefan Debener. “Look now and hear what’s coming: On the functional role of cross-modal phase reset”. In: *Hearing Research* 307 (Jan. 2014), pp. 144–152. DOI: 10.1016/j.heares.2013.07.002.

[57] Benedict Shien Wei Ng, Tim Schroeder, and Christoph Kayser. "A Precluding But Not Ensuring Role of Entrained Low-Frequency Oscillations for Auditory Perception". In: *The Journal of Neuroscience* 32.35 (Aug. 2012), pp. 12268–12276. DOI: 10.1523/jneurosci.1877-12.2012.

[58] Ian C. Fiebelkorn and Sabine Kastner. "A Rhythmic Theory of Attention". In: *Trends in Cognitive Sciences* 23.2 (Feb. 2019), pp. 87–101. DOI: 10.1016/j.tics.2018.11.009.

[59] Rufin VanRullen. "Attention Cycles". In: *Neuron* 99.4 (Aug. 2018), pp. 632–634. DOI: 10.1016/j.neuron.2018.08.006.

[60] Bradley Lega et al. "Slow-Theta-to-Gamma Phase–Amplitude Coupling in Human Hippocampus Supports the Formation of New Episodic Memories". In: *Cerebral Cortex* 26.1 (Oct. 2014), pp. 268–278. DOI: 10.1093/cercor/bhu232.

[61] Sanne ten Oever, Peter de Weerd, and Alexander T. Sack. "Phase-dependent amplification of working memory content and performance". In: *Nature Communications* 11.1 (2020), p. 1832. DOI: 10.1038/s41467-020-15629-7.

[62] Randolph F. Helfrich et al. "Neural Mechanisms of Sustained Attention Are Rhythmic". In: *Neuron* 99.4 (Aug. 2018), 854–865.e5. DOI: 10.1016/j.neuron.2018.07.032.

[63] Randolph F. Helfrich, Janna D. Lendner, and Robert T. Knight. "Aperiodic sleep networks promote memory consolidation". In: *Trends in Cognitive Sciences* 25.8 (Aug. 2021), pp. 648–659. DOI: 10.1016/j.tics.2021.04.009.

[64] Athanassios G. Siapas, Evgueniy V. Lubenov, and Matthew A. Wilson. "Prefrontal Phase Locking to Hippocampal Theta Oscillations". In: *Neuron* 46.1 (Apr. 2005), pp. 141–151. DOI: 10.1016/j.neuron.2005.02.028.

[65] Matthew W. Jones and Matthew A. Wilson. "Phase precession of medial prefrontal cortical activity relative to the hippocampal theta rhythm". In: *Hippocampus* 15.7 (2005), pp. 867–873. DOI: 10.1002/hipo.20119.

[66] Karim Benchenane et al. "Coherent Theta Oscillations and Reorganization of Spike Timing in the Hippocampal- Prefrontal Network upon Learning". In: *Neuron* 66.6 (June 2010), pp. 921–936. DOI: 10.1016/j.neuron.2010.05.013.

[67] Kristopher L. Anderson et al. "Theta Oscillations Mediate Interaction between Prefrontal Cortex and Medial Temporal Lobe in Human Memory". In: *Cerebral Cortex* 20.7 (Oct. 2009), pp. 1604–1612. DOI: 10.1093/cercor/bhp223.

[68] Raphael Kaplan et al. "Medial prefrontal theta phase coupling during spatial memory retrieval". In: *Hippocampus* 24.6 (Feb. 2014), pp. 656–665. DOI: 10.1002/hipo.22255.

[69] Alexander R. Backus et al. "Hippocampal-Prefrontal Theta Oscillations Support Memory Integration". In: *Current Biology* 26.4 (Feb. 2016), pp. 450–457. DOI: 10.1016/j.cub.2015.12.048.

[70] Michael X Cohen and James F. Cavanagh. "Single-Trial Regression Elucidates the Role of Prefrontal Theta Oscillations in Response Conflict". In: *Frontiers in Psychology* 2 (2011). DOI: 10.3389/fpsyg.2011.00030.

[71] James F. Cavanagh and Michael J. Frank. "Frontal theta as a mechanism for cognitive control". In: *Trends in Cognitive Sciences* 18.8 (Aug. 2014), pp. 414–421. DOI: 10.1016/j.tics.2014.04.012.

[72] Baltazar Zavala et al. "Cognitive control involves theta power within trials and beta power across trials in the prefrontal-subthalamic network". In: *Brain* 141.12 (Oct. 2018), pp. 3361–3376. DOI: 10.1093/brain/awy266.

[73] John O'Keefe and Michael L. Recce. "Phase relationship between hippocampal place units and the EEG theta rhythm". In: *Hippocampus* 3.3 (1993), pp. 317–330. DOI: 10.1002/hipo.450030307.

[74] Matthijs A. A. van der Meer and A. David Redish. "Theta phase precession in rat ventral striatum links place and reward information". In: *Journal of Neuroscience* 31.8 (2011), pp. 2843–2854. DOI: 10.1523/JNEUROSCI.4869-10.2011.

[75] Salman E. Qasim, Itzhak Fried, and Joshua Jacobs. "Phase precession in the human hippocampus and entorhinal cortex". In: *Cell* 184.12 (2021), 3242–3255.e10. DOI: 10.1016/j.cell.2021.04.017.

[76] Leila Reddy et al. "Theta-phase dependent neuronal coding during sequence learning in human single neurons". In: *Nature Communications* 12.1 (2021), p. 4839. DOI: 10.1038/s41467-021-25150-0.

[77] Miles Wischnewski et al. "Induced neural phase precession through exogenous electric fields". In: *Nature Communications* 15.1 (Feb. 2024). DOI: 10.1038/s41467-024-45898-5.

[78] John E. Lisman and Ole Jensen. "The theta–gamma neural code". In: *Neuron* 77.6 (2013), pp. 1002–1016. DOI: 10.1016/j.neuron.2013.03.007.

[79] John Widloski and Ila R. Fiete. "A model of grid cell development through spatial exploration and spike time-dependent plasticity". In: *Neuron* 83.2 (2014), pp. 481–495. DOI: 10.1016/j.neuron.2014.06.018.

[80] Gyorgy Buzsaki and David Tingley. "Space and time: The hippocampus as a sequence generator". In: *Trends in Cognitive Sciences* 22.10 (2018), pp. 853–869. DOI: 10.1016/j.tics.2018.07.006.

[81] Magdalene I Schlesiger et al. “The medial entorhinal cortex is necessary for temporal organization of hippocampal neuronal activity”. In: *Nature Neuroscience* 18.8 (June 2015), pp. 1123–1132. DOI: 10.1038/nn.4056.

[82] Peter Brown. “Oscillatory nature of human basal ganglia activity: Relationship to the pathophysiology of Parkinson’s disease”. In: *Movement Disorders* 18.4 (Dec. 2002), pp. 357–363. DOI: 10.1002/mds.10358.

[83] Constance Hammond, Hagai Bergman, and Peter Brown. “Pathological synchronization in Parkinson’s disease: networks, models and treatments”. In: *Trends in Neurosciences* 30.7 (July 2007), pp. 357–364. DOI: 10.1016/j.tins.2007.05.004.

[84] Simon Little and Peter Brown. “The functional role of beta oscillations in Parkinson’s disease”. In: *Parkinsonism & amp; Related Disorders* 20 (Jan. 2014), S44–S48. DOI: 10.1016/s1353-8020(13)70013-0.

[85] Wolf-Julian Neumann et al. “Subthalamic synchronized oscillatory activity correlates with motor impairment in patients with Parkinson’s disease”. In: *Movement Disorders* 31.11 (Aug. 2016), pp. 1748–1751. DOI: 10.1002/mds.26759.

[86] Gerd Tinkhauser et al. “Beta burst dynamics in Parkinson’s disease OFF and ON dopaminergic medication”. In: *Brain* 140.11 (Oct. 2017), pp. 2968–2981. DOI: 10.1093/brain/awx252.

[87] Roxanne Lofredi et al. “Beta bursts during continuous movements accompany the velocity decrement in Parkinson’s disease patients”. In: *Neurobiology of Disease* 127 (July 2019), pp. 462–471. DOI: 10.1016/j.nbd.2019.03.013.

[88] Roxanne Lofredi et al. “Pallidal Beta Activity Is Linked to Stimulation-Induced Slowness in Dystonia”. In: *Movement Disorders* 38.5 (Feb. 2023), pp. 894–899. DOI: 10.1002/mds.29347.

[89] Peter Brown et al. "Dopamine Dependency of Oscillations between Subthalamic Nucleus and Pallidum in Parkinson's Disease". In: *The Journal of Neuroscience* 21.3 (Feb. 2001), pp. 1033–1038. DOI: 10.1523/jneurosci.21-03-01033.2001.

[90] A. A. Kuhn et al. "High-Frequency Stimulation of the Subthalamic Nucleus Suppresses Oscillatory Activity in Patients with Parkinson's Disease in Parallel with Improvement in Motor Performance". In: *Journal of Neuroscience* 28.24 (June 2008), pp. 6165–6173. DOI: 10.1523/jneurosci.0282-08.2008.

[91] A. Eusebio et al. "Deep brain stimulation can suppress pathological synchronisation in parkinsonian patients". In: *Journal of Neurology, Neurosurgery & amp; Psychiatry* 82.5 (Oct. 2010), pp. 569–573. DOI: 10.1136/jnnp.2010.217489.

[92] Christoph S. Herrmann et al. "Transcranial alternating current stimulation: a review of the underlying mechanisms and modulation of cognitive processes". In: *Frontiers in Human Neuroscience* 7 (2013). DOI: 10.3389/fnhum.2013.00279.

[93] Yuchen He et al. "Neurophysiological mechanisms of transcranial alternating current stimulation". In: *Frontiers in Neuroscience* 17 (Apr. 2023). DOI: 10.3389/fnins.2023.1091925.

[94] Randolph F. Helfrich et al. "Entrainment of Brain Oscillations by Transcranial Alternating Current Stimulation". In: *Current Biology* 24.3 (Feb. 2014), pp. 333–339. DOI: 10.1016/j.cub.2013.12.041.

[95] M. M. Ali, K. K. Sellers, and F. Frohlich. "Transcranial Alternating Current Stimulation Modulates Large-Scale Cortical Network Activity by Network Resonance". In: *Journal of Neuroscience* 33.27 (July 2013), pp. 11262–11275. DOI: 10.1523/jneurosci.5867-12.2013.

[96] A.J. Woods et al. "A technical guide to tDCS, and related non-invasive brain stimulation tools". In: *Clinical Neurophysiology* 127.2 (Feb. 2016), pp. 1031–1048. DOI: 10.1016/j.clinph.2015.11.012.

[97] Marom Bikson et al. “Safety of Transcranial Direct Current Stimulation: Evidence Based Update 2016”. In: *Brain Stimulation* 9.5 (Sept. 2016), pp. 641–661. DOI: 10.1016/j.brs.2016.06.004.

[98] A. Antal et al. “Low intensity transcranial electric stimulation: Safety, ethical, legal regulatory and application guidelines”. In: *Clinical Neurophysiology* 128.9 (Sept. 2017), pp. 1774–1809. DOI: 10.1016/j.clinph.2017.06.001.

[99] Sanne ten Oever et al. “Stimulus Presentation at Specific Neuronal Oscillatory Phases Experimentally Controlled with tACS: Implementation and Applications”. In: *Frontiers in Cellular Neuroscience* 10 (Oct. 2016). DOI: 10.3389/fncel.2016.00240.

[100] Rafael Polanía, Walter Paulus, and Michael A. Nitsche. “Modulating cortico-striatal and thalamo-cortical functional connectivity with transcranial direct current stimulation”. In: *Human Brain Mapping* 33.10 (Sept. 2011), pp. 2499–2508. DOI: 10.1002/hbm.21380.

[101] Eugen Kvašňák et al. “10 Minutes Frontal 40 Hz tACS—Effects on Working Memory Tested by Luck-Vogel Task”. In: *Behavioral Sciences* 13.1 (Dec. 2022), p. 39. DOI: 10.3390/bs13010039.

[102] Jonas Rauh et al. “Comparison of transcranial brain stimulation approaches: prefrontal theta alternating current stimulation enhances working memory performance”. In: *Frontiers in Psychiatry* 14 (June 2023). DOI: 10.3389/fpsyt.2023.1140361.

[103] Katharina Klink et al. “The Modulation of Cognitive Performance with Transcranial Alternating Current Stimulation: A Systematic Review of Frequency-Specific Effects”. In: *Brain Sciences* 10.12 (Dec. 2020), p. 932. DOI: 10.3390/brainsci10120932.

[104] Inge Leunissen et al. “Effects of beta-band and gamma-band rhythmic stimulation on motor inhibition”. In: *iScience* 25.5 (May 2022), p. 104338. DOI: 10.1016/j.isci.2022.104338.

[105] Jane Tan et al. “Dual-Site Beta ¡scp¿tACS¡/scp¿ Over the ¡scp¿rIFG¡/scp¿ and ¡scp¿preSMA¡/scp¿-Induced Phase-Specific Changes in Functional Connectivity but not Response Inhibition Performance in Older Adults”. In: *Psychophysiology* 62.5 (May 2025). DOI: 10.1111/psyp.70060.

[106] Matteo Feurra et al. “Frequency-Dependent Tuning of the Human Motor System Induced by Transcranial Oscillatory Potentials”. In: *The Journal of Neuroscience* 31.34 (Aug. 2011), pp. 12165–12170. DOI: 10.1523/jneurosci.0978-11.2011.

[107] Ekaterina Lyzhko et al. “Offline 20 Hz transcranial alternating current stimulation over the right inferior frontal gyrus increases theta activity during a motor response inhibition task”. In: *Neurophysiologie Clinique* 53.3 (June 2023), p. 102887. DOI: 10.1016/j.neucli.2023.102887.

[108] Marius Moisa et al. “Brain Network Mechanisms Underlying Motor Enhancement by Transcranial Entrainment of Gamma Oscillations”. In: *The Journal of Neuroscience* 36.47 (Nov. 2016), pp. 12053–12065. DOI: 10.1523/jneurosci.2044-16.2016.

[109] Viola Rjosk et al. “Transcranial Alternating Current Stimulation at Beta Frequency: Lack of Immediate Effects on Excitation and Interhemispheric Inhibition of the Human Motor Cortex”. In: *Frontiers in Human Neuroscience* 10 (Nov. 2016). DOI: 10.3389/fnhum.2016.00560.

[110] C. Wach et al. “Effects of 10Hz and 20Hz transcranial alternating current stimulation (tACS) on motor functions and motor cortical excitability”. In: *Behavioural Brain Research* 241 (Mar. 2013), pp. 1–6. DOI: 10.1016/j.bbr.2012.11.038.

[111] Danielle L. Kurtin et al. “Moving from phenomenological to predictive modelling: Progress and pitfalls of modelling brain stimulation in-silico”. In: *NeuroImage* 272 (May 2023), p. 120042. DOI: 10.1016/j.neuroimage.2023.120042.

[112] Kym Wansbrough et al. “Recent advancements in optimising transcranial electrical stimulation: reducing response variability through individualised stimulation”. In: *Current Opinion in Behavioral Sciences* 56 (Apr. 2024), p. 101360. DOI: 10.1016/j.cobeha.2024.101360.

[113] Vincent Rochas et al. “MRI-individualized, multi-electrode tACS enhances the induced electrical field strength in the targeted area of mild cognitive impairment patients”. In: *Clinical Neurophysiology* 177 (Sept. 2025), p. 2110930. DOI: 10.1016/j.clinph.2025.2110930.

[114] Matteo Feurra et al. “State-Dependent Effects of Transcranial Oscillatory Currents on the Motor System during Action Observation”. In: *Scientific Reports* 9.1 (Sept. 2019). DOI: 10.1038/s41598-019-49166-1.

[115] Jinwen Wei et al. “State-Dependent tACS Effects Reveal the Potential Causal Role of Prestimulus Alpha Traveling Waves in Visual Contrast Detection”. In: *The Journal of Neuroscience* 44.27 (May 2024), e2023232024. DOI: 10.1523/jneurosci.2023-23.2024.

[116] Desmond Agboada, Zhihe Zhao, and Miles Wischnewski. “Neuroplastic effects of transcranial alternating current stimulation (tACS): from mechanisms to clinical trials”. In: *Frontiers in Human Neuroscience* 19 (Mar. 2025). DOI: 10.3389/fnhum.2025.1548478.

[117] Matthew R. Krause et al. “Transcranial alternating current stimulation entrains single-neuron activity in the primate brain”. In: *Proceedings of the National Academy of Sciences* 116.12 (Mar. 2019), pp. 5747–5755. DOI: 10.1073/pnas.1815958116.

[118] Osama Elyamany et al. “Transcranial alternating current stimulation (tACS): from basic mechanisms towards first applications in psychiatry”. In: *European Archives of Psychiatry and Clinical Neuroscience* 271.1 (Nov. 2020), pp. 135–156. DOI: 10.1007/s00406-020-01209-9.

[119] Wei A. Huang et al. "Transcranial alternating current stimulation entrains alpha oscillations by preferential phase synchronization of fast-spiking cortical neurons to stimulation waveform". In: *Nature Communications* 12.1 (May 2021). DOI: 10.1038/s41467-021-23021-2.

[120] Lars Riecke et al. "Neural Entrainment to Speech Modulates Speech Intelligibility". In: *Current Biology* 28.2 (Jan. 2018), 161–169.e5. DOI: 10.1016/j.cub.2017.11.033.

[121] Florian H. Kasten et al. "Integrating electric field modeling and neuroimaging to explain inter-individual variability of tACS effects". In: *Nature Communications* 10.1 (Nov. 2019). DOI: 10.1038/s41467-019-13417-6.

[122] Da-Wei Zhang, Alexandros Moraidis, and Torkel Klingberg. "Individually tuned theta HD-tACS improves spatial performance". In: *Brain Stimulation* 15.6 (Nov. 2022), pp. 1439–1447. DOI: 10.1016/j.brs.2022.10.009.

[123] Flavio Frohlich and Leah Townsend. "Closed-Loop Transcranial Alternating Current Stimulation: Towards Personalized Non-invasive Brain Stimulation for the Treatment of Psychiatric Illnesses". In: *Current Behavioral Neuroscience Reports* 8.2 (Mar. 2021), pp. 51–57. DOI: 10.1007/s40473-021-00227-8.

[124] Luke Johnson et al. "Dose-dependent effects of transcranial alternating current stimulation on spike timing in awake nonhuman primates". In: *Science Advances* 6.36 (Sept. 2020). DOI: 10.1126/sciadv.aaz2747.

[125] Yao Wang et al. "The influence of different current-intensity transcranial alternating current stimulation on the eyes-open and eyes-closed resting-state electroencephalography". In: *Frontiers in Human Neuroscience* 16 (Aug. 2022). DOI: 10.3389/fnhum.2022.934382.

[126] Abhishek Datta et al. “Gyri-precise head model of transcranial direct current stimulation: Improved spatial focality using a ring electrode versus conventional rectangular pad”. In: *Brain Stimulation* 2.4 (Oct. 2009), 201–207.e1. DOI: 10.1016/j.brs.2009.03.005.

[127] Alexander Opitz et al. “Determinants of the electric field during transcranial direct current stimulation”. In: *NeuroImage* 109 (Apr. 2015), pp. 140–150. DOI: 10.1016/j.neuroimage.2015.01.033.

[128] Toralf Neuling, Stefan Rach, and Christoph S. Herrmann. “Orchestrating neuronal networks: sustained after-effects of transcranial alternating current stimulation depend upon brain states”. In: *Frontiers in Human Neuroscience* 7 (2013). DOI: 10.3389/fnhum.2013.00161.

[129] Alexandra Vossen, Joachim Gross, and Gregor Thut. “Alpha Power Increase After Transcranial Alternating Current Stimulation at Alpha Frequency (alpha-tACS) Reflects Plastic Changes Rather Than Entrainment”. In: *Brain Stimulation* 8.3 (May 2015), pp. 499–508. DOI: 10.1016/j.brs.2014.12.004.

[130] Miles Wischnewski, Dennis J. L. G. Schutter, and Michael A. Nitsche. “Effects of beta-tACS on corticospinal excitability: A meta-analysis”. In: *Brain Stimulation* 12.6 (2019), pp. 1381–1389. DOI: 10.1016/j.brs.2019.07.023.

[131] Aaron P. Jones et al. “Closed-Loop tACS Delivered during Slow-Wave Sleep Reduces Retroactive Interference on a Paired-Associates Learning Task”. In: *Brain Sciences* 13.3 (Mar. 2023), p. 468. DOI: 10.3390/brainsci13030468.

[132] Tobias Schwippel et al. “Closed-Loop Transcranial Alternating Current Stimulation for the Treatment of Major Depressive Disorder: An Open-Label Pilot Study”. In: *American Journal of Psychiatry* 181.9 (Sept. 2024), pp. 842–845. DOI: 10.1176/appi.ajp.20230838.

[133] Natalie Schaworonkow et al. "EEG-triggered TMS reveals stronger brain state-dependent modulation of motor evoked potentials at weaker stimulation intensities". In: *Brain Stimulation* 12.1 (Jan. 2019), pp. 110–118. DOI: 10.1016/j.brs.2018.09.009.

[134] Anke Karabanov, Axel Thielscher, and Hartwig Roman Siebner. "Transcranial brain stimulation: closing the loop between brain and stimulation". In: *Current Opinion in Neurology* 29.4 (Aug. 2016), pp. 397–404. DOI: 10.1097/wco.0000000000000342.

[135] Jeongwook Kwon and Byoung-Kyong Min. "Deep learning-based electroencephalic decoding of the phase-lagged transcranial alternating current stimulation". In: *Frontiers in Human Neuroscience* 19 (June 2025). DOI: 10.3389/fnhum.2025.1545726.

[136] John-Stuart Brittain et al. "Tremor Suppression by Rhythmic Transcranial Current Stimulation". In: *Current Biology* 23.5 (Mar. 2013), pp. 436–440. DOI: 10.1016/j.cub.2013.01.068.

[137] Sebastian R. Schreglmann et al. "Non-invasive suppression of essential tremor via phase-locked disruption of its temporal coherence". In: *Nature Communications* 12.1 (Jan. 2021). DOI: 10.1038/s41467-020-20581-7.

[138] Freek Nieuwhof et al. "Phase-locked transcranial electrical brain stimulation for tremor suppression in dystonic tremor syndromes". In: *Clinical Neurophysiology* 140 (Aug. 2022), pp. 239–250. DOI: 10.1016/j.clinph.2022.03.020.

[139] Xueli Chen et al. "Alpha oscillatory activity is causally linked to working memory retention". In: *PLOS Biology* 21.2 (Feb. 2023). Ed. by Simon Hanslmayr, e3001999. DOI: 10.1371/journal.pbio.3001999.

[140] David Haslacher et al. "Working memory enhancement using real-time phase-tuned transcranial alternating current stimulation". In: *Brain Stimulation* 17.4 (July 2024), pp. 850–859. DOI: 10.1016/j.brs.2024.07.007.

[141] Georgy Zarubin et al. “Transient Amplitude Modulation of Alpha-Band Oscillations by Short-Time Intermittent Closed-Loop tACS”. In: *Frontiers in Human Neuroscience* 14 (Sept. 2020). DOI: 10.3389/fnhum.2020.00366.

[142] Farrokh Mansouri et al. “A Fast EEG Forecasting Algorithm for Phase-Locked Transcranial Electrical Stimulation of the Human Brain”. In: *Frontiers in Neuroscience* 11 (July 2017). DOI: 10.3389/fnins.2017.00401.

[143] Kristoffer Hougaard Madsen et al. “No trace of phase: Corticomotor excitability is not tuned by phase of pericentral mu-rhythm”. In: *Brain Stimulation* 12.5 (Sept. 2019), pp. 1261–1270. DOI: 10.1016/j.brs.2019.05.005.

[144] L. L. Chen et al. “Real-Time Brain Oscillation Detection and Phase-Locked Stimulation Using Autoregressive Spectral Estimation and Time-Series Forward Prediction”. In: *IEEE Transactions on Biomedical Engineering* 60.3 (Mar. 2013), pp. 753–762. DOI: 10.1109/tbme.2011.2109715.

[145] Christoph Zrenner et al. “Real-time EEG-defined excitability states determine efficacy of TMS-induced plasticity in human motor cortex”. In: *Brain Stimulation* 11.2 (Mar. 2018), pp. 374–389. DOI: 10.1016/j.brs.2017.11.016.

[146] Aqsa Shakeel, Toshihisa Tanaka, and Keiichi Kitajo. “Time-Series Prediction of the Oscillatory Phase of EEG Signals Using the Least Mean Square Algorithm-Based AR Model”. In: *Applied Sciences* 10.10 (May 2020), p. 3616. DOI: 10.3390/app10103616.

[147] Aqsa Shakeel et al. “Real-Time Implementation of EEG Oscillatory Phase-Informed Visual Stimulation Using a Least Mean Square-Based AR Model”. In: *Journal of Personalized Medicine* 11.1 (Jan. 2021), p. 38. DOI: 10.3390/jpm11010038.

[148] Sina Shirinpour et al. “Experimental evaluation of methods for real-time EEG phase-specific transcranial magnetic stimulation”. In: *Journal of Neural Engineering* 17.4 (July 2020), p. 046002. DOI: 10.1088/1741-2552/ab9dba.

[149] Michael Rosenblum et al. “Real-time estimation of phase and amplitude with application to neural data”. In: *Scientific Reports* 11.1 (Sept. 2021). DOI: 10.1038/s41598-021-97560-5.

[150] J R McIntosh and P Sajda. “Estimation of phase in EEG rhythms for real-time applications”. In: *Journal of Neural Engineering* 17.3 (May 2020), p. 034002. DOI: 10.1088/1741-2552/ab8683.

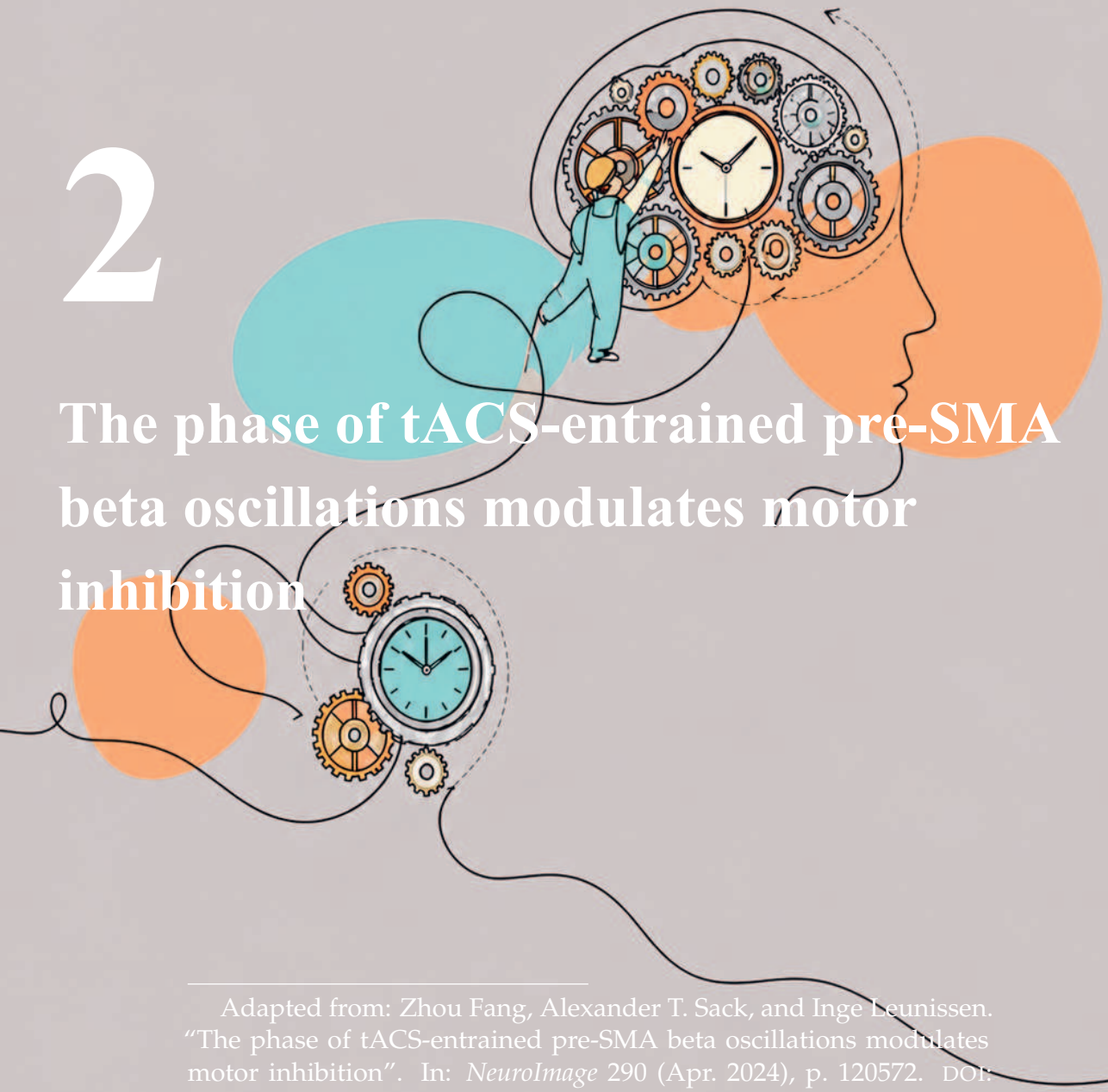
[151] Hao Liu et al. “A Novel Real-time Phase Prediction Network in EEG Rhythm”. In: *Neuroscience Bulletin* 41.3 (Nov. 2024), pp. 391–405. DOI: 10.1007/s12264-024-01321-z.

[152] Hanna Pankka et al. “Enhanced EEG Forecasting: A Probabilistic Deep Learning Approach”. In: *Neural Computation* 37.4 (Mar. 2025), pp. 793–814. DOI: 10.1162/neco_a_01743.

[153] Cristian Rodriguez Rivero and Jochen Ditterich. “A user-friendly algorithm for adaptive closed-loop phase-locked stimulation”. In: *Journal of Neuroscience Methods* 347 (Jan. 2021), p. 108965. DOI: 10.1016/j.jneumeth.2020.108965.

2

The phase of tACS-entrained pre-SMA beta oscillations modulates motor inhibition



Adapted from: Zhou Fang, Alexander T. Sack, and Inge Leunissen. "The phase of tACS-entrained pre-SMA beta oscillations modulates motor inhibition". In: *NeuroImage* 290 (Apr. 2024), p. 120572. DOI: 10.1016/j.neuroimage.2024.120572.

Abstract

Inhibitory control has been linked to beta oscillations in the fronto-basal ganglia network. Here we aim to investigate the functional role of the phase of this oscillatory beta rhythm for successful motor inhibition. We applied 20 Hz transcranial alternating current stimulation (tACS) to the pre-supplementary motor area (pre-SMA) while presenting stop signals at 4 (Experiment 1) and 8 (Experiment 2) equidistant phases of the tACS entrained beta oscillations. Participants showed better inhibitory performance when stop signals were presented at the trough of the beta oscillation whereas their inhibitory control performance decreased with stop signals being presented at the oscillatory beta peak. These results are consistent with the communication through coherence theory, in which postsynaptic effects are thought to be greater when an input arrives at an optimal phase within the oscillatory cycle of the target neuronal population. The current study provides mechanistic insights into the neural communication principles underlying successful motor inhibition and may have implications for phase-specific interventions aimed at treating inhibitory control disorders such as PD or OCD.

2.1 Introduction

Motor inhibition is a crucial cognitive function that allows us to rapidly adapt to our ever-changing environment by cancelling or suppressing planned movements. Previous studies have found that this essential inhibitory control is associated with the activation of a fronto-basal ganglia network, including the pre-supplementary motor area (preSMA), the right inferior frontal cortex (rIFC), and the subthalamic nucleus (STN) [1]. These key nodes of the fronto-basal ganglia inhibition network are presumed to interact with each other via the so-called "hyperdirect pathway" [2, 3, 1].

There is concrete evidence suggesting that this inter-regional information exchange is directly related to beta-band oscillatory mechanisms within the fronto-basal ganglia circuit. Intracranial recordings from these regions revealed increased oscillatory activity in the beta frequency band during successful inhibition [4, 5, 6, 7, 8, 9, 10, 11], and this increase in beta activity relates to inhibitory performance [12, 13, 14]. Moreover, the hyperdirect pathway is overactive in Parkinson's disease (PD) [1], resulting in excessive beta oscillations in the STN and cortical motor areas [15], which are associated with bradykinesia, rigidity, and freezing symptoms [16, 17, 18, 19]. Finally, entraining beta oscillations by means of transcranial alternating current stimulation (tACS) promotes inhibition of unintended movements [20], [13, 21], suggesting that the power ('amplitude') of beta oscillations is causally related to successful motor inhibition. However, although the functional implications of beta oscillations for motor inhibition have been demonstrated in previous research, not much is known yet about the exact temporal dynamics of neural communication within the fronto-basal ganglia circuit.

Long-range neural communication is thought to come about through groups of neurons engaging in rhythmic synchronization, creating short temporal windows of low and high excitability of the respective regions [22]. Effective neural communication between such regions requires a stable phase relation between sending and receiving populations,

known as coherence. The disruption of beta phase coherency between the STN and motor/premotor regions by deep brain stimulation suggests that it is in fact the phase of oscillatory beta that may play a crucial role in successful inhibitory control [23, 24, 25]. In line with this notion, local broadband neuronal activity in the motor cortex seems to be entrained on the phase of the beta rhythm [26] and motor cortex excitability is beta-phase dependent [27, 28, 29, 30, 31].

Conventional methods for investigating oscillatory phase, such as magneto-/electroencephalography, are limited by their post-hoc nature and by providing only correlational evidence. This is particularly problematic when investigating stimuli that require a psychophysical staircase, such as the stop signal delay in a stop signal task which is typically staircased to maintain a 50% stopping accuracy to allow for an estimation of stopping speed [32]. In contrast, tACS can phase align cortical neural activity with the externally applied current [33, 34], transforming the phase of oscillatory brain activity into an experimentally controlled independent variable [35]. In the current experiment we applied beta tACS over the preSMA to experimentally control the phase of oscillatory beta activity while presenting behaviorally relevant stop signals precisely time-locked to 4 (experiment 1) or 8 (experiment 2) pre-determined equidistance phases of the tACS waveform. Stop signal delay staircases were run in parallel for the different phase conditions in order to investigate the causal role of the beta phase for successful motor inhibition. Assuming that the fronto-basal ganglia network makes use of the beta rhythm to convey the need for inhibition between the pre-SMA / frontal regions and the subcortical downstream nodes of the fronto-basal ganglia network, we expected that stop signals presented at specific and distinct beta phases would lead to improved inhibitory control whereas other beta phases may cause decreased motor inhibition performance.

2.2 Methods

To investigate the relationship between the oscillatory phase and inhibitory performance, we conducted two related experiments (Exp 1 and Exp 2), with Exp 2 adding four more conditions on top of Exp 1. The following section describes the experimental procedures of Exp 1 and 2 as well as how they differ.

2.2.1 Participants

Thirty-two healthy, right-handed (the mean laterality quotient score is 96.3, with a range of 70-100 [36]) 18-35 year-old (mean age 25.3; 13 males and 19 females) volunteers were recruited for this study. All 32 participants were involved in Exp 1 and 16 of them took part in both Exp 1 and Exp 2 (mean age 24.3; 8 males and 8 females). Standard screening verified that there were no contraindications to non-invasive brain stimulation [37, 38]. All procedures were approved by the local ethical committee and written informed consent was obtained from all participants.

2.2.2 General experiment procedure

In all experiments, participants received 20 Hz (beta) tACS stimulation during the performance of a stop-signal task. In Exp 1, the stop signals were presented at 4 equidistant phases of one oscillatory cycle of the tACS signal: 90°, 180°, 270°, and 360° (0°). The procedure of Exp 2 was split into two days more than 48 hours apart, with four phase conditions completed each day: day 1: 90°, 180°, 270°, and 360° (0°) and day 2: 45°, 135°, 225°, and 315°. The order of the two sets of conditions was counterbalanced across participants.

At the beginning of each experimental session, a 3-minute resting EEG was recorded while participants kept their eyes open and fixed on a black screen. Subsequently, participants practised the stop signal task by performing 20 go trials, followed by 20 trials in which go and stop

trials were mixed and next performed four experimental blocks, each including 180 trials. Therefore, Exp 1 contained 720 trials per subject, and Exp 2 had a total of 1440 trials. Participants had a 3-5-minute break between each block. After the task, the post-EEG was recorded in the same way as the pre-EEG.

Participants were asked to report their self-perceived level of fatigue before and after the session, and their tACS discomfort level after the experiment on a Visual Analogue Scale (VAS). The VAS consisted of a 10 cm horizontal line with two opposing limits displayed at either end of the line (no discomfort-worst discomfort for the discomfort level and not tired-exhausted for the fatigue level).

2.2.3 Stop-signal paradigm

Participants were asked to sit comfortably, 1 meter away from the screen (refresh rate 240 Hz) and perform an anticipated response stop-signal task [39, 40, 41] as shown in Figure 2.1 A. The stop-signal task was programmed in LabVIEW (National Instruments, Austin, TX). Each trial started with the display of an empty bar in the centre of the screen, with an indicator filling it over the course of 1000 ms at a constant speed from bottom to top. A target line was positioned at 800 ms from the onset. Participants were instructed to pinch a force transducer (OMEGA Engineering, Norwalk, CT, USA) with their right index finger and thumb to stop the indicator when it reached the target line. A force response threshold was initially set at 25% of their maximal voluntary force (MVF), which could be lowered in 5% increments until participants were able to comfortably reach the threshold during the whole session (mean is 23.3%; range is 10% 25%). MVF was determined as the highest force value measured during 3 maximal strength pinches of 5s. Participants were encouraged to stop the indicator at the target line as accurately as possible. The target line changed colour at the end of the trial as feedback on their performance. There were 4 colour options: green, yellow, orange, and red, indicating the distance between the indicator and the target line within 20, 40, 60, and $>$60 ms, respectively.

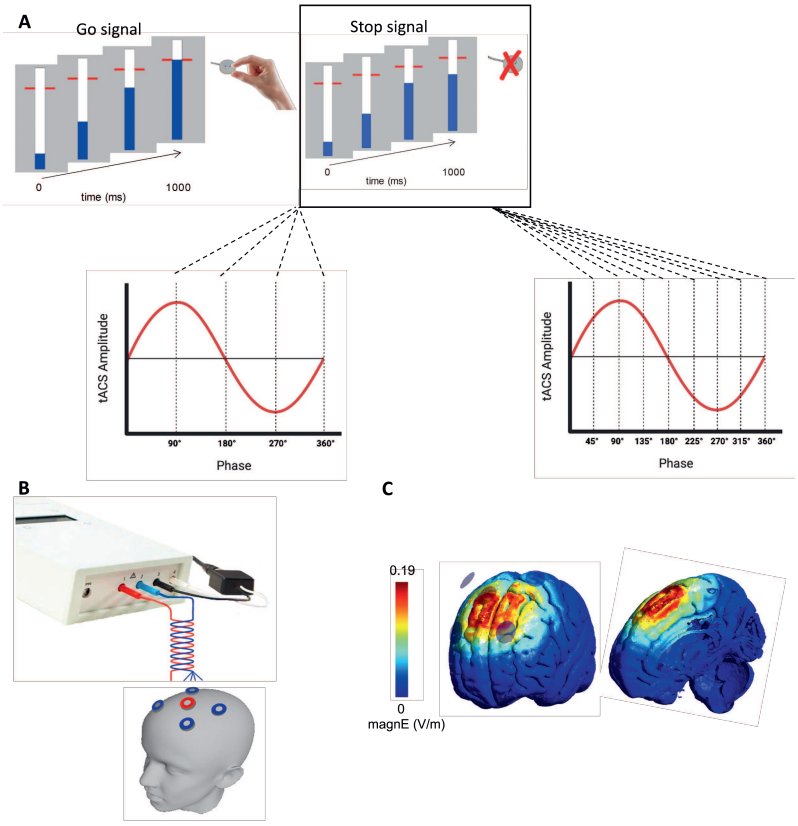


Figure 2.1: **Experimental methods**. (A) Stop-signal paradigm. The blue indicator filled the empty bar at a constant speed. In go trials, it rose from the bottom to the top and participants were asked to stop it at the target line. In stop trials, the indicator stopped increasing before the target line. In this case, participants had to withhold their responses. Stop signals were aligned with the 4 (Exp 1) and 8 (Exp 2) desired phases of the tACS wave. (B) tACS electrode montage. The centre electrode ring is placed over FCz and surrounded by four electrode rings at a centre-to-centre distance of 5 cm. (C) Simulated electrical field distribution generated by the tACS setup in an example brain.

33% of the trials were stop-signal trials, in which the indicator automatically stopped before reaching the target line. In this case, participants had to refrain from pinching the sensor. Throughout stop-signal trials, the indicator was equally likely to stop at 110 ms, 150 ms, 190 ms, 230 ms, and 270 ms before the target line. The timing was slightly shifted (maximally $\pm$25 ms) to match the closest desired phase of the tACS wave. After 1s the indicator was reset to empty. The inter-trial interval jittered between 2.7-3.7 ms. Participants completed four task runs per session, each comprising 120 go and 60 stop trials presented in a pseudorandomized order (720 trials per session in total). Each task run contained stop signals presented at one of the four desired phases at all possible stop-signal delays. For more information on the synchronization between tACS wave and stop-signal presentation see section: tACS phase locked stop-signal presentation.

The force signal was captured through a digital-analog converter (DAC) from National Instruments (Austin, TX, USA) and saved trial-by-trial (from the indicator starting filling up to 1700 ms) using LabChart with a sampling rate of 1000 Hz. Stop trials were classified as failed stop trials if the force produced exceeded the response threshold. If the force remained below the threshold, the trial was classified as successfully inhibited.

2.2.4 tACS procedures

20 Hz tACS was applied using a 4$\times$1 HD-tACS setup (DC STIMULATOR PLUS, NeuroConn, GmbH, Ilmenau, Germany). Custom made gel-filled cup-electrodes made out of plastic cylinders ($\varnothing$2cm at top, 2.5cm at bottom) were mounted in an EEG cap (EASYCAP GmbH, Germany) and filled with electrode gel (OneStep Cleargel) before an EEG Ag/AgCl ring electrode was fastened into the cup. The target electrode was placed over the preSMA (FCz) and four surrounding electrodes were positioned at F1, F2, C1, and C2 based on the international 10-20 coordinate system (Figure 2.1 B). The impedance of the tACS electrodes was kept below 10 kΩ (8.4 $\pm$ 1.6 kΩ) and the peak-to-peak amplitude of

the stimulation was set to 2 mA by default, which was reduced if the participant were too uncomfortable with the stimulation resulting in the mean intensity being 1.97 ± 0.11 mA. The stimulation was ramped up and down for 10 s and lasted 9.6 min in total per block leading to a 38.4 min total stimulation received by the participants per session. The electrical field distribution generated by our tACS setup was simulated by a simNIBs pipeline based on the 2 mA peak-to-peak intensity of the current on a sample brain. All electrodes were modeled as a 2mm thick rubber layer with a conductivity of 0.1 S/m and the conductive gel was set as 1mm thick with a conductivity of 3 S/m. We normalized the electric field distribution mesh and transferred it to nifty. The modelled current flow in individuals suggests that the extent of the electric field yielded by this 4×1 electrode montage is confined to the region of the preSMA (Figure 2.1 C).

2.2.5 tACS phase-locked stop signal presentation

In order to understand how phase modulates inhibition, we aligned the stop signal onset with the 4 (Exp 1) and 8 (Exp 2) desired phases of the entraining tACS oscillation as shown in Figure 2.1 A. The experimental setup of the phase-locked stimulus presentation system was previously accomplished and described in [35]. In the setup, source files created in MATLAB (TheMathWorks Inc., Natick, Massachusetts, USA) containing values oscillating between -1 and +1 are loaded into DataStreamer, a custom PC software (https://osf.io/h6b8v/). DataStreamer scales the predetermined tACS waveform signals to the desired tACS intensity and feeds them through a digital-analog converter (DAC) from National Instruments (Austin, TX, USA). A standard BNC cable connected the DAC to the remote input connection of the tACS stimulator. The resolution of the tACS waveform in the source files was 10000 Hz. In a secondary timeline in the source file, stimulus triggering pulses were coded to indicate the timing (by their position in the timeline with respect to the tACS waveform) and parameters (by their numerical value). The digital values were communicated by DataStreamer via the DAC

to the PC running the stop signal task in Labview which continuously detected incoming triggering pulses. The pulses triggered the start of each trial and the presentation of the stop signals (stopping of indicator before reaching the target line). The pulses for the stop signal were aligned to the desired phase on the tACS waveform closest to the desired stop signal delay. We quantified the delay between the trigger sent out and the timestamps of the actual stop signal occurrence provided by the task software. The mean of the absolute delay in the 95% range (2.5th to 97.5th percentile) was 1.11 ms and within 2.86 ms, which was calculated per participant and per phase condition (Table S2.3 and Table S2.4). Note that these values are additionally constrained to the frame rate of the LCD monitor which was 240 Hz (4.16 ms per frame). When the program received a stop trigger, the actual stop signal would be presented at the next frame (the delay is between 0 and 4.16 ms). The presentation frame rate constrained the number of possible phase bins (20 Hz is 50 ms/cycle, for 8 phase bins, 6.25 ms/bin), but was still acceptable for an 8-phase condition.

2.2.6 EEG procedures

In experiment 2, EEG signals were recorded through actiCHamp Plus amplifier (Brain Products, Germany) from 8 Ag/AgCl electrodes (Fz, FC1, FC2, C3, Cz; A1, A2 as the references; and AFz as the ground). The sampling rate was 1000 Hz and the impedance was kept below 20 kΩ. In addition, an electrooculogram (EOG) was recorded from the electrodes located at the corner of both eyes as well as both above and below the left eye.

2.2.7 Behavioral analysis

MATLAB 2022a (Mathworks, Natick, MA, USA) was used to analyze behavioral data. The force data collected trial-by-trial were converted from Volt to Newton. Next, a fifth-order 20 Hz low pass Butterworth filter was applied to filter the force data. In each trial, the average force

of the data between -650 ms and -400 ms before the target time was subtracted to correct the baseline. After preprocessing the force data, we calculated the following for all stop trials: (1) peak force, the maximum force of the trial; (2) peak force rate, which was the maximum rate of change in the force signal; The force measures above that were larger than 2.5×SD of their mean value were seen as the outliers values and deleted. For both the peak force and the peak force rate, we determine the median per phase condition as the distributions were strongly left skewed.

Reaction time (RT) was computed based on the time that the response threshold was initially reached (typically 25% of MVF). We determined the mean RT on failed stops (RTsf) and RT on go trials (RTgo). The go trials with an RT $<$ 400 ms or RT $>$ 990 ms, identified as early response or no response errors, were removed from the dataset. To be able to calculate the Stop Signal Reaction Time (SSRT), the dataset had to satisfy the assumption of the independent race model (Verbruggen et al., 2019) (i.e., go trials and stop trials needed to behave independently). We compared the mean RTgo against the mean RTsf to see if the former was larger than the latter. The SSRT was then calculated using integration methods [32].

The percent of successful stops (P(inhibition)) for each phase condition was calculated based on all five stop signal delays (SSD).

2.2.8 EEG analysis

The resting EEG data were analyzed using FieldTrip [42], in MATLAB 2022a. We pre-processed data by: (1) re-referencing data of each channel to the average of left and right reference channels (A1, A2); (2) removing linear trend and baseline correcting; (3) filtering with a 1-300 Hz band pass filter and a 50 Hz FIR band stop filter; (4) Regressing out eye movements using the function *scrls_regression* of the Eeglab plugin AAR [43] (filter order 3; forgetting factor 0.999; sigma 0.01; precision 50). Data from both pre and post stimulation periods were segmented into

1 s epochs. The epochs including noisy signals were rejected by visual detection. Then, the EEG data underwent a fast Fourier transformation (FFT) in a 4-45 Hz frequency range and a Hanning window with a 10s zeros-padding. Subsequently, the mean absolute beta power at 13-30 Hz was determined and compared between pre and post stimulation.

For the purpose of investigating the correlation between subjects' individual beta frequency (IBF) and the degree of phase modulation on performance, the averaged pre-resting EEG spectra were log-transformed and fitted by a linear trend in a least-squares manner to remove the $1/f$ property of the spectra [44, 45]. The IBF was then obtained by finding the peak from a 3^{rd} order Gaussian curve fitted to the EEG spectra.

2.2.9 Statistical analysis

All analyses were carried out using MATLAB 2022a and IBM SPSS Statistics 27. In order to validate the hypothesis that inhibition performance is influenced by phase conditions and oscillates along with neuronal oscillations entrained by tACS, we investigated: (a) the presence of tACS-phase effects, and (b) a one-cycle sinus matched the pattern of behavioral outcomes over the sampled phase conditions. Commencing the analysis, a repeated measures ANOVA was performed to assess the difference of stimulation-related discomfort ($\text{VAS}_{discomfort}$) and fatigue ($\text{VAS}_{fatigue}$) between sessions (Exp 2) and time (pre- and post-stimulation) on the subjective level.

For both Exp 1 and Exp 2, we evaluated the impact of the beta tACS phase on inhibition performance by comparing the outcome measures (SSRT, percent of successful inhibition, peak force and peak force rate) on different phase conditions (4 phase conditions in Exp 1 and 8 in Exp 2). The individual outcome measures were averaged per phase. Repeated measures ANOVA was used to analyze SSRT, RTsf, and P(inhibition), while the Friedman test was employed for assessing the significance of differences in non-normally distributed peak force and peak force rate (Shapiro-Wilk test $p < 0.05$). Post-hoc tests were

conducted to identify specific phases that significantly influenced inhibition behavior in terms of SSRT, RTsf, and P(inhibition). Wilcoxon Signed Rank test was used to assess peak force and peak force rate. On both the group level and the individual level, a performance pattern yielded by the outcome measures over tACS oscillatory phase conditions was fitted with a single sinusoidal cycle by the Matlab function 'fminsearch' where parameters of the best-fitting phase and amplitude were determined based on minimization of squared errors [46, 47, 48, 49]. The explained variance (R^2) of the fitted pattern was obtained to evaluate the goodness of fit. The calculation of the R^2 was based on values at the 4 or 8 sample points. Inspired by previous reports we multiplied R^2 by the variance of the best fitting sinusoid to obtain 'relevance values' [46, 47, 48, 49]. As we had so few sample points, we calculated the variance of the best fitting sinusoid not only based on the sinusoid values at the sample points but calculated population variance of 100 equidistant values on one full cycle of the best fitting sinusoid. This variance measure of the full sinusoid was multiplied with R^2, which was calculated as 1-(SSM/SST), where SST was the sum of squared differences between observed data at sample points and their mean, and SSM was the sum of squared differences between observed data at sample points and the sinusoid values at those sample points. The resulting hybrid measure of relevance value should reflect both the goodness of fit (R^2) and the extent of modulation of performance by tACS [49]. The relevance value was then used to perform a permutation test and quantify the related p-values. Conducting permutation test, we built a null distribution with 2,000 relevance values that came from the same processing procedure as above, but with the label (phase)-shuffled data. In this way, the null distribution represented the case where the beta phase had no quantitative effect on relevance values. We compared the obtained relevance value against the null distribution and the reported p-values reflect the proportion of the label-shuffled values that have a test statistic larger than that of the non-shuffled data. The relevance value would be deemed statistically significant if it is located within the last 0.05 of the null distribution.

The method described above assumes that individual results are phase-aligned. For various reasons (e.g., transmission time, cortical anatomy), it is not a priori expected that, even in the case of successful tACS entrainment, individual results should phase-align. Considering that mismatched optimal phases might cancel the values of each other out on the group level, we also performed an analysis in which we aligned phases per individual before averaging. Since the phases of individuals were calibrated by shifting the maximum value (peak) of the sinusoidal pattern to the same position (slot 1 in Exp 1 and slot 2 in Exp 2), the statistical results on slot 1 in Exp 1 and slot 2 in Exp 2 should not be considered for subsequent discussions.

2.3 Results

2.3.1 Experiment 1

All participants (N = 32) of experiment 1 tolerated the stimulation well as indicated by the VAS fatigue and discomfort rating score (Table S2.1). Although there is a significant change between pre-and-post fatigue scores, the overall fatigue and discomfort levels are within the mild range. Three participants were excluded from further analyses. Data for one participant was lost due to a technical issue; another participant had an average stop rate $> 70\%$; and the last participant violated the context independence assumption, resulting in a total of 29 participants.

Behavioral results

A repeated measures ANOVA was used to compare the effect of phase on SSRT, RTsf, and P(inhibition), and a Friedman test was performed on force peak and force peak rate. The results show that all behavioral outcomes differ significantly between phases (Table 2.1). Post-hoc tests revealed a significant difference in both SSRT and P(inhibition) between 90° and 270° - 360°, and 180° and 270° - 360° phase conditions ($p < 0.05$);

Table 2.1: **Group results (Experiment 1).**

Parameter	Phases				Phase effects
	90°	180°	270°	360° (0°)	
P(inhibit) (%)	50.92±6.60	50.40±5.58	56.55±8.18	58.39±6.32	F(3,84)=31.39** $p < .001$
SSRT (ms)	218.33±26.50	222.97±13.16	198.33±20.84	200.41±19.33	F(2.26,63.30)=13.54** $p < .001$
RTsf (ms)	813.25±10.61	810.22±11.02	804.76±9.92	813.97±11.86	F(3,84)=11.36** $p < .001$
Peak force (N)	10.19±5.89	11.46±6.70	7.47±5.41	6.33±5.36	$\chi^2(3)$=28.862** $p < .001$
Peak force rate (N/s)	166.95±105.88	181.84±107.03	131.05±89.74	108.12±84.78	$\chi^2(3)$=22.08** $p < .001$

The phase effects with p-value were calculated from repeated measures ANOVA.

* The within-subjects effects are significant at the 0.05 level

** The within-subjects effects are significant at the 0.01 level

in RTsf between 270° and 90° - 180° - 360°, and 180° and 270° - 360° ($p < 0.05$). Wilcoxon Signed Rank test results show a significant difference in both the peak force and peak force rate of stop trials, between 90° and 270° - 360°, and 180° and 270° - 360° phases ($p < 0.05$) (Table S2.5, S2.6). The post-hoc analysis yielded compelling results indicating that subjects exhibited significantly higher accuracy and faster response times when stop signals were presented at 270° - 360° compared to 90° - 180°. Furthermore, the reaction times on fail stop trials were the shortest at 270°, reflecting that only the fastest go processes could overcome the inhibition at this phase. The Wilcoxon Signed Rank test further revealed that participants exerted less force and lower force rate on stop trials at 270° - 360° compared to 90° - 180°, indicating a significant increase in inhibitory control. In conclusion, the findings highlight a greater degree of inhibition at the trough phase, 270° - 360°.

Figure 2.2 shows the group results from Exp.1 across 4 tACS-phase conditions, superimposed with the best-fitting one-cycle sinusoids. In line with the results of the ANOVA, the curve-fitting results also show a significant phase modulation of behaviour that matches a one-cycle sinusoid. However, the interpretation of these results warrants some caution as a sinusoidal curve fitting with only four data points can lead to inaccurate outcomes. This led to Exp.2 where we increased the phase conditions to 8.

Although similar patterns of phase dependency were observed for all

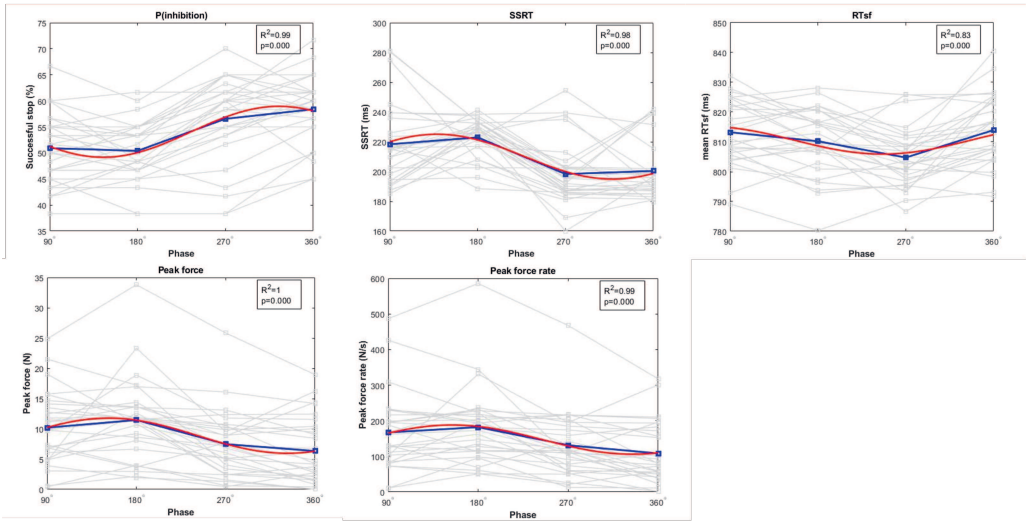


Figure 2.2: **Group behavioral results of Exp.1.** P(inhibition): the percent of successful stops; SSRT: stop signal reaction time; RTsf: reaction time on failed stops; Peak force: the maximum force;Peak force rate: the maximum rate of change in the force signal. The individual behavioral outcomes are shown as grey lines. The group average value is in blue, and the best-fitting sinusoid is in red. In the legend boxes, the R^2, which indicates the goodness of fit, along with the p-value based on the permutation test on the relevance value are provided.

participants, with a sine wave shaped relation, the best inhibitory performance does not necessarily occur at the same beta phase in each participant. In the event that the optimal phase varies between participants, averaging data in each phase condition might conceal an existing phase dependency on the group level. To this end, the peaks of individual subject data were re-aligned to the 90° phase before averaging across participants. Such realignment creates an artificially positive modulation at the optimal phase, therefore the data were tested against shuffled data that underwent the same peak realignment procedure. The results of this phase-aligned analysis can be found in the supplement (Figure S2.1).

2.3.2 Experiment 2

In Exp.2, the VAS fatigue and discomfort scores indicated that all the participants (N = 16) tolerated the stimulation well in both sessions (Table S2.2). Repeated measures ANOVA shows no difference between the two sessions. The participant that had a successful stop percentage $> 70\%$ and the one that was lost due to the technical issue were excluded from further analyses. As a result, 14 participants remained.

Behavioral results over phases

We ran a repeated measures ANOVA to determine if there was a statistically significant difference in SSRT, RTsf and percent of successful stops between each of the eight phases. For the non-normally distributed measures, peak force and peak force rate, we used a Friedman test. The statistic results are shown in Table 2.2. All measures show significant effects from phase conditions. Post hoc results show a significant change in P(inhibition) between 90° and 360°, 180° and 270° - 360°; in SSRT between 135° and 270°; in RTsf between 270° and 90° - 135° (Table S2.7); Wilcoxon Signed Rank test results indicate that in peak force, there is a significant difference between 270° and 90° - 135° - 180° - 360°, 315° and

90° - 135° - 225°, 360° and 90° - 135° - 180° - 270° - 225°; in peak force rate between270° and 180° - 225° - 360°, 315° and 180° - 225°, 360° and 90° - 135° - 180° - 270° (Table S2.8). Aligned with the findings of Exp 1, the post hoc analysis and Wilcoxon Signed Rank test consistently show that 270° - 360° elicits the highest accuracy in successful stops and the shortest reaction times on stop trials. Notably, at 270°, the reaction time on failed stop trials was significantly reduced. Additionally, at 270° - 360°, both force and force rate were significantly lower. These converging findings demonstrate that participants displayed better inhibition when stop signals were at the trough phases of beta oscillations.

Table 2.2: **Group results (Experiment 2).**

Parameter	Phases								Phase effects
	45°	**90°**	**135°**	**180°**	**225°**	**270°**	**315°**	**360°**	
P(inhibition) (%)	53.40±6.60	50.83±7.18	51.25±8.79	50.48±6.49	50.24±13.30	55.60±8.61	53.21±10.30	59.29±7.70	F(3.42,44.46)=4.03** P=0.001
SSRT (ms)	211.46±24.73	219.29±29.84	233.89±28.97	220.89±15.04	225.14±41.95	197.00±20.79	207.61±34.90	200.36±19.56	F(7,91)=3.39** P=0.003
RTsf (ms)	812.47±13.41	814.92±12.14	816.87±11.65	810.92±13.14	810.07±14.91	804.53±10.13	812.76±13.60	814.12±14.15	F(7,91)=2.94** P=0.008
Peak force (N)	9.77±6.23	9.93±5.90	11.12±6.19	11.25±6.35	10.85±7.33	7.87±5.72	8.22±5.15	5.94±5.14	$\chi^2(7)$=26.31** $p < .001$
Peak force rate (N/s)	148.19±76.99	161.11±73.47	163.45±77.43	184.64±79.59	168.44±93.25	139.18±74.82	132.36±69.14	103.62±66.45	$\chi^2(7)$=24.79** p=0.001

Behavioral variances across 8 phase conditions, and the effects of phase modulation effects resulting from the repeated measures ANOVA

*. The within-subjects effects are significant at the 0.05 level

**. The within-subjects effects are significant at the 0.01 level

Then we looked at the causal role of the tACS phase on inhibition. Figure 2.3 depicts the group results of behavioral outcomes over eight phase conditions (blue plot), with best-fitting sinusoids in red. The fitted sinusoids reveal significant effects on P(inhibition) (R^2 = 0.61), SSRT (R^2 = 0.75), RTsf (R^2 = 0.59), peak force (R^2 = 0.42) and peak force rate (R^2 = 0.64), $p < 0.05$, showing that these measures are highly dependent on the phase where inhibition occurs. These results indicate that inhibitory performance over tACS-phases matches a sinusoidal oscillatory pattern, and inhibition is at its greatest when the stimuli are presented at the trough of the tACS oscillation, which is in line with the results of Exp. 1.

EEG results

All results are based on the signal recorded at Fz as it is located over the preSMA and neighbours FCz which is the central tACS electrode.

Pre- and post-resting EEG We conducted a paired t-test to compare the absolute power of the pre- and post- beta (15-30 Hz) band during the resting state, averaged over participants in each session (N = 28) (Figure 2.4 A). The results revealed a significant increase after stimulation (0.051 ± 0.073) compared to before (0.015 ± 0.008), t(27) = 2.573, p = 0.016. The results indicated that the overall rest-state beta power significantly increased after the experiment session.

Individual beta peak frequency When aligning stimuli to the tACS waveform, it is crucial that the tACS entrains the endogenous oscillations for one to be able to observe a phase modulation in behaviour. It is likely that the strength of entrainment varies between individuals. Based on previous studies, demonstrating that 20 Hz is the central beta frequency in the motor system [50, 51, 52], we set the tACS stimulation frequency as 20 Hz over the pre-SMA area to modulate inhibition

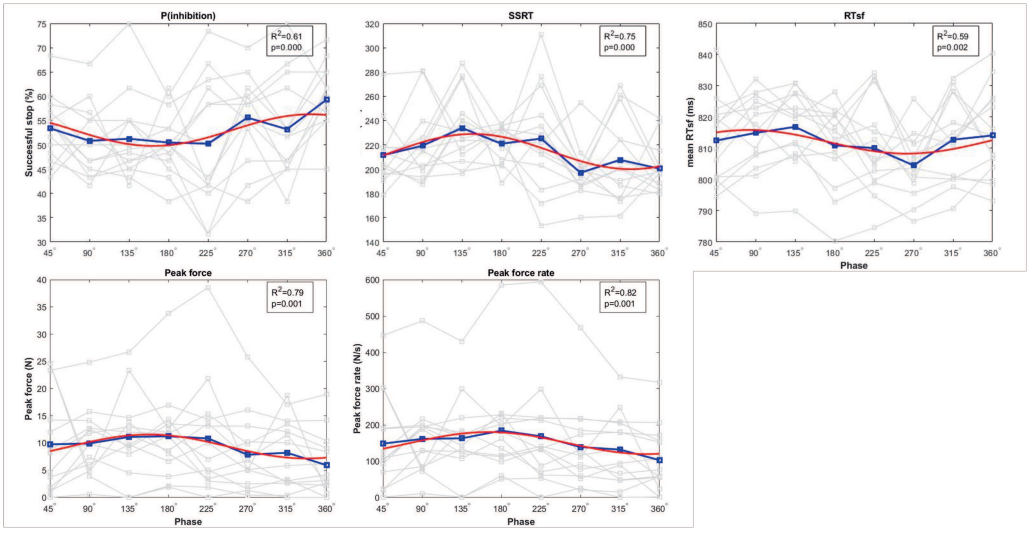


Figure 2.3: **Group behavioral results of Exp.2.** P(inhibition): the percent of successful stops; SSRT: stop signal reaction time; RTsf: reaction time on failed stops; Peak force: the maximum force; Peak force rate: the maximum rate of change in the force signal. The individual behavioral outcomes are shown as grey lines. The group average value is in blue, and the best-fitting sinusoid is in red. In the legend boxes, the R^2, which indicates the goodness of fit, along with the p-value is provided.

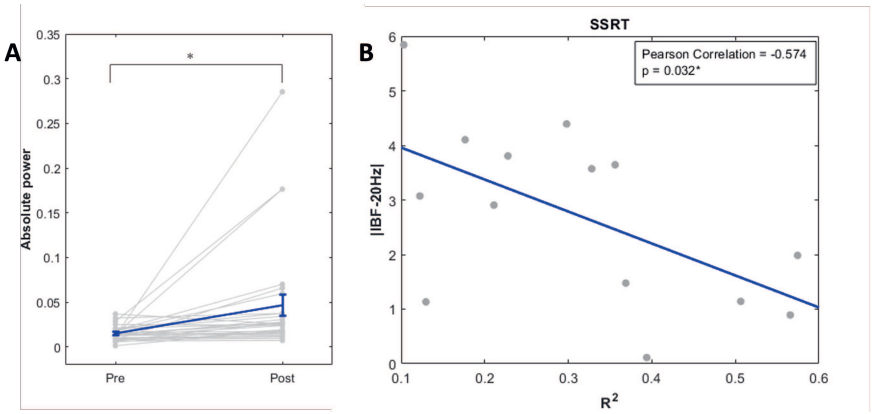


Figure 2.4: **EEG results.** (A) Pre-post beta absolute power with 95% confidence interval error bars. (B) Correlation between R^2 of measures and distance between IBF and 20 Hz.

behaviour. According to the Arnold tongue principle, entrainment happens when the external stimulation frequency is close to the intrinsic oscillation frequency and/or the stimulation intensity is sufficiently high [53]. To investigate whether the phase modulation effects were stronger when the endogenous oscillations were closest to 20Hz, we correlated the individual beta frequency based on the pre-resting state EEG of each participant in Exp 2 with the R^2 of their inhibition performance variables (Figure 2.4 B). The Rsq of SSRT, peak force and peak force rate showed a significant correlation with the distance between IBF and stimulation frequency (20 Hz) (SSRT: r = -0.574, p = 0.032; Peak force: r = -0.696, p = 0.006; Peak force rate: r = -0.561, p = 0.037), indicating that the closer the frequency of the endogenous brain oscillation to the external stimulation, the stronger the phase modulation of behavior.

2.4 Discussion

The aim of the current study was to investigate the functional role of the oscillatory beta phase within the fronto-basal ganglia network for suc-

cessful motor inhibition. We presented inhibition stimuli at various pre-determined and experimentally controlled phases of tACS entrained beta oscillations. This methodology was achieved with the setup developed by ten Oever et al. and previously used in phase-dependent studies by [49] and [48]. Using this setup, we experimentally aligned the stop signal onset with the 4 (Exp 1) and 8 (Exp 2) pre-determined phases of the entraining tACS oscillation. Successful inhibitory control at each of these phases was assessed by participants' performance in the stop signal task, where their stop-signal reaction time (SSRT), successful stop rate (P(inhibition)), the reaction time of stop fail (RTsf), peak force and peak force rate in stop trials were tracked. We found that inhibition performance was systematically affected by the beta phase at which stop signals were presented. Moreover, aligned with our a priori hypotheses, group results showed that inhibition outcomes over these selected phases fit a sinusoidal pattern. Specifically, better inhibitory control was observed at the trough of the beta phase whereas inhibition control for stop stimuli presented at the peak was significantly decreased.

2.4.1 Effect of beta oscillatory phase on inhibitory motor control

Previous studies have consistently shown that successful motor inhibition is associated with increased beta power and beta bursting in both frontal and subcortical nodes of the motor inhibition network [7, 54, 9, 4, 55, 12, 56], suggesting that the fronto-basal ganglia circuit fine-tunes inhibitory motor control by adequately regulating beta oscillatory network activity. More conclusive evidence for a causal link between beta oscillatory activity and motor inhibition stems from transcranial electric stimulation studies demonstrating that increasing the amplitude of beta oscillations in the motor system results in stronger motor inhibition [20, 13, 21].

However, to fully understand the dynamics within this circuit during motor inhibition we must consider the role of oscillatory beta phase. Phase coherence between brain areas is believed to facilitate effective

communication by creating windows in which information can be transmitted most efficiently [22, 57]. Delivering stimuli during an optimal phase should therefore enhance behavioral performance. Such a relationship between the phase-coupled presentation of stimuli and performance has been shown in other cognitive domains such as sensory perception [58, 59], attention [60] and memory [61]. With respect to motor inhibition, stronger coherence in the beta band has been associated with faster inhibitory control [7, 14]. However, until now, it was unclear whether inhibitory control performance functionally depends on the phase at which the stop signal is presented.

Our study provides causal evidence for a modulatory role of the beta oscillatory phase on motor inhibition that follows a one-cycle sinusoidal pattern. Specifically, we discovered that inhibitory control performance was improved for stop signals presented at the trough phase of the experimentally controlled oscillatory beta wave, while inhibition performance was decreased at the peak of the beta phase. This relationship was systematic within participants and surprisingly consistent across participants. This consistent relation between experimentally controlled beta-phase and inhibitory control performance supports the notion that input arriving at the excitatory phase of the local neuronal ensemble increases the efficiency of information transfer when task-induced coherence connects the cortical neural population (preSMA) to the functional brain network [62, 63]. The degree of consistency in this systematic phase-dependency indicates that the optimal phase relation is stabilized and brought about by the enduring anatomical structure of the network pathway [64].

The beta-phase-dependent inhibitory control in this study corroborates the findings that motor cortex excitability varies with the beta oscillatory phase. [26] demonstrated that the beta rhythm acts as a suppressive mechanism to actively gate local motor cortex activity, with the highest activity on the falling flank of the beta cycle. This also aligns with the finding of [65] that motor commands are released between 120°-140° along the beta cycle, and that TMS stimulation on the falling flank of the beta wave results in the highest motor evoked potentials (MEP),

whereas stimulation on the trough or rising flank results in smaller MEPs ([30, 31], but note that different phases have been reported as well: [48, 27, 29]). Interestingly, [66] found that action potentials in the STN are typically phase locked to the 270° phase of frontal beta oscillations. In addition, GABAa-dependent intracortical inhibition in M1 is largest at the 270° phase [67]. Together, these findings suggest that (dis)inhibitory signals can be transmitted from the frontal cortex to M1 via the basal ganglia - thalamo circuits at beta frequency with an optimal window for motor inhibition and initiation at opposing phases of this oscillatory beta cycle.

Our results highlight the role of the beta phase in neuronal hypo- or hyper-synchronization where (de)synchronization within brain networks helps to weaken or facilitate communication in a phase-specific manner. Interfering with a specific phase could therefore disrupt dysfunctional communication resulting from abnormal synchronization in neurological and psychiatric disorders. Excessive synchronization of beta oscillations attributed to dopamine deficiency in PD has for example been observed across cortical areas and the BG [68, 69, 70, 71], and disrupting beta synchronization in cortical [72] and BG nodes, including striatum [73, 74], pallidum [75], subthalamic nucleus [76, 77] and thalamus [78], results in improvements of bradykinesia, rigidity, and freezing. Precisely timing transcranial magnetic stimulation (TMS) to the opposing phase of the optimal window of ongoing beta oscillations in cortical regions may likewise present an effective non-invasive intervention for personalized modulation [79, 80], similar as has been demonstrated for phase-specific STN stimulation [24].

2.4.2 Phase modulation in relation to tACS entrainment

By employing tACS and pre-programming the presentation of the stop signals at specific phases of the tACS wave, we were able to conduct psychophysical staircases over each of the experimentally controlled phase conditions. However, one crucial factor in studying phase modulation with tACS is the entrainment of cortical areas to external stimula-

tion. The pre-post EEG comparison shows a significant increase in beta power suggesting a potential aftereffect of the stimulation, which could indicate successful entrainment. However, due to the absence of a sham condition, we cannot rule out the possibility that the observed increase in beta power might be attributed to task performance, rather than solely tACS entrainment. The Arnold tongue principle illustrates that external stimulation with a frequency close to the underlying internal frequency in the cortical area leads to the highest entrainment [53] (i.e., highest phase-locking between endogenous and exogenous oscillations with a consistent phase difference [81, 82]), and this entrainment is dose-dependent [83]. In our study, we revealed a significant correlation between the distance of the individual peak frequency from the 20 Hz stimulation frequency and the degree of phase modulation of inhibitory control performance ($r = 0.574$, $p = 0.032$), indicating that better entrainment with tACS led to a more sinusoidal pattern of inhibitory control performance. This phenomenon is likely attributed to the strong alignment between endogenous beta oscillations and the tACS waveform. Consequently, stop signals, synchronized with the phase of the tACS waveform, reached the desired phase of the intrinsic brainwave with greater precision.

2.5 Conclusion

The current study provides evidence for a functional modulatory role of the oscillatory beta phase within the fronto-basal-ganglia network for inhibitory motor control performance. We revealed that the trough of experimentally controlled beta oscillations in the preSMA provides an optimal window for exerting inhibition control over presented stop signals. In addition, participants with an individual beta peak frequency close to the 20Hz tACS stimulation frequency showed the strongest phase-dependent modulation of inhibitory motor control performance, further suppo

References

[1] Marjan Jahanshahi et al. "A fronto-striato-subthalamic-pallidal network for goal-directed and habitual inhibition". In: *NATURE REVIEWS NEUROSCIENCE* 16.12 (2015), pp. 719–732. DOI: https://doi.org/10.1038/nrn4038.

[2] Adam R. Aron et al. "Triangulating a Cognitive Control Network Using Diffusion-Weighted Magnetic Resonance Imaging (MRI) and Functional MRI". In: *The Journal of Neuroscience* 27.14 (Apr. 2007), pp. 3743–3752. DOI: 10.1523/jneurosci.0519-07.2007.

[3] Adam R. Aron, Trevor W. Robbins, and Russell A. Poldrack. "Inhibition and the right inferior frontal cortex: one decade on". In: *Trends in Cognitive Sciences* 18.4 (2014), pp. 177–185. DOI: https://doi.org/10.1016/j.tics.2013.12.003.

[4] Manuel Alegre et al. "The subthalamic nucleus is involved in successful inhibition in the stop-signal task: A local field potential study in Parkinson's disease". In: *Experimental Neurology* 239 (Jan. 2013), pp. 1–12. DOI: 10.1016/j.expneurol.2012.08.027.

[5] Andrea A. Kühn et al. "The relationship between local field potential and neuronal discharge in the subthalamic nucleus of patients with Parkinson's disease". In: *Experimental Neurology* 194.1 (2005), pp. 212–220. DOI: https://doi.org/10.1016/j.expneurol.2005.02.010.

[6] Nicole Swann et al. "Intracranial EEG Reveals a Time- and Frequency-Specific Role for the Right Inferior Frontal Gyrus and Primary Motor Cortex in Stopping Initiated Responses". In: *The Journal of Neuroscience* 29.40 (Oct. 2009), pp. 12675–12685. DOI: 10.1523/jneurosci.3359-09.2009.

[7] Nicole C. Swann et al. "Roles for the pre-supplementary motor area and the right inferior frontal gyrus in stopping action: Electrophysiological responses and functional and structural

connectivity". In: *NeuroImage* 59.3 (Feb. 2012), pp. 2860–2870. DOI: 10.1016/j.neuroimage.2011.09.049.

[8] Johanna Wagner et al. "Establishing a Right Frontal Beta Signature for Stopping Action in Scalp EEG: Implications for Testing Inhibitory Control in Other Task Contexts". In: *Journal of Cognitive Neuroscience* 30.1 (Jan. 2018), pp. 107–118. DOI: 10.1162/jocn_a_01183.

[9] Jan R. Wessel and Adam R. Aron. "Unexpected Events Induce Motor Slowing via a Brain Mechanism for Action-Stopping with Global Suppressive Effects". In: *The Journal of Neuroscience* 33.47 (Nov. 2013), pp. 18481–18491. DOI: 10.1523/jneurosci.3456-13.2013.

[10] Jan R Wessel et al. "Surprise disrupts cognition via a fronto-basal ganglia suppressive mechanism". In: *Nature communications* 7.1 (2016), p. 11195. DOI: https://doi.org/10.1038/ncomms11195.

[11] Anna Castiglione et al. "Preventing a Thought from Coming to Mind Elicits Increased Right Frontal Beta Just as Stopping Action Does". In: *Cerebral Cortex* 29.5 (Feb. 2019), pp. 2160–2172. DOI: https://doi.org/10.1093/cercor/bhz017.

[12] Michael Schaum et al. "Right inferior frontal gyrus implements motor inhibitory control via beta-band oscillations in humans". In: *eLife* 10 (Mar. 2021). DOI: 10.7554/elife.61679.

[13] Inge Leunissen et al. "Effects of beta-band and gamma-band rhythmic stimulation on motor inhibition". In: *iScience* 25.5 (May 2022), p. 104338. DOI: 10.1016/j.isci.2022.104338.

[14] Qian Ding et al. "Individual differences in beta-band oscillations predict motor-inhibitory control". In: *Frontiers in Neuroscience* 17 (2023). DOI: https://doi.org/10.3389/fnins.2023.1131862.

[15] P Brown. “Abnormal oscillatory synchronisation in the motor system leads to impaired movement”. In: *Current Opinion in Neurobiology* 17.6 (Dec. 2007), pp. 656–664. DOI: 10.1016/j.conb.2007.12.001.

[16] Andrea A. Kühn et al. “High-Frequency Stimulation of the Subthalamic Nucleus Suppresses Oscillatory β Activity in Patients with Parkinson’s Disease in Parallel with Improvement in Motor Performance”. In: *Journal of Neuroscience* 28.24 (2008), pp. 6165–6173. DOI: https://doi.org/10.1523/JNEUROSCI.0282-08.2008.

[17] S. Little et al. “Beta band stability over time correlates with Parkinsonian rigidity and bradykinesia”. In: *Experimental Neurology* 236.2 (Aug. 2012), pp. 383–388. DOI: 10.1016/j.expneurol.2012.04.024.

[18] Chiung Chu Chen et al. “Complexity of subthalamic 13-35Hz oscillatory activity directly correlates with clinical impairment in patients with Parkinson’s disease”. In: *Experimental Neurology* 224.1 (July 2010), pp. 234–240. DOI: 10.1016/j.expneurol.2010.03.015.

[19] Jon B. Toledo et al. “High beta activity in the subthalamic nucleus and freezing of gait in Parkinson’s disease”. In: *Neurobiology of Disease* 64 (Apr. 2014), pp. 60–65. DOI: 10.1016/j.nbd.2013.12.005.

[20] Raed A. Joundi et al. “Driving Oscillatory Activity in the Human Cortex Enhances Motor Performance”. In: *Current Biology* 22.5 (Mar. 2012), pp. 403–407. DOI: 10.1016/j.cub.2012.01.024.

[21] Jane Tan et al. “The Effects of Dual-Site Beta tACS over the rIFG and preSMA on Response Inhibition in Young and Older Adults”. In: (Dec. 2022). DOI: 10.1101/2022.11.30.518460.

[22] Pascal Fries. "A mechanism for cognitive dynamics: neuronal communication through neuronal coherence". In: *Trends in Cognitive Sciences* 9.10 (2005), pp. 474–480. DOI: https://doi.org/10.1016/j.tics.2005.08.011.

[23] Ashwini Oswal et al. "Deep brain stimulation modulates synchrony within spatially and spectrally distinct resting state networks in Parkinson's disease". In: *Brain* 139.5 (Mar. 2016), pp. 1482–1496. DOI: https://doi.org/10.1093/brain/aww048.

[24] Abbey B. Holt et al. "Phase-Dependent Suppression of Beta Oscillations in Parkinson's Disease Patients". In: *Journal of Neuroscience* 39.6 (2019), pp. 1119–1134. DOI: https://doi.org/10.1523/JNEUROSCI.1913-18.2018.

[25] Yousef Salimpour et al. "Phase- targeted stimulation modulates phase-amplitude coupling in the motor cortex of the human brain". In: *Brain Stimulation* 15.1 (2022), pp. 152–163. DOI: https://doi.org/10.1016/j.brs.2021.11.019.

[26] Kai J. Miller et al. "Human Motor Cortical Activity Is Selectively Phase-Entrained on Underlying Rhythms". In: *PLoS Computational Biology* 8.9 (Sept. 2012). Ed. by Tim Behrens, e1002655. DOI: 10.1371/journal.pcbi.1002655.

[27] Gijs van Elswijk et al. "Corticospinal Beta-Band Synchronization Entails Rhythmic Gain Modulation". In: *The Journal of Neuroscience* 30.12 (Mar. 2010), pp. 4481–4488. DOI: 10.1523/jneurosci.2794-09.2010.

[28] Julian Keil et al. "Prestimulus Beta Power and Phase Synchrony Influence the Sound-Induced Flash Illusion". In: *Cerebral Cortex* 24.5 (Jan. 2013), pp. 1278–1288. DOI: 10.1093/cercor/bhs409.

[29] Fatemeh Khademi, Vladimir Royter, and Alireza Gharabaghi. "Distinct Beta-band Oscillatory Circuits Underlie Corticospinal Gain Modulation". In: *Cerebral Cortex* 28.4 (Feb. 2018), pp. 1502–1515. DOI: https://doi.org/10.1093/cercor/bhy016.

[30] Flavie Torrecillos et al. “Motor Cortex Inputs at the Optimum Phase of Beta Cortical Oscillations Undergo More Rapid and Less Variable Corticospinal Propagation”. In: *Journal of Neuroscience* 40.2 (2020), pp. 369–381. DOI: https://doi.org/10.1523/JNEUROSCI.1953-19.2019.

[31] Miles Wischnewski et al. “The phase of sensorimotor mu and beta oscillations has the opposite effect on corticospinal excitability”. In: *Brain Stimulation* 15.5 (2022), pp. 1093–1100. DOI: https://doi.org/10.1016/j.brs.2022.08.005.

[32] Frederick Verbruggen et al. “A consensus guide to capturing the ability to inhibit actions and impulsive behaviors in the stop-signal task”. In: *eLife* 8 (Apr. 2019). DOI: 10.7554/elife.46323.

[33] Gregor Thut, Philippe G. Schyns, and Joachim Gross. “Entrainment of Perceptually Relevant Brain Oscillations by Non-Invasive Rhythmic Stimulation of the Human Brain”. In: *Frontiers in Psychology* 2 (2011). DOI: 10.3389/fpsyg.2011.00170.

[34] Christoph S. Herrmann et al. “Transcranial alternating current stimulation: a review of the underlying mechanisms and modulation of cognitive processes”. In: *Frontiers in Human Neuroscience* 7 (2013). DOI: 10.3389/fnhum.2013.00279.

[35] Sanne ten Oever et al. “Stimulus Presentation at Specific Neuronal Oscillatory Phases Experimentally Controlled with tACS: Implementation and Applications”. In: *Frontiers in Cellular Neuroscience* 10 (Oct. 2016). DOI: 10.3389/fncel.2016.00240.

[36] R. C. Oldfield. “The assessment and analysis of handedness: The Edinburgh inventory”. In: *Neuropsychologia* 9.1 (1971), pp. 97–113. DOI: 10.1016/0028-3932(71)90067-4.

[37] Marom Bikson, Abhishek Datta, and Maged Elwassif. “Establishing safety limits for transcranial direct current stimulation”. In: *Clinical Neurophysiology* 120.6 (June 2009), pp. 1033–1034. DOI: 10.1016/j.clinph.2009.03.018.

[38] A.J. Woods et al. "A technical guide to tDCS, and related non-invasive brain stimulation tools". In: *Clinical Neurophysiology* 127.2 (Feb. 2016), pp. 1031–1048. DOI: 10.1016/j.clinph.2015.11.012.

[39] A. T. Slater-Hammel. "Reliability, Accuracy, and Refractoriness of a Transit Reaction". In: *Research Quarterly. American Association for Health, Physical Education and Recreation* 31.2 (May 1960), pp. 217–228. DOI: 10.1080/10671188.1960.10613098.

[40] James P. Coxon, Cathy M. Stinear, and Winston D. Byblow. "Intracortical Inhibition During Volitional Inhibition of Prepared Action". In: *Journal of Neurophysiology* 95.6 (June 2006), pp. 3371–3383. DOI: 10.1152/jn.01334.2005.

[41] Inge Leunissen et al. "Reliable estimation of inhibitory efficiency: to anticipate, choose or simply react?" In: *European Journal of Neuroscience* 45.12 (June 2017). Ed. by Susan Rossell, pp. 1512–1523. DOI: 10.1111/ejn.13590.

[42] Robert Oostenveld et al. "FieldTrip: Open Source Software for Advanced Analysis of MEG, EEG, and Invasive Electrophysiological Data". In: *Computational Intelligence and Neuroscience* 2011 (2011), pp. 1–9. DOI: 10.1155/2011/156869.

[43] German Gomez-Herrero. "Automatic artifact removal (AAR) toolbox v1.3 (Release 09.12.2007) for MATLAB". In: *Technology* 3 (Jan. 2007), pp. 1–23.

[44] Saskia Haegens et al. "Inter- and intra-individual variability in alpha peak frequency". In: *NeuroImage* 92 (May 2014), pp. 46–55. DOI: 10.1016/j.neuroimage.2014.01.049.

[45] V.V. Nikulin and T. Brismar. "Phase synchronization between alpha and beta oscillations in the human electroencephalogram". In: *Neuroscience* 137.2 (Jan. 2006), pp. 647–657. DOI: 10.1016/j.neuroscience.2005.10.031.

[46] Ian C. Fiebelkorn et al. “Ready, Set, Reset: Stimulus-Locked Periodicity in Behavioral Performance Demonstrates the Consequences of Cross-Sensory Phase Reset”. In: *Journal of Neuroscience* 31.27 (2011), pp. 9971–9981. DOI: https://doi.org/10.1523/JNEUROSCI.1338-11.2011.

[47] Sanne ten Oever and Alexander T. Sack. “Oscillatory phase shapes syllable perception”. In: *Proceedings of the National Academy of Sciences* 112.52 (2015), pp. 15833–15837. DOI: https://doi.org/10.1073/pnas.1517519112.

[48] Lukas Schilberg et al. “Phase of beta-frequency tACS over primary motor cortex modulates corticospinal excitability”. In: *Cortex* 103 (2018), pp. 142–152. DOI: 10.1016/j.cortex.2018.03.001.

[49] Tom A. de Graaf et al. “Does alpha phase modulate visual target detection? Three experiments with tACS-phase-based stimulus presentation”. In: *European Journal of Neuroscience* 51.11 (2020), pp. 2299–2313. DOI: https://doi.org/10.1111/ejn.14677.

[50] Vihren Chakarov et al. “Beta-Range EEG-EMG Coherence With Isometric Compensation for Increasing Modulated Low-Level Forces”. In: *Journal of Neurophysiology* 102.2 (2009). PMID: 19458142, pp. 1115–1120. DOI: https://doi.org/10.1152/jn.91095.2008.

[51] Suresh D. Muthukumaraswamy. “Functional Properties of Human Primary Motor Cortex Gamma Oscillations”. In: *Journal of Neurophysiology* 104.5 (2010). PMID: 20884762, pp. 2873–2885. DOI: https://doi.org/10.1152/jn.00607.2010.

[52] Petra Fischer et al. “Subthalamic nucleus gamma activity increases not only during movement but also during movement inhibition”. In: *eLife* 6 (July 2017). Ed. by Eilon Vaadia, e23947. DOI: https://doi.org/10.7554/eLife.23947.

[53] Mohsin M. Ali, Kristin K. Sellers, and Flavio Fröhlich. "Transcranial Alternating Current Stimulation Modulates Large-Scale Cortical Network Activity by Network Resonance". In: *Journal of Neuroscience* 33.27 (2013), pp. 11262–11275. DOI: https://doi.org/10.1523/JNEUROSCI.5867-12.2013.

[54] Nicola J. Ray et al. "The role of the subthalamic nucleus in response inhibition: Evidence from local field potential recordings in the human subthalamic nucleus". In: *NeuroImage* 60.1 (Mar. 2012), pp. 271–278. DOI: 10.1016/j.neuroimage.2011.12.035.

[55] Yvonne M. Fonken et al. "Frontal and motor cortex contributions to response inhibition: evidence from electrocorticography". In: *Journal of Neurophysiology* 115.4 (Apr. 2016), pp. 2224–2236. DOI: 10.1152/jn.00708.2015.

[56] Darcy A. Diesburg and Jan R. Wessel. "The Pause-then-Cancel model of human action-stopping: Theoretical considerations and empirical evidence". In: *Neuroscience & Biobehavioral Reviews* 129 (Oct. 2021), pp. 17–34. DOI: 10.1016/j.neubiorev.2021.07.019.

[57] Pascal Fries. "Rhythms for Cognition: Communication through Coherence". In: *Neuron* 88.1 (2015), pp. 220–235. DOI: https://doi.org/10.1016/j.neuron.2015.09.034.

[58] Daniel Bush et al. "Spike-timing dependent plasticity and the cognitive map". In: *Frontiers in Computational Neuroscience* 4 (2010). DOI: https://doi.org/10.3389/fncom.2010.00142.

[59] Florian H. Kasten and Christoph S. Herrmann. "The hidden state-dependency of transcranial alternating current stimulation (tACS)". In: *bioRxiv* (2020). DOI: https://doi.org/10.1101/2020.12.23.423984.

[60] Rufin VanRullen. "Attention Cycles". In: *Neuron* 99.4 (2018), pp. 632–634. DOI: https://doi.org/10.1016/j.neuron.2018.08.006.

[61] Sanne Ten Oever et al. “Phase-Coded Oscillatory Ordering Promotes the Separation of Closely Matched Representations to Optimize Perceptual Discrimination”. In: *iScience* 23.7 (2020), p. 101282. DOI: https://doi.org/10.1016/j.isci.2020.101282.

[62] Alberto Pérez-Cervera, Tere M. Seara, and Gemma Huguet. “Phase-locked states in oscillating neural networks and their role in neural communication”. In: *Communications in Nonlinear Science and Numerical Simulation* 80 (2020), p. 104992. DOI: https://doi.org/10.1016/j.cnsns.2019.104992.

[63] Marius Schneider et al. “A mechanism for inter-areal coherence through communication based on connectivity and oscillatory power”. In: *Neuron* 109.24 (2021), 4050–4067.e12. DOI: https://doi.org/10.1016/j.neuron.2021.09.037.

[64] Gustavo Deco and Morten L. Kringelbach. “Metastability and Coherence: Extending the Communication through Coherence Hypothesis Using A Whole-Brain Computational Perspective”. In: *Trends in Neurosciences* 39.3 (2016), pp. 125–135. DOI: https://doi.org/10.1016/j.tins.2016.01.001.

[65] Sara J Hussain et al. “Voluntary Motor Command Release Coincides with Restricted Sensorimotor Beta Rhythm Phases”. In: *The Journal of Neuroscience* 42.29 (June 2022), pp. 5771–5781. DOI: 10.1523/jneurosci.1495-21.2022.

[66] Hayriye Cagnan et al. “Temporal evolution of beta bursts in the parkinsonian cortical and basal ganglia network”. In: *Proceedings of the National Academy of Sciences* 116.32 (2019), pp. 16095–16104. DOI: https://doi.org/10.1073/pnas.1819975116.

[67] Andrea Guerra et al. “Phase Dependency of the Human Primary Motor Cortex and Cholinergic Inhibition Cancelation During Beta tACS”. In: *Cerebral Cortex* 26.10 (Sept. 2016), pp. 3977–3990. DOI: https://doi.org/10.1093/cercor/bhw245.

[68] David Williams et al. "Dopamine-dependent changes in the functional connectivity between basal ganglia and cerebral cortex in humans". In: *Brain* 125.7 (July 2002), pp. 1558–1569. DOI: https://doi.org/10.1093/brain/awf156.

[69] Vladimir Litvak et al. "Resting oscillatory cortico-subthalamic connectivity in patients with Parkinson's disease". In: *Brain* 134.2 (Dec. 2010), pp. 359–374. DOI: https://doi.org/10.1093/brain/awq332.

[70] J. Hirschmann et al. "Distinct oscillatory STN-cortical loops revealed by simultaneous MEG and local field potential recordings in patients with Parkinson's disease". In: *NeuroImage* 55.3 (Apr. 2011), pp. 1159–1168. DOI: 10.1016/j.neuroimage.2010.11.063.

[71] Or Koren et al. "Dopaminergic medication reduces interhemispheric hyper-synchronization in Parkinson's disease". In: *Parkinsonism & Related Disorders* 97 (2022), pp. 39–46. DOI: https://doi.org/10.1016/j.parkreldis.2022.02.009.

[72] L. M. F. Doyle Gaynor et al. "Suppression of beta oscillations in the subthalamic nucleus following cortical stimulation in humans". In: *European Journal of Neuroscience* 28.8 (2008), pp. 1686–1695. DOI: https://doi.org/10.1111/j.1460-9568.2008.06363.x.

[73] Rui M Costa et al. "Rapid alterations in corticostriatal ensemble coordination during acute dopamine-dependent motor dysfunction". In: *Neuron* 52.2 (2006), pp. 359–369. DOI: https://doi.org/10.1016/j.neuron.2006.07.030.

[74] M. M. McCarthy et al. "Striatal origin of the pathologic beta oscillations in Parkinson's disease". In: *Proceedings of the National Academy of Sciences* 108.28 (2011), pp. 11620–11625. DOI: https://doi.org/10.1073/pnas.1107748108.

[75] Andrea A. Kühn et al. “Increased beta activity in dystonia patients after drug-induced dopamine deficiency”. In: *Experimental Neurology* 214.1 (2008), pp. 140–143. DOI: https://doi.org/10.1016/j.expneurol.2008.07.023.

[76] Camille de Solages et al. “Bilateral symmetry and coherence of subthalamic nuclei beta band activity in Parkinson’s disease”. In: *Experimental Neurology* 221.1 (2010), pp. 260–266. DOI: https://doi.org/10.1016/j.expneurol.2009.11.012.

[77] Natasha Darcy et al. “Spectral and spatial distribution of subthalamic beta peak activity in Parkinson’s disease patients”. In: *Experimental Neurology* 356 (2022), p. 114150. DOI: https://doi.org/10.1016/j.expneurol.2022.114150.

[78] Ysbrand D Van Der Werf et al. “The neural response to transcranial magnetic stimulation of the human motor cortex. II. Thalamocortical contributions”. In: *Experimental brain research* 175.2 (2006), pp. 246–255. DOI: https://doi.org/10.1007/s00221-006-0548-x.

[79] Michael Cassidy et al. “Movement-related changes in synchronization in the human basal ganglia”. In: *Brain* 125.6 (June 2002), pp. 1235–1246. DOI: https://doi.org/10.1093/brain/awf135.

[80] Andrew Sharott et al. “Spatio-temporal dynamics of cortical drive to human subthalamic nucleus neurons in Parkinson’s disease”. In: *Neurobiology of Disease* 112 (2018), pp. 49–62. DOI: https://doi.org/10.1016/j.nbd.2018.01.001.

[81] Ehsan Negahbani et al. “Transcranial Alternating Current Stimulation (tACS) Entrains Alpha Oscillations by Preferential Phase Synchronization of Fast-Spiking Cortical Neurons to Stimulation Waveform”. In: *bioRxiv* (2019). DOI: https://doi.org/10.1101/563163.

[82] Sreekari Vogeti, Cindy Boetzel, and Christoph S. Herrmann. "Entrainment and Spike-Timing Dependent Plasticity - A Review of Proposed Mechanisms of Transcranial Alternating Current Stimulation". In: *Frontiers in Systems Neuroscience* 16 (2022). DOI: https://doi.org/10.3389/fnsys.2022.827353.

[83] Luke Johnson et al. "Dose-dependent effects of transcranial alternating current stimulation on spike timing in awake nonhuman primates". In: *Science Advances* 6.36 (Sept. 2020). DOI: 10.1126/sciadv.aaz2747.

2.6 Supplementary information

Table S2.1: Experiment 1 VAS and discomfort rating score.

	Pre/Post	Subjective rating between 1-10	Main effect of time (pre, post)
Fatigue	Pre	2.44±1.80	F(1,28)=1.073
	Post	3.80±1.95	p=0.003
Discomfort	Post	3.46±0.28	-

Table S2.2: Experiment 2 VAS and discomfort rating score.

Subjective rating between1-10		Session 1	Session 2	Statistic	
				Main effect of phase sessions	Main effect of time (pre, post)
Discomfort		3.01±0.19	2.57±1.36	F(1,14)=0.41 p=0.064	-
Fatigue	Pre	2.62±2.15	2.83±2.04	F(1,14)=0.02 p=0.700	F=2.54$p < .001$
	Post	4.15±2.00	4.54±2.36	F(1,14)=0.04 p=0.538	

Figure S2.1: Phase-aligned group results of Exp.1

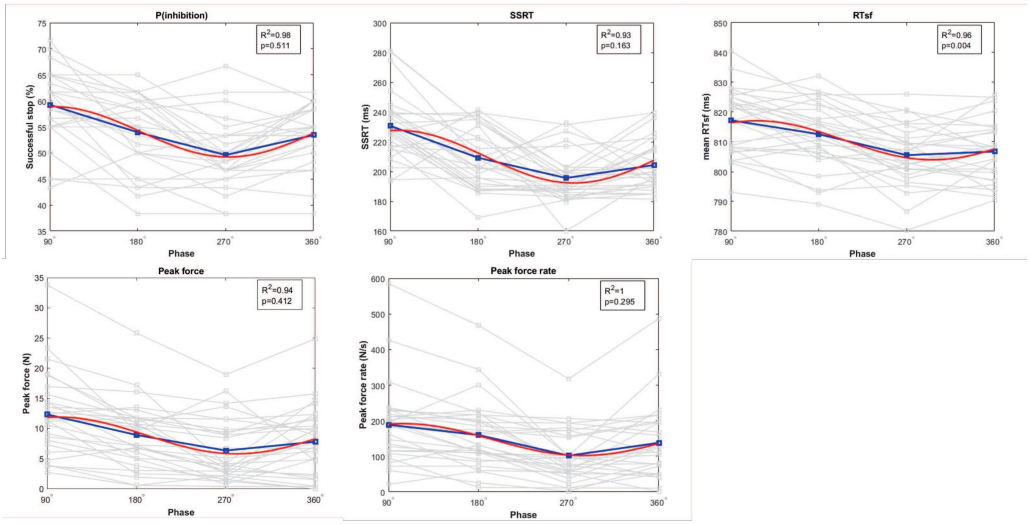


Figure S2.2: Phase-aligned group results of Exp.2

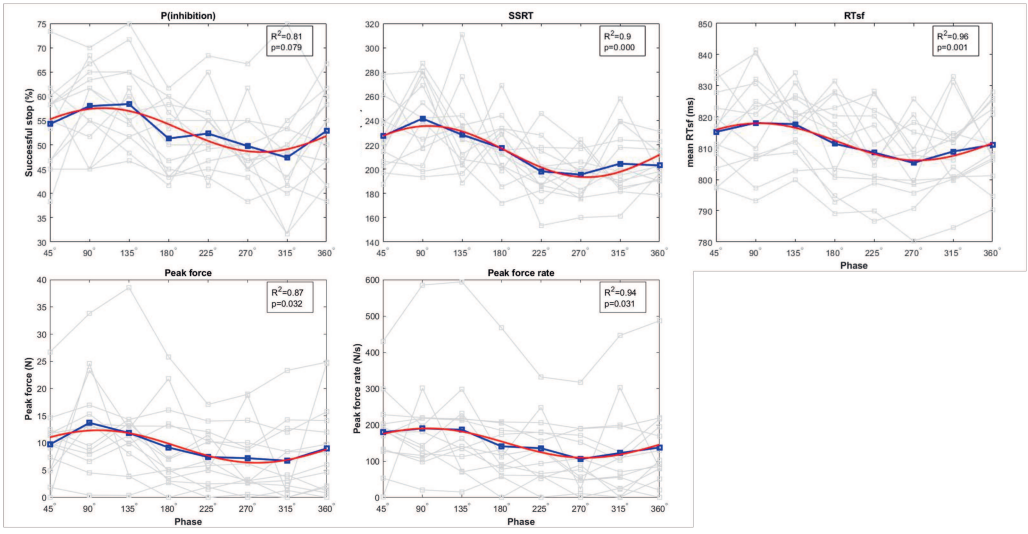


Table S2.3: Experiment 1 95% range values of recorded stimulus trigger to stimulus delays, in milliseconds, per phase and participant.

Participant	90°	180°	270°	360°
1	0.940	0.983	1.153	0.943
2	1.290	1.170	1.167	1.031
3	0.913	0.860	1.223	1.027
4	1.127	1.027	1.139	0.832
5	1.110	0.900	1.142	1.120
6	1.047	0.925	1.115	0.897
7	1.087	1.113	1.020	0.963
8	1.095	1.113	0.963	1.013
9	0.930	1.110	1.070	0.993
10	0.937	1.197	1.136	1.017
11	1.017	1.120	1.023	0.897
12	1.103	0.797	0.892	0.939
13	1.017	1.169	0.827	0.927
14	0.953	0.875	0.875	1.091
15	1.068	1.044	1.020	0.950
16	1.146	1.187	1.119	0.990
17	0.969	1.053	1.197	1.041
18	1.183	1.003	1.140	0.900
19	1.100	1.053	1.003	2.105
20	1.110	1.130	1.027	0.986
21	1.040	1.040	1.064	1.037
22	1.113	0.839	1.033	1.163
23	1.197	1.037	1.138	1.040
24	1.173	1.122	1.010	1.287
25	1.120	1.063	1.061	1.060
26	1.260	1.083	1.339	0.897
27	1.253	1.123	1.170	0.927
28	0.933	1.127	1.122	0.940
29	1.157	0.937	2.862	1.246
30	1.220	0.907	1.093	0.980
Mean	1.087	1.037	1.138	1.041
SD	0.191	0.197	0.378	0.266

Table S2.4: Experiment 2 95% range values of recorded stimulus trigger to stimulus delays, in milliseconds, per phase and participant.

Participants	45°	90°	135°	180°	225°	270°	315°	360°
1	1.000	1.146	1.007	1.187	1.223	1.119	0.766	0.990
2	1.127	1.183	1.075	1.003	1.053	1.140	1.373	0.900
3	1.063	1.100	1.166	1.053	0.973	1.003	1.227	2.105
4	1.107	1.110	1.197	1.130	1.034	1.027	1.070	0.986
5	1.197	1.040	0.900	1.040	1.010	1.064	1.133	1.037
6	2.396	1.113	2.350	0.839	2.098	1.033	2.119	1.163
7	1.147	1.197	1.040	1.037	1.149	1.138	1.027	1.040
8	1.186	1.173	1.010	1.122	1.115	1.010	0.875	1.287
9	1.054	1.120	1.112	1.063	0.953	1.061	1.167	1.060
10	0.997	1.260	0.897	1.083	1.013	1.339	1.007	0.897
11	0.820	1.253	1.107	1.123	0.993	1.170	0.987	0.927
12	1.159	0.933	1.117	1.127	1.077	1.122	1.153	0.940
13	1.085	1.157	1.132	0.937	1.247	2.862	1.092	1.246
14	1.159	1.220	1.037	0.907	1.210	1.093	1.037	0.980
Mean	1.178	1.143	1.153	1.047	1.154	1.227	1.145	1.111
SD	0.339	0.080	0.331	0.090	0.268	0.445	0.295	0.289

Table S2.5: Post hoc tests results of P(inhibition), SSRT and RTsf in Exp. 1.

		P(inhibition)			SSRT			RTsf		
		Mean diff.	SE	Sig.	Mean diff.	SE	Sig.	Mean diff.	SE	Sig.
90°	180°	0.517	0.864	1.000	-4.638	4.999	1.000	3.025	1.479	0.303
	270°	-5.632**	0.966	0.000	20.000**	5.402	0.006	8.491**	1.527	0.000
	360°	-7.471**	1.212	0.000	17.914*	6.160	0.042	-0.720	1.686	1.000
180°	270°	-6.149**	0.880	0.000	24.638**	3.898	0.000	5.466*	1.734	0.023
	360°	-7.989**	1.038	0.000	22.552**	3.417	0.000	-3.744	2.107	0.519
270°	360°	-1.839	1.070	0.580	-2.086	4.311	1.000	-9.210**	1.930	0.000

Table S2.6: Wilcoxon signed-rank test results of peak force and peak force rate of stop trials in Exp. 1.

		Peak force		Peak force rate	
		Z	Sig.	Z	Sig.
90°	180°	1.027	0.304	1.027	0.304
	270°	-2.995**	0.003	-2.152*	0.031
	360°	-3.189**	0.001	-2.843**	0.004
180°	270°	-4.206**	0.000	-3.860**	0.000
	360°	-4.271**	0.000	-4.054**	0.000
270°	360°	-2.281*	0.023	-2.281*	0.023

Table S2.7: Post hoc tests results of P(inhibition), SSRT and RTsf in Exp. 2

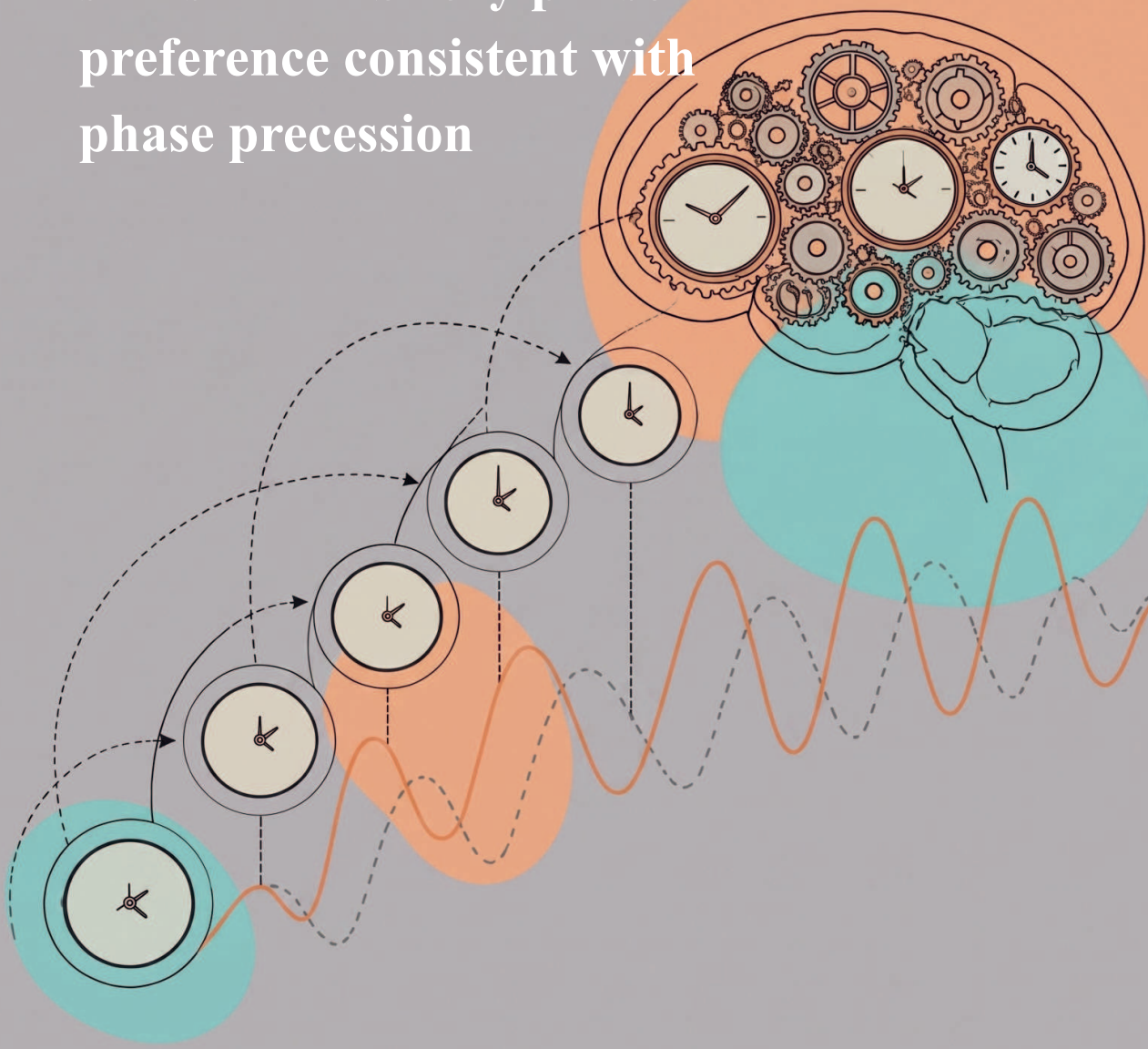
		P(inhibition)			SSRT			RTsf		
		Mean Diff.	SE	Sig.	Mean Diff.	SE	Sig.	Mean Diff.	SE	Sig.
45	90	2.565	1.723	1.000	-7.821	7.597	1.000	-2.458	3.246	1.000
	135	2.149	2.234	1.000	-22.429	10.014	1.000	-4.404	2.979	1.000
	180	2.922	2.020	1.000	-9.429	6.059	1.000	1.548	3.137	1.000
	225	3.160	2.920	1.000	-13.679	13.099	1.000	2.396	4.063	1.000
	270	-2.197	2.230	1.000	14.464	7.468	1.000	7.940	3.026	0.589
	315	0.184	1.896	1.000	3.857	10.522	1.000	-0.290	2.532	1.000
	360	-5.888	2.319	0.692	11.107	6.620	1.000	-1.653	3.367	1.000
90	135	-0.416	2.145	1.000	-14.607	11.315	1.000	-1.946	2.333	1.000
	180	0.357	1.080	1.000	-1.607	7.473	1.000	4.006	2.117	1.000
	225	0.595	2.647	1.000	-5.857	12.495	1.000	4.854	3.376	1.000
	270	-4.762	1.317	0.088	22.286	8.684	0.657	10.398**	2.164	0.010
	315	-2.381	1.762	1.000	11.679	9.714	1.000	2.168	3.270	1.000
	360	-8.452*	1.941	0.022	18.929	10.003	1.000	0.805	2.224	1.000
135	180	0.773	2.169	1.000	13.000	9.157	1.000	5.952	2.691	1.000
	225	1.011	2.550	1.000	8.750	10.096	1.000	6.801	2.292	0.305
	270	-4.346	2.119	1.000	36.893*	8.665	0.026	12.344*	2.828	0.021
	315	-1.965	2.135	1.000	26.286	10.043	0.596	4.114	2.257	1.000
	360	-8.037	2.558	0.218	33.536	10.015	0.147	2.751	3.384	1.000
180	225	0.238	3.100	1.000	-4.250	11.970	1.000	0.849	3.793	1.000
	270	-5.119*	1.139	0.017	23.893	6.524	0.080	6.392	2.446	0.600
	315	-2.738	2.387	1.000	13.286	9.392	1.000	-1.838	3.328	1.000
	360	-8.810**	1.435	0.001	20.536	5.353	0.058	-3.201	3.131	1.000
225	270	-5.357	2.622	1.000	28.143	9.803	0.368	5.544	3.972	1.000
	315	-2.976	1.817	1.000	17.536	13.555	1.000	-2.686	2.540	1.000
	360	-9.048	3.291	0.463	24.786	13.537	1.000	-4.049	4.420	1.000
270	315	2.381	2.159	1.000	-10.607	9.435	1.000	-8.230	3.419	0.887
	360	-3.690	1.367	0.509	-3.357	6.747	1.000	-9.593	2.789	0.123
315	360	-6.071	2.548	0.927	7.250	9.424	1.000	-1.363	3.623	1.000

Table S2.8: Wilcoxon signed-rank test results of peak force and peak force rate of stop trials in Exp. 2.

		Peak force		Peak force rate	
		Z	Sig.	Z	Sig.
45	90	1.528	0.124	1.601	0.109
	135	1.601	0.109	1.664	0.096
	180	1.475	0.140	1.852	0.064
	225	1.601	0.109	2.229*	0.026
	270	0.973	0.331	1.036	0.300
	315	-0.094	0.925	0.282	0.778
	360	-0.973	0.331	-0.659	0.510
90	135	0.031	0.975	-0.785	0.433
	180	1.161	0.245	1.664	0.096
	225	-0.094	0.925	-0.094	0.925
	270	-2.471*	0.016	-1.601	0.109
	315	-1.977*	0.048	-1.412	0.158
	360	-2.982**	0.003	-2.542*	0.011
135	180	-0.345	0.730	1.224	0.221
	225	-0.094	0.925	0.534	0.594
	270	-2.229*	0.026	-1.036	0.300
	315	-2.040*	0.041	-1.789	0.074
	360	-2.919**	0.004	-2.605*	0.009
180	225	-0.220	0.826	-0.534	0.594
	270	-3.296**	0.001	-2.982**	0.003
	315	-1.852	0.064	-2.354*	0.019
	360	-3.170*	0,002	-3.107**	0.002
225	270	-1.475	0.140	-1.475	0.140
	315	-2.480*	0.013	-2.480*	0.013
	360	-2.354*	0.019	-2.542*	0.011
270	315	-0.220	0.826	-0.659	0.510
	360	-2.354*	0.019	-2.345*	0.019
315	360	-1.224	0.221	-1.224	0.221

3

TACS induces state-dependent shifts in inhibitory phase preference consistent with phase precession



Adapted from: Zhou Fang et al. "tACS induces state-dependent shifts in inhibitory phase preference consistent with phase precession". In: (Dec. 2025). DOI: 10.64898/2025.11.28.691215.

Abstract

Phase-dependent modulation of motor inhibition suggests that oscillatory timing plays a key role in inhibitory control. Here we show that rhythmic brain stimulation can selectively alter this timing in a manner consistent with phase precession. Participants performed an anticipatory stop-signal task while receiving 20 Hz transcranial alternating current stimulation (tACS) over the pre-supplementary motor area, with stop signals presented at defined phases of the stimulation waveform. An additional control experiment with no tACS was conducted, in which the stop signal phase was derived post-hoc from the ongoing EEG. In both tACS and control sessions, stopping efficacy varied sinusoidally with beta phase, confirming that inhibitory control is intrinsically phase-dependent. During tACS, however, the phase associated with the strongest inhibition advanced progressively across the session by about 180°, and this effect was specific to failed-stop trials. No comparable shift occurred without stimulation. These findings indicate that rhythmic drive can bias the temporal phase at which inhibition is most effective when the brain is in an error-prone state, revealing a state-dependent, precession-like reorganization of inhibitory timing. We propose that tACS interacts with error-related plasticity to promote gradual phase advancement, placing the system within spike-timing-dependent learning windows, whereas intrinsic fluctuations alone appear insufficient to facilitate cumulative precession. More broadly, these results suggest that phase precession may represent a general coding principle extending beyond hippocampal circuits, enabling the motor system to adaptively adjust inhibitory control through oscillatory timing mechanisms.

3.1 Introduction

Neural oscillations are fundamental to brain function, providing a temporal framework that regulates the timing of neuronal activity and thereby supports synaptic plasticity, information transfer, and large-scale integration across cortical and subcortical networks [1, 2]. One striking oscillatory phenomenon is phase precession, a coding mechanism in which neural spikes shift progressively earlier relative to the phase of an ongoing oscillation across successive cycles. This phenomenon was first described in the hippocampus of rodents during spatial navigation [3] and has since been observed in regions such as the ventral striatum [4] and frontal cortex [5], suggesting that it represents a general computational principle extending beyond the hippocampal system. By advancing spike timing across successive oscillatory cycles, neurons can represent behavioral sequences that unfold over longer timescales within the faster temporal structure of ongoing rhythms [6, 7]. This temporal compression is thought to "bind" distributed neural events into coherent, rapidly accessible representations, supporting associative learning and flexible behavior [6, 7, 8, 9]. Recent invasive recordings have further demonstrated phase precession in the human hippocampus [10, 11], underscoring its relevance for human neural coding.

A critical next step is to determine whether phase precession in humans can be induced or promoted experimentally. Establishing causal control over this phenomenon would be important not only for testing its proposed roles in sequence learning, temporal binding, and predictive coding, but also for exploring how this mechanism might be harnessed to modulate cognition and behavior. Transcranial alternating current stimulation (tACS) provides a promising approach. By applying low-intensity alternating currents at specific frequencies, tACS can bias ongoing rhythms, promote phase alignment of neuronal spiking time [12, 13, 14], and modulate brain oscillations through a process known as entrainment [15, 16]. At the cellular level, alternating currents have been shown to advance spike phase relative to an imposed oscillation,

providing a mechanistic precedent for externally driven precession [17, 18]. While most human tACS studies have demonstrated stable phase alignment rather than progressive phase shifts, recent work has shown that rhythmic stimulation can induce phase precession in the motor cortex [19]. This raises the question of whether tACS-induced phase precession generalizes beyond simple motor cortex activity and whether its expression is directly linked to cognitive function and behavior.

Building on these findings, the present study investigates whether tACS can enable phase precession-like dynamics during inhibitory control. Specifically, we tested whether rhythmic stimulation over the pre-supplementary motor area (preSMA) could induce systematic phase advancement during motor inhibition, a process in which stopping efficiency has been shown to depend on the beta oscillatory phase [20]. We propose that tACS provides a rhythmic scaffold that aligns neural activity in time, allowing intrinsic excitatory-inhibitory interactions to gradually advance the phase of optimal motor inhibition within this externally synchronized rhythm. Such temporal compression of neural activity has been proposed to facilitate spike-timing-dependent plasticity and adaptive coding in animal models [21, 22]. Accordingly, we hypothesized that if tACS promotes phase precession-like dynamics, inhibitory performance should exhibit a progressive shift over time in the optimal stimulation phase at which the stop-signal arrives. In contrast, this shift should be absent without external rhythmic drive in a control experiment, indicating that precession reflects an interaction between stimulation-induced synchronization and endogenous network adaptation.

3.2 Methods

3.2.1 Overview

This study comprised two experiments. In Experiment 1, we reanalyzed the dataset reported in [20] to address a distinct question regarding

tACS-induced phase precession. The experimental design has been described in detail previously [20] and is summarized here. In Experiment 2, an independent cohort performed the same stop-signal task but without active tACS, providing a control condition. Common procedures and key differences between the two experiments are outlined below.

3.2.2 Participants

In Experiment 1, twenty-nine healthy, right-handed adults (13 males, 19 females; mean age = 25.3 years, range 18-35) participated. Handedness was confirmed using the Edinburgh Handedness Inventory (mean laterality quotient = 96.3, range 70-100; [23]). In Experiment 2, eighteen healthy, right-handed adults (6 males, 12 females; mean age = 24.0 years, range 18-30, mean laterality quotient = 89.4, range 65-100) participated. All participants had no contraindications to non-invasive brain stimulation [24, 25], and provided written informed consent. The protocol was approved by the Ethics Review Committee Psychology and Neuroscience of Maastricht University, the Netherlands (ERCPN Approval code: OZL_204_04_02_2019).

3.2.3 Task and stimulation protocol

In both experiments, participants performed an anticipatory version of a stop signal task [26, 27, 28]. As shown in the Figure 3.1, the trial starts with a moving indicator filling up an empty bar (1000 ms) with a consistent speed. Participants were asked to stop the indicator as close to a fixed target line (800 ms) as possible by pinching a force transducer (OMEGA Engineering, Norwalk, CT, USA) using their right thumb and index finger. Immediate feedback indicated absolute error: green, yellow, orange, or red for ≤ 20, ≤ 40, ≤ 60, or > 60 ms, respectively. Response was triggered when their force exceeds a threshold which was determined from individual maximal voluntary force (MVF). MVF was defined as the highest value obtained across three 5 s maximal pinches. The threshold was initially set to 25% MVF and could be reduced in

5% increments for comfort (mean 23.3%, range 10-25%). In 30% of the trials, the bar stopped before reaching the target, signaling participants to withhold their response. Failed stop trials (SF) were those where force exceeded the response thresholds, while successful stop trials (SS) involved forces below this threshold.

In Experiment 1, the session comprised 240 stop trials and 480 go trials presented in pseudorandom order. Stop-signal delays (SSD) occurred approximately 110, 150, 190, 230, and 270 ms prior to the target line and shifted up to $\pm$ 25 ms to match the intended tACS phase. Inter-trial intervals jittered between 2.7 and 3.7 s. tACS (DC STIMULATOR PLUS, NeuroConn, GmbH, Ilmenau, Germany) was placed using a 1×4 electrode configuration over the preSMA, with the central electrode located at FCz and four surrounding electrodes at F1, F2, C1, and C2 based on the 10-20 system. The electrodes were embedded in gel-filled cup that was made out of plastic cylinders ($\varnothing$2 cm at top, 2.5 cm at bottom) and mounted in an EEG cap (EASYCAP GmbH, Germany). The stop signals were presented at 90° (peak), 180°, 270°, and 360° relative to the tACS waveform at 20 Hz using a phase-locked stimulus presentation system [29], as shown in Figure.3.1 (B).

Experiment 2 involved 101 stop trials and 308 go trials, presented in 3 blocks of 136 trials. We used a staircase tracking algorithm that adjusts the SSD in 16.667 ms increments based on the participant's performance to maintain a 50% inhibition accuracy in stopping responses on stop trials. During the experiment, tACS electrodes were positioned as in Experiment 1. Stimulation was delivered only during the first 10 seconds of each task block, leaving the remainder 10 min tACS-free. For the purpose of estimating the stop-signal phase relative to the ongoing oscillatory phase, EEG was recorded using a BrainAmp system (Brain Products GmbH, Germany) at a sampling rate of 5000 Hz from 32 Ag/AgCl electrodes according to the 10-20 system (channels included F7, FC5, C3, Fz, FC1, Cz, FC2, C4, FC6, F8, T7, T8 as implicit reference; AFz as ground). In addition, four electro-oculographic (EOG) electrodes (UVEOG, LVEOG, RHEOG, and LHEOG) were placed to monitor eye movements. Impedances were maintained below 10 $k\Omega$ and signals

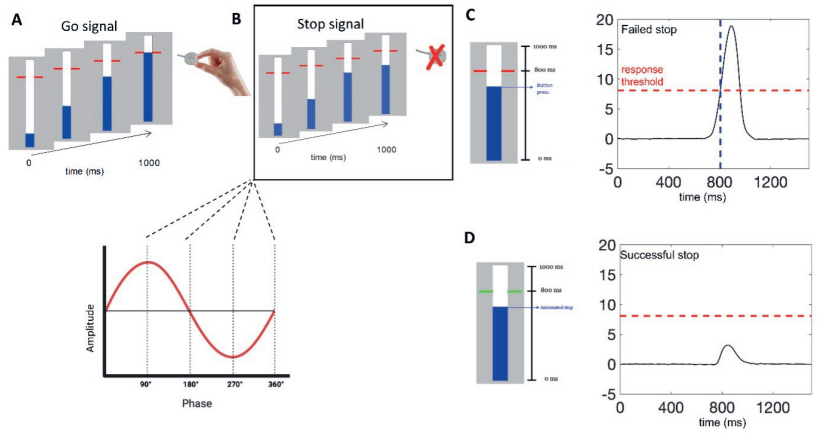


Figure 3.1: **Anticipatory stop-signal task and trial classification.** (**A**) In the go trials, participants squeezed a force sensor as a bar reached the target. (**B**) In stop trials (30% of the total trials), the bar stopped early, requiring inhibition. In Experiment 1, the stop signals were presented equiprobably at four phase angles (90°, 180°, 270°, 360°) relative to the tACS; in Experiment 2, the instantaneous phase at the stop signals was estimated post hoc and assigned to the same four phase bins. (**C**) Stop-failed (SF) were defined as responses exceeding the response threshold. The target line turned red to indicate failed inhibition. (**D**) Stop-successful (SS) were those in which force remained below the threshold; the target line turned green to indicate successful inhibition.

were sampled at 5000 Hz. Processing performed in MATLAB R2022a using FieldTrip [30] comprised (1) re-referencing each channel to T7; (2) demeaning and detrending; (3) filtering with a 1-300 Hz band pass filter and a 50 Hz FIR notch filter; (4) regressing out eye movement noise by an EEGlab plugin, AAR (order = 3, $\lambda = 0.9999$, $\sigma = 0.01$, precision = 50). The phase at the moment of the stop signal was determined post-hoc based on the Fz channel: it was first segmented from -0.5 to 0 s relative to the stop signal, and a one-pass FIR bandpass filter (18-22 Hz) was applied. The edge of 32 data points preceding the stop signal was removed to mitigate boundary artifacts introduced by filtering. An autoregressive (AR) model (order 30) was then fitted to predict 64 data points forward. The Hilbert transform was applied to the segment, estimating the phase at the instant corresponding to the original endpoint. Estimated phases were categorized into four bins: 90° ($\geq 45°$ to $< 135°$), 180° ($\geq 135°$ to $< 225°$), 270° ($\geq 225°$ to $< 315°$), and 360° ($\geq 315°$ to $< 360°$ or $\geq 0°$ to $< 45°$).

3.2.4 Force metrics

The force signal was acquired via a digital-to-analog converter (DAC) from National Instruments (Austin, TX, USA) and recorded in LabChart with a sampling rate of 1000 Hz. Data were saved on a trial-by-trial basis from the onset of the fill indicator to 1700 ms.

Behavioral force data were analyzed using MATLAB R2022a (MathWorks, Natick, MA, USA). For both Experiment 1 and 2, raw force signals recorded on a trial-by-trial basis were first converted from volts to newtons. A fifth-order 20 Hz low-pass Butterworth filter was applied to remove high-frequency noise. Baseline correction was performed by subtracting the mean force measured between -650 ms and -400 ms relative to target onset for each trial.

For all stop trials, the peak force, i.e. the maximum force within the trial, was extracted and normalized to the participant's MVF, yielding a percentage measure. Trials with force values exceeding $\pm$ 2.5 standard

deviations from the participant's mean were considered outliers and removed from further analysis.

3.2.5 Data analysis

Phase dependency and phase precession of motor inhibition were both quantified from normalized peak force values across the four stop-signal phase bins (90°, 180°, 270°, 360°). The phase dependency analysis assessed how stopping efficacy varied across these phases, whereas phase precession was evaluated using the same procedure but within a sliding time window across the experimental session.

3.2.6 Phase dependency analysis

For each experiment, normalized peak force values were compared across the four phase bins. In Experiment 1 (SS), data violated the assumption of normality (Shapiro-Wilk test, $p < 0.05$); therefore, a Friedman test (non-parametric test for repeated measures) was used. For Experiment 1 (SF) and Experiment 2, a repeated-measures ANOVA (rm-ANOVA) was applied. Post hoc tests examined pairwise differences between phase bins. To characterize the sinusoidal modulation of inhibition, normalized peak force values were first averaged across participants within each phase bin, and a sine wave was fitted to the group means. The goodness-of-fit (R^2) was compared against a permutation-based null distribution obtained by shuffling phase labels at the individual level to assess the reliability of the modulation. The preferred phase was defined as the trough of the fitted sine wave (reflecting the phase of strongest inhibition), and the weight of the preferred phase was taken as the amplitude of the sine wave, indicating the magnitude of modulation.

3.2.7 Phase precession analysis

Phase precession was assessed by re-computing the preferred phase and weight within a sliding window across the experiment. In each window, a sine wave was fitted to normalized peak force values averaged across participants for the four phase bins, and the trough and amplitude were extracted as the preferred phase and weight, respectively. In Experiment 1, each window included at least 80 stop-signal trials (covering four phase bins, five SSDs, and two conditions: SS and SF). A final window size of 96 trials (40% of total; 16 steps of 9 trials) was used. In Experiment 2, the staircase procedure concentrated SSDs near the center of the distribution; to maintain comparability, a minimum window of 48 trials was selected, corresponding to a window size of 50 trials ($\approx$ 49.5% of total; 8 steps of 6 trials). Analyses were conducted separately for SS and SF trials.

Finally, linear-circular correlations between fitted preferred phases and trial progression were computed at the group level for SS and SF trials in both experiments. The statistical significance of the phase precession effect was determined by a nonparametric permutation test: phase labels were shuffled 10,000 times at the individual trial level to generate a null distribution, and p-values were obtained as the proportion of permutations exceeding the observed correlation coefficient. Additional analyses using different window sizes are reported in the Supplementary Information.

3.3 Results

3.3.1 Experiment 1 (tACS)

We first tested whether the phase of tACS at stop-signal onset influences inhibitory performance. Figure 3.2 (A) and (B) show the averaged SS and SF normalized peak force across stop signal phases with the best-fitting sinusoidal curve. We found a significant modulation of normalized peak force by stimulation phase for SS trials

($\chi^2(3, N = 28) = 31.757$, $p < 0.001$, Shapiro–Wilk test $p < 0.05$) and SF trials ($F(3, 81) = 3.016$, $p = 0.050$). Post-hoc Wilcoxon signed-rank tests confirmed significant pairwise differences between phases, indicating phase-dependent force modulation under tACS (see Table S3.1). Specifically, normalized peak force in SS trials was significantly lower at 90° compared to 180° ($p = 0.009$), 270° ($p < 0.001$), and 360° ($p < 0.001$). In addition, force at 180° was lower than at 270° ($p = 0.036$), while 270° showed higher force than 360° ($p = 0.031$). In SF trials, the force at 90° was significantly higher than at 180° ($p = 0.001$). Sinusoidal fits captured the phase-dependent modulation robustly (SS: $R^2 = 1.00$, $p < 0.001$; SF: $R^2 = 0.99$, $p < 0.001$), indicating significant modulation relative to a permutation-based null distribution. The trough (preferred) phases occurred at 67.3° for SS and 132.8° for SF trials, reflecting the phases of maximal inhibition.

To assess temporal changes in phase-dependent inhibition, we performed a sliding-window analysis (96 trials, 15 steps). Normalized force values were averaged across trials within each stimulation-phase bin and then across participants to determine the phase associated with the lowest force on stop trials, indexing the point of strongest inhibition. In failed stop (SF) trials, this optimal phase shifted progressively forward over the session (from approximately 120° to 300°), suggesting a gradual drift in the phase associated with maximal inhibition (Linear–circular correlations: $R = 0.887$, $p < 0.001$). This was not evident in SS (tACS) trials ($R = 0.327$, $p = 0.216$) (Figure 3.2 (C)–(D)). This pattern is held under multiple analysis windows (Figure S3.1). A permutation test with 10,000 shuffled phase labels at the individual trial level confirmed the significance of this effect in SF trials only ($p < 0.001$) (Figure S3.3).

These results suggest that under tACS, the beta phase associated with the strongest inhibitory drive shifted forward across failed inhibition trials by time, implying that error-prone states might be accompanied by preferred phase recalibration. The absence of precession in SS indicates that low-error states maintain the spike-phase relationship supporting inhibitory control.

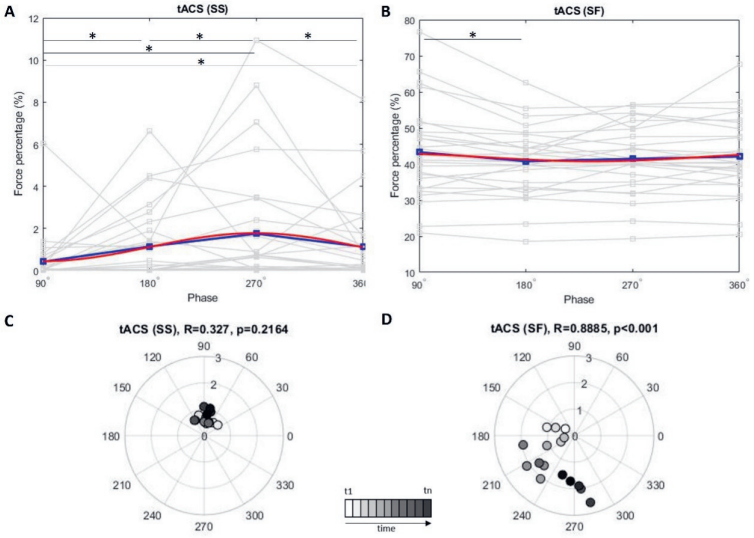


Figure 3.2: **Experiment 1**. (**A**)–(**B**), plots of peak force normalized with respect to the maximal voluntary force across tACS beta phases for stop success (SS) and stop failure (SF) trials. Gray lines represent individual data points. The blue lines indicate the average data, while the red curve shows the best-fitting sinusoidal pattern for each condition. Less force refers to greater inhibition. (**C**)–(**D**), polar plots of phase shifting of inhibition over time. Angular position represents preferred phase of inhibition, and radius represents the weight. A significant shift is observed in the SF group ($\sim$120° to $\sim$300°, $R = 0.889$, $p < 0.001$), but not the SS ($R = 0.327$, $p = 0.216$).

3.3.2 Experiment 2 (sham-tACS)

In the no-tACS experiment, we also first assessed whether inhibitory performance depends on the stop-signal phase. As shown in Figure 3.3 (A)-(B), force output during SS trials exhibited a significant phase-dependent modulation (rm-ANOVA: $F(3, 51) = 3.170$, $p = 0.05$). Post hoc comparisons revealed significantly lower force in the $90°$ bin compared to both $180°$ ($p = 0.038$) and $270°$ ($p = 0.020$, Table S3.2), suggesting enhanced inhibition when the stop signal coincided at $90°$. SF trials did not show significant phase-dependent modulation ($F(3, 51) = 0.210$, $p = 0.889$). The best-fitting sinusoidal functions showed significant phase-dependent modulation (SS: $R^2 = 1.00$, $p < 0.001$; SF: $R^2 = 1.00$, $p < 0.001$) relative to a permutation-based null distribution. Preferred trough phases were $82.5°$ for SS and $357.8°$ for SF trials, indicating maximal inhibition.

Results in Experiment 2 show successful stopping remains phase dependent with a stable optimum at $\sim 90°$. But there is no robust evidence for phase precession without stimulation. Taken together, the phase dependence of inhibition is a common property of the SS condition across experiments. The optimal beta oscillatory timing for successful stopping is stable irrespective of stimulation. SF trials showed moderate phase dependency under tACS, while no effect in the sham condition. Nevertheless, the relative phase of greatest inhibitory engagement occurred at a distinct angle compared to SS trials in both experiments, suggesting differential network recruitment between successful and failed inhibition [31]. Interestingly, SF trials in the tACS condition (Experiment 1) showed a systematic advance of the optimal phase and survived rigorous permutation testing, implying that the emergence of phase precession is specific to tACS and selectively during trials where inhibitory control fails.

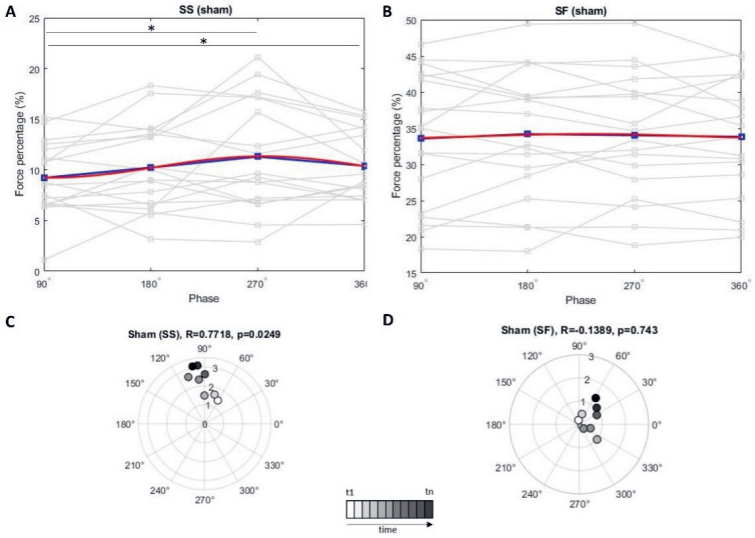


Figure 3.3: **Experiment 2**. (**A**)–(**B**), plots of normalized peak force across Fz-EEG beta phases for stop success (SS) and stop failure (SF) trials. Gray lines represent individual data points. The blue lines indicate the average data, while the red curve shows the best-fitting sinusoidal pattern for each condition. (**C**)–(**D**), polar plots of phase shifting of inhibition over time.

3.4 Discussion

The present study tested whether externally applied rhythmic stimulation can shift the optimal oscillatory phase at which inhibitory control is strongest. Our previous work showed that stopping efficiency depends on the beta phase at which the stop-signal is presented [20]. Consistent with this, we observed a robust phase dependency of inhibitory performance in both the tACS and control experiments, confirming that phase-dependent inhibition is an intrinsic property of the motor system. Importantly, during tACS, the phase associated with the strongest inhibition advanced progressively over time $\sim 180°$, and this shift was specific to stop-failed (SF) trials. No comparable effect was observed without stimulation. This pattern suggests that external rhythmic stimulation can selectively induce the precession of phase at which inhibitory control is most effective during unsuccessful inhibition, gradually altering the coupling between oscillatory activity and behavioral performance. Although our measures do not capture neuronal spiking directly, these behavioral phase shifts are consistent with a precision-like adjustment in the functional timing of inhibitory control.

3.4.1 External rhythmic stimulation alters phase preference of inhibitory control

Our work extends previous findings that beta-band stimulation can modulate motor system function at multiple levels. tACS has been shown to influence motor excitability [32, 33], alter motor performance [34, 35], and affect inhibitory control [36, 37]. Here we go beyond these observations by showing that rhythmic stimulation not only entrains oscillatory activity but can also bias the temporal phase at which inhibitory control is most effective when the brain is at an error-prone state, revealing a state-dependent modulation of oscillatory timing.

In line with [19], our findings support the notion that tACS can induce precession-like phase shifts, not only at rest but also during active motor

inhibition, with stronger effects observed during failed inhibition trials. A possible mechanistic account is that rhythmic stimulation may create network conditions conducive to precession-like dynamics, rather than directly imposing phase shifts. In hippocampal models, phase precession has been attributed to asymmetric excitation-inhibition interactions, where excitatory ramping activity gradually outpaces inhibitory feedback, causing neurons to fire at progressively earlier oscillatory phases [38]. By synchronizing membrane potential fluctuations across populations, tACS could enhance such asymmetries, effectively amplifying small phase advances that accumulate over time. In this view, rhythmic stimulation provides a temporal scaffold within which intrinsic network dynamics can reorganize, giving rise to precession-like phase advancement without direct control of spike timing.

The predominance of precession-like phase advancement during failed stops suggests that tACS interacts most effectively with networks in an adaptive, plastic state. Failed inhibition is accompanied by dopaminergic learning signals and transient reorganization of beta activity [39], reflecting ongoing error-driven updating of inhibitory control. During this phase, excitatory-inhibitory balance and oscillatory coupling likely fluctuate, placing neuronal populations within spike-timing-dependent plasticity (STDP) windows in which small timing shifts can alter synaptic strength [21, 7]. tACS, by providing a weak but consistent rhythmic input, may bias these timing relationships, promoting earlier activation on subsequent cycles and thereby amplifying endogenous phase advancement.

At the network level, failed inhibition also entails broader recruitment of fronto-basal ganglia and salience circuits [40, 31, 41, 42]. This broader and more variable network configuration introduces phase heterogeneity and reduces global phase stability, making the system more susceptible to external modulation. In such a regime, a weak periodic drive can steer the relative timing among coupled oscillators, allowing cumulative phase advances to emerge over time. By contrast, successful stopping probably engages a more phase-stable, beta-synchronized circuit that resists such perturbation. This trial-specific susceptibility

mirrors the state-dependent effects frequently reported in tACS studies [43, 44], where stimulation interacts most strongly with networks that are already dynamically engaged in adaptation or learning. Together, these properties may help to explain why precession-like dynamics were observed specifically during failed stops, when both local plasticity and large-scale network variability could create conditions favorable for tACS-induced timing shifts.

3.4.2 Broader theoretical implications

Our findings contribute to a growing theoretical framework in which phase precession serves as a general temporal coding mechanism in the brain. In the hippocampus, phase precession is thought to compress temporally extended events within individual oscillatory cycles, thereby supporting sequence learning and predictive coding [7]. By mapping sequences of experience onto the phase of an ongoing oscillation, neural systems can link distributed events across time and space into coherent representations.

A similar principle may apply to motor inhibition. During failed stops, precession-like shifts may serve to temporally compress error-related neural dynamics, enabling the system to rapidly integrate these events into adaptive control policies. Such temporal compression could enhance the salience of behavioral errors, facilitating reinforcement-based updating of inhibitory strategies. More broadly, this framework supports the idea that phase precession is not restricted to hippocampal navigation or memory but may represent a domain-general coding principle for aligning temporally distributed neural events. From this perspective, the phase advancement observed during tACS may reflect a fundamental property of neural computation, i.e., the ability to use oscillatory phase as a temporal reference frame for linking sequential events across multiple timescales. As a result, precession enables more efficient temporal alignment of error-related neural events, potentially supporting precise action-outcome encoding and rapid adaptation for following errors. This coding strategy could underlie diverse cognitive

operations, from motor adaptation and executive control to reinforcement learning and predictive processing, suggesting that oscillatory phase alignment may be a universal mechanism for temporal organization, adaptation, and plasticity in the brain.

3.4.3 Limitations and future directions

In a single stimulation session, the effects of tACS on inhibitory timing are likely transient, reflecting short-term adjustments in network synchrony and excitability. With repeated exposure, however, such phase-specific modulation could begin to engage longer-term plasticity mechanisms, leading to more stable adaptations in inhibitory control. The link between precession-like dynamics and spike-timing-dependent plasticity (STDP) supports this possibility [22, 19]: by aligning neural activity within potentiation windows, rhythmic stimulation may gradually reinforce phase relationships that enhance inhibitory performance. In this way, tACS could not only modulate ongoing oscillations but also shape the temporal organization of neural activity, potentially improving network efficiency over time. These considerations imply that tACS might serve to strengthen the individual capacity of error-based learning.

However, several limitations warrant caution. Inference about phase precession in the present study is indirect, relying on behavioral performance and modeled oscillatory phase rather than direct recordings of spiking activity. Consequently, the observed phase shifts should not be interpreted as evidence of neuronal precession but rather as macroscopic signatures of gradual temporal reorganization under rhythmic drive. Future studies combining tACS with invasive electrophysiology or high-resolution source imaging will be crucial to determine whether similar progressive phase shifts occur at the neuronal ensemble level.

An additional possibility is that the observed phase advancement arises from changes in coupling strength between the exogenous tACS field

and endogenous oscillations rather than from intrinsic timing adjustments. According to coupled-oscillator models such as the Kuramoto framework [45], dynamic fluctuations in coupling can shift the phase relationship between two oscillators without altering intrinsic spike timing. Although such a mechanism could, in principle, explain gradual phase drift, the outcome-specific pattern observed here argues against a purely coupling-based explanation: during successful-stop trials, the tACS-EEG beta phase relationship remained stable.

Future work combining rhythmic stimulation with computational modeling, MEG/EEG source reconstruction, and invasive recordings will be essential to distinguish genuine intrinsic precession from changes in network-level coupling. These approaches will also help determine whether repeated induction of precession-like shifts can produce lasting improvements in inhibitory control and behavioral flexibility, offering a pathway toward rhythm-based modulation of adaptive cognition.

3.5 Conclusion

Taken together, our results show that neuronal phase preference under tACS can shift over time during goal-directed inhibition, and that this effect is contingent on behavioral outcome. These findings suggest that phase precession is not only a biophysical phenomenon but also one shaped by cognitive demands and capable of interacting with plasticity mechanisms. More broadly, our work provides a methodological framework for probing phase dynamics in motor control and highlights the potential of outcome-contingent stimulation paradigms to harness precession as a mechanism for adaptive neuromodulation.

References

[1] Gyorgy Buzsaki and Andreas Draguhn. “Neuronal oscillations in cortical networks”. In: *Science* 304.5679 (2004), pp. 1926–1929. DOI: 10.1126/science.1099745.

[2] Christian Beste, Alexander Münchau, and Christian Frings. "Towards a systematization of brain oscillatory activity in actions". In: *Communications Biology* 6.1 (Feb. 2023). DOI: 10.1038/s42003-023-04531-9.

[3] John O'Keefe and Michael L. Recce. "Phase relationship between hippocampal place units and the EEG theta rhythm". In: *Hippocampus* 3.3 (1993), pp. 317–330. DOI: 10.1002/hipo.450030307.

[4] Matthijs A. A. van der Meer and A. David Redish. "Theta phase precession in rat ventral striatum links place and reward information". In: *Journal of Neuroscience* 31.8 (2011), pp. 2843–2854. DOI: 10.1523/JNEUROSCI.4869-10.2011.

[5] Matthew W. Jones and Matthew A. Wilson. "Phase precession of medial prefrontal cortical activity relative to the hippocampal theta rhythm". In: *Hippocampus* 15.7 (2005), pp. 867–873. DOI: 10.1002/hipo.20119.

[6] John E. Lisman and Ole Jensen. "The theta–gamma neural code". In: *Neuron* 77.6 (2013), pp. 1002–1016. DOI: 10.1016/j.neuron.2013.03.007.

[7] John Widloski and Ila R. Fiete. "A model of grid cell development through spatial exploration and spike time-dependent plasticity". In: *Neuron* 83.2 (2014), pp. 481–495. DOI: 10.1016/j.neuron.2014.06.018.

[8] Gyorgy Buzsaki and David Tingley. "Space and time: The hippocampus as a sequence generator". In: *Trends in Cognitive Sciences* 22.10 (2018), pp. 853–869. DOI: 10.1016/j.tics.2018.07.006.

[9] Magdalene I Schlesiger et al. "The medial entorhinal cortex is necessary for temporal organization of hippocampal neuronal activity". In: *Nature Neuroscience* 18.8 (June 2015), pp. 1123–1132. DOI: 10.1038/nn.4056.

[10] Salman E. Qasim, Itzhak Fried, and Joshua Jacobs. "Phase precession in the human hippocampus and entorhinal cortex". In: *Cell* 184.12 (2021), 3242–3255.e10. DOI: 10.1016/j.cell.2021.04.017.

[11] Leila Reddy et al. "Theta-phase dependent neuronal coding during sequence learning in human single neurons". In: *Nature Communications* 12.1 (2021), p. 4839. DOI: 10.1038/s41467-021-25150-0.

[12] Simal Ozen et al. "Transcranial Electric Stimulation Entrains Cortical Neuronal Populations in Rats". In: *The Journal of Neuroscience* 30.34 (Aug. 2010), pp. 11476–11485. DOI: 10.1523/jneurosci.5252-09.2010.

[13] Luke Johnson et al. "Dose-dependent effects of transcranial alternating current stimulation on spike timing in awake nonhuman primates". In: *Science Advances* 6.36 (Sept. 2020). DOI: 10.1126/sciadv.aaz2747.

[14] Matthew R. Krause et al. "Transcranial alternating current stimulation entrains single-neuron activity in the primate brain". In: *Proceedings of the National Academy of Sciences* 116.12 (Mar. 2019), pp. 5747–5755. DOI: 10.1073/pnas.1815958116.

[15] Gregor Thut, Philippe G. Schyns, and Joachim Gross. "Entrainment of Perceptually Relevant Brain Oscillations by Non-Invasive Rhythmic Stimulation of the Human Brain". In: *Frontiers in Psychology* 2 (2011). DOI: 10.3389/fpsyg.2011.00170.

[16] Christoph S. Herrmann et al. "Shaping Intrinsic Neural Oscillations with Periodic Stimulation". In: *The Journal of Neuroscience* 36.19 (May 2016), pp. 5328–5337. DOI: 10.1523/jneurosci.0236-16.2016.

[17] Jeffrey C. Magee. "Dendritic Mechanisms of Phase Precession in Hippocampal CA1 Pyramidal Neurons". In: *Journal of Neurophysiology* 86.1 (July 2001), pp. 528–532. DOI: 10.1152/jn.2001.86.1.528.

[18] Rishikesh Narayanan and Daniel Johnston. "The h Channel Mediates Location Dependence and Plasticity of Intrinsic Phase Response in Rat Hippocampal Neurons". In: *The Journal of Neuroscience* 28.22 (May 2008), pp. 5846–5860. DOI: 10.1523/jneurosci.0835-08.2008.

[19] Miles Wischnewski et al. "Induced neural phase precession through exogenous electric fields". In: *Nature Communications* 15.1 (Feb. 2024). DOI: 10.1038/s41467-024-45898-5.

[20] Zhou Fang, Alexander T. Sack, and Inge Leunissen. "The phase of tACS-entrained pre-SMA beta oscillations modulates motor inhibition". In: *NeuroImage* 290 (Apr. 2024), p. 120572. DOI: 10.1016/j.neuroimage.2024.120572.

[21] Yang Dan and Mu-ming Poo. "Spike timing-dependent plasticity: From synapse to perception". In: *Physiological Reviews* 86.3 (2006), pp. 1033–1048. DOI: 10.1152/physrev.00030.2005.

[22] Mate Lengyel et al. "Matching storage and recall: Hippocampal spike timing-dependent plasticity and phase response curves". In: *Nature Neuroscience* 8.12 (2005), pp. 1677–1683. DOI: 10.1038/nn1561.

[23] R. C. Oldfield. "The assessment and analysis of handedness: The Edinburgh inventory". In: *Neuropsychologia* 9.1 (1971), pp. 97–113. DOI: 10.1016/0028-3932(71)90067-4.

[24] Marom Bikson, Abhishek Datta, and Maged Elwassif. "Establishing safety limits for transcranial direct current stimulation". In: *Clinical Neurophysiology* 120.6 (June 2009), pp. 1033–1034. DOI: 10.1016/j.clinph.2009.03.018.

[25] A.J. Woods et al. "A technical guide to tDCS, and related non-invasive brain stimulation tools". In: *Clinical Neurophysiology* 127.2 (Feb. 2016), pp. 1031–1048. DOI: 10.1016/j.clinph.2015.11.012.

[26] A. T. Slater-Hammel. “Reliability, Accuracy, and Refractoriness of a Transit Reaction”. In: *Research Quarterly. American Association for Health, Physical Education and Recreation* 31.2 (May 1960), pp. 217–228. DOI: 10.1080/10671188.1960.10613098.

[27] James P. Coxon, Cathy M. Stinear, and Winston D. Byblow. “Intracortical Inhibition During Volitional Inhibition of Prepared Action”. In: *Journal of Neurophysiology* 95.6 (June 2006), pp. 3371–3383. DOI: 10.1152/jn.01334.2005.

[28] Inge Leunissen et al. “Reliable estimation of inhibitory efficiency: to anticipate, choose or simply react?” In: *European Journal of Neuroscience* 45.12 (June 2017). Ed. by Susan Rossell, pp. 1512–1523. DOI: 10.1111/ejn.13590.

[29] Sanne ten Oever et al. “Stimulus Presentation at Specific Neuronal Oscillatory Phases Experimentally Controlled with tACS: Implementation and Applications”. In: *Frontiers in Cellular Neuroscience* 10 (Oct. 2016). DOI: 10.3389/fncel.2016.00240.

[30] Robert Oostenveld et al. “FieldTrip: Open Source Software for Advanced Analysis of MEG, EEG, and Invasive Electrophysiological Data”. In: *Computational Intelligence and Neuroscience* 2011 (2011), pp. 1–9. DOI: 10.1155/2011/156869.

[31] Weidong Cai et al. “Dissociable Roles of Right Inferior Frontal Cortex and Anterior Insula in Inhibitory Control: Evidence from Intrinsic and Task-Related Functional Parcellation, Connectivity, and Response Profile Analyses across Multiple Datasets”. In: *The Journal of Neuroscience* 34.44 (Oct. 2014), pp. 14652–14667. DOI: 10.1523/jneurosci.3048-14.2014.

[32] Miles Wischnewski, Dennis J. L. G. Schutter, and Michael A. Nitsche. “Effects of beta-tACS on corticospinal excitability: A meta-analysis”. In: *Brain Stimulation* 12.6 (2019), pp. 1381–1389. DOI: 10.1016/j.brs.2019.07.023.

[33] Lukas Schilberg et al. “Phase of beta-frequency tACS over primary motor cortex modulates corticospinal excitability”. In: *Cortex* 103 (2018), pp. 142–152. DOI: 10.1016/j.cortex.2018.03.001.

[34] Alek Pogosyan et al. “Boosting Cortical Activity at Beta-Band Frequencies Slows Movement in Humans”. In: *Current Biology* 19.19 (Oct. 2009), pp. 1637–1641. DOI: 10.1016/j.cub.2009.07.074.

[35] Sybren Van Hoornweder et al. “The causal role of beta band desynchronization: Individualized high-definition transcranial alternating current stimulation improves bimanual motor control”. In: *NeuroImage* 312 (May 2025), p. 121222. DOI: 10.1016/j.neuroimage.2025.121222.

[36] Inge Leunissen et al. “Effects of beta-band and gamma-band rhythmic stimulation on motor inhibition”. In: *iScience* 25.5 (May 2022), p. 104338. DOI: 10.1016/j.isci.2022.104338.

[37] Tingting Zhu, Alexander T. Sack, and Inge Leunissen. “In-phase and anti-phase dual-site beta tACS differentially influence functional connectivity and motor inhibition”. In: (May 2025). DOI: 10.1101/2025.04.28.651005.

[38] Mayank R. Mehta, Albert K. Lee, and Matthew A. Wilson. “Role of experience and oscillations in transforming a rate code into a temporal code”. In: *Nature* 417.6890 (2002), pp. 741–746. DOI: 10.1038/nature00807.

[39] Henning Schroll et al. “Reinforcement magnitudes modulate subthalamic beta band activity in patients with Parkinson’s disease”. In: *Scientific Reports* 8.1 (June 2018). DOI: 10.1038/s41598-018-26887-3.

[40] Alexei Samsonovich and Bruce L. McNaughton. “Path integration and cognitive mapping in a continuous attractor neural network model”. In: *Journal of Neuroscience* 17.15 (1997), pp. 5900–5920. DOI: 10.1523/JNEUROSCI.17-15-05900.1997.

[41] Roberto Limongi and Francisco J. Pérez. "Successful and unsuccessful response inhibitions differentially affect the effective connectivity between insular, presupplementary-motor, and striatal areas." In: *Behavioral Neuroscience* 131.1 (2017), pp. 20–32. DOI: 10.1037/bne0000175.

[42] Scott JS Isherwood et al. "Multi-study fMRI outlooks on subcortical BOLD responses in the stop-signal paradigm". In: (Jan. 2025). DOI: 10.7554/elife.88652.3.

[43] Beatrix Krause and Roi Cohen Kadosh. "Not all brains are created equal: the relevance of individual differences in responsiveness to transcranial electrical stimulation". In: *Frontiers in Systems Neuroscience* 8 (2014). DOI: 10.3389/fnsys.2014.00025.

[44] Sankaraleengam Alagapan et al. "Modulation of Cortical Oscillations by Low-Frequency Direct Cortical Stimulation Is State-Dependent". In: *PLOS Biology* 14.3 (Mar. 2016). Ed. by Ole Jensen, e1002424. DOI: 10.1371/journal.pbio.1002424.

[45] Yoshiki Kuramoto. *Chemical Oscillations, Waves, and Turbulence*. Berlin: Springer, 1984. DOI: 10.1007/978-3-642-69689-3.

3.6 Supplementary information

3.6.1 Post hoc comparisons of force modulation by beta phase

3.6.2 Phase precession pattern using multiple window sizes

Phase precession plots using different window sizes for experiment 1 (tACS) and 2 (sham) are shown in S3.1 and S3.2. In the SS trials, the phase range was relatively small (60°-120°). The significant shift seen with larger time windows in this case is likely due to noise being smoothed out, rather than a meaningful underlying signal. On the other hand, in the SF trials, the phase shift was much larger (130°-300°), indicating a stronger effect than noise. Using large windows may have

Table S3.1: **Post hoc comparisons of force modulation by beta phase in Experiment 1 (tACS)**

		SS (tACS)		SF (tACS)	
		Main diff (N)	p	Main diff (N)	p
90°	180°	-2.596	0.009	-2.521	0.008
	270°	-4.600	<0.001	-1.848	0.125
	360°	-3.962	<0.001	-1.229	0.120
180°	270°	-2.095	0.036	0.637	0.444
	360°	-0.091	0.927	1.292	0.072
270°	360°	2.163	0.031	0.619	0.438

Post hoc analyses followed the Friedman test for SS and repeated-measures ANOVA for SF. No correction was applied. Bold values indicate statistically significant differences at $p < 0.05$. Significant differences were found in SS between 90° and 180°–270°–360°, 180° and 270°, and between 270° and 360° phases (Wilcoxon signed-rank tests). In SF, a significant difference was observed between 90° and 180°.

averaged out important circular changes, making the precession harder to detect.

This interpretation is supported by a permutation test, which validates that the significance shift was only observed in Experiment 1-SF (Figure S3).

3.6.3 Permutation test results

Table S3.2: **Post hoc comparisons of force modulation by beta phase in Experiment 2 (sham)**

		SS (sham)	
		Mean diff (N)	p
90°	180°	-1.017	0.116
	270°	-2.097	0.038
	360°	-1.190	0.020
180°	270°	-1.080	0.183
	360°	-0.173	0.750
270°	360°	0.907	0.223

Post hoc analyses conducted after repeated-measures ANOVA. No correction was applied. Bold values indicate statistically significant differences at $p < 0.05$. Significant differences were found only in SS between 90° and 270°–360°.

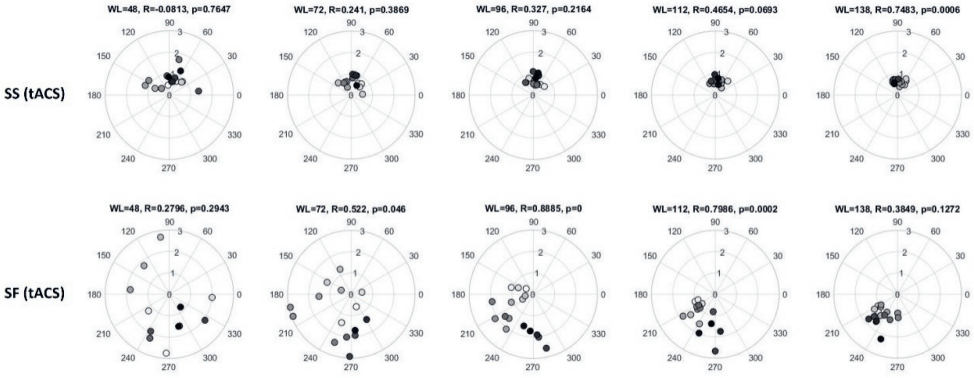


Figure S3.1: **Experiment 1.** Phase precession plots using different sliding window lengths (WL) with a fixed 16-step resolution. In some cases (e.g., WL = 48), fewer than 16 steps were available when, within a given window, one or more participants lacked SS or SF trials in every phase bin, making the phase estimation impossible.

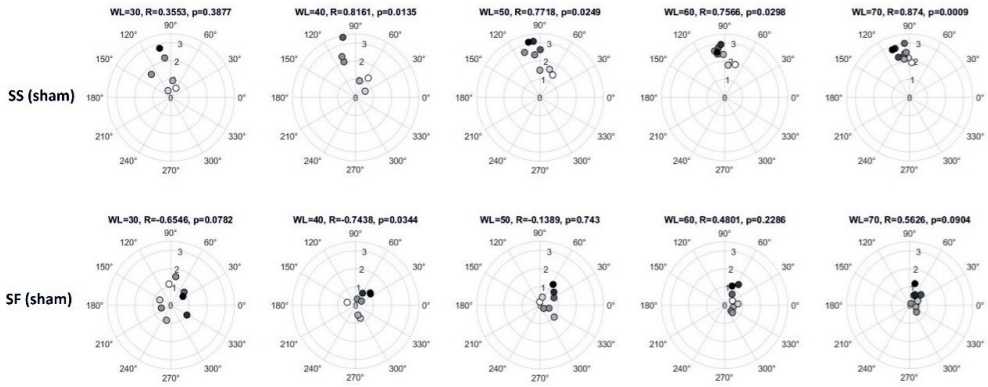


Figure S3.2: **Experiment 2.** Preferred phase precession with different sliding window lengths (WL) and a fixed 8-step resolution. In some cases, fewer than 8 steps were possible when, within a given window, one or more participants lacked SS or SF trials in any of the phase bins, making the phase estimation impossible.

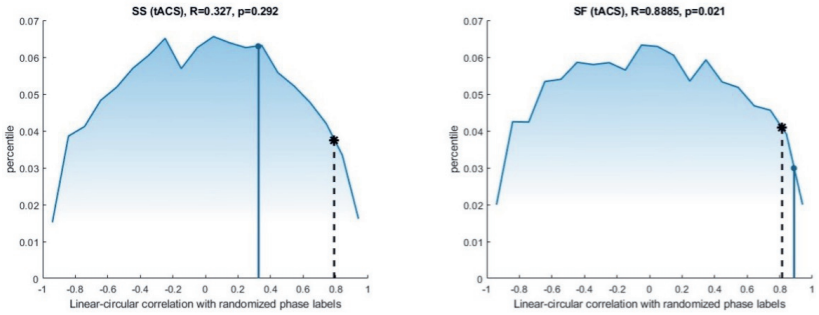


Figure S3.3: Permutation test with 10000 permutations randomizing the phase labels on linear-circular correlations between phases and force in the tACS group. The observed correlations are marked by the blue dots ($p = 0.292$ in SS (tACS) (left); $p = 0.021$ in SF (tACS) (right)). The black dashed lines with asterisks indicate the 95th percentile of the distribution. In SF (tACS) trials, the observed correlation laying beyond the 95th percentile, indicating a significant correlation between preferred phase and time points. In other trials, the observed correlation falls within the distribution, indicating a non-significant.

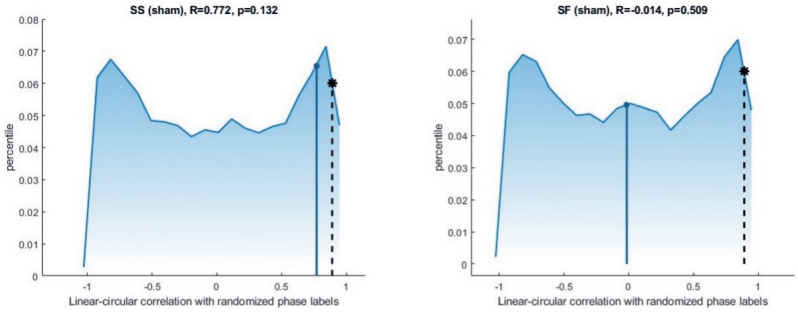
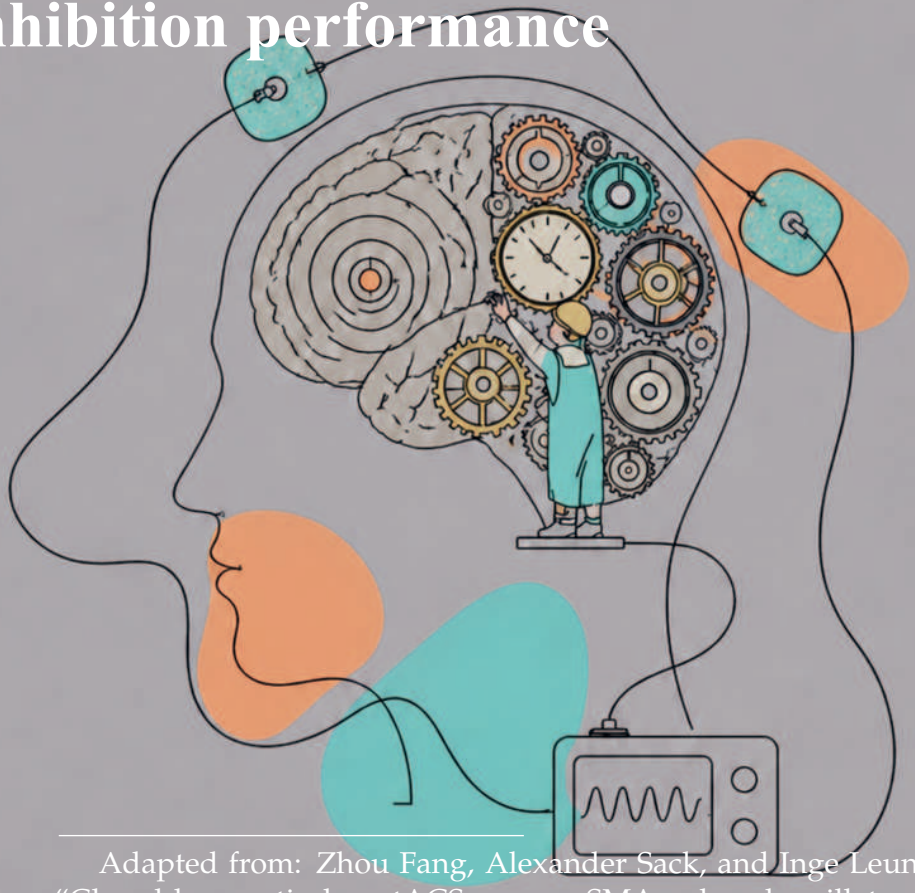


Figure S3.4: Permutation test with 10000 permutations randomizing the phase labels on linear-circular correlations between phases and force in the sham group. The observed correlations are marked by the blue dots ($p = 0.132$ in SS (sham) (left); $p = 0.509$ in SF (sham) (right)). The black dashed lines with asterisks indicate the 95th percentile of the distribution. Neither SS and SF of sham has passed the test.

4

Closed-loop anti-phase tACS over preSMA reduced oscillatory beta synchronization and modulated motor inhibition performance



Adapted from: Zhou Fang, Alexander Sack, and Inge Leunissen. "Closed-loop anti-phase tACS over preSMA reduced oscillatory beta synchronization and modulated motor inhibition performance". In: (Nov. 2025). DOI: 10.1101/2025.11.25.690566.

Abstract

Motor control depends on flexible modulation of beta-band oscillations (15-30 Hz) within cortical-basal ganglia circuits. In Parkinson's disease (PD), beta synchronization becomes pathologically elevated, contributing to motor slowing and rigidity and motivating the need for non-invasive strategies that can suppress excessive beta activity. Transcranial alternating stimulation (tACS) provides a non-invasive approach to modify endogenous oscillatory activity, yet conventional open-loop tACS typically reinforces, rather than disrupts, endogenous synchrony. Here, we developed an online adaptive EEG-guided closed-loop system that continuously tracked the instantaneous beta phase and delivered stimulation either aligned (in-phase) or 180 degrees opposed (anti-phase) to the ongoing beta rhythm. Thirty-eight right-handed healthy participants performed a stop-signal task while receiving 4×1 HD-tACS over pre-supplementary motor cortex (preSMA) in three conditions: in-phase, anti-phase, and sham.

Anti-phase tACS produced a robust suppression of beta relative to both in-phase and sham stimulation, consistent with destructive interference of the endogenous rhythm. Behaviorally, anti-phase tACS slowed the stopping process, whereas in-phase stimulation reduced peak force rate during go trials and decreased variability of the go response, consistent with increased inhibitory tone and stabilization of ongoing motor states. These results provide converging behavioral and neurophysiological evidence for destructive interference of anti-phase tACS and establish a mechanistic framework for phase-specific closed-loop neuromodulation, paving the way to implement a noninvasive therapeutic strategy aimed at desynchronizing pathological beta in Parkinson's disease.

4.1 Introduction

Neural oscillations provide a temporal framework for coordinating communication across distributed brain networks. Among these rhythms, beta oscillations (15-30 Hz) are especially central to sensorimotor control. In a healthy brain, beta oscillations naturally desynchronize during movement initiation and execution, and re-synchronize when a rapid halt is required [1, 2, 3, 4, 5, 6]. These state-dependent shifts enable flexible transitions between executing and withholding actions, and disruptions to this dynamic can have profound consequences for motor control.

Parkinson's disease (PD) provides a prominent example of such a disruption. In PD, beta synchronization within and between nodes of the cortical-basal ganglia circuit becomes pathologically elevated, and this excessive coupling is strongly associated with the severity of the bradykinesia and rigidity [7, 8, 9, 10]. Consequently, reducing pathological beta synchrony may serve as a pivotal strategy for restoring motor function in PD. Current treatments such as levodopa therapy and deep brain stimulation (DBS) indeed reduce the degree of beta synchronization [11, 12]; however, both approaches have limitations, including side effects, invasiveness, and variable efficacy over time [13, 14]. This motivates the development of non-invasive methods that can modulate pathological beta dynamics.

Transcranial alternating current stimulation (tACS) offers a non-invasive avenue for interacting with endogenous neural rhythms and has therefore gained significant interest as a potential tool for modulating beta activity. By delivering low-intensity sinusoidal currents at targeted frequencies, tACS can induce phase alignment of neuronal spiking activity [15, 16, 17] and modulate brain oscillations through a process known as entrainment [18, 19]. Enhancing beta oscillations with tACS in healthy young adults leads to reduced motor output and stronger motor inhibition [20, 21, 3, 22]. However, conventional open-loop tACS typically reinforces the oscillatory synchrony when applied for extended durations [23]. This property

fundamentally limits its therapeutic potential in PD, where the clinical objective is to reduce pathologically elevated beta. To overcome this constraint, we propose the application of tACS in anti-phase relative to the endogenous beta oscillations, leveraging phase cancellation as a mechanism to actively disrupt pathological beta synchrony.

Phase cancellation, a fundamental concept in wave physics, involves destructive interference between two waves of the same frequency but opposite phases. In neuroscience, this principle has been translated into the idea that externally applied stimulation can reduce ongoing neural oscillations when delivered in the opposite phase. Preliminary research indicates that this approach holds promise for modulating pathological neural oscillations. For example, [13] demonstrated that delivering tACS in the opposing phase to the tremor rhythm can reduce Parkinsonian tremor. Similarly, computational modelling by [24] suggests that when the phase offset between tACS and ongoing neural oscillations approaches 180 degrees, a transient reduction in oscillation amplitude occurs. With the first indications that this idea works in an experimental context at alpha frequencies [25].

Given the potential risk of inadvertently exacerbating beta synchronization in patients with Parkinson's disease (PD) if the approach proves ineffective, we first designed a proof-of-concept study in healthy volunteers. We employed a closed-loop strategy in which beta oscillations in the pre-supplementary motor area (preSMA) were monitored in real-time using electroencephalogram (EEG), and phase-locked tACS sequences were administered in response to the ongoing beta phase. Participants performed a stop-signal task [26, 27, 28], which probes both movement execution and inhibition, providing a suitable paradigm to assess motor control. This setup enabled us to investigate the impact of phase mismatches between cortical stimulation and brain oscillations on (1) endogenous beta de-/synchronization, and (2) motor performance.

As a first step, we evaluated the accuracy and precision of the closed-loop tACS system, which integrates a phase prediction method to phase-

lock tACS to brain oscillations while compensating for system delay [29, 30]. Our results revealed that the accuracy and precision of the phase locking are sufficiently high to deliver in-/anti-phase stimulation effectively. We then evaluated beta de-/synchronization and motor performance across three stimulation conditions: in-phase, anti-phase and sham. Our findings indicate that compared to the sham condition, in-phase tACS increases beta synchronization and improves motor inhibition, whereas anti-phase tACS reduces beta synchronization and disrupts inhibition. Finally, we observed a positive correlation between the degree of beta de-/entrainment induced by tACS and corresponding behavioral changes.

These findings suggest that phase-specific tACS can bidirectionally modulate beta oscillations and motor control, offering a potential non-invasive approach for disrupting pathological beta synchronization in PD. Future work should assess whether anti-phase stimulation can translate into therapeutic benefit in PD.

4.2 Methods

4.2.1 Participants

38 (16 males) healthy, right-handed (laterality range 20-100, mean 94.61) 18-35-year-old (mean age: 20.47 ± 2.54) participants were enrolled in this study. Standard screening verified that there were no contraindications for non-invasive brain stimulation [31, 32]. The study protocol was approved by the local ethical committee and all participants gave written informed consent prior to participation.

4.2.2 Experimental procedures

Figure 4.1 illustrates the general experiment procedure. During the experiment, participants underwent a single session with three different stimulation conditions. The session began with a practice block of the

stop-signal task [26, 27] including 20 go-only trials and 20 go/stop-mixed trials (detailed in the following section). Subsequently, we recorded one minute resting EEG while participants kept their eyes open and fixed on a black screen, followed by one minute of task-EEG during performance of the stop signal task. The individual beta peak frequency (IBF) was calculated based on the task-EEG and used as a stimulation frequency for closed-loop tACS (see IBF determination section for more detail). Next, the pre-supplementary motor area (preSMA) was stimulated using tACS either in-phase or anti-phase relative to the ongoing endogenous beta oscillations, based on real-time EEG monitoring. Additionally, a sham condition was included, in which only a brief, one-cycle 0.5 Hz current was applied to mimic the sensation of stimulation without effectively modulating brain activity.

Each stimulation condition commenced with a one-minute resting-state EEG while participants kept their eyes open and fixed on a black screen, followed by a block of the stop-signal task containing 50 go/stop trials with concurrent tACS stimulation applied. Within each trial, the tACS train lasted 2 seconds, with the stop-signal task trial occurring for 1 second in the middle of the stimulation period. The inter-trial interval was set to 5 seconds, during which a white fixation cross was presented on the black screen, and the ongoing EEG signal was used to calculate and predict the optimal phase for timing the onset of the next tACS sequence. This "rest and task" combination was repeated three times within the same condition, and a final one-minute of resting EEG segment was collected before concluding the stimulation block. Resulting in 150 trials (of which 50 stop trials) and about 21 minutes in each condition. The order of the go/stop trials within each block and the sequence of stimulation conditions were pseudo-randomized and counterbalanced across participants to control for order effects.

After completion of each stimulation condition, participants were given a 10-minute break and were asked to fill out a Visual Analogue Scale (VAS) questionnaire to assess stimulation-induced discomfort. The VAS consisted of a 10 cm horizontal line with two opposing limits displayed

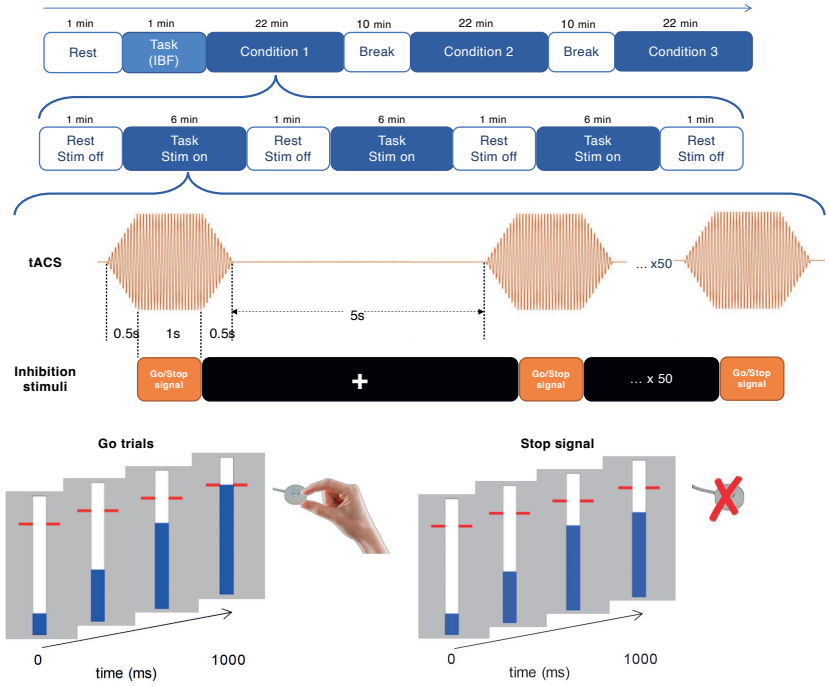


Figure 4.1: **Experimental Procedure and Stop-Signal Task Design.** Top Panel: The experimental timeline consists of three conditions (in-phase, anti-phase, and sham). Each condition includes three alternating blocks of resting EEG (1 minute) and task EEG (6 minutes) with concurrent tACS stimulation. A 10-minute break separates the conditions.
Middle Panel: Timing of tACS stimulation and stop-signal task within a trial. Stimulation lasts for 2 seconds, with the stop-signal task occurring during the middle 1 second.
Bottom Panel: Stop-signal task. In the majority of trials, participants pinch a force transducer to stop a moving visual indicator as close as possible to the target line. In stop-signal trials, the blue indicator stopped automatically before reaching the target line, serving as a cue for participants to attempt to withhold their response.

at either end of the line ("no feeling" to "strong pain/discomfort"). The total duration of an experimental session was 83 minutes.

4.2.3 Stop-signal task

Participants were asked to comfortably sit 1 meter away from the screen (refresh rate 240 Hz) and perform an anticipated version of the stop-signal task [26, 27, 33] (Figure 4.1 bottom panel). The task was adapted from the Open-Source Anticipated Response Inhibition Task (OSARI; [34]) and implemented in PsychoPy (version 2020.2.10; [35]). Modifications were made to the OSARI script to enable precise trial synchronization with the tACS stimulation, allowing for real-time alignment of task events with the stimulation protocol. Each trial began with the display of an empty bar at the center of the screen, with an indicator that progressively filled it from bottom to the top in 1000 ms. Two arrows located adjacent to the bar at the 800 ms marked the target line, the color of which changed every time at the end of the trial as feedback on their performance (green, yellow, orange, and red, indicate the distance between the indicator and the target line within 20, 40, 60, and $>$60 ms). Participants were instructed to pinch a force transducer (OMEGA Engineering, Norwalk, CT, USA) with their right index finger and thumb to stop the indicator as close to the target line as possible. The force response threshold was initially set at 25% of their maximum voluntary force (MVF), but could be reduced in 5% increments if needed, allowing participants to comfortably reach the threshold throughout the session (mean: 24.1%; range: 15%-25%). MVF was determined as the highest force recorded during three 5-second maximal strength pinches.

In 33% of the trials, known as stop trials, the bar would unexpectedly stop filling before reaching the target line. In these cases, participants were instructed to withhold pressing the sensor. A staircasing algorithm was used to adjust the stop signal delay (SSD), enforcing a 50% success rate in inhibiting responses within each condition (initial SSD 600 ms; step size 25 ms). Stop trials were considered as failed stops (SF) if the participant pressed the sensor hard enough to cross the 25% MVF

threshold or successful stops (SS) if their response remained below this threshold. Feedback on stop trials was provided through color changes in the arrows: green for SS trials and red for SF trials.

The force signal was acquired with an A/D Instruments Powerlab 26 Series (Dunedin, New Zealand) and stored on a trial-by-trial basis—from the moment the indicator began to fill until 1000 ms—using LabChart, with a sampling rate of 1000 Hz.

4.2.4 tACS

tACS was applied using a 4×1 HD-tACS (DC STIMULATOR PLUS, NeuroConn, GmbH, Ilmenau, Germany) setup. The electrodes were embedded in a gel-filled cup that was made out of plastic (⌀2cm at top, 2.5 cm at bottom, height: 1.3 cm) and mounted in an EEG cap (EASYCAP GmbH, Germany). Electrodes were placed over the preSMA, with the central electrode located at FCz and four others surrounding it at F1, F2, C1, and C2 based on the 10-20 system (Figure 4.2 A). Electrode gel (OneStep Cleargel) was filled in the cup to achieve an impedance level below 10 kΩ. Across all participants, the mean impedance averaged over channels was 7.46 ± 3.10 kΩ.

The default peak-to-peak stimulation amplitude was set at 2 mA, but it was reduced if the participant experienced discomfort. For one participant, the amplitude was set to 1.6 mA, resulting in an average intensity of 1.99 ± 0.08 mA.

In in-phase and anti-phase trials, stimulation was delivered at the individual beta frequency (IBF) measured during the stop-signal task. Each train consisted of a 0.5-second ramp-up, one second of continuous stimulation time-locked to the stop signal task trial, and a 0.5-second ramp-down. In the sham condition, a 0.5 Hz one-circle current starting at the rising phase (0∘) was employed for two seconds without ramp-up/down.

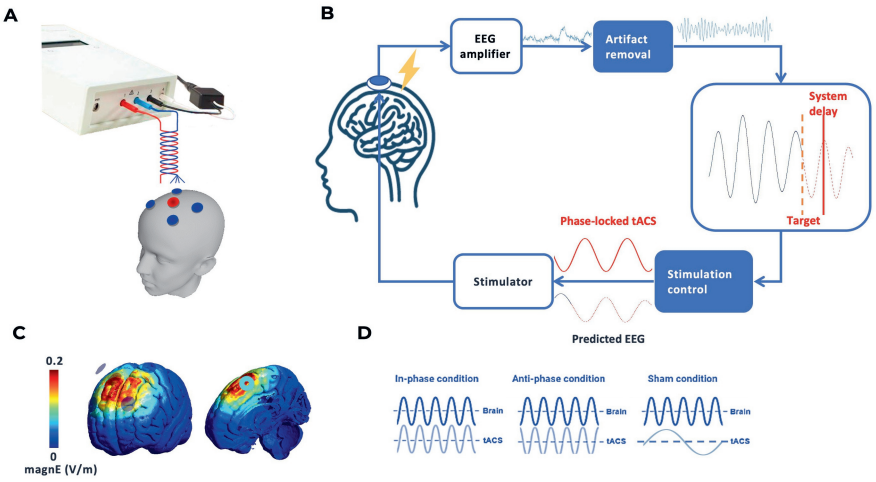


Figure 4.2: **Closed-Loop tACS-EEG System Setup.** (**A**) 4×1 tACS setup with electrodes placed over the preSMA (centered at FCz) and surrounding regions (F1, F2, C1, C2). (**B**) Real-time closed-loop tACS-EEG system workflow. EEG data from preSMA is processed to predict the phase of beta oscillations, enabling phase-locked tACS delivery synchronized with the stop-signal task. (**C**) Simulated electric field distribution. (**D**) Phase locked tACS for in-phase, anti-phase, and sham conditions.

4.2.5 EEG

EEG was recorded using the actiChamp Plus amplifier (Brain Products GmbH, Gilching, Germany) with passive Ag/AgCl electrodes secured in plastic EEG caps (EASYCAP GmbH, Germany). The EEG signal was streamed in real time via Lab stream layer (LSL) using the ActiChamp LSL Connector (sampling rate: 10000Hz) [36]. The electrode placement followed the 10-20 system for localization, with 6 electrodes positioned at Fz, FC1, FC2, Cz, A2 (reference), and Afz (ground). By applying the Onestep Cleargel from Medcat (Klazienaveen, the Netherlands), the impedance was kept below 10 kΩ. Event markers were recorded for the beginning of the trial, the stop signals, and responses.

4.2.6 Online phase-locked closed-loop tACS-EEG

IBF determination

The individual beta frequency (IBF) was determined as follows. A Laplacian montage was first applied to channel Fz by subtracting the average of surrounding channels (Cz, FC1, and FC2). The spatially filtered signal was then zero-phase FIR filtered (order 128, two-pass) in the beta frequency band (18-22 Hz) using the FieldTrip toolbox [37]. The FFT of the filtered signal was calculated with zero-padding to 4096 points, and the IBF was detected as the frequency with maximum magnitude in the spectrum [38, 39]. Across participants, the IBF was 20.07 ± 1.28 Hz (mean $\pm$ SD; n = 29).

Online EEG analysis and phase estimation

To deliver the tACS sequence with a predetermined phase with respect to endogenous beta oscillations, an online phase-locked closed-loop tACS-EEG system was established, as illustrated in Figure 4.2 B. End-to-end system delay was empirically measured and compensated in the code (Supplementary 4.6.1). The script that was used to process

the EEG data and send triggers to the tACS remote was customized in MATLAB R2022a based on the script from Shirinpour et al. [30]. A 500-ms time window was applied to the streamed data, updating with each new sample chunk (8∼12 samples every 0.01 s). The EEG data within this time window underwent the following steps: (1) re-referencing using a surface Laplacian approach, computed by subtracting the average of the surrounding electrodes from (Cz, FC1 and FC2) from the central electrode (Fz); (2) filtered by a zero-phase band-pass FIR filter in the range of IBF $\pm$ 2; (3) the signal edges were trimmed to remove filtering artifacts; and (4) the data was fed into an Autoregressive algorithm (https://github.com/OpitzLab/CL-phase/tree/master/AR), where AR coefficients were generated using the Yule-Walker method to forward-predict the beta wave (as detailed in Zrenner et al. [40]); (5) the instantaneous phase of the predicted wave was determined via the Hilbert transform; (6) once the predicted phase reached $90° \pm 5.73°$ (peak), a digital trigger was sent simultaneously to initiate the tACS sequence and Stop-signal trials via an LPT port. With a system delay of 16 ms, the phase 16 ms ahead was predicted, ensuring perfect synchronization of the task onset and phase-locked tACS sequence. To accommodate the 0.5-second ramp-up period for tACS, a corresponding 0.5-second delay was implemented in Psychopy for trial initiation, ensuring that the task period coincides with the 2-mA stabilized tACS current. The tACS onset phase for each trial was set to $90°$ for in-phase, $0°$ for sham, and $270°$ for anti-phase conditions. The performance of the closed-loop system was evaluated using measures of phase prediction accuracy, bias, and variance, as detailed in Supplementary 4.6.1.

4.2.7 EEG analysis

The EEG data were preprocessed using the FieldTrip toolbox [37] in MATLAB 2022a. Offline analyses focused on channels FC1 and FC2 based on their proximity to fronto-central regions likely associated with pre-supplementary motor area (preSMA) activity during motor inhibition [41, 42, 43], and adjacent to contralateral sensorimotor cortex

that are known generators of post-movement beta rebound (PMBR) [44].

Inter-stimulation rest EEG

EEG data were first segmented into epochs ranging from 0.1 seconds to 3 seconds after the stimulation. Preprocessing involved demeaning, detrending, and filtering. A bandpass filter (1-100 Hz) removed low-frequency drifts and high-frequency noise, while a notch filter (49-51 Hz) eliminated power line interference. Next, EEG data were re-referenced to the common average of all channels. Trials containing artifacts were detected via visual inspection and removed to preserve data integrity. The same preprocessing pipeline was applied to all conditions. EEG data of two participants were removed due to excessive noise at FC1.

We employed a wavelet-based time-frequency decomposition to analyze the spectral content of EEG signals over time. The continuous wavelet transform was applied using a frequency range of 1-45 Hz (0.5 Hz steps) and a time range of the whole epoch (0.02-second steps). The wavelet width increased linearly from 1 to 13 cycles across frequencies to balance temporal and spectral resolution. The analysis generates power spectra averaged across trials within each condition. Time-frequency representations were saved for each participant, condition (in-, anti-phase, and sham), and trial type (go (GO), stop-signal (SS), and stop-failure (SF)), for statistical analyses.

Pre/post rest EEG

The one-minute pre- and post-EEG for each condition was extracted, epoched into 1-second segments and preprocessed with the same steps as the inter-stimulation rest EEG. A fast Fourier transform (FFT) was performed using the multi-taper method with a Hanning taper. Power spectra were computed across a 1-45 Hz range with a 1 Hz frequency

resolution, and data were padded in a 10-s window to enhance spectral resolution. The resulting spectra were then averaged over epochs. The 1/f component was removed by using a log-linear fit to the power spectrum [45, 46]. Individual spectra were averaged, with the standard deviation represented illustrating variability across participants.

Task EEG

We previously demonstrated that inhibition success depends on the phase of the beta cycle at which the stop-signal is presented [47]. To investigate how tACS in- or anti-phase with respect to the endogenous beta rhythm would affect this relationship, we determined the stimulation phase at which stop signals were presented. For each trial, we computed the instantaneous phase of the in-/anti-phase tACS waveform at the moment of stop-signal onset. The analytic phase was then estimated using a Hilbert transform. Then, we categorized the stop trials (SS and SF) into 'up' or 'down' trials based on the stop signals at the 'up phase' (0∘-180∘) or 'down phase' (180∘-360∘), respectively.

To establish a reference for how beta activity normally evolves during the task in the absence of stimulation, we also analyzed task EEG data from the sham condition. The data were first segmented into epochs from 0.3 to 1.7 seconds relative to sham stimulation onset (the stop signal task duration is from 0.5 to 1.5 seconds to the stimulation). A bandpass filter (5-300 Hz) was applied to remove low-frequency drifts including the sham tACS noise and high-frequency artifacts. The following steps are similar to the aftereffects EEG data: a notch filter (49-51 Hz) was applied; bad epochs were excluded by visual detection; re-referencing based on the average of all channels; wavelet-based time-frequency decomposition was performed to generate power spectra. Time-frequency representations were categorized into: GO, SS and SF for further comparison.

4.2.8 Behavioral analysis

Force

Force data, originally recorded in volts, was converted to Newtons. A fifth-order 20 Hz low-pass Butterworth filter was applied to remove high-frequency noise, and baseline correction was performed by subtracting the average force from 400 to 150 ms before the target line. Force measures - peak force (maximum force), peak force rate (force increase rate), and onset of the force - were computed for each trial. Outliers of the force measures were defined as values exceeding 2.5 standard deviations above or below the median and were excluded. We categorized the force metrics into GO, SS, and SF trials across different stimulation conditions.

Response times

Average response times (RT) in GO and SF trials were calculated. Trials with early responses (>400 ms before the target) or omissions (>1000 ms) were considered errors and removed from both the force and RT data.

Non-parametric analysis

Stop-signal reaction time (SSRT) estimation depends on the independent race model, which assumes context independence between go and stop processes, we verified this assumption. As expected, response time on go trials (RTGOs) were longer than response times on stop-failed trials (RTSFs, Figure S4.2, [28, 48]). SSRT was estimated non-parametrically using the integration method with replacement of go omissions [28]. For each condition, we also calculated the probability of early respond go trials (P(Go errors)), go omission (P(Go omission)), successful inhibition (P(Inhibition)) and mean stop signal delay (SSD).

Parametric analysis: Bayesian modelling

To analyze the stop-signal performance data parametrically under three conditions (in-phase, anti-phase, and sham tACS), we employed the hierarchical BEESTS-CV modeling (Bayesian Ex-Gaussian Estimation of Stop-Signal RT-Context-Independence Violation) [49]. This approach is based on the horse-race model assuming that response inhibition depends on the relative finishing times of go and stop processes [50, 51]. On a stop signal trial, SS occurs if the go process takes longer to complete than the SSD and the time required for the stop process to finish. While if the go process completes faster than this combined time (SSD + stop process finishing time), SF occurs.

The go and stop runners' finishing time follows an ex-Gaussian distribution with parameters μ, σ, and τ. For each condition (in-phase, anti-phase, and sham), we estimated nine parameters per participant: μ_{go}, σ_{go}, and τ_{go} for the go process, μ_{stop}, σ_{stop}, and τ_{stop} for the stop process, PTF for the probability of trigger failures, PGF for the probability of go failures, M and S indicating the finishing time distribution (location and scale) of the go runners that were shaped by the filled-interval illusion on stop-signal trials [52]. PTF and PGF parameters were transformed into a probability scale. Considering the truncated distribution, we transformed the location and scale of the parameters into means and standard deviations. The mean go reaction time (GORT) and Stop signal reaction time (SSRT) on the population level was estimated by computing $\mu_{\text{go}} + \tau_{\text{go}}$, and $\mu_{\text{stop}} + \tau_{\text{stop}}$, from the posterior distributions.

The analysis was conducted using the EXG-SS model type of the Dynamic Models of Choice (DMC, [53]) package in the R programming environment (R Core Team, 2015). Non-hierarchical Bayesian estimation was first performed to fit individual-level data. The initial priors of the non-hierarchical fitting with down and bounds were reported in the Supplementary 4.6.4. Hierarchical fitting was then performed using the estimated parameters from the non-hierarchical fitting as

the initial values. Differential Evolution Markov Chain Monte Carlo (DE-MCMC, [54]) sampling with 100 iterations per chain was used to generate posterior distributions for each parameter. We modeled the data for each condition separately.

To evaluate the goodness of fit of the BEESTS-CV model, we employed two complementary approaches. First, we assessed the descriptive accuracy of the censored BEESTS model by simulating 1000 new data sets from the posterior distribution of participant-level parameters and comparing the predicted data against the observed data with respect to: the average cumulative distribution functions of GORTs and signal-respond RTs (SSRTs), inhibition functions, and median SSRTs across SSDs. Across all measures, the predicted data closely resembled the observed distributions (Figure S4.3, S4.4), demonstrating that the model provided a good account of the behavioral performance. Second, we examined whether the context independence assumption of the race model was satisfied by computing a delta function from the difference between the cumulative distribution functions (CDFs) of GORTs and SSRTs across different probabilities [49]. A positive and increasing delta function suggests that context independence holds. On the other hand, if the delta function is negative or decreasing, it indicates a violation of context independence. Goodness of fitness is assessed visually based on the discrepancies between the observed delta function and delta functions generated by the 1000 posterior predictive simulations. As shown in Figure S4.5, the observed delta function is positive and has a steeply increasing pattern in all conditions, meaning that the model with context independence describes the data very well.

4.2.9 Statistical analysis

All statistical analyses were carried out using R 4.5.0 (R Core Team, 2021) and Matlab R2022a (Mathworks, Natick, MA, USA).

VAS

The VAS scores of discomfort for each stimulation condition were analyzed using repeated measures ANOVA with stimulation condition as the within-subject factor (Table S4.1, S4.2).

Force outcomes

Linear mixed-effects (LME) models were used to analyze force outcomes (peak force, peak force rate, total force, onset time, and time to peak) with stimulation conditions (in-phase, anti-phase, sham) and trial type (GO, SS, and SF) as fixed factors. Random intercepts were modeled at the subject level to account for individual variability in force output, and models were fitted using restricted maximum likelihood (REML). F-statistics, degrees of freedom, and p-values of the LME result are reported. Tukey post-hoc contrasts were further examined, with p-values and estimates (mean difference $\pm$ standard error) reported. The analysis was performed in R, utilizing packages nlme 3.1-147 [55] and multcomp 1.4-13 [56], for lme model fitting, post-hoc testing, and result extraction.

To test whether stopping performance depended on the relative phase of the tACS waveform, we compared force measures between stop signals presented at the up phase (0∘-180∘) and down phase (180∘-360∘) of the stimulation cycle. Paired-samples t-tests were conducted within each stimulation condition (in-phase, anti-phase) to assess differences between up- and down-phase for both failed (SF) and successful stop (SS) trials.

Non-parametric estimates

To compare non-parametric estimates of stop-signal performance across in-, anti-phase and sham groups, we applied a Friedman test followed

by Wilcoxon signed-rank tests for P(Inhibition), as the data violated the assumption of normality (Shapiro-Wilk test $p < 0.05$). We conducted repeated measures ANOVA with post-hoc tests for the remaining dependent variables (GORT, SSRT, SFRT, SSD, P(Go errors), and P(Go omissions)).

BEESTS-CV parameters

The mean of the posterior distributions of the BEESTS model parameters in three stimulation conditions were reported with a 95% credible interval (CI; $2.5^{th} - 97.5^{th}$ percentiles). To evaluate group differences, Bayesian p-values were indicated as the proportion of samples in one group's distribution exceeding those in another, with values near 0 or 1 indicating significant shifts toward lower or higher parameter estimates, respectively. See [57] and [58] for more detail on this approach.

EEG measures

Statistical comparisons of time-frequency representations were conducted using non-parametric cluster-based permutation tests applied to: (1) inter-stimulation post-task EEG (time range: 0.25-1 s after stimulation), comparing conditions (in-phase, anti-phase, sham) both across all trial types and within each trial type (GO, SS, SF); (2) post-task EEG in the sham condition, comparing trial types (GO, SS, SF); and (3) on-task EEG in the sham condition, comparing trial types (GO, SS, SF). A Monte Carlo approach with 1000 randomizations was applied, using a significance threshold of $p < 0.05$. The design matrix accounted for within-subject dependencies, and significant clusters were outlined in the visualized results.

Paired t-tests were used to identify significant differences in IBF-centered power spectra between pre- and post-rest-EEG for each condition (in-phase, sham, and anti-phase). Significant differences ($p < 0.05$) were highlighted in the plots with shaded regions.

EEG-behavior correlations

To investigate the relationship between post-stimulation beta power and online inhibitory performance, a plausible correlation analysis was applied between posterior SSRT estimated from the BEESTS model posterior and post-stimulation EEG beta power density. Beta power was extracted within the 0.25-1 s window following stimulation and within the individualized beta frequency band (IBF $\pm$ 2 Hz), and averaged across all trials per condition. A Bayesian hierarchical approach was then used to obtain the population-level distribution of correlation coefficients. Significance was indicated by the probability that the true correlation exceeds zero ($p(r > 0)$) is larger than 0.95 or smaller than 0.05.

4.3 Results

4.3.1 Inter-stimulation EEG

All inter-stimulation EEG analyses focused on 0.25-1 s after tACS offset (2.25-3.0 s relative to tACS onset), centered on the individual beta frequency (IBF) at FC1/FC2. Statistical significance was determined using cluster-based permutation testing, with a threshold of $p < 0.05$.

Induced beta dynamics in the inter-stimulation interval

Figure 4.3 illustrates post-stimulation beta activity averaged across all trials for each condition. Figure 4.3 A shows the EEG power spectrum baseline-corrected to the end of the stimulation-free segment (4.5-4.7 s, z-score), and Figure 4.3 B shows paired t-statistic contrasts. These maps indicate that anti-phase stimulation yielded a significant reduction in beta power relative to both sham and in-phase, with clusters centered on IBF and extending up to ~ 0.95 s after stimulation offset. No significant clusters were observed for the in-phase vs. sham comparison.

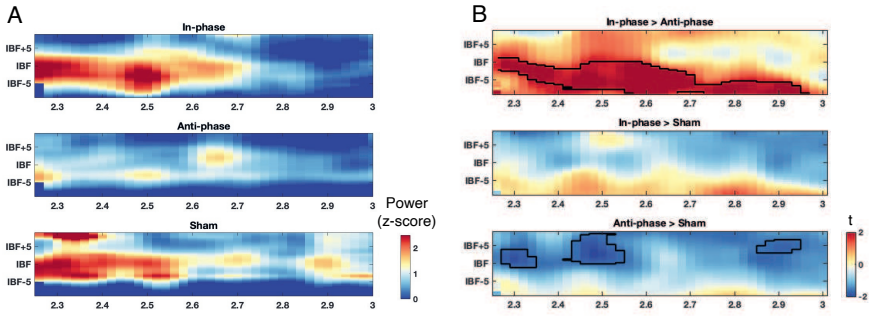


Figure 4.3: **Time-frequency representations (x: time [s], y: frequency [Hz]) of tACS aftereffects at FC1/FC2 during the inter-stimulation interval (0.25-1 s post stimulation), aligned to each participant's individual beta frequency (IBF).** (**A**) Baseline-corrected power (z-score; baseline 4.5-4.7 s) shown separately for in-phase, anti-phase, and sham. (**B**) Cluster-based paired t-contrasts ($p < 0.05$, TFCE corrected) between conditions: in-phase ¿ anti-phase, in-phase ¿ sham, and anti-phase ¿ sham. Significant clusters are outlined in black.

Phase-specific modulation of trial-type dynamics

To establish a functional baseline for trial-type comparisons, we first examined beta activity under sham stimulation (Figure 4.4). Time-frequency maps revealed significantly stronger beta activity following GO and SF trials compared to SS trials, consistent with the established association between PMBR and motor execution [59, 60, 61] (Figure 4.4 AB). In contrast, SS trials did not involve movement execution and therefore did not evoke a PMBR, but rather showed beta synchronization directly after the stop signal during stimulation (Figure 4.4 CD). This baseline analysis confirmed that movement and inhibition engage different beta dynamics, providing a reference for assessing stimulation effects.

We then examined how stimulation modulated these trial-type specific dynamics (Figure 4.5). The most robust effect was observed for anti-phase stimulation, which significantly disrupted the beta rebound

relative to sham. Following GO trials (Figure 4.5 A), anti-phase stimulation led to a marked suppression of beta activity around the IBF, lasting up to ~ 0.95 s post-stimulation (Figure 4.5 A). For SF trials, anti-phase again produced significant suppression of beta power, elicited at 0.3-0.5 s around IBF (Figure 4.5 B). For SS trials (Figure 4.5 C), anti-phase reduced stop-signal-related beta synchronization relative to sham and in-phase, with a transient effect at 0.5-0.6 s. Together, these results show that anti-phase stimulation consistently attenuates both motor- and inhibition-related beta dynamics across trial types.

4.3.2 Pre-post rest EEG results

Paired t-test between 5-second pre- and post-rest EEG power spectra (FC1/FC2) revealed a significant decrease within the frequency band of IBF$\pm$1 Hz after stimulation (Figure 4.6). This reduction was not present in the in-phase and sham conditions. Taken together, anti-phase tACS induces frequency-specific suppression of post-stimulation beta oscillations.

4.3.3 BEESTS-CV model results

The inhibitory performance in each stimulation condition was estimated based on the finishing time distributions of the 'go' and 'stop' runners, as captured by the parameter estimates from the BEESTS-CV-DMC model. Table 4.1 summarizes the posterior means and 95% credible intervals (CIs) for each model parameter across conditions, along with the difference between posterior distributions. Statistical significance is represented by Bayesian p-values, defined as the proportion of the posterior distribution of the latter condition that exceeds $(p > 0.95)$ or falls below $(p < 0.05)$ the former condition. Figure 4.7 presents the posterior distributions for each population-level parameter, aligning with the statistics in Table 4.1.

For the 'stop' process, we observed an increase in μ_{stop} in the anti-phase (196 ms) compared to the in-phase (191 ms) condition, suggesting that

anti-phase stimulation might slow the stop process. Moreover, τ_{stop} was higher in the in-phase (21 ms) condition relative to the anti-phase (12 ms). The overall SSRT remained comparable across conditions, likely due to a trade-off between μ_{stop} and τ_{stop} components. For the 'go' process, the posterior distribution of σ_{go} is significantly lower in the in-phase condition (33 ms) compared to sham (35 ms). τ_{go} was increased in both the in-phase (18 ms) and anti-phase (18 ms) conditions relative to sham (9 ms), while no significant difference was found in μ_{go}, which was translated into a significantly slower mean GORT $(\mu_{\text{go}} + \tau_{\text{go}})$ in the anti-phase conditions (823 ms) than in sham (815 ms). This pattern suggests that anti-phase tACS did not change the central tendency of the go process, but selectively increased the tail of the finishing time distribution, reflecting a higher frequency of slow responses. In contrast, in-phase tACS appeared to reduce variability of the go finishing time, yet at the same time induced more frequent slow responses.

Finally, we observed significant conditional impacts on the filled-interval illusion, as reflected in the parameters M (shift) and S (spread) of the go finishing distribution on stop-signal trials influenced by the illusion. The M parameter was lower in the in-phase condition (3.6) relative to sham (5.7), suggesting a reduced elongation of the perceived interval following stop signals. In addition, S was significantly lower in the anti-phase condition (1.07) relative to sham (1.14), reflecting reduced variability in interval estimation under anti-phase stimulation.

We did not observe significant differences in PTF and PGF across stimulation conditions. This stable likelihood for both go and stop trigger failures indicates that the observed changes in stop and go distributions are unlikely to stem from attentional fluctuations, but rather reflect changes in inhibitory efficiency caused by the stimulation [51].

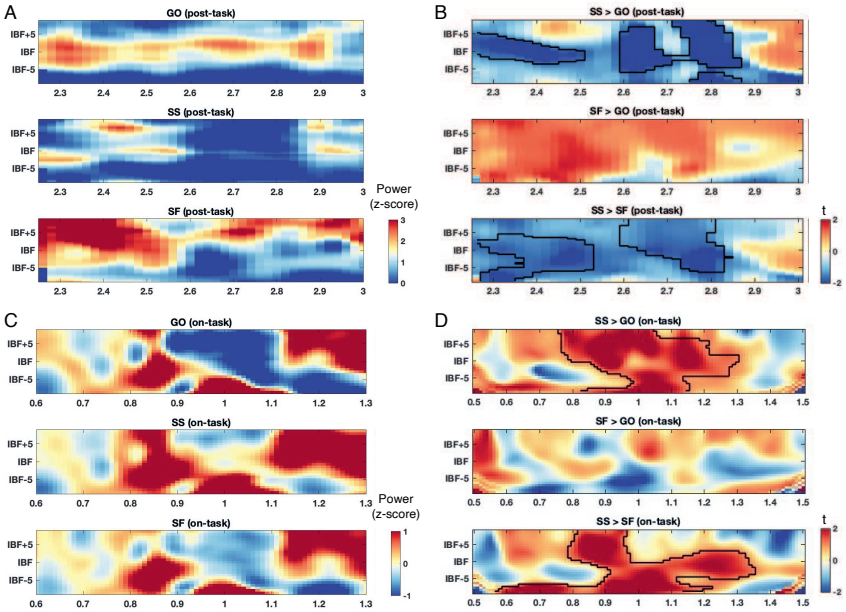


Figure 4.4: **Time-frequency representations (x: time [s], y: frequency [Hz]) at FC1/FC2, aligned to each participant's individual beta frequency (IBF).** (**A**) Post-task baseline-corrected power (z-score; baseline 4.5-4.7 s) shown separately for go, stop-successful (SS) and stop-failed (SF) trials during the inter-stimulation interval (2.1-3.0 s). (**B**) Cluster-based paired t-contrasts ($p < 0.05$, cluster corrected) of post-task EEG power between trial types (GO > SS, GO > SF, SF > SS). Significant clusters are outlined in black. (**C**) On-task baseline-corrected power (z-score; baseline 0.7-1.1 s, average stop signal presentation time = 1.1) shown separately for go, stop-successful (SS) and stop-failed (SF) trials. (**D**) Cluster-based paired t-contrasts ($p < 0.05$, cluster corrected) of on-task EEG power between trial types (GO > SS, GO > SF, SF > SS). Significant clusters are outlined in black.

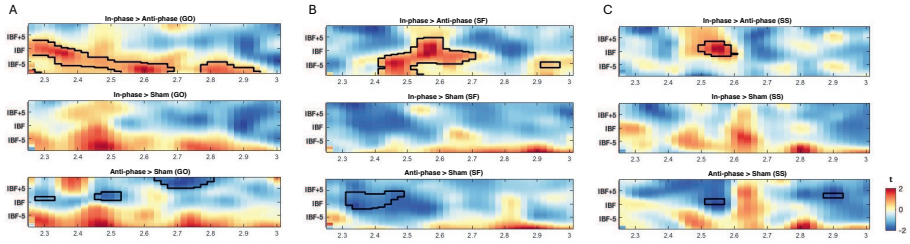


Figure 4.5: **Time-frequency representations (x: time [s], y: frequency [Hz]) for cluster-based paired t-statistic ($p < 0.05$, TFCE corrected) between conditions within each trial type. Spectrums are at FC1/FC2 during the inter-stimulation interval (2.25-3.0 s), aligned to each participant's individual beta frequency (IBF). Panels depict** (**A**) GO, (**B**) SF, and (**C**) SS trials. Rows show condition contrasts: in-phase vs anti-phase (top), in-phase vs sham (middle), and anti-phase vs sham (bottom). Significant clusters are outlined in black ($p < 0.05$).

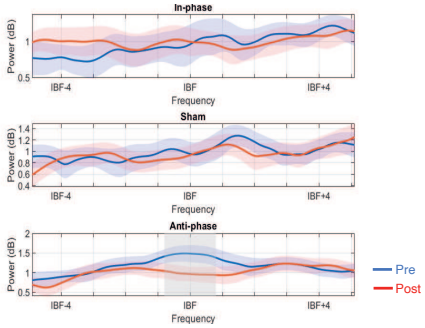


Figure 4.6: **Pre- and post-stim EEG power spectra (IBF$\pm$5 Hz) across three conditions.** Pre-spectra is in blue, and post-spectra is in red. Shaded regions represent variability ($\pm$SEM), and gray areas indicate frequency ranges with significant pre-post differences from the paired t-test. Anti-phase stimulation resulted in a significant decrease in beta power around IBF$\pm$1 Hz.

Table 4.1: **Posterior means and 95% credible intervals (CIs) of the population-level mean parameters across stimulation conditions.**

	Mean (95% CI)			In.- Anti.		In. - Sham		Anti. - Sham	
Parameter	In-phase	Anti-phase	Sham	Main diff. (95% CI)	p	Main diff.	p	Main diff.	p
P_{TF}	0.949 (-1.386-8.528)	1.899 (-1.386-11.393)	1.947 (-1.386-11.751)	1.079 (-7.845-10.613)	.587	1.173 (-7.905-11.081)	.591	0.093 (-9.990-10.637)	.505
P_{GF}	2.778 (0.370-6.861)	2.594 (0.370-5.436)	2.547 (0.370-5.723)	-0.330 (-4.852-3.487)	.462	-0.339 (-4.936-3.738)	.449	-0.009 (-3.526-3.597)	.492
μ_{stop}	191.265 (187.335-195.320)	196.216 (187.335-199.551)	192.475 (187.335-196.375)	4.951 (-0.267-10.061)	**.968***	1.210 (-4.304-6.623)	.67	-3.740 (-8.936-1.489)	.078
σ_{stop}	10.195 (3.446-17.502)	8.843 (3.446-15.118)	7.487 (3.446-13.240)	-1.352 (-11.800-8.669)	.402	-2.708 (-12.659-6.732)	.293	-1.356 (-10.390-7.455)	.385
τ_{stop}	21.437 (13.855-26.133)	12.542 (13.855-19.677)	18.898 (13.855-25.881)	-8.894 (-19.079-1.312)	**.043***	-2.539 (-12.666-9.273)	.292	6.355 (-5.295-19.312)	.853
SSRT	212.701 (204.361-219.072)	208.500 (204.361-216.505)	211.349 (204.361-219.484)	-4.202 (-15.843-7.185)	.233	-1.353 (-12.938-11.521)	.389	2.849 (-9.953-16.662)	.664
μ_{go}	801.298 (797.328-805.281)	804.326 (797.328-808.074)	805.808 (797.328-810.306)	3.028 (-2.516-8.465)	.861	4.510 (-1.460-10.669)	.933	1.482 (-4.211-7.341)	.696
σ_{go}	32.929 (31.347-34.512)	34.470 (31.347-35.967)	35.397 (31.347-36.881)	1.541 (-0.663-3.702)	.922	2.468 (0.254-4.681)	**.984***	0.927 (-1.197-3.059)	.812
τ_{go}	18.039 (15.846-20.121)	18.737 (15.846-21.460)	9.128 (15.846-13.828)	0.698 (-2.730-4.534)	.648	-8.911 (-14.085–2.457)	**.004****	-9.609 (-15.406–2.900)	**.002****
GORT	819.337 (814.760-823.786)	823.064 (814.760-827.737)	814.809 (814.760-821.470)	3.727 (-2.845-10.374)	.871	-4.527 (-12.603-4.325)	.145	-8.254 (-16.579-0.609)	**.034***
M	3.565 (1.697-5.446)	5.735 (1.697-7.800)	5.868 (1.697-7.869)	2.170 (-0.647-4.980)	.936	2.303 (-0.429-5.144)	**.952***	0.133 (-2.831-3.083)	.538
S	1.119 (1.065-1.174)	1.066 (1.065-1.115)	1.139 (1.065-1.184)	-0.053 (-0.127-0.019)	.076	0.020 (-0.052-0.089)	.715	0.073 (0.006-0.139)	**.984***

Values are reported for in-phase, anti-phase, and sham conditions. Pairwise contrasts are reported alongside the corresponding 'Main diff' (i.e., the value computed by subtracting the posterior samples of the latter condition from the former condition, such that positive values indicate higher estimates in the first condition) and Bayesian p-values (i.e., posterior probabilities that the parameter value in the second condition exceeds that in the first) indicated with $p < .05$ (*) and $p < .01$ (**).

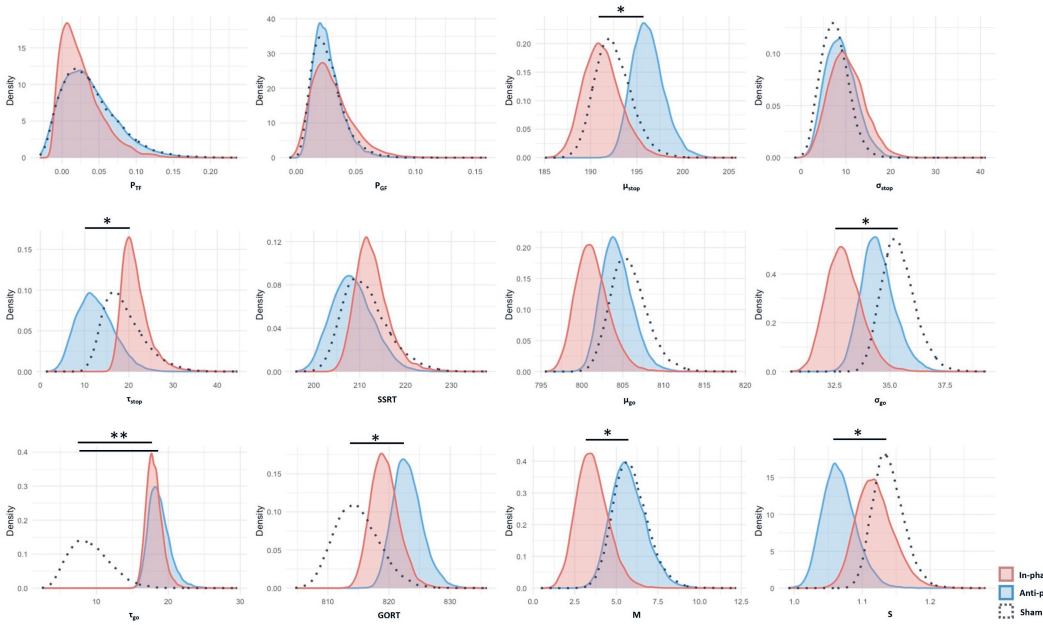


Figure 4.7: **Posterior distributions of population-level parameters estimated by the BEESTS-CV-DMC model across in-phase (red), anti-phase (blue), and sham (dot) conditions**. Asterisks indicate that the Bayesian p-values > 0.95 or < 0.05.

4.3.4 Force results

A linear mixed-effects model was conducted to examine the effects of stimulation condition (in-phase, anti-phase, and sham) on force outcomes. The analysis revealed a statistically significant main effect of stimulation on peak force rate during GO trials ($F(2, 10034) = 4.68, p < 0.001$) and on response onset time during stop-signal (SS) trials ($F(2, 2296) = 3.18, p = 0.04$; Table 4.2). Post-hoc pairwise comparisons (Tukey-HSD) revealed that in-phase elicited significantly lower peak force rate during GO trials compared with both anti-phase ($z = -2.45, p = 0.04$) and sham ($z = -2.8, p = 0.01$; $SE = 2.32$). For SS

trials, onset time was significantly longer under in-phase than sham stimulation (in-phase - sham: $z = 2.4, p = 0.04$, $SE = 2.87$).

Table 4.2: **Effect of stimulation on force measures.**

Trial type	Measures	Summary			LME statistic
		Inphase	Antiphase	Sham	Main effect
GO	Peak force (N)	30.48±9.09	30.59±9.52	30.37±9.08	F(2,10042)=2.5, p=.08
	Peak force rate (N/s)	355.57±125.33	361.6±128.85	362±156.87	**F(2,10034)=4.68, p<.001***
	Onset time (ms)	703.78±51.26	704.72±55.06	703.45±53.6	F(2,9984)=0.59, p=.56
SF	Peak force (N)	25.10±7.61	25.15±8.01	25.12±7.52	F(2,2362)=0.002, p=1
	Peak force rate (N/s)	329.32±120.86	330.11±117.46	332.88±118.8	F(2,2352)=0.89, p=.41
	Onset time (ms)	703.78±51.26	704.72±55.06	703.45±53.60	F(2,9984)=0.59, p=.56
SS	Peak force (N)	6.80±6.37	7.24±7.15	6.93±6.44	F(2,2566)=1.27, p=.28
	Peak force rate (N/s)	103.85±98.09	107.83±101.12	115.85±257.15	F(2,2744)=1.45, p=.23
	Onset time (ms)	711.5±64.05	705.45±66.51	704.68±62.16	**F(2,2296)=3.18, p=0.04***

Linear mixed-effects (LME) model results for peak force, peak force rate, and onset time across in-phase, anti-phase and sham stimulation conditions during go (GO), stop-failed (SF), and stop-successful (SS) trials. Asterisks (*) denote statistically significant effects at $p < 0.05$.

These findings suggest that in-phase tACS attenuates motor output and enhances inhibitory control, as reflected in reduced peak force rate during voluntary responses and delayed response onset during inhibition.

4.3.5 Correlations between beta power and behavioral measures

Plausible correlation analysis (SSRT-beta power)

To assess the relationship between post-stimulation beta power and the SSRT posterior estimates from the BEESTS model, we employed a plausible correlation analysis using Bayesian hierarchical modeling that accounts for individual-level uncertainty and provides a population-level distribution of correlation coefficients. The result revealed a reliable negative association in both sham and in-phase stimulation between SSRT and post-stimulation beta power (Figure 4.8). Specifically, participants eliciting stronger post-stimulation beta power tended to exhibit shorter SSRTs (sham: $r = -0.221$, 95% CI $[-0.461, -0.040]$, $p = 0.048$;

In-phase: $r = -0.265$, 95% CI $[-0.505, 0.003]$, $p = 0.027$). In contrast, no significant correlations were observed in the anti-phase.

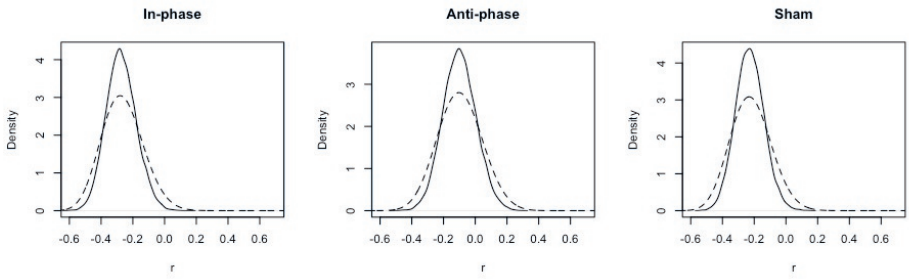


Figure 4.8: **Posterior density estimates of plausible correlations (r) between IBF $\pm$ 2 EEG power and hierarchical SSRT.** Solid lines represent the individual-level plausible correlation distributions, and dashed lines represent the population-level posterior distributions obtained using a uniform prior ($\kappa = 1$).

These correlations suggest that enhanced beta synchronization during the post-stimulation phase is linked to faster stopping processes. While anti-phase tACS may disrupt the natural relation between inhibitory efficiency and post-movement cortical beta dynamics.

4.3.6 Phase-dependency of inhibition performance

To examine whether in-phase versus anti-phase tACS influences the relationship between stop-signal presentation phase and inhibitory control, we conducted paired t-tests comparing peak force on stop trials (SS and SF) between stop signals delivered at the down versus up phases of the online tACS waveform. Building on our previous finding that inhibition success depends on the phase of the endogenous beta cycle at which the stop signal is processed [47], this analysis tested whether externally aligning or misaligning tACS with that rhythm modulates the phase-specific effect.

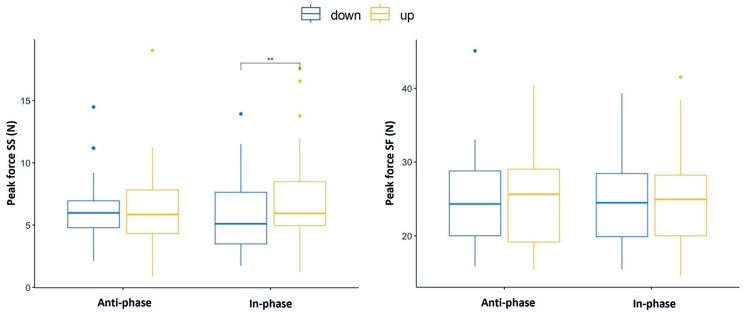


Figure 4.9: **Box plots of peak force (N) at the up and down phases on SS and SF trials under in- and anti-phase tACS stimulation.** Down and up phases refer to the tACS waveform at the time of the stop signal presentation, respectively. The double asterisk (**) indicates a significant difference between up and down stop signal phases ($p = 0.005$).

The analysis revealed a significant phase-dependent modulation of peak force during SS trials exclusively under in-phase tACS: peak force was significantly lower when the stop signal occurred at the down phase compared to the up phase of the stimulation waveform ($t(32) = -3.04$; $p = 0.005$) (Figure 4.9). By contrast, anti-phase tACS did not produce any phase-dependent effects on peak force in SS trials ($t(32) = -0.16$, $p = 0.88$), nor were significant differences observed in SF trials under either stimulation condition (In-phase: $t(32) = -0.79$, $p = 0.43$; Anti-phase: $t(32) = 0.03$, $p = 0.97$). The in-phase results closely replicate our prior finding [47] that inhibition is strongest when the stop signal coincides with the preferred phase of the beta oscillation, suggesting that in-phase tACS preserves this stable phase relationship. In contrast, anti-phase stimulation appears to disrupt this alignment, attenuating the phase-dependent modulation of inhibitory control.

4.4 Discussion

Pathologically elevated beta synchronization is a defining neurophysiological feature of Parkinson's disease (PD) and a key therapeutic target

for neuromodulation [62]. Motivated by this need to suppress aberrant oscillatory coupling, we developed a closed-loop tACS-EEG system delivering stimulation precisely aligned, or opposed in phase, to ongoing beta activity in the pre-supplementary motor area (preSMA). Using this approach, we investigated how phase-specific stimulation influences neural dynamics and motor inhibition. Our findings demonstrate that anti-phase tACS disrupts beta synchronization and modulates motor inhibition performance, mirroring the therapeutic goal in PD treatment.

4.4.1 Phase-specific effects of closed-loop tACS on beta synchrony

TACS can entrain neural activity and modulate oscillatory power in a frequency- and phase-specific manner [15, 16, 17, 18, 19, 63, 64]. Recent work highlights that the phase relationship between externally applied currents and intrinsic rhythms determines whether stimulation amplifies or disrupts oscillatory activity [24, 25, 65, 66]. In vitro, in-phase fields promote synchrony, whereas out-of-phase fields reduce it [67, 68]. Clinically, phase-locked tACS applied at the tremor frequency has been shown to suppress tremor [13].

In line with these predictions, our inter-stimulation EEG analyses revealed robust suppression of beta power following anti-phase tACS compared with both sham and in-phase stimulation, with effects centered around the individual beta frequency. This attenuation likely reflects destructive interference, whereby stimulation delivered in the opposite phase counteracts ongoing oscillatory activity. This suppression may represent the destructive counterpart of an outlasting 'echo' of tACS entrainment [69].

By contrast, in-phase tACS did not significantly increase beta power, likely due to the short stimulation trains (2 s including 0.5 s ramp-up/down), which may have limited entrainment accumulation. Nevertheless, subtle behavioral modulations emerged under in-phase tACS,

including reduced peak force and lower response variability during movement.

4.4.2 Ongoing brain state shapes the phase effects

In line with numerous previous studies, our sham-condition EEG analyses replicated well-established task-related beta patterns: (1) a stop-signal-locked beta increase associated with successful inhibition [70, 71, 3], and (2) a post-movement beta enhancement following GO and SF trials, reflecting a re-establishment of the motor state after voluntary movement [59, 60, 72, 61]. Going and stopping rely on partly distinct networks: go responses engage motor and premotor regions, whereas stopping recruits the rIFG-preSMA-STN inhibitory circuit [73, 74, 75]. Failed stops instead involve enhanced rAI-preSMA coupling linked to salience monitoring [76, 77].

Across all trial types, anti-phase tACS reduced post-stimulation beta power, consistent with destructive interference. This effect was strongest in GO and SF trials, where stimulation ended during the natural beta rebound, producing a desynchronization "echo". In contrast, in successful stops (SS), beta re-synchronizes earlier, time-locked to the stop signal occurring during stimulation, leaving fewer active dynamics to be disrupted. The modest desynchronization in SS trials may also reflect compensatory overshoot or recruitment of alternative networks to sustain inhibition [78, 79, 80]. These observations align with prior work showing that tACS effects are state-dependent, varying with ongoing neural activity and task engagement [81, 82, 83]. Anti-phase stimulation thus most effectively disrupts beta synchrony when delivered during strong endogenous coupling.

4.4.3 Behavioral consequences of phase-specific tACS

Beyond the neural effects, stimulation also modulated behavior. Consistent with the observed beta desynchronization, anti-phase tACS

impaired inhibitory control, as reflected in a higher μ_{stop} estimated with the BEESTS model. Because μ_{stop} represents the mean of the Gaussian component of the stop-signal reaction time (SSRT) distribution, it captures the typical latency of the stopping process. An increase in μ_{stop} therefore indicates slower and less efficient inhibition, supporting the view that beta synchrony facilitates rapid stopping. However, neither the overall SSRT derived from the integration method nor the BEESTS-estimated mean SSRT differed significantly across conditions, implying that compensatory mechanisms (e.g., proactive slowing or adaptive plasticity in fronto-basal ganglia circuits) may have helped to maintain performance despite local beta disruption. Importantly, the correlation between post-stimulation beta power and SSRT that was evident in the sham and in-phase conditions was absent during anti-phase stimulation, suggesting that anti-phase tACS disrupted the normal coupling between cortical beta synchronization and inhibitory efficiency.

In a similar way, anti-phase stimulation also abolished the phase-dependent modulation of stopping that was observed when stimulation was aligned with ongoing beta activity. Peak force on stop trials was lower when the stop signal coincided with the down phase of the in-phase waveform, but this modulation was not present when the phase relationship was reversed. This mirrors our prior finding that inhibition efficiency depends on the phase of the stimulation waveform at which the stop signal occurs [47]. Together, these observations suggest that aligning stimulation with endogenous beta preserves functional phase relationships, whereas misalignment disrupts the propagation of stop signals through the network.

In-phase tACS reduced the rate of force in go trials and showed delayed force onset in successful stops. The reduction in peak force rate resembles earlier findings that beta-frequency stimulation can act as an active "brake" on the motor system [20, 21, 3], potentially reflecting a transient increase in inhibitory tone or reduced corticospinal drive. At the same time, in-phase stimulation decreased σ_{go}, indicating lower variability in go-process finishing times and the increased τ_{go}. This pattern could suggest a stabilization of internal response timing, i.e., less

trial-to-trial variability, but occasional longer responses when flexibility was required. Such an effect would be consistent with proposals that beta activity contributes to the maintenance of ongoing sensorimotor states and temporal regularity [5, 4, 84, 6]. However, the precise functional contribution of beta remains debated, and these findings could also arise from enhanced timing precision, altered temporal weighting, or other network-level adjustments induced by stimulation. Thus, while in-phase stimulation appears to have modulated both the strength and stability of motor responses, the relative contribution of inhibitory versus stabilizing mechanisms cannot yet be fully dissociated.

4.4.4 Implications and limitations

These findings provide causal evidence that phase alignment governs the behavioral impact of brain stimulation. By demonstrating that identical stimulation can either impair or facilitate inhibition depending on its phase relation to ongoing beta activity, the results highlight the importance of timing stimulation to the brain's intrinsic dynamics.

Several limitations should be acknowledged. First, our primary neurophysiological analyses focused on the after-effects of stimulation. While these after-effects suggest sustained modulation, our results were largely blind to the immediate, online impact of tACS on neural oscillations. Second, we employed only two phase conditions, in-phase and anti-phase, which limits our ability to precisely map the full spectrum of phase-dependent effects. Finally, the efficacy of tACS can vary significantly across individuals due to distinct coupling strengths to external stimulation. Future research should account for these individual differences, exploring optimized stimulation durations and intensities to enhance precision and efficacy.

Despite these constraints, the results provide a mechanistic framework for state- and phase-dependent brain stimulation. In clinical contexts such as Parkinson's disease, where excessive beta synchrony

impairs movement, anti-phase stimulation could be leveraged to transiently desynchronize pathological rhythms, whereas in-phase or phase-adaptive approaches may help restore deficient coupling in other contexts. Ultimately, closed-loop tACS offers a promising route toward individualized, temporally precise neuromodulation that aligns intervention with the brain's natural oscillatory architecture.

4.5 Conclusion

This study shows that the behavioral impact of beta-frequency tACS depends critically on its phase alignment with ongoing neural activity. Anti-phase tACS disrupted beta synchrony and impaired inhibitory control. In contrast, phase-aligned stimulation modulated go performance through reduced force output and lower response variability, consistent with increased inhibitory tone and greater temporal stability. These findings offer mechanistic insight into how the precise timing of stimulation relative to intrinsic neural dynamics governs its functional outcome. Moreover, they establish a framework for individualized, temporally adaptive neuromodulation that could serve as a non-invasive therapeutic approach to desynchronize pathological beta activity in Parkinson's disease.

References

[1] Jan R. Wessel and Adam R. Aron. "Unexpected Events Induce Motor Slowing via a Brain Mechanism for Action-Stopping with Global Suppressive Effects". In: *The Journal of Neuroscience* 33.47 (Nov. 2013), pp. 18481–18491. DOI: 10.1523/jneurosci.3456-13.2013.

[2] Michael Schaum et al. "Right inferior frontal gyrus implements motor inhibitory control via beta-band oscillations in humans". In: *eLife* 10 (Mar. 2021). DOI: 10.7554/elife.61679.

[3] Inge Leunissen et al. "Effects of beta-band and gamma-band rhythmic stimulation on motor inhibition". In: *iScience* 25.5 (May 2022), p. 104338. DOI: 10.1016/j.isci.2022.104338.

[4] Bjørg Elisabeth Kilavik et al. "The ups and downs of beta oscillations in sensorimotor cortex". In: *Experimental Neurology* 245 (July 2013), pp. 15–26. DOI: 10.1016/j.expneurol.2012.09.014.

[5] Andreas K Engel and Pascal Fries. "Beta-band oscillations — signalling the status quo?" In: *Current Opinion in Neurobiology* 20.2 (Apr. 2010), pp. 156–165. DOI: 10.1016/j.conb.2010.02.015.

[6] Jacopo Barone and Holly E. Rossiter. "Understanding the Role of Sensorimotor Beta Oscillations". In: *Frontiers in Systems Neuroscience* 15 (May 2021). DOI: 10.3389/fnsys.2021.655886.

[7] A. A. Kuhn et al. "High-Frequency Stimulation of the Subthalamic Nucleus Suppresses Oscillatory Activity in Patients with Parkinson's Disease in Parallel with Improvement in Motor Performance". In: *Journal of Neuroscience* 28.24 (June 2008), pp. 6165–6173. DOI: 10.1523/jneurosci.0282-08.2008.

[8] S. Little et al. "Beta band stability over time correlates with Parkinsonian rigidity and bradykinesia". In: *Experimental Neurology* 236.2 (Aug. 2012), pp. 383–388. DOI: 10.1016/j.expneurol.2012.04.024.

[9] Chiung Chu Chen et al. "Complexity of subthalamic 13-35Hz oscillatory activity directly correlates with clinical impairment in patients with Parkinson's disease". In: *Experimental Neurology* 224.1 (July 2010), pp. 234–240. DOI: 10.1016/j.expneurol.2010.03.015.

[10] Jon B. Toledo et al. "High beta activity in the subthalamic nucleus and freezing of gait in Parkinson's disease". In: *Neurobiology of Disease* 64 (Apr. 2014), pp. 60–65. DOI: 10.1016/j.nbd.2013.12.005.

[11] Prashant Tiwari et al. “Evidences of possible side effects of neuroleptic drugs: A systematic review”. In: *Asian Pacific Journal of Reproduction* 1.4 (Dec. 2012), pp. 330–336. DOI: 10.1016/s2305-0500(13)60105-0.

[12] N.J. Ray et al. “Local field potential beta activity in the subthalamic nucleus of patients with Parkinson’s disease is associated with improvements in bradykinesia after dopamine and deep brain stimulation”. In: *Experimental Neurology* 213.1 (Sept. 2008), pp. 108–113. DOI: 10.1016/j.expneurol.2008.05.008.

[13] John-Stuart Brittain, Andrew Sharott, and Peter Brown. “The highs and lows of beta activity in cortico-basal ganglia loops”. In: *European Journal of Neuroscience* 39.11 (Apr. 2014), pp. 1951–1959. DOI: 10.1111/ejn.12574.

[14] Kai-Hsiang Stanley Chen and Robert Chen. “Invasive and Noninvasive Brain Stimulation in Parkinson’s Disease: Clinical Effects and Future Perspectives”. In: *Clinical Pharmacology & Therapeutics* 106.4 (July 2019), pp. 763–775. DOI: 10.1002/cpt.1542.

[15] Simal Ozen et al. “Transcranial Electric Stimulation Entrains Cortical Neuronal Populations in Rats”. In: *The Journal of Neuroscience* 30.34 (Aug. 2010), pp. 11476–11485. DOI: 10.1523/jneurosci.5252-09.2010.

[16] Luke Johnson et al. “Dose-dependent effects of transcranial alternating current stimulation on spike timing in awake nonhuman primates”. In: *Science Advances* 6.36 (Sept. 2020). DOI: 10.1126/sciadv.aaz2747.

[17] Matthew R. Krause et al. “Transcranial alternating current stimulation entrains single-neuron activity in the primate brain”. In: *Proceedings of the National Academy of Sciences* 116.12 (Mar. 2019), pp. 5747–5755. DOI: 10.1073/pnas.1815958116.

[18] Gregor Thut, Philippe G. Schyns, and Joachim Gross. "Entrainment of Perceptually Relevant Brain Oscillations by Non-Invasive Rhythmic Stimulation of the Human Brain". In: *Frontiers in Psychology* 2 (2011). DOI: 10.3389/fpsyg.2011.00170.

[19] Christoph S. Herrmann et al. "Shaping Intrinsic Neural Oscillations with Periodic Stimulation". In: *The Journal of Neuroscience* 36.19 (May 2016), pp. 5328–5337. DOI: 10.1523/jneurosci.0236-16.2016.

[20] Alek Pogosyan et al. "Boosting Cortical Activity at Beta-Band Frequencies Slows Movement in Humans". In: *Current Biology* 19.19 (Oct. 2009), pp. 1637–1641. DOI: 10.1016/j.cub.2009.07.074.

[21] Raed A. Joundi et al. "Driving Oscillatory Activity in the Human Cortex Enhances Motor Performance". In: *Current Biology* 22.5 (Mar. 2012), pp. 403–407. DOI: 10.1016/j.cub.2012.01.024.

[22] Jane Tan et al. "The Effects of Dual-Site Beta tACS over the rIFG and preSMA on Response Inhibition in Young and Older Adults". In: (Dec. 2022). DOI: 10.1101/2022.11.30.518460.

[23] Anke Karabanov, Axel Thielscher, and Hartwig Roman Siebner. "Transcranial brain stimulation: closing the loop between brain and stimulation". In: *Current Opinion in Neurology* 29.4 (Aug. 2016), pp. 397–404. DOI: 10.1097/wco.0000000000000342.

[24] Matthew R. Krause et al. "Brain stimulation competes with ongoing oscillations for control of spike timing in the primate brain". In: *PLOS Biology* 20.5 (May 2022). Ed. by Huan Luo, e3001650. DOI: 10.1371/journal.pbio.3001650.

[25] Xueli Chen et al. "Alpha oscillatory activity is causally linked to working memory retention". In: *PLOS Biology* 21.2 (Feb. 2023). Ed. by Simon Hanslmayr, e3001999. DOI: 10.1371/journal.pbio.3001999.

[26] A. T. Slater-Hammel. “Reliability, Accuracy, and Refractoriness of a Transit Reaction”. In: *Research Quarterly. American Association for Health, Physical Education and Recreation* 31.2 (May 1960), pp. 217–228. DOI: 10.1080/10671188.1960.10613098.

[27] James P. Coxon, Cathy M. Stinear, and Winston D. Byblow. “Intracortical Inhibition During Volitional Inhibition of Prepared Action”. In: *Journal of Neurophysiology* 95.6 (June 2006), pp. 3371–3383. DOI: 10.1152/jn.01334.2005.

[28] Frederick Verbruggen et al. “A consensus guide to capturing the ability to inhibit actions and impulsive behaviors in the stop-signal task”. In: *eLife* 8 (Apr. 2019). DOI: 10.7554/elife.46323.

[29] Takayuki Onojima and Keiichi Kitajo. “A closed-loop stimulation approach with real-time estimation of the instantaneous phase of neural oscillations by a Kalman filter”. In: (Apr. 2021). DOI: 10.1101/2021.04.25.441309.

[30] Sina Shirinpour et al. “Experimental evaluation of methods for real-time EEG phase-specific transcranial magnetic stimulation”. In: *Journal of Neural Engineering* 17.4 (July 2020), p. 046002. DOI: 10.1088/1741-2552/ab9dba.

[31] Marom Bikson, Abhishek Datta, and Maged Elwassif. “Establishing safety limits for transcranial direct current stimulation”. In: *Clinical Neurophysiology* 120.6 (June 2009), pp. 1033–1034. DOI: 10.1016/j.clinph.2009.03.018.

[32] A.J. Woods et al. “A technical guide to tDCS, and related non-invasive brain stimulation tools”. In: *Clinical Neurophysiology* 127.2 (Feb. 2016), pp. 1031–1048. DOI: 10.1016/j.clinph.2015.11.012.

[33] Inge Leunissen et al. “Reliable estimation of inhibitory efficiency: to anticipate, choose or simply react?” In: *European Journal of Neuroscience* 45.12 (June 2017). Ed. by Susan Rossell, pp. 1512–1523. DOI: 10.1111/ejn.13590.

[34] Jason L. He et al. “OSARI, an Open-Source Anticipated Response Inhibition Task”. In: *Behavior Research Methods* 54.3 (Nov. 2021), pp. 1530–1540. DOI: 10.3758/s13428-021-01680-9.

[35] Jonathan Peirce et al. “PsychoPy2: Experiments in behavior made easy”. In: *Behavior Research Methods* 51.1 (Feb. 2019), pp. 195–203. DOI: 10.3758/s13428-018-01193-y.

[36] Christian Kothe et al. “The Lab Streaming Layer for Synchronized Multimodal Recording”. In: *Imaging Neuroscience* 3 (2025), IMAG.a.136. DOI: 10.1162/IMAG.a.136.

[37] Robert Oostenveld et al. “FieldTrip: Open Source Software for Advanced Analysis of MEG, EEG, and Invasive Electrophysiological Data”. In: *Computational Intelligence and Neuroscience* 2011 (2011), pp. 1–9. DOI: 10.1155/2011/156869.

[38] Farrokh Mansouri et al. “A Fast EEG Forecasting Algorithm for Phase-Locked Transcranial Electrical Stimulation of the Human Brain”. In: *Frontiers in Neuroscience* 11 (July 2017). DOI: 10.3389/fnins.2017.00401.

[39] Aqsa Shakeel, Toshihisa Tanaka, and Keiichi Kitajo. “Time-Series Prediction of the Oscillatory Phase of EEG Signals Using the Least Mean Square Algorithm-Based AR Model”. In: *Applied Sciences* 10.10 (May 2020), p. 3616. DOI: 10.3390/app10103616.

[40] Christoph Zrenner et al. “Real-time EEG-defined excitability states determine efficacy of TMS-induced plasticity in human motor cortex”. In: *Brain Stimulation* 11.2 (Mar. 2018), pp. 374–389. DOI: 10.1016/j.brs.2017.11.016.

[41] Hanne Schevernels et al. “Electrophysiological evidence for the involvement of proactive and reactive control in a rewarded stop-signal task”. In: *NeuroImage* 121 (Nov. 2015), pp. 115–125. DOI: 10.1016/j.neuroimage.2015.07.023.

[42] Matthias Liebrand et al. “Temporal Dynamics of Proactive and Reactive Motor Inhibition”. In: *Frontiers in Human Neuroscience* 11 (Apr. 2017). DOI: 10.3389/fnhum.2017.00204.

[43] Jan R. Wessel. "beta-Bursts Reveal the Trial-to-Trial Dynamics of Movement Initiation and Cancellation". In: *The Journal of Neuroscience* 40.2 (Nov. 2019), pp. 411–423. DOI: 10.1523/jneurosci.1887-19.2019.

[44] Pasquale Cardellicchio et al. "Beta Rebound as an Index of Temporal Integration of Somatosensory and Motor Signals". In: *Frontiers in Systems Neuroscience* 14 (Sept. 2020). DOI: 10.3389/fnsys.2020.00063.

[45] Saskia Haegens et al. "Inter- and intra-individual variability in alpha peak frequency". In: *NeuroImage* 92 (May 2014), pp. 46–55. DOI: 10.1016/j.neuroimage.2014.01.049.

[46] V.V. Nikulin and T. Brismar. "Phase synchronization between alpha and beta oscillations in the human electroencephalogram". In: *Neuroscience* 137.2 (Jan. 2006), pp. 647–657. DOI: 10.1016/j.neuroscience.2005.10.031.

[47] Zhou Fang, Alexander T. Sack, and Inge Leunissen. "The phase of tACS-entrained pre-SMA beta oscillations modulates motor inhibition". In: *NeuroImage* 290 (Apr. 2024), p. 120572. DOI: 10.1016/j.neuroimage.2024.120572.

[48] Patrick G Bissett et al. "Design issues and solutions for stop-signal data from the Adolescent Brain Cognitive Development (ABCD) study". In: *eLife* 10 (Mar. 2021). DOI: 10.7554/elife.60185.

[49] Dora Matzke et al. "Stopping timed actions." In: (Mar. 2021). DOI: 10.31234/osf.io/9h3v7.

[50] Dora Matzke et al. "Bayesian parametric estimation of stop-signal reaction time distributions." In: *Journal of Experimental Psychology: General* 142.4 (Nov. 2013), pp. 1047–1073. DOI: 10.1037/a0030543.

[51] Dora Matzke, Jonathon Love, and Andrew Heathcote. "A Bayesian approach for estimating the probability of trigger failures in the stop-signal paradigm". In: *Behavior Research Methods* 49.1 (Jan. 2016), pp. 267–281. DOI: 10.3758/s13428-015-0695-8.

[52] Robert Evan Ornstein. *On the Experience of Time*. Harmondsworth, England: Penguin Books, 1969.

[53] Andrew Heathcote et al. "Dynamic models of choice". In: *Behavior Research Methods* 51.2 (June 2018), pp. 961–985. DOI: 10.3758/s13428-018-1067-y.

[54] Cajo J. F. Ter Braak. "A Markov Chain Monte Carlo version of the genetic algorithm Differential Evolution: easy Bayesian computing for real parameter spaces". In: *Statistics and Computing* 16.3 (Sept. 2006), pp. 239–249. DOI: 10.1007/s11222-006-8769-1.

[55] José Pinheiro and Douglas Bates. *nlme: Linear and Nonlinear Mixed Effects Models*. Nov. 1999. DOI: 10.32614/cran.package.nlme.

[56] Torsten Hothorn, Frank Bretz, and Peter Westfall. "Simultaneous Inference in General Parametric Models". In: *Biometrical Journal* 50.3 (June 2008), pp. 346–363. DOI: 10.1002/bimj.200810425.

[57] Dora Matzke et al. "Inhibiting responses to difficult choices." In: *Journal of Experimental Psychology: General* 148.1 (Jan. 2019), pp. 124–142. DOI: 10.1037/xge0000525.

[58] Yoojeong Choo et al. "Right inferior frontal gyrus damage is associated with impaired initiation of inhibitory control, but not its implementation". In: *eLife* 11 (Dec. 2022). DOI: 10.7554/elife.79667.

[59] G. Pfurtscheller, A. Stancák, and C. Neuper. “Post-movement beta synchronization. A correlate of an idling motor area?” In: *Electroencephalography and Clinical Neurophysiology* 98.4 (Apr. 1996), pp. 281–293. DOI: 10.1016/0013-4694(95)00258-8.

[60] François Cassim et al. “Does post-movement beta synchronization reflect an idling motor cortex?” In: (Dec. 2001). DOI: 10.1097/00001756-200112040-00051.

[61] Huiling Tan, Cian Wade, and Peter Brown. “Post-Movement Beta Activity in Sensorimotor Cortex Indexes Confidence in the Estimations from Internal Models”. In: *The Journal of Neuroscience* 36.5 (Feb. 2016), pp. 1516–1528. DOI: 10.1523/jneurosci.3204-15.2016.

[62] P Brown. “Abnormal oscillatory synchronisation in the motor system leads to impaired movement”. In: *Current Opinion in Neurobiology* 17.6 (Dec. 2007), pp. 656–664. DOI: 10.1016/j.conb.2007.12.001.

[63] Randolph F. Helfrich et al. “Entrainment of Brain Oscillations by Transcranial Alternating Current Stimulation”. In: *Current Biology* 24.3 (Feb. 2014), pp. 333–339. DOI: 10.1016/j.cub.2013.12.041.

[64] Philip Tseng et al. “The critical role of phase difference in gamma oscillation within the temporoparietal network for binding visual working memory”. In: *Scientific Reports* 6.1 (Aug. 2016). DOI: 10.1038/srep32138.

[65] Matthew R. Krause, Pedro G. Vieira, and Christopher C. Pack. “Transcranial electrical stimulation: How can a simple conductor orchestrate complex brain activity?” In: *PLOS Biology* 21.1 (Jan. 2023), e3001973. DOI: 10.1371/journal.pbio.3001973.

[66] David Haslacher et al. “Working memory enhancement using real-time phase-tuned transcranial alternating current stimulation”. In: *Brain Stimulation* 17.4 (July 2024), pp. 850–859. DOI: 10.1016/j.brs.2024.07.007.

[67] Flavio Fröhlich and David A. McCormick. "Endogenous Electric Fields May Guide Neocortical Network Activity". In: *Neuron* 67.1 (July 2010), pp. 129–143. DOI: 10.1016/j.neuron.2010.06.005.

[68] Davide Reato et al. "Low-Intensity Electrical Stimulation Affects Network Dynamics by Modulating Population Rate and Spike Timing". In: *The Journal of Neuroscience* 30.45 (Nov. 2010), pp. 15067–15079. DOI: 10.1523/jneurosci.2059-10.2010.

[69] Asher Geffen, Nicholas Bland, and Martin V. Sale. "μ-Transcranial Alternating Current Stimulation Induces Phasic Entrainment and Plastic Facilitation of Corticospinal Excitability". In: *European Journal of Neuroscience* 61.5 (Mar. 2025). DOI: 10.1111/ejn.70042.

[70] Nicole Swann et al. "Intracranial EEG Reveals a Time- and Frequency-Specific Role for the Right Inferior Frontal Gyrus and Primary Motor Cortex in Stopping Initiated Responses". In: *The Journal of Neuroscience* 29.40 (Oct. 2009), pp. 12675–12685. DOI: 10.1523/jneurosci.3359-09.2009.

[71] Johanna Wagner et al. "Establishing a Right Frontal Beta Signature for Stopping Action in Scalp EEG: Implications for Testing Inhibitory Control in Other Task Contexts". In: *Journal of Cognitive Neuroscience* 30.1 (Jan. 2018), pp. 107–118. DOI: 10.1162/jocn_a_01183.

[72] Teodoro Solis-Escalante et al. "Cue-induced beta rebound during withholding of overt and covert foot movement". In: *Clinical Neurophysiology* 123.6 (June 2012), pp. 1182–1190. DOI: 10.1016/j.clinph.2012.01.013.

[73] Adam R. Aron et al. "Triangulating a Cognitive Control Network Using Diffusion-Weighted Magnetic Resonance Imaging (MRI) and Functional MRI". In: *The Journal of Neuroscience* 27.14 (Apr. 2007), pp. 3743–3752. DOI: 10.1523/jneurosci.0519-07.2007.

[74] Charlotte L. Rae et al. “The Prefrontal Cortex Achieves Inhibitory Control by Facilitating Subcortical Motor Pathway Connectivity”. In: *The Journal of Neuroscience* 35.2 (Jan. 2015), pp. 786–794. DOI: 10.1523/jneurosci.3093-13.2015.

[75] Sara Jahfari et al. “Effective Connectivity Reveals Important Roles for Both the Hyperdirect (Fronto-Subthalamic) and the Indirect (Fronto-Striatal-Pallidal) Fronto-Basal Ganglia Pathways during Response Inhibition”. In: *The Journal of Neuroscience* 31.18 (May 2011), pp. 6891–6899. DOI: 10.1523/jneurosci.5253-10.2011.

[76] Weidong Cai et al. “Dissociable Roles of Right Inferior Frontal Cortex and Anterior Insula in Inhibitory Control: Evidence from Intrinsic and Task-Related Functional Parcellation, Connectivity, and Response Profile Analyses across Multiple Datasets”. In: *The Journal of Neuroscience* 34.44 (Oct. 2014), pp. 14652–14667. DOI: 10.1523/jneurosci.3048-14.2014.

[77] Roberto Limongi and Francisco J. Pérez. “Successful and unsuccessful response inhibitions differentially affect the effective connectivity between insular, presupplementary-motor, and striatal areas.” In: *Behavioral Neuroscience* 131.1 (2017), pp. 20–32. DOI: 10.1037/bne0000175.

[78] Magdalena Nowak et al. “Driving Human Motor Cortical Oscillations Leads to Behaviorally Relevant Changes in Local GABAAInhibition: A tACS-TMS Study”. In: *The Journal of Neuroscience* 37.17 (Mar. 2017), pp. 4481–4492. DOI: 10.1523/jneurosci.0098-17.2017.

[79] Wing Ting To et al. “Changing Brain Networks Through Noninvasive Neuromodulation”. In: *Frontiers in Human Neuroscience* 12 (Apr. 2018). DOI: 10.3389/fnhum.2018.00128.

[80] Aref Pariz et al. “Selective control of synaptic plasticity in heterogeneous networks through transcranial alternating current stimulation (tACS)”. In: *PLOS Computational Biology* 19.4 (Apr.

2023). Ed. by Daniel Bush, e1010736. DOI: 10.1371/journal.pcbi.1010736.

[81] Ines R Violante et al. "Externally induced frontoparietal synchronization modulates network dynamics and enhances working memory performance". In: *eLife* 6 (Mar. 2017). DOI: 10.7554/elife.22001.

[82] Johannes Vosskuhl, Daniel Strüber, and Christoph S. Herrmann. "Non-invasive Brain Stimulation: A Paradigm Shift in Understanding Brain Oscillations". In: *Frontiers in Human Neuroscience* 12 (May 2018). DOI: 10.3389/fnhum.2018.00211.

[83] Kilian Abellaneda-Pérez et al. "Differential tDCS and tACS Effects on Working Memory-Related Neural Activity and Resting-State Connectivity". In: *Frontiers in Neuroscience* 13 (Jan. 2020). DOI: 10.3389/fnins.2019.01440.

[84] Bernhard Spitzer and Saskia Haegens. "Beyond the Status Quo: A Role for Beta Oscillations in Endogenous Content (Re)Activation". In: *eneuro* 4.4 (July 2017), ENEURO.0170–17.2017. DOI: 10.1523/eneuro.0170-17.2017.

4.6 Supplementary information

4.6.1 Closed-loop evaluation

To evaluate the performance of the closed-loop system, we recorded ∼10-minute tACS-free EEG data where one participant was performing the stop-signal task to simulate 10,000 trials of real-time beta peak detection (the algorithm iteratively continued until 10,000 peaks were detected). The performance of phase prediction was quantified offline based on accuracy, bias, and variance [1]. The accuracy was evaluated by the equation:

$$1 - \frac{1}{N \times 180} \sum_{i=1}^{N} |\theta_i - \theta_0|$$

where N is the number of trials used to estimate the phase; θ_i is the estimated phase in the trials i; θ_0 is the target phase, 0°. An accuracy of 1 means that the phase has been estimated precisely every time, whereas an accuracy of 0 means that the phase has been detected opposite to the target phase, e.g., peaks instead of troughs. With an accuracy of 0.5, phase estimation is uniformly randomly distributed. Bias was determined by computing the average difference between the estimated and target phases, revealing any systematic deviations from the intended outcome. Variance, quantified using standard deviation, indicates the spread of the outcome distribution, reflecting the consistency of phase estimation across trials. Figure S4.1 A shows the distribution of system delays over 10.000 simulated trials for in-phase and anti-phase stimulation, with the median delay (red line) at 16 ms for both conditions. Statistical comparison revealed no significant difference in delay between in- and anti-phase tACS (paired t-test: $t(28) = 1.648$, $p = 0.110$), indicating consistent timing performance across stimulation modes.

Figure S4.1 B presents the accuracy of the phase prediction algorithm, depicted as the distribution of phase differences (in degrees) between the actual EEG phase at stimulation onset and the targeted phase, accounting for the measured 16 ms system delay. The clustering of phase differences near the target indicates the system's reliable phase-locked stimulation capability, essential for accurate closed-loop tACS delivery.

4.6.2 Self-report discomfort scores

Table S4.1: **Mean ± standard deviation of self-reported discomfort scores (range: 0–100) after each stimulation condition.**

Stimulation condition	Discomfort score (0-100)	Main effect of stimulation
In-phase	35.8±22.64	F(2, 68)=16.85, p<0.001*
Anti-phase	38.74±20.76	
Sham	20.43±21.66	

A repeated measures ANOVA revealed a significant main effect of stimulation condition on perceived discomfort ($F(2, 68) = 16.85, p < 0.001$).

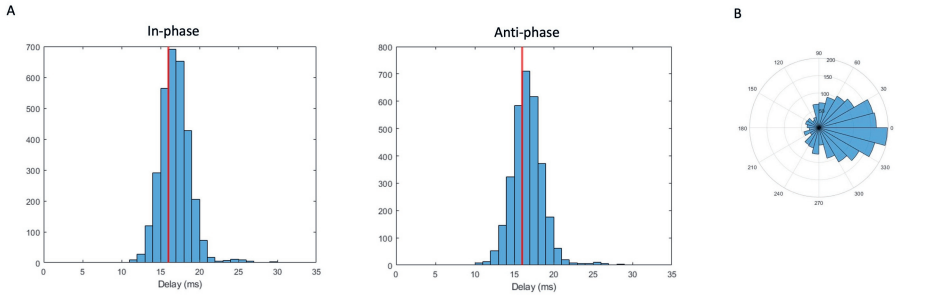


Figure S4.1: **Closed-loop system evaluation.** (**A**) Distribution of system delays measured over 10000 trials for in-phase and anti-phase tACS. Median delay (red line) was 16 ms for both(**B**) Polar histogram of phase prediction accuracy, showing the distribution of phase differences between actual and targeted EEG phases (accounting for 16 ms delay), demonstrating precise phase-locking of the closed-loop tACS system.

Table S4.2: **Tukey's HSD post-hoc comparisons of discomfort scores across stimulation conditions.**

group1	group2	Mean diff	p	lower	upper
Anti-phase	In-phase	2.9429	0.8378	-9.3944	15.2801
Anti-phase	Sham	-15.3714	0.0105*	-27.7087	-3.0342
In-phase	Sham	-18.3143	0.0018*	-30.6515	-5.977

Asterisks denote significance ($p < .05$). Sham was rated significantly lower in discomfort than both In-phase and Anti-phase, while no significant difference was found between In-phase and Anti-phase.

4.6.3 Context violation and non-parametric integration estimates comparisons

Non-parametric estimated behavioral metrics of stop-signal performance are summarized in Table S4.3. SSRT was estimated using the integration method with replacement of go omissions [2]. The staircase algorithm successfully maintained stopping accuracy near the target 50%, with no significant main effect (Friedman test, $\chi^2(2) = 2.9$, $p = 0.23$). The GORT differed significantly across conditions (ANOVA, $F(2, 68) = 4.04$, $p = 0.022$), with follow-up comparisons revealing

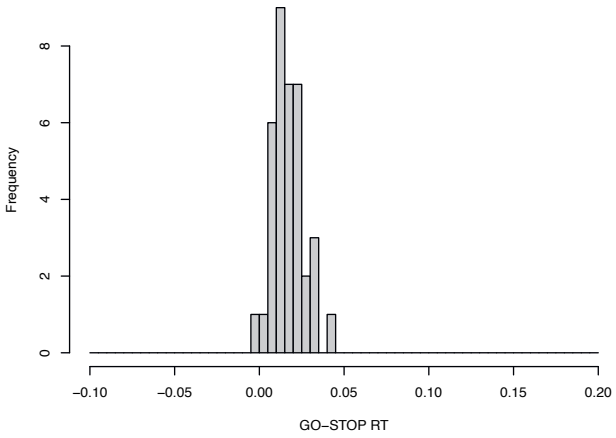


Figure S4.2: **Assessment of context independence.** GO-STOP RT: Go reaction time - Failed stop reaction time. The dataset didn't show severe independence violation.

faster responses in the sham vs. anti-phase condition ($p = 0.03$) and slower responses in the in-phase vs. sham ($p = 0.01$). No significant main effects were observed for SSRT or stop-signal delay (SSD), with respective ANOVA results of $F(2, 68) = 0.14$ ($p = 0.87$) and $F(2, 68) = 1.27$ ($p = 0.29$). Pairwise comparisons for these measures did not reveal any significant differences.

Table S4.3: **Summary of descriptive statistics, main effects, and post hoc comparisons across tACS phase conditions for non-parametric estimates.**

	Mean (SD)			Main Effect (F/χ^2, p)	In.- Anti.		In. - Sham		Anti. - Sham	
Parameter	**In-phase**	**Anti-phase**	**Sham**		**Main diff.**	**p**	**Main diff.**	**p**	**Main diff.**	**p**
P(Inhibition) †	54.29 (2.12)	53.94 (1.91)	53.31 (3.82)	$\chi^2(2)=2.9$, p=.23	144.50	.28	105.00	.05	-129.00	.54
RTGO (ms)	818.20 (12.68)	822.50 (13.11)	818.11 (13.62)	**F(2,68)=4.04, p=.022**	**-2.71**	**.01**	0.05	.96	**2.30**	**.03**
SSRT (ms)	208.73 (16.94)	209.46 (13.54)	209.61 (15.43)	F(2,68)=0.14, p=.87	-0.39	.70	-0.52	.61	-0.08	.94
SFRT (ms)	801.17 (16.41)	805.89 (15.44)	800.87 (17.52)	F(2,68)=2.31, p=.11	-1.82	.08	0.10	.92	**2.19**	**.04**
SSD (ms)	604.87 (17.70)	608.54 (14.51)	606.03 (19.01)	F(2,68)=1.27, p=.29	-1.43	.16	-0.54	.59	1.08	.29
P(Go errors)	0	0	0	NA	NA	NA	NA	NA	NA	NA
P(Go omissions)	2.49 (3.02)	2.40 (2.53)	2.34 (3.16)	$\chi^2(2)=0.48$, p=.79	201.00	.78	149.00	.99	-141.50	.82

Main effects and post-hoc results were tested using repeated measures ANOVA and paired t-tests. No corrections were applied to p values.
† Friedman test with Wilcoxon signed-rank tests was conducted for non-normal distributed data.
SSRT=Stop signal reaction time, estimated using the integration method with replacement of go omissions [2]. RTGO=mean reaction time of go trials; SSRT=Stop-signal reaction time; RTSF=mean reaction time of Stop-failed trials; SSD=Stop-signal delay.

4.6.4 BEESTS-CV model prior distributions

The prior distributions:

$$\begin{aligned}
\mu_{go} &\sim Normal(0.5, 0.50)[0, 1], \\
\mu_{stop} &\sim Normal(0.2, 0.50)[0, 1], \\
\sigma_{go}, \sigma_{stop} &\sim Normal(0.03, 0.35)[0, 1], \\
\tau_{go}, \tau_{stop} &\sim Normal(0.03, 0.35)[0, 1], \\
\phi^{-1}(P_{TF}), \phi^{-1}(P_{GF}) &\sim Normal(-1.28, 3), \\
M &\sim Normal(0, 3), \\
S &\sim Normal(1, 3)[0, \infty].
\end{aligned} \tag{S4.1}$$

The hyper-prior location parameter distributions:

$$\begin{aligned}
\mu_{\mu_{go}} &\sim Normal(0.5, 0.5)[0, 1], \\
\mu_{\mu_{stop}} &\sim Normal(0.2, 0.5)[0, 1], \\
\mu_{\sigma_{go}}, \mu_{\sigma_{stop}} &\sim Normal(0.04, 0.35)[0, \infty], \\
\mu_{\tau_{go}}, \mu_{\tau_{stop}} &\sim Normal(0.04, 0.35)[0, \infty], \\
\mu_{\phi^{-1}(P_{TF})}, \mu_{\phi^{-1}(P_{GF})} &\sim Normal(-1.28, 3)[-\infty, \infty], \\
\mu_M &\sim Normal(0, 3)[-\infty, \infty], \\
\mu_S &\sim Normal(0, 1)[0, \infty].
\end{aligned} \tag{S4.2}$$

The hyper-prior scale parameters:

$$\sigma_p \sim Exponential(1) \tag{S4.3}$$

For each parameter $p \in \{\mu_{go}, \mu_{stop}, \sigma_{go}, \sigma_{stop}, \tau_{go}, \tau_{stop}, P_{TF}, P_{GF}, M, S\}$.

4.6.5 BEESTS-CV model fitting and context independence

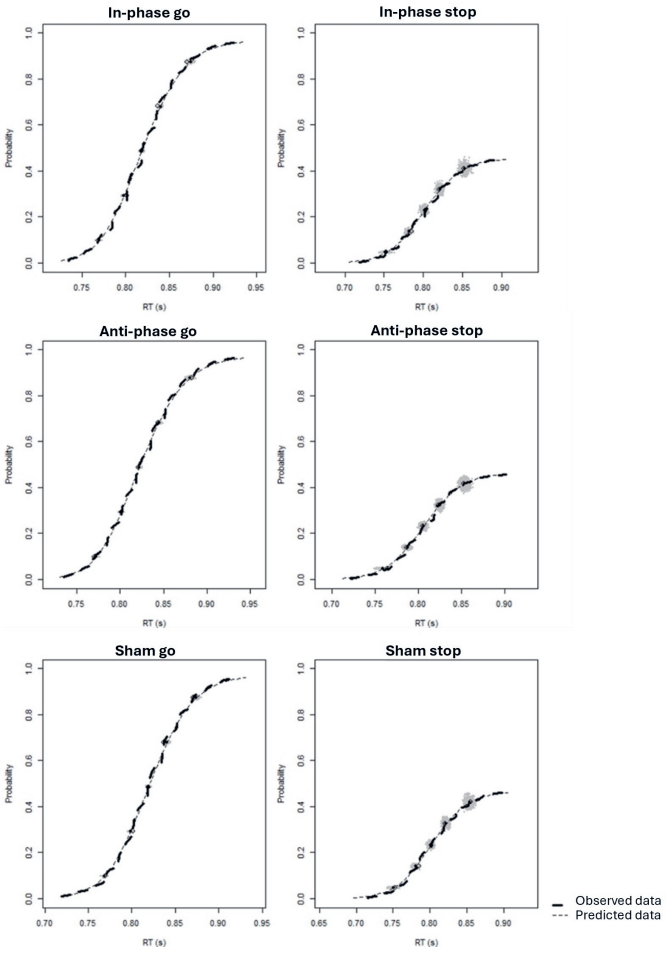


Figure S4.3: **Averaged observed and predicted cumulative distribution functions of reaction time (RTs) for go signal (left panels) and stop signals (right panels) collapsed (due to the SSDs determined by a staircase algorithm) across SSDs in three conditions.** The thick dashed lines show the observed data. The grey dots show the prediction samples from the joint posterior distribution of the model parameters. The thin dashed lines show the average of the predictions.

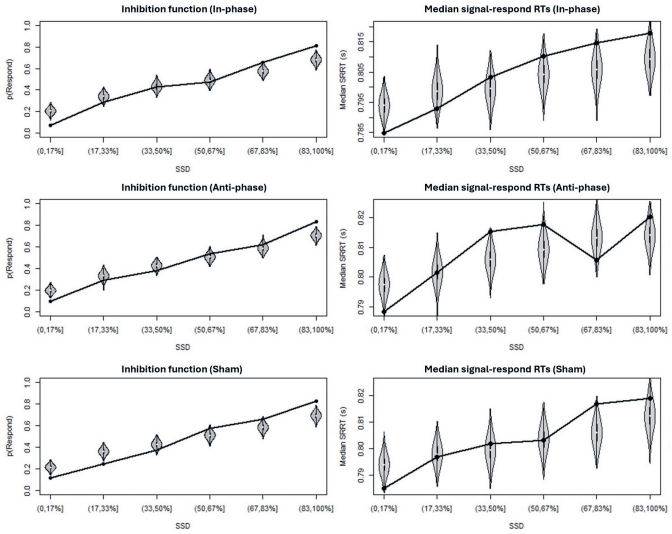


Figure S4.4: **Observed vs predicted inhibition functions (left panels) and median signal-respond RT as a function of stop-signal delay (SSD; right panels) for three stimulation conditions.** Black bullets show the observed data. Grey violin plots show the distribution of the predictions of the BEESTS-CV model.

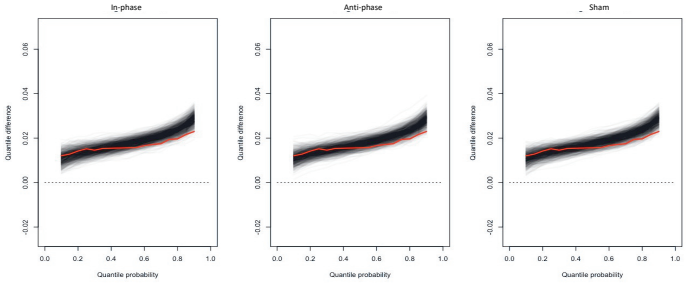


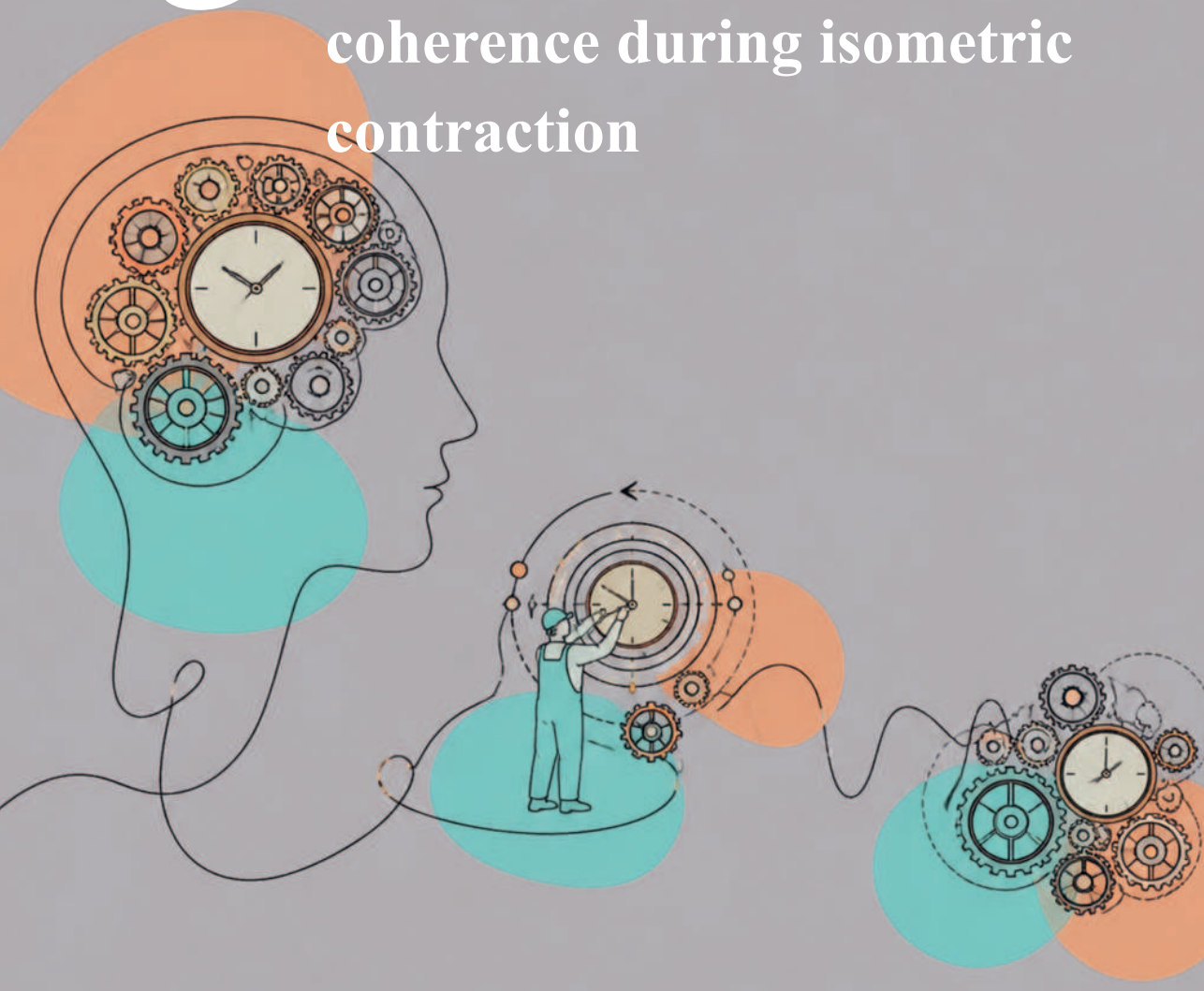
Figure S4.5: **Average delta functions in three conditions: in-, anti-phase and sham.** The red line shows the observed delta functions averaged across participants. The black lines show 1000 posterior predictive delta functions averaged across participants obtained from fitting the data with the BEESTS-CV model assuming context independence; the darker the area, the denser the predicted delta function.

Supplementary references

[1] Sina Shirinpour et al. “Experimental evaluation of methods for real-time EEG phase-specific transcranial magnetic stimulation”. In: *Journal of Neural Engineering* 17.4 (July 2020), p. 046002. DOI: 10.1088/1741-2552/ab9dba.

[2] Frederick Verbruggen et al. “A consensus guide to capturing the ability to inhibit actions and impulsive behaviors in the stop-signal task”. In: *eLife* 8 (Apr. 2019). DOI: 10.7554/elife.46323.

5 Anti-phase closed-loop tACS disrupts cortico-muscular coherence during isometric contraction



Abstract

Non-invasive interventions such as transcranial alternating current stimulation (tACS) can interact with endogenous oscillations by rhythmically biasing membrane potentials and shifting spike timing, yet conventional tACS ignores ongoing phase and has limited ability to disrupt pathological synchrony. Here, we tested closed-loop, phase-specific tACS over primary motor cortex (M1) during sustained isometric force in healthy adults (N = 25), systematically varying stimulation duration (1, 1.5, 2, and 5 s) and predefined onset phase of the tACS waveform, in-phase (0°), anti-phase (180°), or sham, relative to endogenous oscillations. We found reliable modulation of stimulation onset phase and duration time on post-stimulation cortico-muscular coherence (CMC) in the beta band. Specifically, brief anti-phase trains (1-2 s) significantly suppressed CMC compared to prolonged anti-phase (5 s), in-phase, and sham conditions, while in-phase tACS consistently increased beta CMC compared to both anti-phase and sham, with longer duration eliciting stronger CMC than shorter ones. No significant effects were observed on local beta power, force output, or resting beta. These findings establish a bidirectional, phase-dependent mechanism of corticospinal coupling and highlight brief anti-phase tACS as an effective means to transiently desynchronize motor networks, offering a potential therapeutic avenue for alleviating pathological synchrony in motor disease.

5.1 Introduction

Non-invasive brain stimulation (NIBS) is now widely used to bias large-scale neural network dynamics and is being explored as a treatment strategy for disorders characterized by dysrhythmic brain activity [1, 2, 3]. Among NIBS techniques, transcranial alternating current stimulation (tACS), delivering weak, sinusoidal currents through the scalp, can interact with endogenous oscillations at targeted frequencies by rhythmically biasing membrane potentials and shift the timing of neuronal

spikes [4, 5, 6, 2]. In humans, concurrent studies have shown frequency- and phase-specific tACS induces phase alignment of ongoing brain oscillations, known as entrainment [7, 8]. This entrainment enables selective enhancement of targeted rhythms, offering a means to probe and potentially modify the network dynamics underlying sensory [7], cognitive [9], and motor functions [10].

The impact of tACS critically depends on its phase relationship with the ongoing neural rhythm. Aligning the external waveform in-phase with endogenous beta tends to reinforce synchrony, whereas stimulation delivered in anti-phase, corresponding to a 180° phase offset, can weaken or cancel ongoing rhythmic activity [11]. Such an idea motivates phase-specific closed-loop tACS, which provides an opportunity to bidirectionally modulate ongoing neural dynamics and, in particular, to suppress pathological oscillations. Phase-specific stimulation has been shown to suppress pathological oscillations such as tremor and to modulate task performance, supporting the feasibility of closed-loop, phase-targeted neuromodulation approaches [12, 13, 14, 15, 16]. However, the magnitude of the phase-dependent entrainment is not clear. Brief anti-phase stimulation may transiently disrupt synchrony, whereas prolonged stimulation could increase the likelihood of re-entraining the targeted neural population, potentially diminishing the intended desynchronizing effect and converging toward in-phase-like outcomes [11]. This principle is recapitulated in our Stuart Landau simulations (Figure S5.1). Therefore, systematically investigating the optimal duration of anti-phase stimulation to achieve maximal desynchronization without unintended entrainment is crucial for developing neuromodulation protocols.

Corticomuscular coherence (CMC) represents a particularly suitable readout for assessing the effects of tACS on motor control in healthy subjects. CMC directly reflects beta-band synchrony that supports coordinated communication across the motor system, linking cortical activity to ongoing muscle output via temporally structured corticospinal interactions [17, 18]. In healthy individuals, beta-CMC is most robust during steady isometric contractions and is widely interpreted as an

index of effective corticospinal communication [19, 20]. Consistent with this interpretation, conventional tACS in the beta-band applied over the primary motor cortex (M1) in healthy participants has been shown to enhance beta-band corticomuscular coupling during isometric contractions, even when behavioral output remains largely unchanged [21, 22, 23]. These coherence changes do not reliably coincide with increases in local cortical beta power, suggesting that tACS can modulate functional coupling without producing a uniform amplification of beta activity at the stimulation site [24, 25].

Whereas 20 Hz tACS over M1 can strengthen beta synchrony and CMC in healthy individuals, the same approach in Parkinson's disease (PD) has been associated with impaired motor performance [26] and further reductions in CMC [22]. These disturbances may arise from disrupted motor network communication in the context of excessive beta dynamics, alongside deficits in sensorimotor processing and movement readiness [27, 28, 29, 30]. Conventional tACS, by its open-loop nature, reinforces the oscillatory synchrony when applied for extended durations [31], which is problematic given that PD is characterized by abnormally elevated beta activity across cortico-basal ganglia circuits [32]. Interventions that reduce pathological beta, such as L-DOPA administration [33] or deep brain stimulation [34, 35], have been shown to diminish elicited beta oscillations and enhance CMC. Together, these findings motivate the hypothesis that a phase-dependent closed-loop tACS approach could more effectively desynchronize abnormally elevated beta in a non-invasive way, thereby normalizing CMC and improving motor function.

In the present study, we investigated whether closed-loop, phase-specific tACS over M1 can modulate CMC, local beta power, and motor output during sustained isometric contraction in healthy participants. We hypothesized that in-phase stimulation would increase CMC, reflecting enhanced motor inhibition, while anti-phase stimulation would reduce CMC by disrupting pathological-like synchrony. A secondary aim was to determine how varying the duration of anti-phase tACS influences its ability to desynchronize

motor networks, thereby informing the design of optimized, phase-targeted neuromodulation strategies. Our results revealed that both the tACS duration and its phase lag to ongoing oscillations jointly determine its aftereffects on corticospinal coupling without altering gross behavior and local power. Our study provides the first empirical evidence constraining the optimal duration for closed-loop anti-phase desynchronization and delineating a temporal window in which rebound entrainment emerges. This framework motivates short anti-phase tACS as a promising approach for normalizing pathological synchrony in motor disorders.

5.2 Methods

5.2.1 Participants

Twenty-five healthy, right-handed adults (7 males; mean age = 23 (18-35)) took part in the study. Right-handedness was confirmed using the Edinburgh Handedness Inventory, mean laterality quotient = 87.7, range = 50-100 [36]. All participants underwent standard screening to rule out contraindications to non-invasive brain stimulation [37, 38]. The experimental procedures were approved by the local ethics committee, and written informed consent was obtained from all participants in accordance with the Declaration of Helsinki.

5.2.2 Experimental design and task

A within-subject design was used, in which each participant completed eight stimulation conditions. These included tACS administered in anti-phase with the endogenous beta rhythm using 1.0, 1.5, 2.0, and 5.0 s trains (A1, A1.5, A2, and A5), tACS administered in-phase with the endogenous beta rhythm using 2.0 and 5.0 s trains (I2 and I5), and sham stimulation of 2.0 and 5.0 s duration (S2 and S5; Figure 5.1 B).

Prior to the experiment, maximum voluntary contraction (MVC) was measured with a precision force transducer (OMEGA Engineering, Norwalk, CT, USA; Sampling rate: 1000 Hz), and the upper and lower force thresholds were determined as 1.25% and 1% of the MVF. The experiment began with a practice session of an isometric contraction task, in which participants were instructed to pinch the force transducer between the upper and lower force threshold guided by real-time visual feedback: a dynamic red trace displayed their exerted force relative to two blue horizontal lines marking the target range. Subsequently, we recorded a two-minute EEG while participants performed the contraction task. The individual beta peak frequency (IBF) was calculated based on the EEG data and used as a stimulation frequency for closed-loop tACS.

Each condition was performed across 12 stimulation blocks (A1×2, A1.5×2, A2×2, A5×2, I2, I5, S2, and S5), with phase-locked delivery based on real-time detection of the endogenous beta phase. The order of conditions was pseudo-randomized and counterbalanced across participants to control for potential order effects. Each block began with a 30-s resting-state EEG followed by a force build-up period during which participants stabilized their pinch force between the upper and lower force threshold with visual feedback (lasting 5-30 s). Once the visual trace disappeared, a green fixation cross signaled the onset of the 3-minute isometric contraction task. During this period, tACS trains were delivered every 5 s, with each onset phase determined by real-time phase detection from the preceding 0.5-second-EEG segment. A final one-minute rest EEG segment was collected at the end of each block.

Between blocks, participants rested for approximately 3 minutes and completed a Visual Analogue Scale (VAS) questionnaire to assess stimulation-related sensations. The VAS consisted of a 10-cm horizontal line anchored at ”no feeling” (0) and ”strong pain/discomfort” (10).

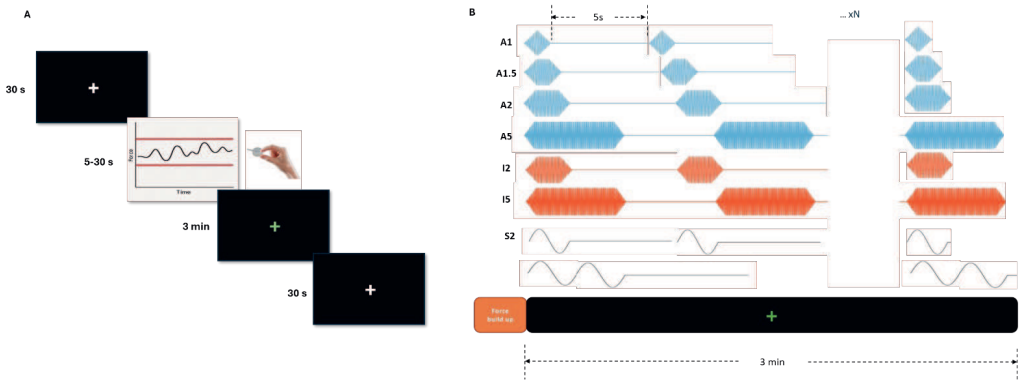


Figure 5.1: **Experiment design and stimulation protocol. (A)** Task sequence. Each block began and ended with a 30-s resting-state EEG (white fixation cross). Participants then performed an isometric pinch contraction at 1-1.25 % of their maximum voluntary contraction (MVC), guided by real-time visual feedback. Once the force stabilized within the target range, the visual trace disappeared, and a green fixation cross indicated the onset of the 3-min contraction task. **(B)** Stimulation protocol. During each 3-min block, closed-loop tACS was applied in eight conditions: anti-phase (A1, A1.5, A2, A5; 1.0-5.0 s trains at 180°), in-phase (I2, I5; 0°), and sham (S2, S5; 90°). The stimulation was phase-locked to the ongoing beta oscillation derived from real-time EEG recordings.

5.2.3 EEG and EMG acquisition

EEG was recorded using an actiChamp Plus amplifier (Brain Products GmbH, Gilching, Germany) with passive Ag/AgCl electrodes mounted in a 32-channel EEG cap (EASYCAP GmbH, Germany). The electrode placement followed the international 10-20 system. The ground electrode was placed at FPz, and the system reference at TP10 (right mastoid). Four additional electrodes recorded horizontal and vertical electrooculograms (EOG) to monitor ocular activity. Electrode impedances were maintained below 10 kΩ using OneStep Cleargel (Medcat, Klazienaveen, the Netherlands). Event markers were simultaneously recorded to indicate the onset of each stimulation train.

Surface EMG was used to record muscle activity from the first dorsal interosseous (FDI). Ag/AgCl electrodes were placed in a bipolar configuration with electrodes positioned over the belly of the FDI and the bone-tendon junction of the index finger. The ground electrode was positioned over the ulnar styloid process. The skin was prepared with fine-grit medical sandpaper and cleaned with 70% isopropyl alcohol to minimize impedance before electrode placement. All the signals were streamed in real time via Lab stream layer (LSL) using the ActiCham LSL Connector (sampling rate: 10000 Hz) to a customized MATLAB script for online phase prediction and stored on local servers.

5.2.4 tACS

tACS was delivered using a 4 x 1 high-definition (HD)-tACS (DC STIMULATOR PLUS, NeuroConn, GmbH, Ilmenau, Germany) setup. Electrodes were embedded in gel-filled plastic cups (diameter: 2 cm at the top, 2.5 cm at the base; height: 1.4 cm) mounted in the EEG cap. The central electrode was positioned over C3 (left M1), and the four return electrodes were placed at Fz, F7, Pz, and P7. Each cup was filled with OneStep Cleargel to maintain electrode impedances below 10 kΩ. The default stimulation amplitude was set to a peak-to-peak value of 2 mA, reduced when participants reported discomfort. Only one participant

required an adjustment with an amplitude of 1.9 mA, resulting in a group mean stimulation amplitude of 1.996 $\pm$ 0.02 mA (mean $\pm$ SD).

In the in-phase and anti-phase conditions, stimulation was applied at each participant's individual beta frequency (IBF) determined during the isometric contraction task. Each tACS train included 0.5 s ramp-up and 0.5 s ramp-down periods. In the sham conditions, stimulation consisted of a brief sinusoidal current at 0.5 Hz for 2 s (S2) or 0.6 Hz for 5 s (S5), both starting at the rising phase (0°) and delivered without ramping periods.

IBF determination

The IBF was estimated from the EEG data recorded during the initial isometric contraction task. Data were preprocessed in FieldTrip [39]. The signal was band-pass filtered between 1-100 Hz with a 50 Hz notch filter to remove line noise. The data were demeaned and detrended, segmented into 1-s non-overlapping epochs, and re-referenced to TP9. Independent component analysis (ICA) was applied to remove components reflecting ocular or muscle activity. Remaining bad epochs were manually rejected after visual inspection. Artifact-free data from the channels of interest (C1/FC1/CP1/FC5/CP5) were then subjected to spectral analysis using multitaper FFT (Hanning taper, 1-45 Hz, 10 s padding). The resulting power spectrum was log-transformed, and the $1/f$ aperiodic component was modeled and subtracted using a first-order polynomial fit in log-log space. The residual spectrum between 14-30 Hz was then fitted with a third-order Gaussian function to identify up to three potential beta peaks [40, 41]. The primary beta peak was defined as the frequency corresponding to the maximum corrected power, and used as the stimulation frequency for closed-loop tACS.

5.2.5 Closed-loop tACS-EEG

Online EEG analysis and phase estimation

A real-time closed-loop system was implemented to stream EEG data via the Lab Streaming Layer (LSL) to MATLAB R2023a (The MathWorks Inc., Natick, MA, USA) for online phase estimation and control of the stimulator (Figure 5.1).

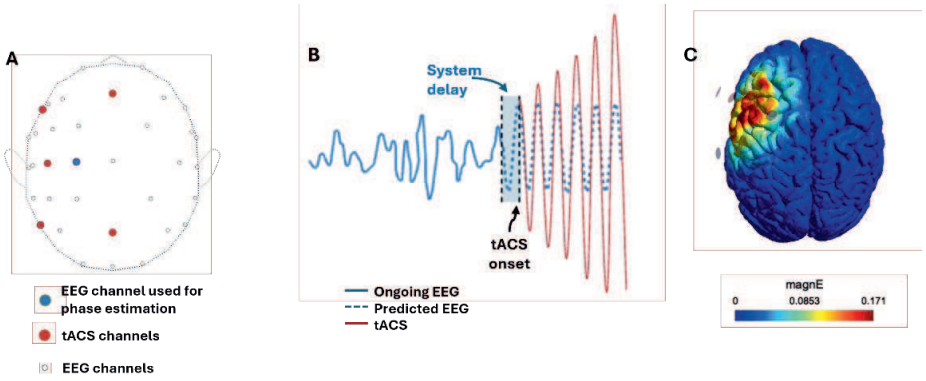


Figure 5.2: **EEG guided closed-loop tACS. (A)** Scalp electrode montage following the standard 10-20 system. The C1 channel was used for real-time phase estimation. 4×1 HD-tACS was applied over the left M1 (anode at C3; return electrodes at Fz, F7, Pz, and P7). **(B)** Real-time beta phase prediction based on an autoregressive (AR) model. The stimulation waveform was triggered when the predicted EEG phase reached the peak, accounting for system delay. As an example, tACS onset with 90° (peak) (in-phase) is shown in the figure. C: Simulated electric field distribution.

The incoming EEG signals were processed in real time using a 500-ms sliding window that updated continuously with each new data chunk (8-12 samples every 0.01 s). For each update, the signal from channel C1 was: (1) re-referenced using a surface Laplacian approach by subtracting the average of the surrounding electrodes from (CP1, CP3, CP5, C5, FC5, FC3, and FC1); (2) filtered using a zero-phase band-pass FIR filter in the range of IBF $\pm$ 2; (3) trimmed at the edges to remove filtering artifacts;

and (4) forwarded to an Autoregressive algorithm for phase prediction (https://github.com/OpitzLab/CL-phase/tree/master/AR). AR coefficients were computed using the Yule-Walker method to forward-predict the ongoing beta oscillation as detailed in [42]. The instantaneous phase of the predicted waveform was then determined via the Hilbert transform, and a digital trigger was sent through an LPT port when the predicted phase reached $90° \pm 5.73°$ (with $90°$ corresponding to the peak). The end-to-end system delay was empirically measured and found to be approximately 19 ms. This delay was compensated in the code by predicting the phase 19 ms ahead, ensuring precise synchronization between the neural oscillation and tACS onset. In-phase stimulation corresponded to a $0°$ phase lag relative to the detected peak of the ongoing beta oscillations and was implemented by starting the tACS waveform at $90°$; For the anti-phase, the onset phase was at $270°$; For the sham, the onset phase was set to $0°$.

Offline closed-loop evaluation

To evaluate the performance of the closed-loop system, we conducted five 3-minute pilot sessions where one participant was performing the isometric contraction task, and tACS-free EEG data were recorded and analyzed offline. A total of 1000 trials were simulated, and the performance of phase prediction was quantified based on the averaged accuracy, bias, and variance [43]. The accuracy was evaluated by the equation:

$$1 - \frac{1}{N \times 180} \sum_{i=1}^{N} |\theta_i - \theta_0|$$

where N is the number of trials (N = 1000) used to estimate the phase; θ_i is the estimated phase in the trials i; θ_0 is the target phase, $0°$. An accuracy of 1 means that the phase has been estimated precisely every time, whereas an accuracy of 0 means that the phase has been detected

opposite to the target phase, e.g., peaks instead of troughs. With an accuracy of 0.5, phase estimation is uniformly randomly distributed. Bias was determined by computing the average difference between the estimated and target phases, revealing any systematic deviations from the intended outcome. Variance, quantified using standard deviation, indicates the spread of the outcome distribution, reflecting the consistency of phase estimation across trials.

5.2.6 Data analysis

Inter-stim EEG

EEG data were preprocessed in MATLAB using the FieldTrip toolbox [39]. Data were segmented into epochs from 0.1 to 3 s post-stimulation. Preprocessing included demeaning, detrending, and filtering. A band-pass filter (1-100 Hz) reduced low-frequency drifts and high-frequency noise, and a notch filter (49-51 Hz) was applied. Vertical and horizontal EOG channels were re-referenced to create bipolar derivations and used for artifact detection. Data were re-referenced to TP9 (left mastoid), and trials containing artifacts were identified by visual inspection and excluded. Independent component analysis (ICA) was used to identify eye movements, blinks, and other non-neural artifacts. Components were rejected based on z-scored kurtosis, EOG component weights, and visual verification.

Time-frequency representations of power were obtained with a Morlet wavelet transform. Frequencies from 1-45 Hz were analyzed in 1-Hz steps with a temporal resolution of 0.05 s. A dynamic width method was applied to balance spectral and temporal precision (1-13 cycles, increasing with frequency).

Power spectra were averaged across trials within each condition for statistical analyses. power spectrum density within the IBF $\pm$ 2 Hz band and the 0.3-0.5 s post-stimulation window were computed separately for each condition.

Inter-stim EMG

EMG data recorded simultaneously with EEG were segmented using the same trial structure as the EEG (0.1-3 s post stimulation). The signal was demeaned, high-pass filtered at 1 Hz, low-pass filtered at 100 Hz, notch-filtered at 50 Hz, and subsequently rectified with 50-ms smoothing to obtain the amplitude envelope.

To assess cortico-muscular coherence (CMC), time-frequency decomposition was performed using a wavelet approach. Fourier spectra were calculated for 1-45 Hz in 0.5-Hz steps, with adaptive time windows corresponding to three cycles per frequency. Coherence between EMG and each EEG channel was then computed using magnitude-squared coherence. This provided time-resolved cortico-muscular coherence estimates for each condition. CMC values within the IBF $\pm$ 2 Hz band and the 0.3-0.5 s post-stimulation window were computed separately for each condition.

Force metrics

Force signals, originally in volts, were converted to Newtons and low-pass filtered at 20 Hz (5th-order Butterworth, zero-phase forward-backward filtering). Baseline correction was performed by subtracting the mean force level of the rest state. The corrected force data were segmented into two types: (1) interval force, defined as the 5-s post-stimulation window; and (2) stimulation force, defined as the tACS-on period. For each epoch, the force-time integral (trapezoidal rule) was computed and normalized by epoch duration (s); condition- and subject-level averages were then computed for statistical comparison.

5.2.7 Statistical analysis

All statistical analyses were performed in MATLAB R2023a (The MathWorks Inc., Natick, MA, USA) and R version 4.4.0 (R Core Team,

2024).

Subjective discomfort ratings (VAS scores) were analyzed using a one-way repeated-measures ANOVA across stimulation conditions. Interval force and stimulation force were assessed with a two-way repeated-measures ANOVA including stimulation condition and interval as within-subject factors.

For EEG and CMC analyses, individual time-frequency spectra were first frequency-aligned to each participant's IBF. Repeated-measures ANOVAs were then conducted at four within-subject levels: (1) Anti-phase duration effect (A1, A1.5, A2, A5); (2) Phase effect at 2-s stimulation (A2, I2, S2); (3) Phase effect at 5-s stimulation (A5, I5, S5); and (4) Phase $\times$ duration interaction across A2, A5, I2, I5, S2, and S5 conditions. Pairwise post hoc comparisons were performed using paired t-tests with Tukey's correction for multiple comparisons. Statistical topographical representations were derived from the corresponding ANOVA or post hoc t-statistics at each electrode, with significance assessed using cluster-based permutation testing for each contrast to visualize condition-specific effects.

For the force data, group-level inference on the normalized interval force and stimulation force was conducted using a two-way repeated measures analysis of variance with both factors treated as within-subject variables. Condition had eight levels (A1, A15, A2, A5, I2, I5, S2, S5), and force type had two levels (interval force and stimulation force).

5.3 Results

5.3.1 Inter-stim EEG power and CMC

Power and coherence density of C1

We first examined post-stimulation EEG beta power and CMC at electrode C1, focusing on the IBF $\pm$ 2 Hz range during the 0.3-1 s post-

stimulation interval. Figure 5.2 illustrates the mean spectral power and CMC values across all stimulation conditions.

The repeated-measures ANOVA revealed no significant main effects of stimulation phase (F(2,38) = 0.65, $p = 0.53$), stimulation duration (F(1,19) = 0.02, p = 0.90), or their interaction (F(2,38) = 0.05, $p = 0.95$) on PSD. Thus, EEG beta power during the inter-stimulus period was not modulated by stimulation phase or duration.

In contrast, CMC analyses revealed robust modulation by both stimulation phase and duration. The repeated-measures ANOVA showed significant main effects of phase (F(2,38) = 58.5, $p < 0.001$) and duration (F(1,19) = 18.0, $p < 0.001$), as well as a significant phase $\times$ duration interaction (F(2,38) = 6.40, $p = 0.004$).

At matched stimulation durations, anti-phase tACS consistently reduced CMC relative to both in-phase and sham stimulation. Following 2s stimulation, CMC was significantly lower after anti-phase stimulation (A2) compared to both in-phase (I2; $p = 0.001$) and sham (S2; $p = 0.001$), whereas in-phase and sham conditions did not differ from each other ($p = 0.78$). A similar pattern was observed after 5s stimulation: CMC following A5 was significantly reduced compared to I5 ($p < 0.001$) and S5 ($p = 0.006$), with no difference between in-phase and sham conditions ($p = 0.84$). Across both durations, no reliable differences were observed between in-phase and sham stimulation, indicating that the observed modulation of corticospinal coupling was specific to anti-phase stimulation.

Within the anti-phase condition, post hoc comparisons (Figure 5.3 B and Table S5.3) showed that CMC increased systematically with stimulation duration in the anti-phase condition. Specifically, CMC following A5 was significantly higher than after A1, A1.5, and A2 (all $p \leq 0.018$). indicating a partial recovery of corticomuscular coupling with longer anti-phase trains. In contrast, stimulation duration had no significant effect on CMC within the in-phase or sham conditions. Note that no reliable differences were found between in-phase and sham conditions at either duration ($p = 0.78$ for 2 s; $p = 0.84$ for 5 s).

Together, these results demonstrate that closed-loop anti-phase tACS selectively disrupts corticomuscular coherence without altering local cortical beta power. This desynchronizing effect is phase-specific and duration-dependent, with maximal suppression following short anti-phase stimulation and partial recovery at longer durations. In contrast, in-phase and sham stimulation yielded comparable levels of cortico-muscular coupling across durations and did not modulate EEG beta power at C1.

Building on these findings, we next examined how the observed phase- and duration-dependent effects distribute across spatial and temporal dimensions.

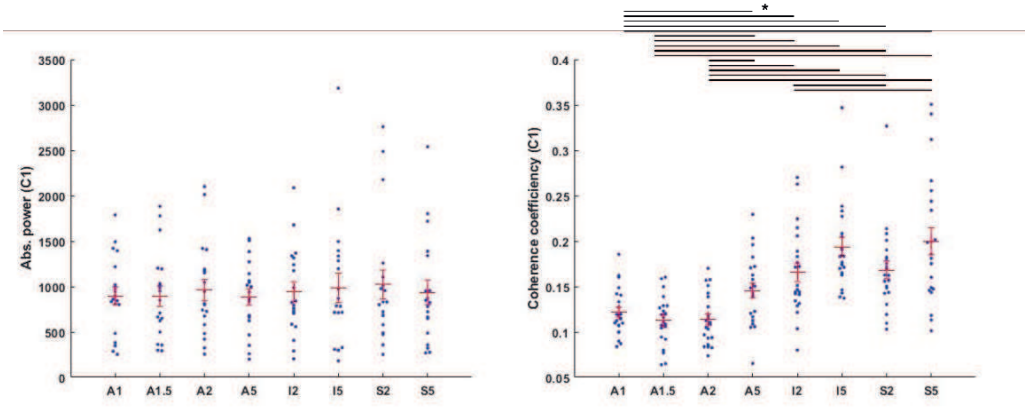


Figure 5.3: **EEG power and cortico-muscular coherence at C1 across stimulation conditions.** Mean EEG beta absolute power (PSD; left) and CMC at electrode C1 (right) are shown for each stimulation condition (A1, A1.5, A2, A5, I2, I5, S2, S5). Error bars denote the standard error of the mean. * indicates significant post-hoc differences ($p < 0.05$).

Spatial and temporal brain pattern of EEG power and CMC

Statistical topographical maps (Figures 5.4 and 5.5) revealed tACS phase and duration effects on post-stimulation (0.3-2 s) CMC and EEG power

in the range of IBF $\pm$ 2. For CMC, anti-phase trains in both 2-s and 5-s conditions produced consistent reduction, presented in a broad central area, relative to in-phase and sham conditions, whereas in-phase stimulation expressed CMC enhancement on top of sham conditions. 2-s anti-phase and in-phase/sham contracted map shows stronger contraction than 5-s conditions. EEG power maps, in contrast, did not show a reliable phase-specific signature across the same windows.

Collapsing within phase, as shown in Figure 5.5, stimulation duration systematically shaped the degree of the effect on CMC. Specifically, short (1-2 s) anti-phase trains produced stronger desynchrony magnitude on CMC than long trains (5 s), indicating an entrainment rebound of ongoing oscillations. EEG power did not yield any expressed changes across conditions, suggesting weak or inconsistent offline power changes during task engagement.

Together, topography results, aligning with the result discussed before, showed that brief, phase-targeted bursts (1-2 s) are sufficient to diminish CMC observed in the inter-stim interval, whereas longer (5 s) trains partially invert the effect.

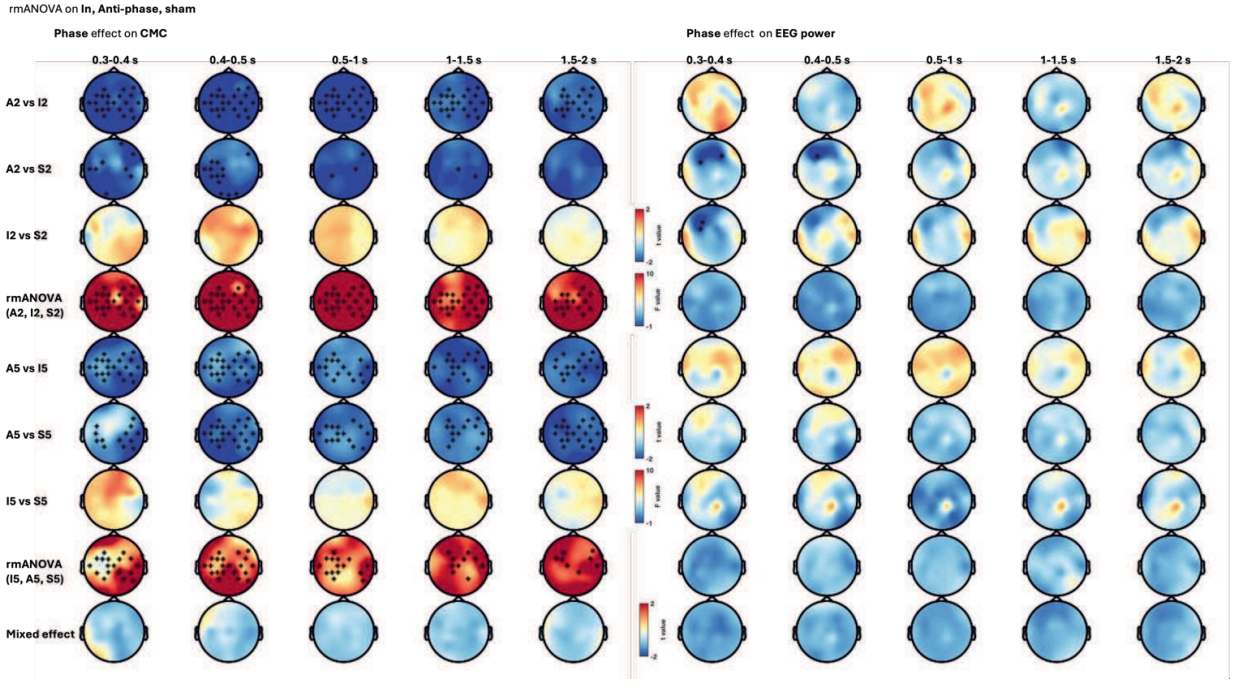


Figure 5.4: **Paired t-test and rm-ANOVA-based topographies of tACS phase effects on cortico-muscular coherence (CMC) and EEG power in the frequency range of IBF±2 across five consecutive post-stimulation windows (0.3-0.4, 0.4-0.5, 0.5-1.0, 1.0-1.5, 1.5-2.0, and 2.0-2.5 s).** The rmANOVA tests a single within-subject factor in a given duration condition, whereas the mixed effects model tests the phase by duration interaction across conditions. Left panel: statistical maps for CMC; Right panel: statistical maps for EEG power.

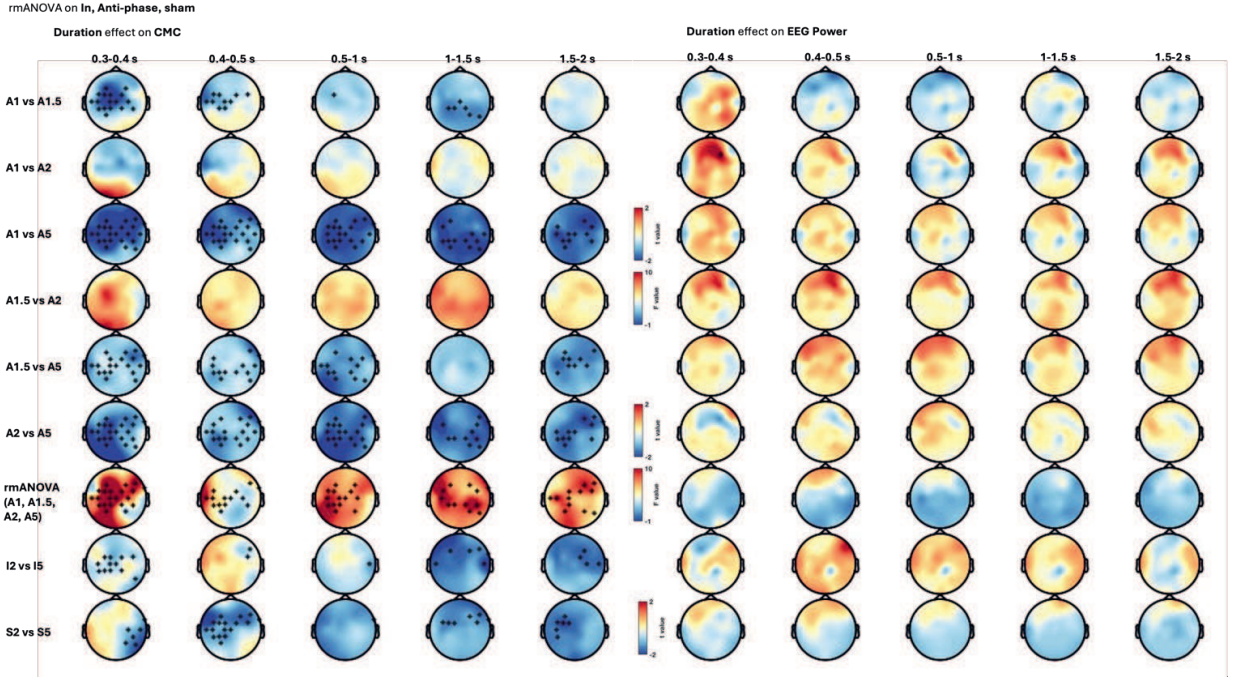


Figure 5.5: **Paired t-test and rm-ANOVA-based topographies of tACS duration effects on cortico-muscular coherence (CMC) and EEG power in the frequency range of IBF $\pm$ 2 across five consecutive post-stimulation windows (0-0.5, 0.5-1.0, 1.0-1.5, 1.5-2.0, and 2.0-2.5 s).** Left panel: statistical maps for CMC; Right panel: statistical maps for EEG power. The rmANOVA tests a single within-subject factor in the anti-phase condition.

Force metrics

Prior to group-level analyses, outliers were identified separately for each condition and measure using a robust median absolute deviation criterion and were excluded, in which one subject was removed (16 of 368 observations total)

Results from a two-way repeated-measures ANOVA on mean normalized force showed no main effects of stimulation conditions, no difference between stimulation on and off, and no interactive effect. Thus, closed-loop tACS did not alter gross motor output.

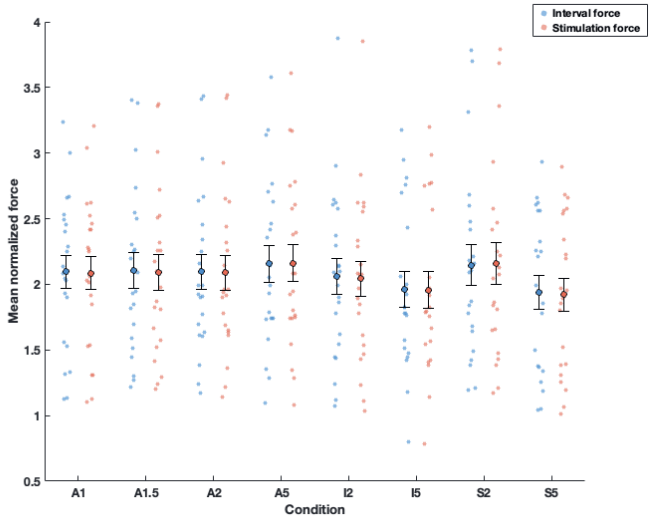


Figure 5.6: **Normalized force across conditions.** Mean normalized force is shown for interval force (5-s post-stimulation window; blue) and stimulation force (tACS-on period; red) across A1, A1.5, A2, A5, I2, I5, S2, and S5 conditions. Colored dots indicate individual participants, and diamonds with error bars indicate group-level central tendency and variability. No significant main effects or interaction were observed.

5.4 Discussion

In this study, we implemented a closed-loop tACS system to investigate the temporal dynamics of neuromodulation during an isometric motor task. We modulated stimulation duration ranging from 1 to 5 seconds in either anti-phase, in-phase, or sham configurations. We demonstrate that short anti-phase stimulation (1-2 s) produced the strongest reduction in CMC compared to in-phase and sham conditions, whereas longer anti-phase trains (5 s) led to partial rebound. In contrast, motor output and post-stimulation beta power remained unchanged across conditions. These findings provide novel evidence that stimulation duration, in addition to phase, critically shapes the neuromodulatory impact of closed-loop tACS on cortico-peripheral coupling, offering new insights for developing targeted, non-invasive interventions for motor disorders. This study intends to establish a specific temporal window for effective interventions in motor disorders.

5.4.1 Brief anti-phase stimulation introduces destructive interference

Accumulated evidence has shown that tACS can entrain neural activity and bias spike timing in a frequency and phase-specific manner [4, 6, 5, 7, 9, 44, 45, 46]. Recent developments in closed-loop tACS, where stimulation is precisely phase-locked to endogenous oscillations, allowing for more targeted disruption or amplification of neural rhythms, have shown improvements in the potential for state-dependent and time-sensitive neuromodulation [12, 14, 15].

Within the motor system, beta oscillations play fundamental roles in movement inhibition and cortico-spinal communication. Excessive beta synchronization is a hallmark of motor disorders such as PD and stroke [47, 48, 49, 50]. While most closed-loop tACS studies have focused on frequency and phase alignment, the temporal length of anti-phase stimulation may determine whether desynchronization is sustained or overridden by rebound entrainment. The question of how

long stimulation should be applied to yield maximal benefit without counterproductive effects is particularly relevant in clinical contexts.

Our study provides the first evidence that closed-loop anti-phase tACS over M1 can disrupt CMC in a phase- and duration-specific manner with healthy adults. Anti-phase tACS significantly reduced CMC compared to both in-phase and sham conditions at both short durations (1-2 s) and long durations (5 s). Specifically, a transcendent anti-phase sequence (1-2 s) produced the most beta-CMC reduction, while longer periods (5 s) led to a partial rebound. The reduction in CMC of our results suggests that aligning the peak of the exogenous waveform with the trough of the endogenous signal can induce destructive interference in endogenous rhythms [51, 44]. This interference is likely from the disruption of the membrane potential modulation cycle, leading to temporal jitter in spike timing [52, 53].

Crucially, we identified a temporal dissociation in efficacy: transient anti-phase stimulation produced stronger disruption than longer stimulation. This suggests while short bursts effectively exert phase cancellation and desynchronization, extended stimulation may inadvertently re-engage the motor network into a synchronized state [11]. Consequently, we propose a critical temporal window (1-2 s) for maximally disrupting beta-band coherence.

5.4.2 Effects of closed-loop tACS are state-, site-, and readout-specific

The absence of offline changes in EEG power in our study is not unprecedented. Prior studies have demonstrated that task engagement could reduce the susceptibility of neural oscillations to exogenous modulation compared to the rest state [54, 55]. This contrasts with our previous findings, in which anti-phase tACS over the pre-supplementary motor area (preSMA) during a stop-signal task selectively reduced local beta power [16]. The dissociation between power modulation observed in

that study and the present work is likely to be attributed to the top-down motor control and sensorimotor feedback loops, which stabilize endogenous beta oscillations and may compete with or override the exogenous electric fields [56, 57, 11]. In contrast, M1 beta during isometric contraction is rigidly stabilized by ”bottom-up” sensorimotor feedback loops [56, 11]. Consequently, while the preSMA is amenable to amplitude suppression, M1 beta is behaviorally ”clamped” by afferent drive, resisting gross power modulation.

A complementary explanation is that the dissociation reflects differences in stimulation site and the specific physiological readout. PreSMA beta is more control- or modulatory-oriented and less tightly locked to the periphery [58, 59]; anti-phase stimulation there can down-modulate local beta power. M1 beta during steady force, by contrast, is tightly coupled to spinal and muscle activity [60, 61], so anti-phase stimulation at M1 disrupts timing (CMC) without necessarily changing local power. In a stop-signal context, preSMA beta ramps and remains labile, making it susceptible to amplitude suppression. During isometric contraction, M1 beta is behaviorally set and stabilized by ongoing sensorimotor and afferent loops; phase jitter introduced by anti-phase stimulation can break cortico-spinal alignment (reducing CMC) while leaving net power unchanged [62, 63]. Power indexes local synchrony, whereas CMC indexes inter-areal or peripheral coupling [64]; thus, anti-phase stimulation can disturb phase alignment without reducing amplitude. Closed-loop alignment to endogenous beta, combined with contraction-related reafference, may favor phase decoherence over amplitude suppression during and after stimulation. Network-wise, preSMA effects likely route via associative basal ganglia-thalamic loops that are amenable to amplitude change, whereas M1 effects during force are constrained by corticospinal drive and proprioceptive feedback, favoring phase effects.

5.4.3 Secondary findings: EEG power, force metrics, and sham group

Another counterintuitive finding was that sham stimulation, which included a sinusoidal waveform (0.5-0.6 Hz) delivered at the 90° phase of ongoing beta oscillations, elicited beta CMC comparable to those seen during in-phase stimulation. Such cross-frequency coupling arises through harmonic or subharmonic resonance, wherein one rhythm can entrain another when their frequencies are related by simple integer ratios [65, 66]. In this scenario, the low-frequency waveform may have interacted nonlinearly with endogenous beta activity, placing the system in a subharmonic resonance regime that facilitated partial entrainment even under sham settings.

Our study found no significant differences in force output across experimental conditions, despite observable changes in CMC. Numerical studies have shown that beta-CMC, reflecting the timing and coordination of corticospinal drive, is most prominent during steady, tonic (isometric) contractions [60, 67] and can be modulated by cognitive load [68], sensory feedback [63], fatigue [69], pharmacological manipulations [70], and noninvasive brain stimulation [71], typically without consistent effects on gross force output. During a steady contraction, descending beta (EEG→EMG) imposes a synchronous template on motoneuron pools, while ascending beta continually recalibrates that template with sensory evidence. Such coupling may reduce drift and variability through improved timing coordination and more economical motor unit recruitment at a given torque, making CMC sensitive to timing perturbations even when mean force remains stable.

5.4.4 Implication and limitation

Our results indicate that phase-locked tACS can bidirectionally modulate the connectivity within corticospinal loops in healthy subjects, which motivates duration- and phase-adaptive closed-loop interventions that maximize the disruption of over-synchrony while minimizing

rebound entrainment. The reduction in CMC induced by anti-phase tACS in healthy participants suggests that phase-specific stimulation can transiently disrupt cortico-peripheral coupling without altering local beta power. While such a disruption might appear maladaptive in the intact motor system, the same mechanism could be beneficial in conditions characterized by excessive and abnormally stable beta synchrony, such as Parkinson's disease. In PD, pathological beta coupling within cortico-basal ganglia circuits may impede effective corticospinal communication, leading to reduced CMC [32, 48]. Dopaminergic treatment that shortens these pathological beta episodes restores CMC by re-aligning descending and ascending signals, as shown in studies demonstrating that levodopa and deep brain stimulation reduce the duration and power of beta bursts in the subthalamic nucleus and motor cortex, thereby normalizing corticomuscular coupling and improving motor performance [33, 34, 72, 35]. Studies using conventional beta-tACS have shown enhanced beta CMC in healthy adults yet reduced beta CMC in PD [22]. By desynchronizing these overly stable oscillations, anti-phase stimulation could potentially restore the temporal flexibility necessary for efficient motor output, thereby normalizing, rather than further reducing, functional CMC.

Several limitations are included in our study: First, the results were obtained solely in healthy adults and therefore may not speak directly for the clinical populations in whom network pathophysiology and treatment state can strongly shape oscillatory dynamics. Future research assessing the modulatory impact of closed-loop tACS on pathological networks are needed. Second, the stimulation duration space was sampled coarsely (four conditions for the anti-phase group) and readouts were only acquired during task state. Future work is suggested to focus on state-specific and time-precise protocols to identify optimal temporal windows for antiphase stimulation the maximize therapeutic outcomes.

5.5 Conclusion

Our study tested a closed-loop, phase-targeted tACS that provides causal control of corticospinal coupling during isometric contraction in healthy adults. Specifically, anti-phase stimulation over M1 reliably reduces beta-CMC compared to in-phase and sham, and this decoupling was strongly duration-dependent: brief bursts (1-2 s) were most effective, whereas longer trains (5 s) showed partial re-entrainment. This destructive interference wasn't accompanied by changes in motor output or offline cortical power changes. Our findings highlight the phase and duration as key for modulating ongoing motor-network dynamics, and bring the potential of closed-loop tACS as an adaptive neuromodulation protocol to normalize pathological oscillations in motor disease.

References

[1] Johannes Vosskuhl, Daniel Strüber, and Christoph S. Herrmann. "Non-invasive Brain Stimulation: A Paradigm Shift in Understanding Brain Oscillations". In: *Frontiers in Human Neuroscience* 12 (May 2018). DOI: 10.3389/fnhum.2018.00211.

[2] Osama Elyamany et al. "Transcranial alternating current stimulation (tACS): from basic mechanisms towards first applications in psychiatry". In: *European Archives of Psychiatry and Clinical Neuroscience* 271.1 (Nov. 2020), pp. 135–156. DOI: 10.1007/s00406-020-01209-9.

[3] Evan Weiss, Michael Kann, and Qi Wang. "Neuromodulation of Neural Oscillations in Health and Disease". In: *Biology* 12.3 (Feb. 2023), p. 371. DOI: 10.3390/biology12030371.

[4] Simal Ozen et al. "Transcranial Electric Stimulation Entrains Cortical Neuronal Populations in Rats". In: *The Journal of Neuroscience* 30.34 (Aug. 2010), pp. 11476–11485. DOI: 10.1523/jneurosci.5252-09.2010.

[5] Matthew R. Krause et al. “Transcranial alternating current stimulation entrains single-neuron activity in the primate brain”. In: *Proceedings of the National Academy of Sciences* 116.12 (Mar. 2019), pp. 5747–5755. DOI: 10.1073/pnas.1815958116.

[6] Luke Johnson et al. “Dose-dependent effects of transcranial alternating current stimulation on spike timing in awake nonhuman primates”. In: *Science Advances* 6.36 (Sept. 2020). DOI: 10.1126/sciadv.aaz2747.

[7] Gregor Thut, Philippe G. Schyns, and Joachim Gross. “Entrainment of Perceptually Relevant Brain Oscillations by Non-Invasive Rhythmic Stimulation of the Human Brain”. In: *Frontiers in Psychology* 2 (2011). DOI: 10.3389/fpsyg.2011.00170.

[8] Christoph S. Herrmann and Daniel Strüber. “What Can Transcranial Alternating Current Stimulation Tell Us About Brain Oscillations?” In: *Current Behavioral Neuroscience Reports* 4.2 (May 2017), pp. 128–137. DOI: 10.1007/s40473-017-0114-9.

[9] Christoph S. Herrmann et al. “Shaping Intrinsic Neural Oscillations with Periodic Stimulation”. In: *The Journal of Neuroscience* 36.19 (May 2016), pp. 5328–5337. DOI: 10.1523/jneurosci.0236-16.2016.

[10] Flavio Fröhlich, Kristin K Sellers, and Asa L Cordle. “Targeting the neurophysiology of cognitive systems with transcranial alternating current stimulation”. In: *Expert Review of Neurotherapeutics* 15.2 (Dec. 2014), pp. 145–167. DOI: 10.1586/14737175.2015.992782.

[11] Matthew R. Krause et al. “Brain stimulation competes with ongoing oscillations for control of spike timing in the primate brain”. In: *PLOS Biology* 20.5 (May 2022). Ed. by Huan Luo, e3001650. DOI: 10.1371/journal.pbio.3001650.

[12] John-Stuart Brittain et al. “Tremor Suppression by Rhythmic Transcranial Current Stimulation”. In: *Current Biology* 23.5 (Mar. 2013), pp. 436–440. DOI: 10.1016/j.cub.2013.01.068.

[13] Abbey B. Holt et al. "Phase-Dependent Suppression of Beta Oscillations in Parkinson's Disease Patients". In: *Journal of Neuroscience* 39.6 (2019), pp. 1119–1134. DOI: https://doi.org/10.1523/JNEUROSCI.1913-18.2018.

[14] Xueli Chen et al. "Alpha oscillatory activity is causally linked to working memory retention". In: *PLOS Biology* 21.2 (Feb. 2023). Ed. by Simon Hanslmayr, e3001999. DOI: 10.1371/journal.pbio.3001999.

[15] David Haslacher et al. "Working memory enhancement using real-time phase-tuned transcranial alternating current stimulation". In: *Brain Stimulation* 17.4 (July 2024), pp. 850–859. DOI: 10.1016/j.brs.2024.07.007.

[16] Zhou Fang, Alexander Sack, and Inge Leunissen. "Closed-loop anti-phase tACS over preSMA reduced oscillatory beta synchronization and modulated motor inhibition performance". In: (Nov. 2025). DOI: 10.1101/2025.11.25.690566.

[17] Christian Gerloff et al. "Coherent corticomuscular oscillations originate from primary motor cortex: Evidence from patients with early brain lesions". In: *Human Brain Mapping* 27.10 (Sept. 2006), pp. 789–798. DOI: 10.1002/hbm.20220.

[18] Jinbiao Liu, Yixuan Sheng, and Honghai Liu. "Corticomuscular Coherence and Its Applications: A Review". In: *Frontiers in Human Neuroscience* 13 (Mar. 2019). DOI: 10.3389/fnhum.2019.00100.

[19] Vihren Chakarov et al. "Beta-Range EEG-EMG Coherence With Isometric Compensation for Increasing Modulated Low-Level Forces". In: *Journal of Neurophysiology* 102.2 (Aug. 2009), pp. 1115–1120. DOI: 10.1152/jn.91095.2008.

[20] Thomas G. Simpson et al. "Cortical beta oscillations help synchronise muscles during static posture holding in healthy motor control". In: *NeuroImage* 298 (Sept. 2024), p. 120774. DOI: 10.1016/j.neuroimage.2024.120774.

[21] Alek Pogosyan et al. “Boosting Cortical Activity at Beta-Band Frequencies Slows Movement in Humans”. In: *Current Biology* 19.19 (Oct. 2009), pp. 1637–1641. DOI: 10.1016/j.cub.2009.07.074.

[22] Beatrix Krause and Roi Cohen Kadosh. “Not all brains are created equal: the relevance of individual differences in responsiveness to transcranial electrical stimulation”. In: *Frontiers in Systems Neuroscience* 8 (2014). DOI: 10.3389/fnsys.2014.00025.

[23] Daisuke Kudo et al. “Individualized beta-band oscillatory transcranial direct current stimulation over the primary motor cortex enhances corticomuscular coherence and corticospinal excitability in healthy individuals”. In: *Brain Stimulation* 15.1 (Jan. 2022), pp. 46–52. DOI: 10.1016/j.brs.2021.11.004.

[24] C. Wach et al. “Effects of 10Hz and 20Hz transcranial alternating current stimulation (tACS) on motor functions and motor cortical excitability”. In: *Behavioural Brain Research* 241 (Mar. 2013), pp. 1–6. DOI: 10.1016/j.bbr.2012.11.038.

[25] Louis-Philippe Lafleur et al. “No aftereffects of high current density 10 Hz and 20 Hz tACS on sensorimotor alpha and beta oscillations”. In: *Scientific Reports* 11.1 (Nov. 2021). DOI: 10.1038/s41598-021-00850-1.

[26] Andrea Guerra et al. “Driving motor cortex oscillations modulates bradykinesia in Parkinson’s disease”. In: *Brain* 145.1 (July 2021), pp. 224–236. DOI: 10.1093/brain/awab257.

[27] Marjan Jahanshahi et al. “A fronto-striato-subthalamic-pallidal network for goal-directed and habitual inhibition”. In: *NATURE REVIEWS NEUROSCIENCE* 16.12 (2015), pp. 719–732. DOI: https://doi.org/10.1038/nrn4038.

[28] Andrea A. Kühn et al. “Reduction in subthalamic 8–35 Hz oscillatory activity correlates with clinical improvement in Parkinson’s disease”. In: *European Journal of Neuroscience* 23.7 (Apr. 2006),

pp. 1956–1960. DOI: 10.1111/j.1460-9568.2006.04717.x.

[29] A. A. Kuhn et al. "High-Frequency Stimulation of the Subthalamic Nucleus Suppresses Oscillatory Activity in Patients with Parkinson's Disease in Parallel with Improvement in Motor Performance". In: *Journal of Neuroscience* 28.24 (June 2008), pp. 6165–6173. DOI: 10.1523/jneurosci.0282-08.2008.

[30] Ying Yu et al. "Parkinsonism Alters Beta Burst Dynamics across the Basal Ganglia–Motor Cortical Network". In: *The Journal of Neuroscience* 41.10 (Jan. 2021), pp. 2274–2286. DOI: 10.1523/jneurosci.1591-20.2021.

[31] Anke Karabanov, Axel Thielscher, and Hartwig Roman Siebner. "Transcranial brain stimulation: closing the loop between brain and stimulation". In: *Current Opinion in Neurology* 29.4 (Aug. 2016), pp. 397–404. DOI: 10.1097/wco.0000000000000342.

[32] P Brown. "Abnormal oscillatory synchronisation in the motor system leads to impaired movement". In: *Current Opinion in Neurobiology* 17.6 (Dec. 2007), pp. 656–664. DOI: 10.1016/j.conb.2007.12.001.

[33] S. Salenius et al. "Defective cortical drive to muscle in Parkinson's disease and its improvement with levodopa". In: *Brain* 125.3 (Mar. 2002), pp. 491–500. DOI: 10.1093/brain/awf042.

[34] Hame Park et al. "Cortico-muscular coherence increases with tremor improvement after deep brain stimulation in Parkinson's disease". In: *NeuroReport* 20.16 (Oct. 2009), pp. 1444–1449. DOI: 10.1097/wnr.0b013e328331a51a.

[35] Katja Airaksinen et al. "Cortico-muscular coherence in advanced Parkinson's disease with deep brain stimulation". In: *Clinical Neurophysiology* 126.4 (Apr. 2015), pp. 748–755. DOI: 10.1016/j.clinph.2014.07.025.

[36] R. C. Oldfield. “The assessment and analysis of handedness: The Edinburgh inventory”. In: *Neuropsychologia* 9.1 (1971), pp. 97–113. DOI: 10.1016/0028-3932(71)90067-4.

[37] Marom Bikson, Abhishek Datta, and Maged Elwassif. “Establishing safety limits for transcranial direct current stimulation”. In: *Clinical Neurophysiology* 120.6 (June 2009), pp. 1033–1034. DOI: 10.1016/j.clinph.2009.03.018.

[38] A.J. Woods et al. “A technical guide to tDCS, and related non-invasive brain stimulation tools”. In: *Clinical Neurophysiology* 127.2 (Feb. 2016), pp. 1031–1048. DOI: 10.1016/j.clinph.2015.11.012.

[39] Robert Oostenveld et al. “FieldTrip: Open Source Software for Advanced Analysis of MEG, EEG, and Invasive Electrophysiological Data”. In: *Computational Intelligence and Neuroscience* 2011 (2011), pp. 1–9. DOI: 10.1155/2011/156869.

[40] Saskia Haegens et al. “Inter- and intra-individual variability in alpha peak frequency”. In: *NeuroImage* 92 (May 2014), pp. 46–55. DOI: 10.1016/j.neuroimage.2014.01.049.

[41] H. Carlqvist et al. “Amplitude and phase relationship between alpha and beta oscillations in the human electroencephalogram”. In: *Medical & amp; Biological Engineering & amp; Computing* 43.5 (Oct. 2005), pp. 599–607. DOI: 10.1007/bf02351033.

[42] Christoph Zrenner et al. “Real-time EEG-defined excitability states determine efficacy of TMS-induced plasticity in human motor cortex”. In: *Brain Stimulation* 11.2 (Mar. 2018), pp. 374–389. DOI: 10.1016/j.brs.2017.11.016.

[43] Sina Shirinpour et al. “Experimental evaluation of methods for real-time EEG phase-specific transcranial magnetic stimulation”. In: *Journal of Neural Engineering* 17.4 (July 2020), p. 046002. DOI: 10.1088/1741-2552/ab9dba.

[44] Randolph F. Helfrich et al. "Entrainment of Brain Oscillations by Transcranial Alternating Current Stimulation". In: *Current Biology* 24.3 (Feb. 2014), pp. 333–339. DOI: 10.1016/j.cub.2013.12.041.

[45] Philip Tseng et al. "The critical role of phase difference in gamma oscillation within the temporoparietal network for binding visual working memory". In: *Scientific Reports* 6.1 (Aug. 2016). DOI: 10.1038/srep32138.

[46] Desmond Agboada, Zhihe Zhao, and Miles Wischnewski. "Neuroplastic effects of transcranial alternating current stimulation (tACS): from mechanisms to clinical trials". In: *Frontiers in Human Neuroscience* 19 (Mar. 2025). DOI: 10.3389/fnhum.2025.1548478.

[47] John N. Caviness et al. "Abnormal corticomuscular coherence is associated with the small amplitude cortical myoclonus in Parkinson's disease". In: *Movement Disorders* 18.10 (Oct. 2003), pp. 1157–1162. DOI: 10.1002/mds.10525.

[48] Nahid Zokaei et al. "Reduced cortico-muscular beta coupling in Parkinson's disease predicts motor impairment". In: *Brain Communications* 3.3 (2021). DOI: 10.1093/braincomms/fcab179.

[49] Yang Zheng et al. "Using Corticomuscular Coherence to Reflect Function Recovery of Paretic Upper Limb after Stroke: A Case Study". In: *Frontiers in Neurology* 8 (Jan. 2018). DOI: 10.3389/fneur.2017.00728.

[50] Rui Xu et al. "Lower-Limb Motor Assessment With Corticomuscular Coherence of Multiple Muscles During Ankle Dorsiflexion After Stroke". In: *IEEE Transactions on Neural Systems and Rehabilitation Engineering* 31 (2023), pp. 160–168. DOI: 10.1109/tnsre.2022.3217571.

[51] M. M. Ali, K. K. Sellers, and F. Frohlich. "Transcranial Alternating Current Stimulation Modulates Large-Scale Cortical Network Activity by Network Resonance". In: *Journal of Neuroscience*

33.27 (July 2013), pp. 11262–11275. DOI: 10.1523/jneurosci.5867-12.2013.

[52] Georgy Zarubin et al. “Transient Amplitude Modulation of Alpha-Band Oscillations by Short-Time Intermittent Closed-Loop tACS”. In: *Frontiers in Human Neuroscience* 14 (Sept. 2020). DOI: 10.3389/fnhum.2020.00366.

[53] Samira Barzegar et al. “Transcranial alternating current stimulation for investigating complex oscillatory dynamics and interactions”. In: *International Journal of Psychophysiology* 212 (June 2025), p. 112579. DOI: 10.1016/j.ijpsycho.2025.112579.

[54] Toralf Neuling, Stefan Rach, and Christoph S. Herrmann. “Orchestrating neuronal networks: sustained after-effects of transcranial alternating current stimulation depend upon brain states”. In: *Frontiers in Human Neuroscience* 7 (2013). DOI: 10.3389/fnhum.2013.00161.

[55] Fatemeh Khademi, Vladislav Royter, and Alireza Gharabaghi. “State-dependent brain stimulation: Power or phase?” In: *Brain Stimulation* 12.2 (Mar. 2019), pp. 296–299. DOI: 10.1016/j.brs.2018.10.015.

[56] Matteo Feurra et al. “State-Dependent Effects of Transcranial Oscillatory Currents on the Motor System: What You Think Matters”. In: *The Journal of Neuroscience* 33.44 (Oct. 2013), pp. 17483–17489. DOI: 10.1523/jneurosci.1414-13.2013.

[57] Robert Schmidt et al. “Beta Oscillations in Working Memory, Executive Control of Movement and Thought, and Sensorimotor Function”. In: *The Journal of Neuroscience* 39.42 (Oct. 2019), pp. 8231–8238. DOI: 10.1523/jneurosci.1163-19.2019.

[58] Parashkev Nachev, Christopher Kennard, and Masud Husain. “Functional role of the supplementary and pre-supplementary motor areas”. In: *Nature Reviews Neuroscience* 9.11 (Oct. 2008), pp. 856–869. DOI: 10.1038/nrn2478.

[59] Adam R. Aron et al. "Frontosubthalamic Circuits for Control of Action and Cognition". In: *The Journal of Neuroscience* 36.45 (Nov. 2016), pp. 11489–11495. DOI: 10.1523/jneurosci.2348-16.2016.

[60] B A Conway et al. "Synchronization between motor cortex and spinal motoneuronal pool during the performance of a maintained motor task in man." In: *The Journal of Physiology* 489.3 (Dec. 1995), pp. 917–924. DOI: 10.1113/jphysiol.1995.sp021104.

[61] Stephan Salenius et al. "Cortical Control of Human Motoneuron Firing During Isometric Contraction". In: *Journal of Neurophysiology* 77.6 (June 1997), pp. 3401–3405. DOI: 10.1152/jn.1997.77.6.3401.

[62] C. Nicholas Riddle and Stuart N. Baker. "Manipulation of peripheral neural feedback loops alters human corticomuscular coherence". In: *The Journal of Physiology* 566.2 (July 2005), pp. 625–639. DOI: 10.1113/jphysiol.2005.089607.

[63] Claire L. Witham et al. "Contributions of descending and ascending pathways to corticomuscular coherence in humans". In: *The Journal of Physiology* 589.15 (July 2011), pp. 3789–3800. DOI: 10.1113/jphysiol.2011.211045.

[64] Rui Xu et al. "Increased Corticomuscular Coherence and Brain Activation Immediately After Short-Term Neuromuscular Electrical Stimulation". In: *Frontiers in Neurology* 9 (Oct. 2018). DOI: 10.3389/fneur.2018.00886.

[65] Thomas Akam and Dimitri M. Kullmann. "Oscillatory multiplexing of population codes for selective communication in the mammalian brain". In: *Nature Reviews Neuroscience* 15.2 (Jan. 2014), pp. 111–122. DOI: 10.1038/nrn3668.

[66] Keith B. Doelling et al. "An oscillator model better predicts cortical entrainment to music". In: *Proceedings of the National Academy of Sciences* 116.20 (Apr. 2019), pp. 10113–10121. DOI: 10.1073/pnas.1816414116.

[67] Tatsuya Mima and Mark Hallett. "Corticomuscular Coherence: A Review". In: *Journal of Clinical Neurophysiology* 16.6 (Nov. 1999), p. 501. DOI: 10.1097/00004691-199911000-00002.

[68] Agnieszka Andrykiewicz et al. "Corticomuscular synchronization with small and large dynamic force output". In: *BMC Neuroscience* 8.1 (Nov. 2007). DOI: 10.1186/1471-2202-8-101.

[69] Franca Tecchio et al. "Cortical short-term fatigue effects assessed via rhythmic brain-muscle coherence". In: *Experimental Brain Research* 174.1 (Apr. 2006), pp. 144–151. DOI: 10.1007/s00221-006-0432-8.

[70] Mark R. Baker and Stuart N. Baker. "Beta-Adrenergic Modulation of Tremor and Corticomuscular Coherence in Humans". In: *PLoS ONE* 7.11 (Nov. 2012). Ed. by James Kilner, e49088. DOI: 10.1371/journal.pone.0049088.

[71] Manuel Zaepffel et al. "Modulations of EEG Beta Power during Planning and Execution of Grasping Movements". In: *PLoS ONE* 8.3 (Mar. 2013). Ed. by Francesco Di Russo, e60060. DOI: 10.1371/journal.pone.0060060.

[72] J. Hirschmann et al. "Differential modulation of STN-cortical and cortico-muscular coherence by movement and levodopa in Parkinson's disease". In: *NeuroImage* 68 (Mar. 2013), pp. 203–213. DOI: 10.1016/j.neuroimage.2012.11.036.

5.6 Supplementary information

5.6.1 Stuart Landau model for phase-specific tACS entrainment

To mechanistically approximate how tACS interacts with an endogenous neural oscillator, we simulated a single Stuart-Landau oscillator [0], the canonical normal form near a supercritical Hopf bifurcation, with an added periodic forcing term representing tACS.

In complex form, the state variable $z(t)$ evolves as

$$\dot{z} = \left(\lambda + i\omega - |z|^2\right) z + ke^{i\omega t + \phi}$$

where λ sets the limit cycle amplitude, ω is the intrinsic frequency, k is the forcing coupling strength (your parameter), and ϕ is the phase lag between stimulation and the ongoing oscillation. Sham is implemented as the same oscillator without the forcing term, enabling a direct comparison between intrinsic dynamics and externally driven dynamics.

As shown in Figure S5.1, Stuart Landau simulations indicate that anti-phase forcing at 180 degrees produces a coupling-dependent transition from transient disruption to post stimulation convergence toward an entrained regime, whereas 0 degree forcing remains stable across coupling strengths.

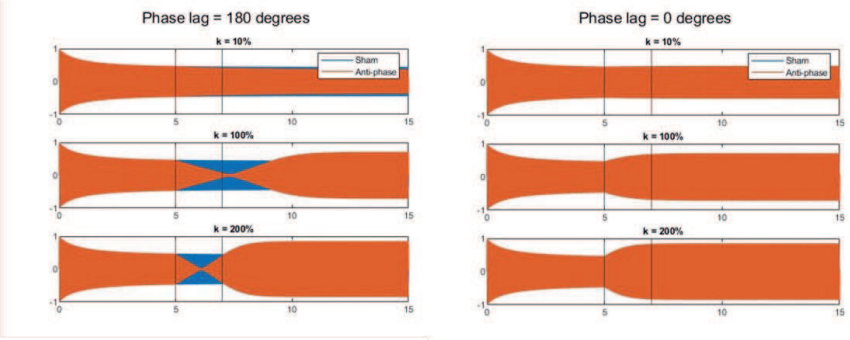


Figure S5.1: **Stuart Landau's simulations of phase-specific tACS entrainment.** The left panel shows a 180-degree phase lag, corresponding to anti-phase stimulation. The left panel shows a 0-degree phase lag, corresponding to in-phase stimulation. Each row includes three coupling strengths, 10%, 100%, and 200%. Orange traces represent the stimulation condition, and blue traces represent the sham. Vertical markers indicate a 2-second stimulation interval.

5.6.2 Self-reported discomfort scores

Perceived discomfort ratings differed significantly across stimulation conditions, as indicated by a repeated-measures ANOVA ($F(7, 168) = 24.40$, $p < 0.001$). Post-hoc Tukey comparisons revealed that both sham conditions were rated significantly less uncomfortable than all active stimulation conditions (all $p < 0.01$), while no significant differences emerged among the in- and anti-phase stimulations.

Table S5.1: **Perceived Discomfort Ratings Across Stimulation Conditions**

Stimulation condition	Discomfort score (Mean $\pm$ SD)	Main effect of condition
A1	2.64 ± 1.44	$F(7, 168) = 24.40$, $p < 0.001$ *
A15	3.16 ± 1.61	
A2	3.72 ± 1.55	
A5	3.96 ± 1.50	
I2	4.04 ± 1.81	
I5	3.84 ± 1.40	
S2	1.20 ± 1.83	
S5	1.32 ± 2.32	

Mean $\pm$ SD of self-reported discomfort ratings (range = 0-10) across all stimulation conditions. A repeated-measures ANOVA revealed a significant main effect of stimulation condition on perceived discomfort.

5.6.3 Paired t-test of CMC

Table S5.2: **Post-Hoc Pairwise Comparisons of Discomfort Ratings Between Stimulation Conditions**

group1	group2	Mean diff	p	lower	upper
A1	A15	0.52	0.961	-0.96	2
A1	A2	1.08	0.334	-0.40	2.56
A1	A5	1.32	0.118	-0.16	2.8
A1	I2	1.4	0.078	-0.08	2.88
A1	I5	1.2	0.208	-0.28	2.68
A1	S2	-1.44	0.063	-2.92	0.04
A1	S5	-1.32	0.118	-2.80	0.16
A15	A2	0.56	0.942	-0.92	2.04
A15	A5	0.8	0.714	-0.68	2.28
A15	I2	0.88	0.605	-0.60	2.36
A15	I5	0.68	0.813	-0.80	2.16
A15	S2	-1.96	**0.006**	-3.44	-0.48
A15	S5	-1.84	**0.009**	-3.32	-0.36
A2	A5	0.24	0.999	-1.24	1.72
A2	I2	0.32	0.996	-1.16	1.8
A2	I5	0.12	1	-1.36	1.6
A2	S2	-2.52	**0.003**	-4.00	-1.04
A2	S5	-2.40	**0.005**	-3.88	-0.92
A5	I2	0.08	1	-1.40	1.56
A5	I5	-0.12	1	-1.60	1.36
A5	S2	-2.76	**0.001**	-4.24	-1.28
A5	S5	-2.64	**0.002**	-4.12	-1.16
I2	I5	-0.20	1	-1.68	1.28
I2	S2	-2.84	**0.001**	-4.32	-1.36
I2	S5	-2.72	**0.002**	-4.20	-1.24
I5	S2	-2.64	**0.002**	-4.12	-1.16
I5	S5	-2.52	**0.003**	-4.00	-1.04
S2	S5	0.12	1	-1.36	1.6

Tukey's HSD post-hoc comparisons of discomfort scores across stimulation conditions. $P < .05$ denote significant difference between conditions.

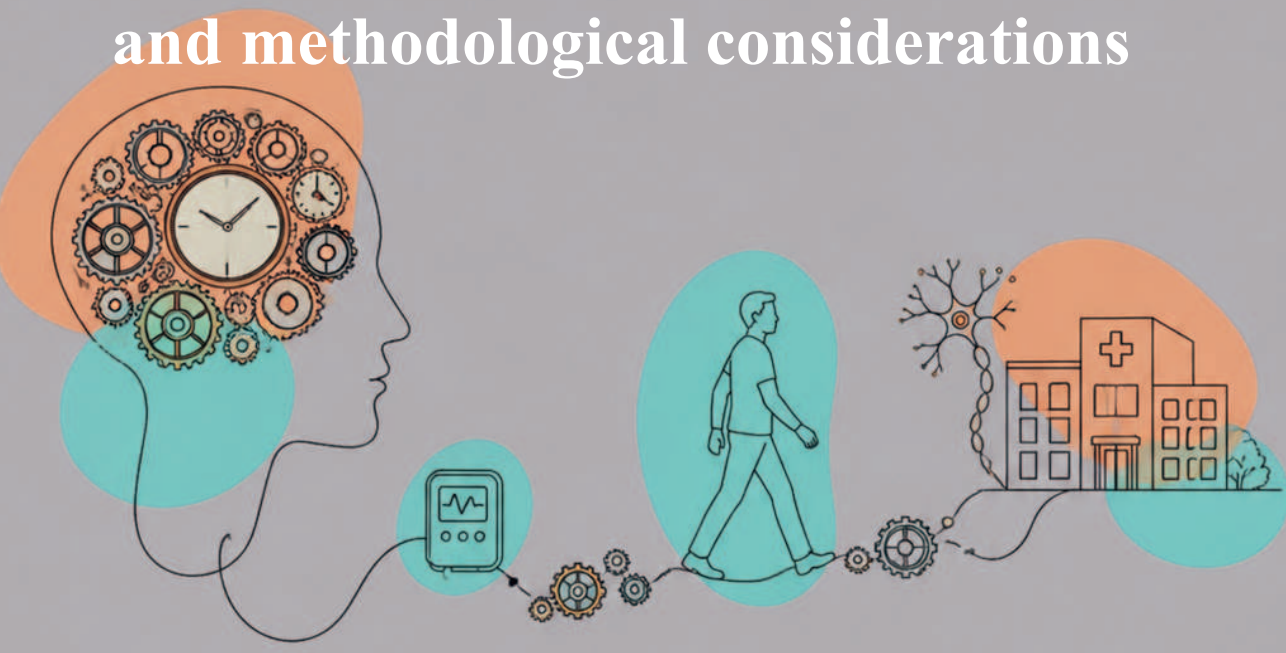
Table S5.3: **Post-hoc pairwise comparisons of cortico-muscular coherence (CMC).**

Group1	Group 2	Mean diff.	SE	p-value	Lower	Upper
A1	A15	0.002	0.008	1	-0.025	0.028
A1	A2	0.007	0.006	0.955	-0.015	0.028
A1	A5	-0.028	0.007	**0.018**	-0.053	-0.004
A1	I2	-0.058	0.013	**0.007**	-0.103	-0.012
A1	I5	-0.092	0.012	< 0.001	-0.131	-0.053
A1	S2	-0.057	0.011	**0.001**	-0.094	-0.02
A1	S5	-0.086	0.01	< 0.001	-0.121	-0.051
A15	A2	0.005	0.008	0.996	-0.02	0.031
A15	A5	-0.03	0.007	**0.008**	-0.054	-0.006
A15	I2	-0.059	0.013	**0.003**	-0.103	-0.016
A15	I5	-0.094	0.01	< 0.001	-0.127	-0.06
A15	S2	-0.058	0.009	< 0.001	-0.089	-0.027
A15	S5	-0.088	0.013	< 0.001	-0.13	-0.045
A2	A5	-0.035	0.009	**0.018**	-0.066	-0.004
A2	I2	-0.065	0.012	< 0.001	-0.103	-0.026
A2	I5	-0.099	0.011	< 0.001	-0.134	-0.064
A2	S2	-0.064	0.009	< 0.001	-0.094	-0.034
A2	S5	-0.093	0.009	< 0.001	-0.123	-0.063
A5	I2	-0.029	0.015	0.513	-0.079	0.02
A5	I5	-0.064	0.012	**0.001**	-0.104	-0.023
A5	S2	-0.028	0.012	0.278	-0.067	0.011
A5	S5	-0.058	0.013	**0.006**	-0.102	-0.013
I2	I5	-0.034	0.016	0.452	-0.089	0.021
I2	S2	0.001	0.013	1	-0.041	0.043
I2	S5	-0.028	0.016	0.62	-0.081	0.024
I5	S2	0.035	0.014	0.215	-0.01	0.081
I5	S5	0.006	0.014	1	-0.041	0.053

Post hoc comparisons across conditions tested using paired t-tests. Values show the estimated mean difference (Group 1 - Group 2), standard error (SE), p-value, and 95% confidence interval (Lower, Upper). No corrections were applied to p values. Significant results ($p < 0.05$) are shown in bold.

6

Online EEG phase tracking for adaptive tACS: practical engineering and methodological considerations



Abstract

Transcranial electrical stimulation (tES) has emerged as a tool to modulate brain oscillations and has shown promising results in influencing cognitive and motor function. This motivates its development as a therapeutic tool for the treatment of psychiatric and neurologic disorders. However, major barriers to reliable application include inter- and intra-individual variability in responsiveness. In addition, conventional open-loop stimulation is by nature entraining, tending to amplify ongoing rhythms, which constrains utility in disorders where pathological oscillations are already excessive, such as Parkinson's disease. Recent advances in computational methods and real-time electrophysiology enable the integration of alternating current stimulation (tACS) with concurrent electroencephalography (EEG), opening the door to closed-loop stimulation strategies. In a phase-dependent closed-loop system, stimulation can be aligned to neural rhythms with a defined phase offset, enabling state-contingent and bidirectional modulation of neural dynamics and behavior. Achieving this demands precise coordination across hardware, software, and experimental design. Success depends on careful control of hardware latency and jitter, robust real-time EEG acquisition during stimulation, accurate causal phase estimation with explicit prediction and compensation, and experimental designs that quantify both neural and behavioral outcomes while controlling for peripheral confounds. Here we provide practical engineering and methodological recommendations for the reproducible implementation of phase-dependent closed-loop tACS, expanding opportunities for mechanistically informed experimental designs and paving the way toward clinical translation.

6.1 Introduction

Transcranial electrical stimulation (tES), transcranial alternating current stimulation (tACS), has emerged as a non-invasive approach for modulating neural oscillations in the human cortex and manipulating cognitive and motor outcomes [1]. By delivering low-intensity currents through the surface, tACS can entrain ongoing cortical activity when delivered at frequencies that match or approximate endogenous rhythms [2]. Converging evidence from cellular and circuit-level studies suggests that a rhythmic external drive can bias neuronal populations toward phase alignment with the applied waveform, thereby shifting oscillatory power, coherence, and downstream information processing [3, 4, 5]. Consistent with this mechanistic account, tACS has been reported to influence behavioral performance across multiple domains, including perceptual detection and multisensory timing [6], visuospatial and sustained attention [7], working memory [8], and motor control [9, 10].

These functional effects are motivating the development of tACS as a therapeutic tool, and early clinical and translational work has begun to evaluate tACS across psychiatric and neurological disorders, including depression and a range of broader neuropsychiatric indications [11, 12]. However, translation remains constrained by several limitations. First, inter- and intra-individual variability in response to the stimulation has been a major barrier to its application [13, 14, 15]. A further and mechanistic limitation is that conventional tACS is, by nature, an entraining intervention that tends to strengthen phase alignment and amplify ongoing oscillatory activity at the driven frequency. This property narrows its utility in disorders characterized by excessive or maladaptive rhythmic synchronization [2, 16]. Parkinson's disease provides a salient example, as pathologically elicited beta synchronization has been a prominent biomarker and linked to bradykinesia and rigidity. In this context, an open-loop entrainment strategy would reinforce the pathological dynamics that are already excessive [17, 18, 19]. These considerations motivate a closed-loop strategy that aims at

suppressing or reshaping ongoing pathological oscillatory dynamics in a phase-dependent manner [20, 21, 22].

Advancements for neuroimaging and electrophysiological readouts provide the sensing substrate for adaptive tACS [23, 24]. Among non-invasive modalities, electroencephalography (EEG) is a well-suited candidate for providing real-time neural dynamic information for a closed-loop tACS system because of its millisecond-scale temporal resolution. EEG enables continuous extraction of the instantaneous oscillatory phase that indexes cortical cyclic fluctuations. A phase-dependent closed-loop tACS can be timed to a specific phase relation relative to an endogenous rhythm to reshape the intrinsic rhythmic synchronization in an intended direction. For example, stimulation with a phase lag of 180 degrees (anti-phase) can reduce phase locking and disrupt oscillatory synchrony.

A practical phase-dependent closed-loop tACS EEG system, therefore, requires three tightly integrated subsystems, as shown in Figure 6.1. First, a front end that acquires EEG with stable timing and sufficient dynamic range, alongside an artifact strategy that preserves the neural signal of interest during or immediately after stimulation. Second, an online signal processing and state estimation module that performs causal filtering, phase estimation, and short-horizon phase prediction, with explicit latency measurement and compensation so that stimulation is delivered at the intended brain phase. Third, a stimulation backend implementing precise waveform phase control and maintaining clock alignment across acquisition, computation, and stimulation hardware.

Accordingly, our purpose is to provide practical engineering and methodological recommendations that enable reproducible implementation of phase-dependent closed-loop tACS, with explicit attention to latency characterization, artifact mitigation, causal phase estimation and prediction, timing validation, and experimental design choices that support interpretable neural and behavioral inference. These practical recommendations aim to expand opportunities for

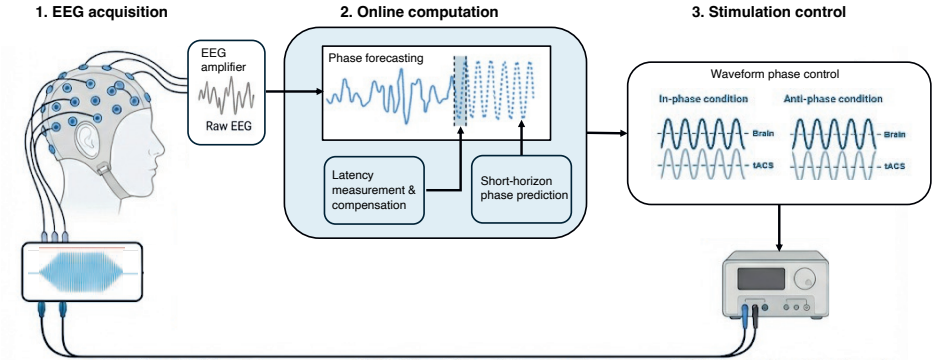


Figure 6.1: **Schematic architecture of an EEG-based phase-dependent closed-loop tACS system.**

mechanistically informed experimental designs that can more cleanly test phase-specific causal hypotheses about oscillatory function and help pave a clearer path from proof of concept demonstrations toward clinical translation of adaptive, phase-dependent tACS interventions.

6.2 A guide for successfully implementing a phase-dependent closed-loop tACS system

6.2.1 Hardware and latency control aligned to the frequency of interest

A reliable closed-loop system integrates three key hardware components: EEG acquisition, computational processing, and stimulation output. Each must operate with predictable latency and minimal jitter relative to the oscillatory period of interest.

Acquisition hardware

An EEG amplifier suitable for closed-loop operation should meet three requirements: (1) Low acquisition delay. Low acquisition delay is criti-

cal for phase targeting: at 20 Hz, a 10 ms acquisition error corresponds to about 72 degrees of phase error, and even a 3 ms shift corresponds to roughly 22 degrees. The acquisition delay typically originates from the amplifier rather than from the acquisition PC, and can range from a few milliseconds up to nearly 100 ms, depending largely on amplifier model and connector or streaming configuration. For example, direct USB streaming with low buffer settings or Ethernet UDP-based streaming designed for online processing can achieve low millisecond latency with sub-millisecond jitter in vendor-validated configurations. Whereas wireless transport typically introduces substantially greater delays. (2) DC coupling and sufficient input range, preventing amplifier saturation from tACS leakage currents, and enabling stable baseline tracking under slow drifts; here, front-end dynamic range and stimulation compatibility features such as high input range and shielding are practical discriminators across amplifier classes. For example, modern DC-coupled research amplifiers may provide EEG input ranges on the order of hundreds of millivolts (for example, $\pm$ 400 mV) with high input impedance and trigger I/O integrated into the same sampling clock, which can be advantageous for stimulation-compatible closed-loop timing. (3) Adequate sampling rate, ideally at least ten times the target frequency band. For example, for beta-range work, 2 kHz is a practical default that supports causal filtering and precise phase tracking.

Table 6.1 shows several EEG amplifiers known for low acquisition delay and minimal jitter, making them recommended for real-time applications.

Operating system

The operating system (OS) and runtime stack must sustain real-time performance without introducing variable delays. RAM should be explicitly allocated for all streaming buffers to avoid dynamic memory calls during execution. The computational load of phase estimation and

Table 6.1: **EEG amplifiers suitable for real-time and closed-loop applications**

Manufacturer & Model	Acquisition Delay	Jitter
Brain Products - actiCHamp Plus (with TurboLink)	< 1.5 ms	~ 0.2 ms
g.tec - g.USBamp/ g.HIamp	~ 0.8-1.2 ms	~ 0.5-1 ms
BioSemi - ActiveTwo	~ 7-8 ms	≤ 1 sample
ANT Neuro - eego (mylab/SPORT)	-	< 1 ms
Bittium - NeurOne Tesla	~ 3.5 ms	~ 0 ms

This table summarizes representative EEG amplifiers that have been demonstrated to support real-time closed-loop applications with low acquisition delay and minimal timing jitter.

feedback control must remain well within the OS's real-time scheduling capacity to prevent jitter accumulation.

End-to-end system latency

For adaptive stimulation to be effective, the total feedback delay from EEG acquisition to tACS delivery must be tightly controlled. Precise synchronization between EEG feedback and stimulator output ensures that each pulse is delivered at the intended cortical phase.

Total loop latency can be expressed as:

$$\tau_{\text{total}} = \tau_{\text{acq}} + \tau_{\text{filter}} + \tau_{\text{est}} + \tau_{\text{comm}} + \tau_{\text{stim}}$$

Where τ_{acq} refers to acquisition delay: time from the analog cortical signal at the electrode to the first digitized samples available to software; τ_{filter} is filtering delay: causal preprocessing delay introduced by real time bandpass and Hilbert pair or other causal transforms; τ_{est} estimation delay: computation time for feature extraction and phase estimation, including windowing, phase unwrap, instantaneous frequency tracking, prediction to the delivery horizon, and decision logic;

τ_{comm} command path delay: time from the decision timestamp to the stimulator input, including OS scheduling, API calls, USB or network transfer, and any digital to analog conversion if an analog control line is used; τ_{stim} stimulator onset delay: time from triggers arrival at the stimulator to current reaching the programmed trajectory at the electrodes.

To compensate for this delay, the target phase command should be advanced by:

$$\phi_{\mathrm{cmd}} = (\phi_{\mathrm{desired}} + 2\pi f \tau_{\mathrm{total}}) \bmod 2\pi$$

Where ϕ_{cmd} is the adjusted phase sent to the stimulator as the trigger target, and ϕ_{desired} is the desired phase at the cortex, which was set to be 0 in Chapters 3 and 4; f is the center frequency of the tracked rhythm. Accurate delay measurement and compensation are essential to maintain consistent phase locking.

6.2.2 Real-time EEG processing and artifact handling

Data buffering

Real-time EEG processing begins with efficient data buffering, maintaining continuous, time-stamped access to the signal stream. Two common open-source systems dominate current implementations: (1) FieldTrip Real-Time Buffer [25] provides a lightweight TCP/IP protocol that streams raw samples in fixed-size chunks; and (2) Lab Streaming Layer (LSL) [26] offers sub-millisecond synchronization across devices using clock offset correction and jitter compensation.

For a real-time system, buffer size (e.g., 32-128 samples) is critical: large buffers increase stability but add latency; smaller buffers improve temporal precision but risk packet underruns. Systems should timestamp each sample before transmission and align clocks via Network Time Protocol (NTP) or LSL's internal time correction. Some of the successful

online phase-dependent stimulation pipelines use double buffering, one buffer for acquisition, one for concurrent processing, ensuring continuous data flow without blocking the amplifier thread [27, 28, 29].

(Re-)reference

Stable phase estimation requires a consistent referencing approach. Common options include unipolar, bipolar, or Laplacian montages, chosen based on the frequency band and cortical target. In multichannel systems, referencing must be fixed prior to model training, as shifts can alter phase offsets and autoregressive model coefficients.

Frequency band selection

Once a stable reference is established, signals should be band-limited to the frequency of interest using causal filters. Key considerations include: (1) Filter type: Causal IIR filters (e.g., Butterworth or Chebyshev Type II) are preferred for low group delay ($<$ 10 ms). FIR filters impose longer delays and are less suited for real-time systems unless very short ($\leq$ 100 taps); (2) Bandwidth: Narrow passbands ($\pm$ 2 Hz around the individual peak frequency) improve phase precision but increase susceptibility to drift; a moderate width ($\pm$ 3-4 Hz) balances stability and adaptability [30, 31]; (3) Adaptation: Dynamic band tracking can be achieved by continuously estimating the dominant spectral peak via short-time FFT or adaptive notch algorithms [32]; (4) Implementation: Filtering is performed sample-by-sample or on small buffered segments to maintain causality. Group delay (τ_{filter}) must be measured and compensated within the total system latency budget.

Artifact handling

Artifact suppression is a major challenge for online processing. Successful implementations employ causal, low-latency detectors combined with: (1) Hardware-level rejection: low impedance acquisition channels and proper grounding reduce motion and mains interference; (2) Adaptive referencing: as discussed above, re-referencing can mitigate slow drifts and line noise without introducing phase distortion; (3) Amplitude and gradient thresholds: Continuous monitoring of signal envelope and its derivative allows immediate rejection of transient artifacts (e.g., eye blinks, muscle bursts). Samples exceeding $z > 3$ of the running mean could be marked as invalid for phase estimation [28]; (4) Artifact masking: During concurrent stimulation, prediction is suspended for 1-2 cycles following each pulse to avoid contamination [33, 34].

Common toolbox for real-time EEG analysis

6.2.3 Phase estimate algorithmic strategies

Precise real-time phase prediction is crucial for a closed-loop stimulation system, accounting for unavoidable system delays and filtering artifacts. Several strategies have been developed to forecast the instantaneous phase of an oscillatory neural signal.

Frequency domain-based sinusoid extrapolation.

A straightforward approach emerges as frequency domain decomposition, where the EEG signal is first band-pass filtered to isolate the frequency band of interest (Figure 6.2.1). A Fast Fourier Transform (FFT) [30] or wavelet method [32] is then computed over a short past window to estimate the dominant oscillation's frequency and phase.

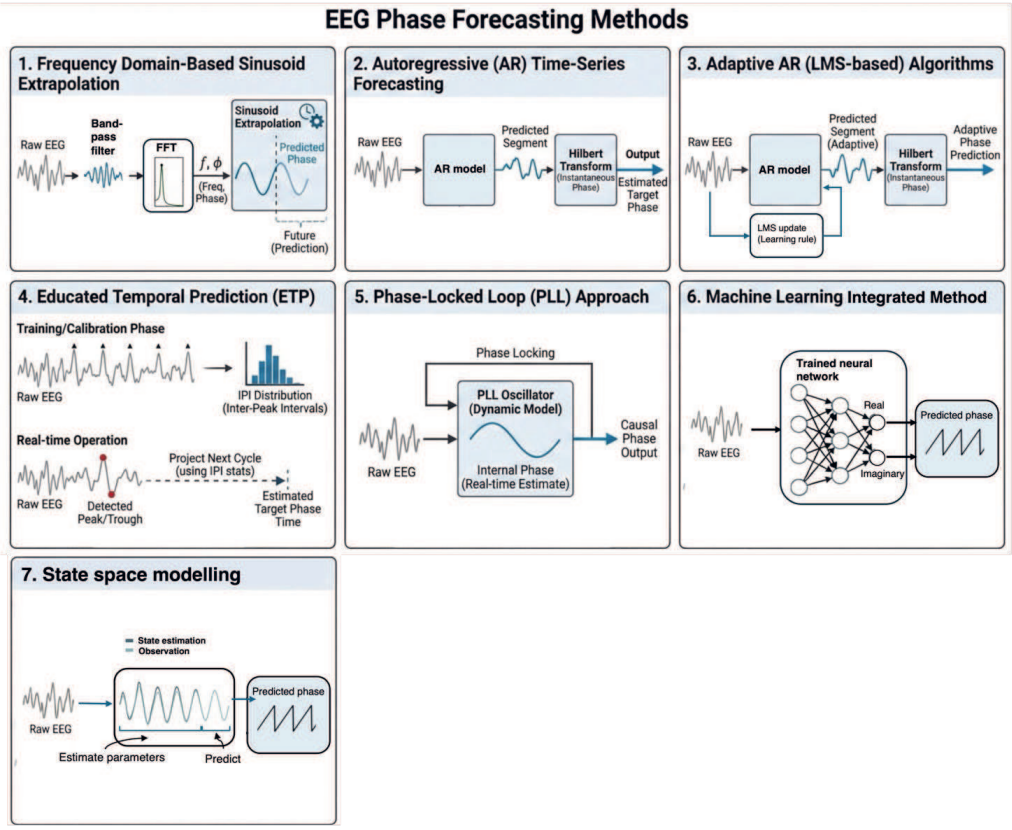


Figure 6.2: **Methods for forecasting the instantaneous phase of oscillatory neural signals.**

Table 6.2: **Open-source toolboxes for online EEG analysis**

Framework	Primary language	Typical latency	Pros	Cons
FieldTrip Real Time Buffer	C, MATLAB, Python	< 5 ms	Lightweight and deterministic. Works well with MATLAB and Python	Minimal GUI. Manual latency calibration required
MNE Realtime and MNE LSL	Python	3-8 ms	Seamless with the MNE ecosystem. Fast prototyping	Python GIL and garbage collection need care for strict timing
BCILAB for EEGLAB	MATLAB	10-20 ms	Rich algorithms and mature tutorials	MATLAB runtime and memory overhead. Less suited to subcycle triggering
OpenViBE	C++	10-15 ms	Visual design with many drivers	Less tuned for sub-20 ms loops. Fewer recent plugins
BCI2000	C++	10-15 ms	Very robust and well documented	Steeper learning curve for custom DSP blocks
BrainFlow	C++, Python, Java, others	< 10 ms	Easy hardware bring-up	Limited advanced buffering controls. Smaller research footprint
Brainstorm online modules	MATLAB	10-20 ms	Strong visualization and source tools	MATLAB dependency and less focus on low latency control
Simulink DSP System Toolbox	MATLAB	5-20 ms	Code generation and fixed step schedulers	License cost and integration effort with neuroscience stacks
PyRiemann realtime pattern tools	Python	Method dependent	Strong accuracy in BCI tasks	Not a full streaming stack. Combine with LSL or FT buffer

Assuming relative stationarity of the oscillation within this brief horizon, the algorithm extrapolates a sinusoidal waveform forward in time to predict the future phase.

Autoregressive (AR) time-series forecasting

A more flexible yet computationally demanding alternative is the autoregressive (AR) time-series forecasting approach (Figure 6.2.2). This method models the EEG signal as a linear combination of its past samples, allowing for short-term extrapolation of the waveform into the

future [31, 33]. The predicted segment then would be used to estimate the instantaneous phase (e.g., with Hilbert), enabling anticipation of when the target phase will occur. AR models generally outperform FFT methods when oscillations are stationary over the prediction horizon, capturing deviations from pure sinusoidal shapes. However, the method's accuracy depends critically on model order, window length, and signal-to-noise ratio (SNR).

As illustrated in Figure 6.2.3, adaptive AR or LMS-based AR algorithms were developed for longer prediction horizons, in which model parameters are continuously updated in real time with learning rules such as the least-mean-square (LMS) algorithm [35, 36]. This adaptivity allows the model to track slow drifts in oscillatory frequency or amplitude, improving phase prediction accuracy under dynamic conditions.

Educated temporal prediction (ETP)

A peak-interval prediction, Educated Temporal Prediction (ETP), uses a training or calibration phase to characterise the distribution of inter-peak intervals (IPI) of the target oscillation under resting conditions. During real-time operation, the system detects each oscillatory peak or trough and projects the next expected cycle using the learned IPI statistics, thereby estimating the future time point at which the desired phase will occur, as depicted in Figure 6.2.4. An ETP approach is recommended when the baseline data are in a low-SNR environment [28].

Phase-locked loop (PLL) approach

The phase-locked loop (PLL) approach, shown in Figure 6.2.5, uses a dynamic oscillator model that continuously locks onto the incoming signal's phase and frequency [37]. The internal phase of the modelled oscillator serves as the real-time estimate of the signal's phase. Such a

causal technique achieves rapid tracking without non-causal operations like the Hilbert transform. This approach is suitable when system latency is constrained. Therefore, it is normally used for hardware embedded phase detection.

Machine learning based methods

Machine learning based methods employ supervised learning techniques, such as convolutional or recurrent neural networks, to learn mappings between raw or pre-processed EEG data and future oscillatory phase [38, 39, 40] (Figure 6.2.6). Machine-learning models can capture non-linear and multi-component patterns in EEG data, offering potentially higher precision and generalisability across subjects. However, their performance depends on the availability of representative training data, and they must be computationally lightweight to satisfy real-time latency constraints.

State space modelling

State space modelling approach can be viewed as model constrained form of sequential learning in which latent oscillatory states, such as phase, amplitude, and frequency, are inferred online from noisy observations [34, 41]. In contrast to purely feedforward neural networks, state space models explicitly encode temporal dynamics and uncertainty, typically using Kalman or Bayesian filtering schemes (Figure 6.2.7). Recent work has demonstrated that oscillatory state space models achieve robust real-time phase tracking and forward prediction under non-stationary and low SNR conditions, often outperforming classical Hilbert or FFT-based estimators. By propagating the inferred latent dynamics forward in time, these models naturally support phase prediction with quantified uncertainty, which is critical for closed-loop stimulation.

Hybrid algorithms

Rodriguez Rivero and Ditterich [42] described an adaptive closed-loop phase-prediction method that integrated onset/offset detection of oscillatory activity with dynamic prediction of the next phase event. These hybrid techniques often employ cascaded filtering, feature extraction, and regression or classification layers to estimate phase with improved robustness. While implementation details vary, hybrid approaches generally provide a balance between computational efficiency and adaptive performance, making them attractive candidates for real-time EEG-based neurostimulation.

In summary, each phase-prediction method offers specific advantages and trade-offs. A comparative summary of the principal EEG phase-prediction algorithms and their characteristic features is presented in Table 6.3. The choice of algorithm ultimately depends on the characteristics of the target oscillation, available computational resources, and the latency constraints of the stimulation hardware.

Comparison of major algorithmic families used for real-time estimation and prediction of EEG oscillatory phase in closed-loop, phase-locked neurostimulation systems. EEG = electroencephalography; FFT = Fast Fourier Transform; AR = autoregressive model; LMS = least mean square; ETP = Educated Temporal Prediction; PLL = phase-locked loop; EPN = EEG Phase Prediction Network; MLOF = multi-layer optimized filter; SNR = signal-to-noise ratio.

6.2.4 Experimental design

Behavioral task

The first prerequisite for successful phase-dependent closed-loop stimulation is to engage a neural rhythm that exhibits stable, high-amplitude

oscillations at the frequency of interest. Such conditions enhance signal-to-noise ratio for real-time phase estimation and ensure that stimulation targets a physiologically meaningful state.

In many cases, empirical evidence shows that tACS effects are most pronounced during active task engagement rather than during rest, when the regarding neural circuits are functionally recruited [43, 44, 45]. Hence, the experimental paradigm should evoke the specific oscillation that the closed-loop system aims to modulate (e.g., beta during motor inhibition, alpha during visuospatial attention, theta during working memory updating).

However, some rhythms (most notably alpha) can exhibit robust, high-amplitude oscillations during rest [46], which may provide sufficiently reliable phase information for closed-loop operation without explicit task demands. Thus, while task engagement is generally advantageous, resting-state paradigms may be appropriate for certain frequencies and research questions.

Target localization and electrode montage

The cortical site chosen for stimulation must correspond to the network generating the oscillation relevant to the cognitive operation under study (for instance, preSMA for motor inhibition or parietal cortex for alpha attention). Ideally, the estimated area for EEG and the target area for tACS should coincide anatomically. However, practical constraints of combined EEG-tACS montages often prevent electrodes and recording sensors from occupying identical scalp locations, introducing small but systematic phase offsets between the measured and the stimulated site.

Beyond these practical limitations, closed-loop approaches need not be restricted to local phase locking. More flexible strategies may intentionally track oscillatory activity in one node of a distributed network and deliver stimulation to another node with a predefined temporal lag (for

example, tracking frontal theta activity and stimulating parietal cortex at a specific phase offset to target frontoparietal communication). Such approaches broaden the scope of closed-loop stimulation from local entrainment to network-level phase coordination.

In all cases, phase-mapping errors and inter-site delays should be explicitly considered and characterize during system calibration. Computational modeling of electric fields can estimate the relative phase distribution under the chosen montage and aid in optimizing electrode geometry to minimize unintended phase lags [47, 48, 49].

Stimulation parameters: amplitude, waveform, and duration

Stimulation amplitude, waveform, and duration critically determine the efficacy and specificity of closed-loop tACS. Intensity should remain within established safety limits while ensuring measurable modulation of the target rhythm. Short bursts of stimulation (1-5 s) synchronized to ongoing oscillations are often sufficient to entrain or disrupt rhythmic activity without inducing adaptation or discomfort. As summarized in Chapter 4, anti-phase tACS of several seconds can transiently desynchronize cortico-muscular coherence, whereas longer trains tend to re-establish entrainment once the system compensates to the external rhythm [50, 51]. Thus, duration should be tailored to the expected neural time constant of adaptation: brief stimulation for transient perturbation, sustained trains for lasting modulation. Alternating current in sinusoidal forms remains the standard for phase-locked protocols, while asymmetric or shaped waveforms may increase specificity but require validation.

Blinding and sensation control

Rigorous blinding is essential for valid behavioral inference. Sensory cues such as tingling, itching, or phosphenes should be perceptually

matched across conditions. A ramp-up/ramp-down sham condition replicating the initial sensations of active stimulation without sustained current is standard practice.

Scaling current intensity individually can control confounding by peripheral feedback, so that subjective ratings of sensation are taken into account when comparing across in-phase, anti-phase, and sham conditions. Automated condition randomization and double-blind control interfaces further ensure unbiased administration.

Table 6.3: **Comparative Summary of EEG Phase-Prediction Algorithms for Closed-Loop Neurostimulation**

Algorithm	Computation load	Adaptivity to non-stationarity	Adaptivity to latency range	Advantage	Limitations
FFT-based sinusoid extrapolation	Very low	Low	Small (past window ∼300ms)	Good when oscillation strong and stable	Poor when frequency drift/multi-component signal
AR	Moderate	Moderate	Past window + AR fit time	Good for short forecasting horizons; many published closed-loop EEG-TMS use	Sensitive to model order/parameters; higher compute
Adaptive AR / LMS-AR	Moderate to high	Higher	Similar to AR but longer horizon possible	Better at tracking frequency drift	Requires adaptation tuning; higher compute
ETP	Low	Low-moderate	Very small buffer + simple extrapolation	Robust, efficient; Shirinpour et al. found ∼70% accuracy in real-time EEG-TMS experiment	Requires training phase; less adaptivity
Causal Oscillator / PLL	Low-medium	Moderate	Very low latency	Suitable for hardware/embedded real-time estimates	Less widely employed in EEG closed-loop stimulation studies; tuning needed
Machine Learning	Potentially high	High	Depends on architecture	Potential highest accuracy; lowest variance vs AR/ETP	Needs training data; generalisability and latency tradeoffs
Hybrid / Optimised Filters	Medium	Variable	Medium	Good compromise between ease and performance (e.g., Rivero et al)	Implementation complexity; may still require tuning

6.3 Future Directions and Emerging Trends

Phase-dependent closed-loop tACS is moving from proof-of-principle demonstrations toward a more generalizable technology for precision neuromodulation. Future work will focus on advancing hardware-level timing control, real-time sensing, and phase estimation algorithms, as well as translational neuroscience.

6.3.1 Research trends and technological advances

Precision phase targeting

Early phase-locked tACS studies typically targeted canonical phases, for example, delivering stimulation at the trough or rising phase of the beta rhythm to maximize corticospinal excitability [52, 53]. However, subsequent work revealed pronounced individual differences: optimal excitability occurs at different phases across participants, and even within individuals over time [54, 55]. The next generation of phase-locked systems should incorporate individualized phase mapping. Brief mapping protocols that systematically sample 8-12 equidistant phases of the target oscillation while measuring corticospinal excitability (via TMS-evoked MEPs), motor performance (reaction time, force output), or cognitive metrics (working memory accuracy), can identify each participant's optimal phase within 15-20 minutes [54, 56].

Moreover, some evidence has shown that the optimal phase is not static but varies with brain state, task demands, and time of day [57, 58, 29]. Adaptive algorithms that continuously update phase targets based on real-time performance feedback or EEG biomarkers represent an important frontier. For example, if motor stopping performance degrades during a session, the system could shift the stimulation phase by 30-60° and reassess, implementing a gradient-descent optimization in phase space [59, 11].

Advanced phase prediction algorithms

Accurate real-time phase estimation remains the key step in a phase-locked system. Current implementations have achieved 60-80% accuracy in hitting target phases, which corresponds to prediction errors of 20-50 ms [28, 33]. Frontiers algorithms aim to close this gap, such as deep learning phase prediction networks [39, 40], and hybrid algorithms combining multiple prediction methods [42, 28]. Moving phase prediction from software to dedicated hardware, e.g., field-programmable gate arrays (FPGAs) or application-specific integrated circuits (ASICs), can reduce latency to under 5 ms, enabling phase-locked control of high-frequency oscillations [60, 37]. An emerging alternative is neuromorphic processing, which models neural oscillations using spiking neural networks. These processors achieve ultra-low latency and power consumption, making them suitable for future wearable or implantable closed-loop devices [61].

Optimizing stimulation waveforms

A typical phase-locked tACS delivers sinusoidal waveforms with fixed amplitude and frequency, adjusting only the timing of stimulation onset to align with the target phase. Emerging evidence suggests that waveform shape, amplitude modulation, and duty cycle critically influence entrainment efficacy and behavioral outcomes.

Non-sinusoidal waveforms: Sawtooth, square, and asymmetric waveforms with faster rising or falling edges may preferentially engage specific phases of endogenous oscillations, enhancing phase-locking strength [62, 63]. For example, a sawtooth waveform with a steep rising edge aligned to the rising phase of beta oscillations could amplify desynchronization during movement preparation, whereas a slow rising edge might stabilize synchrony during tonic contraction. Computational

models of cortical networks predict that waveform asymmetry interacts with the intrinsic rise/fall time constants of membrane potentials, creating phase-dependent resonances [64, 4].

Amplitude modulation: Fixed-amplitude stimulation may be suboptimal when endogenous oscillation amplitude fluctuates across task epochs or brain states. Closed-loop amplitude-modulated (CLAM) tACS systems that increase stimulation intensity when target oscillations are weak and decrease it when oscillations are strong can maintain consistent entrainment despite non-stationarity [65, 66]. Phase-amplitude modulation, where stimulation amplitude is dynamically adjusted based on both instantaneous phase and amplitude of the target oscillation, represents a further refinement [67].

Burst coupling stimulation: Brief, high-intensity bursts (50-200 ms) delivered at target phases may induce stronger phase-resetting and longer-lasting aftereffects than continuous stimulation, while minimizing sensory percepts and adaptation [68, 69]. Burst protocols are particularly promising for sleep applications, where stimulation timed to slow-wave up-states enhances memory consolidation without disrupting sleep architecture [69].

Personalized dosimetry: computational modeling and electric field optimization

Inter-individual variability in tACS response is partly driven by anatomical differences—skull thickness, CSF volume, gyral geometry—that determine electric field strength and distribution at the cortical target [70, 71]. Finite element models (FEMs) constructed from individual T1- and T2-weighted MRI scans predict field intensities with high spatial resolution, revealing that nominally identical electrode montages can produce 2-5 fold differences in cortical field strength across individuals [13, 72].

Closed-loop systems that integrate computational head models can adjust stimulation intensity in real time to achieve target field strengths at the cortical site of interest. For example, if the model predicts that 1 mA surface current yields only 0.3 V/m at M1 in a participant with a thick skull, the system could increase current to 1.5 mA to reach the desired 0.5 V/m threshold for entrainment [11]. Inverse modeling approaches that solve for optimal electrode configurations (position, size, current) given a desired field distribution can further enhance targeting precision, though these typically require offline computation and custom electrode arrays [73, 74].

An emerging frontier is real-time field estimation using concurrent EEG. Changes in oscillatory power, coherence, or phase-locking induced by tACS provide indirect readouts of effective field strength, enabling adaptive dosing without requiring MRI [75, 76]. For instance, if phase-locked beta tACS fails to modulate beta power within the first 2 minutes, the system could incrementally increase intensity until target engagement is achieved, implementing a closed-loop dose-finding algorithm.

State-dependent phase-locked tACS: Triggering stimulation during optimal brain states

Brain state—defined by oscillatory power, phase coherence, and connectivity patterns—fluctuates on timescales from milliseconds to hours, profoundly influencing tACS efficacy [57, 76]. Delivering phase-locked stimulation only when the brain is in favorable states can maximize entrainment and behavioral effects while minimizing exposure and side effects.

Oscillatory burst detection: Beta oscillations are not continuous but occur in transient bursts lasting 100-300 ms, with burst incidence and duration correlating with motor symptoms in Parkinson's disease and inhibitory control in healthy individuals [77, 78, 79, 80]. Phase-locked tACS triggered contingent on burst onset—delivering anti-phase stimulation to disrupt pathological bursts or in-phase stimulation to enhance

physiological bursts—represents a mechanistically targeted intervention. Burst detection algorithms based on amplitude thresholds, time-frequency decomposition, or machine learning classifiers can identify burst onset within 20-50 ms, enabling rapid triggering [81, 77].

Task-event triggering: Cognitive and motor processes unfold in discrete epochs with distinct oscillatory signatures. Phase-locked tACS delivered selectively during task-relevant epochs, for example, at cue onset in a stop-signal task, during retention in working memory, or at movement initiation, can enhance specificity and effect sizes. Event-related designs that synchronize stimulation to behavioral markers (button press, eye movement) or neural markers (event-related potentials) provide temporal precision beyond continuous stimulation.

6.3.2 Research-grade closed-loop platforms

Phase-locked tACS has matured into a research-ready technology integrating simultaneous EEG acquisition, real-time phase detection, and adaptive stimulation control.

NeuroConn LOOP IT integrates acquisition and online analysis in a single controller to drive state-contingent stimulation without the need for phase extrapolation, with constant delays reported around one millisecond, which is suitable for phase-specific interventions in beta or alpha bands.

Neuroelectrics provides a multicomponent stack where NIC2 streams EEG in real time, and MatNIC2 exposes programmatic control so that algorithms can adapt waveform phase or amplitude on the fly during experiments.

EGI has developed a research-grade closed-loop EEG stimulation ecosystem centered around high-density EEG acquisition and low-latency data streaming. The EGI Net Amps platform supports real-time EEG access via dedicated streaming protocols, enabling external real-time processing and control.

Collectively, these platforms enable state-contingent phase targeting, rapid adaptation of stimulation parameters, and reproducible integration with common analysis stacks, which are essential for testing mechanistic hypotheses about oscillatory control and for advancing precision network therapeutics in clinical research.

6.3.3 Clinical Trends and Translational Pathways

Parkinson's disease (PD)

PD is characterised by exaggerated beta oscillations in basal ganglia networks, which are associated with rigidity, bradykinesia, and impaired movement initiation [82, 83, 84, 85]. Applying conventional tACS in the beta band tends to promote motor inhibition [86, 10, 87], but might risk reinforcing the abnormal synchrony in PD [88]. Closed-loop phase-locked tACS that allows the system to dynamically enhance or suppress intrinsic synchrony depending on therapeutic intent is conceptually attractive in PD. By delivering anti-phase stimulation precisely aligned to pathological beta activity or transient beta bursts, closed-loop tACS provides a mechanistically grounded means to desynchronize maladaptive neural coupling, thereby avoiding the synchrony-reinforcing limitations of conventional open-loop beta-tACS.

Growing evidence from both invasive and non-invasive studies supports the therapeutic potential of phase-locked stimulation: phase-specific DBS locked to each patient's tremor phase produced robust, energy-efficient tremor suppression [89]; Phase-locked tACS targeting M1 and timed to the anti-phase of peripheral tremor (detected via accelerometry or EMG) has demonstrated robust tremor amplitude reduction in Parkinsonian rest tremor and essential tremor [90, 91]. Similarly, [21] demonstrated that STN beta oscillations can be suppressed when consecutive electrical pulses arrive at a specific phase of the oscillation. Furthermore, [92] reported cerebellar phase-locked tACS modulates dystonic tremor, but only in sinusoidal (non-jerky)

phenotypes, highlighting the importance of oscillatory regularity for successful phase-targeted interventions.

Alzheimer's disease (AD)

Alzheimer's disease is increasingly conceptualized as degeneration of cortico-hippocampal circuits, which disrupts the temporal code supporting memory [93]. Multiple lines of evidence reported reduced or altered theta-gamma coupling in AD that scales with cognitive impairment [94]. 40 Hz tACS shows encouraging entrainment and short-term cognitive gains but heterogeneous effects [93]. The plausible and variable effects likely depends on depend on disease stage, montage and field distribution, baseline oscillatory integrity, and the cognitive state during stimulation [95, 96]. Another consideration is that 40 Hz power modulation alone may not be the most specific therapeutic control variable for memory, because memory deficits in AD map strongly onto impaired temporal coordination, especially theta-organized gamma dynamics, rather than isolated gamma amplitude changes.

Recent studies have demonstrated that phase-locked gamma tACS delivered at optimal theta phase (normally peak) can improve memory encoding and retrieval efficiency and strengthen frontotemporal theta-gamma coupling [97, 98, 99, 100]. For AD, the next generation of protocols should aim to restore theta gamma coupling. A phase-dependent closed-loop architecture offers a concrete route: estimate ongoing theta phase from EEG, deliver brief gamma bursts only within a narrow phase window during task-relevant epochs, and adapt parameters to the patient's current theta frequency and coupling quality.

Major depressive disorder (MDD)

Major depressive disorder (MDD) is conceptualized as a disorder where aberrant rhythmic activity and dysregulated inter-regional coupling

constrain affective processing, cognitive control, and reward-guided behavior. Pathologically elevated alpha band activity over prefrontal regions and frontal alpha asymmetry are associated with depression symptoms in subsets of patients [101]. Thus, reducing this excessive alpha activity could potentially mitigate symptoms. Several open-loop tACS studies delievering alpha or theta oscillations in MDD, with modest effects on target-engagement [102, 103].

Closed-loop phase-locked tACS in depression remains scarce. [104] piloted a closed-loop system that detects fluctuations in individual alpha frequency power and triggers a brief period of tACS, resulting in increased left frontal alpha power and 30-40% reductions in depression severity. A phase-dependent closed-loop tACS approach is potentially effective because, first, it can reduce the risk that open-loop stimulation inadvertently reinforces an already dominant rhythm; and second, it can promote network-level re-coordination by driving a controlled phase lag between bilateral prefrontal sites, or between prefrontal control regions and limbic hubs, to restore more functional communication patterns [8, 2]. Its future clinical credibility in MDD will depend on robust EEG biomarker stratification and explicit demonstration of target engagement at the individual level.

Schizophrenia

Schizophrenia is strongly associated with dysconnectivity and aberrant rhythmic coordination across cortical networks, with impaired gamma band synchronization and altered alpha band dynamics in frontotemporal circuits that are relevant to auditory verbal hallucinations [105]. Protocols typically use 10 Hz stimulation over the dorsolateral prefrontal cortex and temporoparietal junction, and show increased alpha with reduced depressive symptoms [106, 107, 108, 57]. [109] used dual-site gamma tACS applied in-phase at frontal and temporal electrodes with the return anti-phase at Cz and found significant reductions in refractory auditory hallucinations.

40 Hz auditory steady state responses provide an attractive closed-loop handle because their deficits are robustly documented in schizophrenia. Future steps for an adaptive stimulation could be timed to when measured 40 Hz phase locking is weak, or enforcing a patient-specific phase relation between prefrontal and temporoparietal nodes when frontotemporal coupling is degraded.

Stroke

Stroke is accompanied by characteristic oscillatory abnormalities, including increased interhemispheric beta synchrony, reduced mu desynchronization during movement, and disrupted beta-burst dynamics within sensorimotor networks [110, 111]. Recent work also highlights that beta activity is best understood as burst-like events whose timing and coupling to movement are altered after stroke [112]. Clinical tACS protocols in stroke have typically used open-loop stimulation in alpha or beta ranges, often paired with behavioral therapy [113, 114, 115]. Looking forward, tACS trailored to modulate abnormal slow cortical oscillations has shown potential as a therapeutic tool [116].

Attention-deficit/hyperactivity disorder (ADHD)

Frontal theta-beta ratio abnormalities and altered alpha dynamics reflect executive dysfunction in ADHD [117]. Closed-loop theta or alpha tACS targeting DLPFC during attention tasks, with stimulation parameters adapted to real-time performance metrics, could enhance sustained attention and inhibitory control. Pediatric populations require careful dosimetry and safety monitoring, but initial feasibility studies are encouraging.

Post-traumatic stress disorder (PTSD) and anxiety disorders

Dysregulated amygdala-prefrontal connectivity and altered theta-alpha oscillations characterize PTSD and generalized anxiety [118]. Closed-loop alpha tACS over the ventromedial prefrontal cortex, delivered during exposure therapy or resting-state periods of heightened arousal, may facilitate extinction learning and emotional regulation [103]. Integration with virtual reality exposure therapy and biofeedback represents a promising multimodal intervention.

Conclusion

Phase-dependent closed-loop tACS marks a transition from 'one-fits-for-all' stimulation to real-time adaptive control, enabling mechanistic interventions such as phase-specific suppression or enhancement rather than generic entrainment. It requires rigorous engineering and validation, including deterministic timing, quantified end-to-end latency and jitter, artifact-aware sensing, and causal phase estimation with prediction and verification of delivered brain phase, alongside standardized reporting and benchmarks for target engagement. Looking forward, with continued methodological advancement, phase-dependent closed-loop tACS has the potential to develop as a clinically credible neuromodulation technology that supports precision therapies in disorders defined by abnormal oscillatory synchronization.

References

[1] Christoph S. Herrmann et al. "Transcranial alternating current stimulation: a review of the underlying mechanisms and modulation of cognitive processes". In: *Frontiers in Human Neuroscience* 7 (2013). DOI: 10.3389/fnhum.2013.00279.

[2] Randolph F. Helfrich et al. “Entrainment of Brain Oscillations by Transcranial Alternating Current Stimulation”. In: *Current Biology* 24.3 (Feb. 2014), pp. 333–339. DOI: 10.1016/j.cub.2013.12.041.

[3] Flavio Fröhlich and David A. McCormick. “Endogenous Electric Fields May Guide Neocortical Network Activity”. In: *Neuron* 67.1 (July 2010), pp. 129–143. DOI: 10.1016/j.neuron.2010.06.005.

[4] Wei A. Huang et al. “Transcranial alternating current stimulation entrains alpha oscillations by preferential phase synchronization of fast-spiking cortical neurons to stimulation waveform”. In: *Nature Communications* 12.1 (May 2021). DOI: 10.1038/s41467-021-23021-2.

[5] Matthew R. Krause et al. “Transcranial alternating current stimulation entrains single-neuron activity in the primate brain”. In: *Proceedings of the National Academy of Sciences* 116.12 (Mar. 2019), pp. 5747–5755. DOI: 10.1073/pnas.1815958116.

[6] Roberto Cecere, Geraint Rees, and Vincenzo Romei. “Individual Differences in Alpha Frequency Drive Crossmodal Illusory Perception”. In: *Current Biology* 25.2 (Jan. 2015), pp. 231–235. DOI: 10.1016/j.cub.2014.11.034.

[7] Teresa Schuhmann et al. “Left parietal tACS at alpha frequency induces a shift of visuospatial attention”. In: *PLOS ONE* 14.11 (Nov. 2019). Ed. by Andrea Antal, e0217729. DOI: 10.1371/journal.pone.0217729.

[8] Rafael Polanía et al. “The Importance of Timing in Segregated Theta Phase-Coupling for Cognitive Performance”. In: *Current Biology* 22.14 (July 2012), pp. 1314–1318. DOI: 10.1016/j.cub.2012.05.021.

[9] Alek Pogosyan et al. “Boosting Cortical Activity at Beta-Band Frequencies Slows Movement in Humans”. In: *Current Biology* 19.19 (Oct. 2009), pp. 1637–1641. DOI: 10.1016/j.cub.2009.07.074.

[10] Inge Leunissen et al. “Effects of beta-band and gamma-band rhythmic stimulation on motor inhibition”. In: *iScience* 25.5 (May 2022), p. 104338. DOI: 10.1016/j.isci.2022.104338.

[11] Flavio Frohlich and Leah Townsend. “Closed-Loop Transcranial Alternating Current Stimulation: Towards Personalized Non-invasive Brain Stimulation for the Treatment of Psychiatric Illnesses”. In: *Current Behavioral Neuroscience Reports* 8.2 (Mar. 2021), pp. 51–57. DOI: 10.1007/s40473-021-00227-8.

[12] Fatemeh Gholamali Nezhad et al. “Transcranial alternating current stimulation for neuropsychiatric disorders: a systematic review of treatment parameters and outcomes”. In: *Frontiers in Psychiatry* 15 (Aug. 2024). DOI: 10.3389/fpsyt.2024.1419243.

[13] Florian H. Kasten et al. “Integrating electric field modeling and neuroimaging to explain inter-individual variability of tACS effects”. In: *Nature Communications* 10.1 (Nov. 2019). DOI: 10.1038/s41467-019-13417-6.

[14] Florian H. Kasten and Christoph S. Herrmann. “The hidden brain-state dynamics of tACS aftereffects”. In: *NeuroImage* 264 (Dec. 2022), p. 119713. DOI: 10.1016/j.neuroimage.2022.119713.

[15] Sankaraleengam Alagapan et al. “Modulation of Cortical Oscillations by Low-Frequency Direct Cortical Stimulation Is State-Dependent”. In: *PLOS Biology* 14.3 (Mar. 2016). Ed. by Ole Jensen, e1002424. DOI: 10.1371/journal.pbio.1002424.

[16] Alexandra Vossen, Joachim Gross, and Gregor Thut. “Alpha Power Increase After Transcranial Alternating Current Stimulation at Alpha Frequency (alpha-tACS) Reflects Plastic Changes Rather Than Entrainment”. In: *Brain Stimulation* 8.3 (May 2015), pp. 499–508. DOI: 10.1016/j.brs.2014.12.004.

[17] Moran Weinberger et al. “Beta Oscillatory Activity in the Subthalamic Nucleus and Its Relation to Dopaminergic Response in Parkinson’s Disease”. In: *Journal of Neurophysiology* 96.6 (Dec. 2006), pp. 3248–3256. DOI: 10.1152/jn.00697.2006.

[18] Andrea A. Kühn et al. “Pathological synchronisation in the subthalamic nucleus of patients with Parkinson’s disease relates to both bradykinesia and rigidity”. In: *Experimental Neurology* 215.2 (Feb. 2009), pp. 380–387. DOI: 10.1016/j.expneurol.2008.11.008.

[19] John-Stuart Brittain, Andrew Sharott, and Peter Brown. “The highs and lows of beta activity in cortico-basal ganglia loops”. In: *European Journal of Neuroscience* 39.11 (Apr. 2014), pp. 1951–1959. DOI: 10.1111/ejn.12574.

[20] Anke Karabanov, Axel Thielscher, and Hartwig Roman Siebner. “Transcranial brain stimulation: closing the loop between brain and stimulation”. In: *Current Opinion in Neurology* 29.4 (Aug. 2016), pp. 397–404. DOI: 10.1097/wco.0000000000000342.

[21] Abbey B. Holt et al. “Phase-Dependent Suppression of Beta Oscillations in Parkinson’s Disease Patients”. In: *Journal of Neuroscience* 39.6 (2019), pp. 1119–1134. DOI: https://doi.org/10.1523/JNEUROSCI.1913-18.2018.

[22] Zhou Fang et al. “tACS induces state-dependent shifts in inhibitory phase preference consistent with phase precession”. In: (Dec. 2025). DOI: 10.64898/2025.11.28.691215.

[23] Christoph Zrenner et al. “Closed-Loop Neuroscience and Non-Invasive Brain Stimulation: A Tale of Two Loops”. In: *Frontiers in Cellular Neuroscience* 10 (Apr. 2016). DOI: 10.3389/fncel.2016.00092.

[24] Ghazaleh Soleimani et al. “Closing the loop between brain and electrical stimulation: towards precision neuromodulation treatments”. In: *Translational Psychiatry* 13.1 (Aug. 2023). DOI: 10.1038/s41398-023-02565-5.

[25] Robert Oostenveld et al. “FieldTrip: Open Source Software for Advanced Analysis of MEG, EEG, and Invasive Electrophysiological Data”. In: *Computational Intelligence and Neuroscience* 2011 (2011), pp. 1–9. DOI: 10.1155/2011/156869.

[26] Christian Kothe et al. “The Lab Streaming Layer for Synchronized Multimodal Recording”. In: *Imaging Neuroscience* 3 (2025), IMAG.a.136. DOI: 10.1162/IMAG.a.136.

[27] Brigitte Zrenner et al. “Brain oscillation-synchronized stimulation of the left dorsolateral prefrontal cortex in depression using real-time EEG-triggered TMS”. In: *Brain Stimulation* 13.1 (Jan. 2020), pp. 197–205. DOI: 10.1016/j.brs.2019.10.007.

[28] Sina Shirinpour et al. “Experimental evaluation of methods for real-time EEG phase-specific transcranial magnetic stimulation”. In: *Journal of Neural Engineering* 17.4 (July 2020), p. 046002. DOI: 10.1088/1741-2552/ab9dba.

[29] Zhou Fang, Alexander Sack, and Inge Leunissen. “Closed-loop anti-phase tACS over preSMA reduced oscillatory beta synchronization and modulated motor inhibition performance”. In: (Nov. 2025). DOI: 10.1101/2025.11.25.690566.

[30] Farrokh Mansouri et al. “A Fast EEG Forecasting Algorithm for Phase-Locked Transcranial Electrical Stimulation of the Human Brain”. In: *Frontiers in Neuroscience* 11 (July 2017). DOI: 10.3389/fnins.2017.00401.

[31] L. L. Chen et al. “Real-Time Brain Oscillation Detection and Phase-Locked Stimulation Using Autoregressive Spectral Estimation and Time-Series Forward Prediction”. In: *IEEE Transactions on Biomedical Engineering* 60.3 (Mar. 2013), pp. 753–762. DOI: 10.1109/tbme.2011.2109715.

[32] Kristoffer Hougaard Madsen et al. “No trace of phase: Corticomotor excitability is not tuned by phase of pericentral mu-rhythm”. In: *Brain Stimulation* 12.5 (Sept. 2019), pp. 1261–1270. DOI: 10.1016/j.brs.2019.05.005.

[33] Christoph Zrenner et al. “Real-time EEG-defined excitability states determine efficacy of TMS-induced plasticity in human motor cortex”. In: *Brain Stimulation* 11.2 (Mar. 2018), pp. 374–389. DOI: 10.1016/j.brs.2017.11.016.

[34] Anirudh Wodeyar et al. “A state space modeling approach to real-time phase estimation”. In: *eLife* 10 (Sept. 2021). DOI: 10.7554/elife.68803.

[35] Aqsa Shakeel, Toshihisa Tanaka, and Keiichi Kitajo. “Time-Series Prediction of the Oscillatory Phase of EEG Signals Using the Least Mean Square Algorithm-Based AR Model”. In: *Applied Sciences* 10.10 (May 2020), p. 3616. DOI: 10.3390/app10103616.

[36] Aqsa Shakeel et al. “Real-Time Implementation of EEG Oscillatory Phase-Informed Visual Stimulation Using a Least Mean Square-Based AR Model”. In: *Journal of Personalized Medicine* 11.1 (Jan. 2021), p. 38. DOI: 10.3390/jpm11010038.

[37] Michael Rosenblum et al. “Real-time estimation of phase and amplitude with application to neural data”. In: *Scientific Reports* 11.1 (Sept. 2021). DOI: 10.1038/s41598-021-97560-5.

[38] J R McIntosh and P Sajda. “Estimation of phase in EEG rhythms for real-time applications”. In: *Journal of Neural Engineering* 17.3 (May 2020), p. 034002. DOI: 10.1088/1741-2552/ab8683.

[39] Hao Liu et al. “A Novel Real-time Phase Prediction Network in EEG Rhythm”. In: *Neuroscience Bulletin* 41.3 (Nov. 2024), pp. 391–405. DOI: 10.1007/s12264-024-01321-z.

[40] Hanna Pankka et al. “Enhanced EEG Forecasting: A Probabilistic Deep Learning Approach”. In: *Neural Computation* 37.4 (Mar. 2025), pp. 793–814. DOI: 10.1162/neco_a_01743.

[41] Anirudh Wodeyar et al. “Different Methods to Estimate the Phase of Neural Rhythms Agree But Only During Times of Low Uncertainty”. In: *eneuro* 10.11 (Oct. 2023), ENEURO.0507–22.2023. DOI: 10.1523/eneuro.0507-22.2023.

[42] Cristian Rodriguez Rivero and Jochen Ditterich. “A user-friendly algorithm for adaptive closed-loop phase-locked stimulation”. In: *Journal of Neuroscience Methods* 347 (Jan. 2021), p. 108965. DOI: 10.1016/j.jneumeth.2020.108965.

[43] Matteo Feurra et al. “State-Dependent Effects of Transcranial Oscillatory Currents on the Motor System: What You Think Matters”. In: *The Journal of Neuroscience* 33.44 (Oct. 2013), pp. 17483–17489. DOI: 10.1523/jneurosci.1414-13.2013.

[44] Philipp Ruhnau et al. “Eyes wide shut: Transcranial alternating current stimulation drives alpha rhythm in a state dependent manner”. In: *Scientific Reports* 6.1 (June 2016). DOI: 10.1038/srep27138.

[45] Ines R Violante et al. “Externally induced frontoparietal synchronization modulates network dynamics and enhances working memory performance”. In: *eLife* 6 (Mar. 2017). DOI: 10.7554/elife.22001.

[46] Wolfgang Klimesch. “EEG alpha and theta oscillations reflect cognitive and memory performance: a review and analysis”. In: *Brain Research Reviews* 29.2-3 (Apr. 1999), pp. 169–195. DOI: 10.1016/s0165-0173(98)00056-3.

[47] Alexander Opitz et al. “Spatiotemporal structure of intracranial electric fields induced by transcranial electric stimulation in humans and nonhuman primates”. In: *Scientific Reports* 6.1 (Aug. 2016). DOI: 10.1038/srep31236.

[48] Ivan Alekseichuk et al. “Electric field dynamics in the brain during multi-electrode transcranial electric stimulation”. In: *Nature Communications* 10.1 (June 2019). DOI: 10.1038/s41467-019-10581-7.

[49] Jimin Park et al. “Transcranial alternating current stimulation over multiple brain areas with non-zero phase delays other than 180 degrees modulates visuospatial working memory performance”. In: *Scientific Reports* 13.1 (Aug. 2023). DOI: 10.1038/s41598-023-39960-3.

[50] Matthew R. Krause et al. “Brain stimulation competes with ongoing oscillations for control of spike timing in the primate brain”. In: *PLOS Biology* 20.5 (May 2022). Ed. by Huan Luo, e3001650. DOI: 10.1371/journal.pbio.3001650.

[51] Harry Tran et al. "Transcranial Alternating Current Stimulation can disrupt or reestablish neural entrainment in a primate model of Parkinson's disease". In: (Sept. 2025). DOI: 10.1101/2025.09.17.676896.

[52] Gijs van Elswijk et al. "Corticospinal Beta-Band Synchronization Entails Rhythmic Gain Modulation". In: *The Journal of Neuroscience* 30.12 (Mar. 2010), pp. 4481–4488. DOI: 10.1523/jneurosci.2794-09.2010.

[53] Til Ole Bergmann et al. "Pulsed Facilitation of Corticospinal Excitability by the Sensorimotor mu-Alpha Rhythm". In: *The Journal of Neuroscience* 39.50 (Nov. 2019), pp. 10034–10043. DOI: 10.1523/jneurosci.1730-19.2019.

[54] Lukas Schilberg et al. "Phase of beta-frequency tACS over primary motor cortex modulates corticospinal excitability". In: *Cortex* 103 (2018), pp. 142–152. DOI: 10.1016/j.cortex.2018.03.001.

[55] Flavie Torrecillos et al. "Motor Cortex Inputs at the Optimum Phase of Beta Cortical Oscillations Undergo More Rapid and Less Variable Corticospinal Propagation". In: *Journal of Neuroscience* 40.2 (2020), pp. 369–381. DOI: https://doi.org/10.1523/JNEUROSCI.1953-19.2019.

[56] Sara J Hussain et al. "Voluntary Motor Command Release Coincides with Restricted Sensorimotor Beta Rhythm Phases". In: *The Journal of Neuroscience* 42.29 (June 2022), pp. 5771–5781. DOI: 10.1523/jneurosci.1495-21.2022.

[57] Jinwen Wei et al. "State-Dependent tACS Effects Reveal the Potential Causal Role of Prestimulus Alpha Traveling Waves in Visual Contrast Detection". In: *The Journal of Neuroscience* 44.27 (May 2024), e2023232024. DOI: 10.1523/jneurosci.2023-23.2024.

[58] Miles Wischnewski et al. "Induced neural phase precession through exogenous electric fields". In: *Nature Communications* 15.1 (Feb. 2024). DOI: 10.1038/s41467-024-45898-5.

[59] Romy Lorenz et al. “Efficiently searching through large tACS parameter spaces using closed-loop Bayesian optimization”. In: *Brain Stimulation* 12.6 (Nov. 2019), pp. 1484–1489. DOI: 10.1016/j.brs.2019.07.003.

[60] Dongjin Seo et al. “Wireless Recording in the Peripheral Nervous System with Ultrasonic Neural Dust”. In: *Neuron* 91.3 (Aug. 2016), pp. 529–539. DOI: 10.1016/j.neuron.2016.06.034.

[61] Giacomo Indiveri and Shih-Chii Liu. “Memory and information processing in neuromorphic systems”. In: (2015). DOI: 10.48550/ARXIV.1506.03264.

[62] James Dowsett and Christoph S. Herrmann. “Transcranial Alternating Current Stimulation with Sawtooth Waves: Simultaneous Stimulation and EEG Recording”. In: *Frontiers in Human Neuroscience* 10 (Mar. 2016). DOI: 10.3389/fnhum.2016.00135.

[63] Zeinab Esmaeilpour et al. “Limited Sensitivity of Hippocampal Synaptic Function or Network Oscillations to Unmodulated Kilohertz Electric Fields”. In: *eneuro* 7.6 (Nov. 2020), ENEURO.0368–20.2020. DOI: 10.1523/eneuro.0368-20.2020.

[64] Jérémie Lefebvre, Axel Hutt, and Flavio Frohlich. “Stochastic resonance mediates the state-dependent effect of periodic stimulation on cortical alpha oscillations”. In: *eLife* 6 (Dec. 2017). DOI: 10.7554/elife.32054.

[65] David Haslacher et al. “Working memory enhancement using real-time phase-tuned transcranial alternating current stimulation”. In: *Brain Stimulation* 17.4 (July 2024), pp. 850–859. DOI: 10.1016/j.brs.2024.07.007.

[66] Toralf Neuling, Stefan Rach, and Christoph S. Herrmann. “Orchestrating neuronal networks: sustained after-effects of transcranial alternating current stimulation depend upon brain states”. In: *Frontiers in Human Neuroscience* 7 (2013). DOI: 10.3389/fnhum.2013.00161.

[67] Xueli Chen et al. “Alpha oscillatory activity is causally linked to working memory retention”. In: *PLOS Biology* 21.2 (Feb. 2023). Ed. by Simon Hanslmayr, e3001999. DOI: 10.1371/journal.pbio.3001999.

[68] Georgy Zarubin et al. “Transient Amplitude Modulation of Alpha-Band Oscillations by Short-Time Intermittent Closed-Loop tACS”. In: *Frontiers in Human Neuroscience* 14 (Sept. 2020). DOI: 10.3389/fnhum.2020.00366.

[69] Aaron P. Jones et al. “Closed-Loop tACS Delivered during Slow-Wave Sleep Reduces Retroactive Interference on a Paired-Associates Learning Task”. In: *Brain Sciences* 13.3 (Mar. 2023), p. 468. DOI: 10.3390/brainsci13030468.

[70] Alexander Opitz et al. “Determinants of the electric field during transcranial direct current stimulation”. In: *NeuroImage* 109 (Apr. 2015), pp. 140–150. DOI: 10.1016/j.neuroimage.2015.01.033.

[71] Yu Huang et al. “Measurements and models of electric fields in the in vivo human brain during transcranial electric stimulation”. In: *eLife* 6 (Feb. 2017). DOI: 10.7554/elife.18834.

[72] Vincent Rochas et al. “MRI-individualized, multi-electrode tACS enhances the induced electrical field strength in the targeted area of mild cognitive impairment patients”. In: *Clinical Neurophysiology* 177 (Sept. 2025), p. 2110930. DOI: 10.1016/j.clinph.2025.2110930.

[73] Jacek P Dmochowski et al. “Optimized multi-electrode stimulation increases focality and intensity at target”. In: *Journal of Neural Engineering* 8.4 (June 2011), p. 046011. DOI: 10.1088/1741-2560/8/4/046011.

[74] Giulio Ruffini et al. “Optimization of multifocal transcranial current stimulation for weighted cortical pattern targeting from realistic modeling of electric fields”. In: *NeuroImage* 89 (Apr. 2014), pp. 216–225. DOI: 10.1016/j.neuroimage.2013.12.002.

[75] Matteo Feurra et al. “State-Dependent Effects of Transcranial Oscillatory Currents on the Motor System during Action Observation”. In: *Scientific Reports* 9.1 (Sept. 2019). DOI: 10.1038/s41598-019-49166-1.

[76] Desmond Agboada, Zhihe Zhao, and Miles Wischnewski. “Neuroplastic effects of transcranial alternating current stimulation (tACS): from mechanisms to clinical trials”. In: *Frontiers in Human Neuroscience* 19 (Mar. 2025). DOI: 10.3389/fnhum.2025.1548478.

[77] Gerd Tinkhauser et al. “Beta burst dynamics in Parkinson’s disease OFF and ON dopaminergic medication”. In: *Brain* 140.11 (Oct. 2017), pp. 2968–2981. DOI: 10.1093/brain/awx252.

[78] Roxanne Lofredi et al. “Beta bursts during continuous movements accompany the velocity decrement in Parkinson’s disease patients”. In: *Neurobiology of Disease* 127 (July 2019), pp. 462–471. DOI: 10.1016/j.nbd.2019.03.013.

[79] Simon Little et al. “Bilateral adaptive deep brain stimulation is effective in Parkinson’s disease”. In: *Journal of Neurology, Neurosurgery & amp; Psychiatry* 87.7 (Sept. 2015), pp. 717–721. DOI: 10.1136/jnnp-2015-310972.

[80] Simon Little et al. “Human motor cortical beta bursts relate to movement planning and response errors”. In: *PLOS Biology* 17.10 (Oct. 2019). Ed. by Karunesh Ganguly, e3000479. DOI: 10.1371/journal.pbio.3000479.

[81] Carina R. Oehrn et al. “Chronic adaptive deep brain stimulation versus conventional stimulation in Parkinson’s disease: a blinded randomized feasibility trial”. In: *Nature Medicine* 30.11 (Aug. 2024), pp. 3345–3356. DOI: 10.1038/s41591-024-03196-z.

[82] A. A. Kuhn et al. “High-Frequency Stimulation of the Subthalamic Nucleus Suppresses Oscillatory Activity in Patients with Parkinson’s Disease in Parallel with Improvement in Motor Per-

formance". In: *Journal of Neuroscience* 28.24 (June 2008), pp. 6165–6173. DOI: 10.1523/jneurosci.0282-08.2008.

[83] S. Little et al. "Beta band stability over time correlates with Parkinsonian rigidity and bradykinesia". In: *Experimental Neurology* 236.2 (Aug. 2012), pp. 383–388. DOI: 10.1016/j.expneurol.2012.04.024.

[84] Chiung Chu Chen et al. "Complexity of subthalamic 13-35Hz oscillatory activity directly correlates with clinical impairment in patients with Parkinson's disease". In: *Experimental Neurology* 224.1 (July 2010), pp. 234–240. DOI: 10.1016/j.expneurol.2010.03.015.

[85] Jon B. Toledo et al. "High beta activity in the subthalamic nucleus and freezing of gait in Parkinson's disease". In: *Neurobiology of Disease* 64 (Apr. 2014), pp. 60–65. DOI: 10.1016/j.nbd.2013.12.005.

[86] Raed A. Joundi et al. "Driving Oscillatory Activity in the Human Cortex Enhances Motor Performance". In: *Current Biology* 22.5 (Mar. 2012), pp. 403–407. DOI: 10.1016/j.cub.2012.01.024.

[87] Jane Tan et al. "The Effects of Dual-Site Beta tACS over the rIFG and preSMA on Response Inhibition in Young and Older Adults". In: (Dec. 2022). DOI: 10.1101/2022.11.30.518460.

[88] Andrea Guerra et al. "Driving motor cortex oscillations modulates bradykinesia in Parkinson's disease". In: *Brain* 145.1 (July 2021), pp. 224–236. DOI: 10.1093/brain/awab257.

[89] Hayriye Cagnan et al. "Stimulating at the right time: phase-specific deep brain stimulation". In: *Brain* 140.1 (Dec. 2016), pp. 132–145. DOI: 10.1093/brain/aww286.

[90] John-Stuart Brittain et al. "Tremor Suppression by Rhythmic Transcranial Current Stimulation". In: *Current Biology* 23.5 (Mar. 2013), pp. 436–440. DOI: 10.1016/j.cub.2013.01.068.

[91] Sebastian R. Schreglmann et al. “Non-invasive suppression of essential tremor via phase-locked disruption of its temporal coherence”. In: *Nature Communications* 12.1 (Jan. 2021). DOI: 10.1038/s41467-020-20581-7.

[92] Freek Nieuwhof et al. “Phase-locked transcranial electrical brain stimulation for tremor suppression in dystonic tremor syndromes”. In: *Clinical Neurophysiology* 140 (Aug. 2022), pp. 239–250. DOI: 10.1016/j.clinph.2022.03.020.

[93] Valerio Manippa et al. “Cognitive and Neuropathophysiological Outcomes of Gamma-tACS in Dementia: A Systematic Review”. In: *Neuropsychology Review* 34.1 (Mar. 2023), pp. 338–361. DOI: 10.1007/s11065-023-09589-0.

[94] Michelle S. Goodman et al. “Theta-Gamma Coupling and Working Memory in Alzheimer’s Dementia and Mild Cognitive Impairment”. In: *Frontiers in Aging Neuroscience* 10 (Apr. 2018). DOI: 10.3389/fnagi.2018.00101.

[95] Giulia Sprugnoli et al. “Impact of multisession 40Hz tACS on hippocampal perfusion in patients with Alzheimer’s disease”. In: *Alzheimer’s Research & amp; Therapy* 13.1 (Dec. 2021). DOI: 10.1186/s13195-021-00922-4.

[96] Maria Luisa De Paolis et al. “Transcranial alternating current stimulation (tACS) at gamma frequency: an up-and-coming tool to modify the progression of Alzheimer’s Disease”. In: *Translational Neurodegeneration* 13.1 (June 2024). DOI: 10.1186/s40035-024-00423-y.

[97] Ivan Alekseichuk et al. “Spatial Working Memory in Humans Depends on Theta and High Gamma Synchronization in the Prefrontal Cortex”. In: *Current Biology* 26.12 (June 2016), pp. 1513–1521. DOI: 10.1016/j.cub.2016.04.035.

[98] Robert M. G. Reinhart and John A. Nguyen. “Working memory revived in older adults by synchronizing rhythmic brain circuits”. In: *Nature Neuroscience* 22.5 (Apr. 2019), pp. 820–827. DOI: 10.1038/s41593-019-0371-x.

[99] Mohammed Abubaker et al. "Theta-gamma-coupling as predictor of working memory performance in young and elderly healthy people". In: *Molecular Brain* 17.1 (Oct. 2024). DOI: 10.1186/s13041-024-01149-8.

[100] Lukas Diedrich et al. "Boosting working memory in the elderly: driving prefrontal theta-gamma coupling via repeated neuromodulation". In: *GeroScience* 47.2 (July 2024), pp. 1425–1440. DOI: 10.1007/s11357-024-01272-3.

[101] Alexander A. Fingelkurts and Andrew A. Fingelkurts. "Altered Structure of Dynamic Electroencephalogram Oscillatory Pattern in Major Depression". In: *Biological Psychiatry* 77.12 (June 2015), pp. 1050–1060. DOI: 10.1016/j.biopsych.2014.12.011.

[102] Morgan L. Alexander et al. "Double-blind, randomized pilot clinical trial targeting alpha oscillations with transcranial alternating current stimulation (tACS) for the treatment of major depressive disorder (MDD)". In: *Translational Psychiatry* 9.1 (Mar. 2019). DOI: 10.1038/s41398-019-0439-0.

[103] Justin Riddle et al. "Reduction in Left Frontal Alpha Oscillations by Transcranial Alternating Current Stimulation in Major Depressive Disorder Is Context Dependent in a Randomized Clinical Trial". In: *Biological Psychiatry: Cognitive Neuroscience and Neuroimaging* 7.3 (Mar. 2022), pp. 302–311. DOI: 10.1016/j.bpsc.2021.07.001.

[104] Tobias Schwippel et al. "Closed-Loop Transcranial Alternating Current Stimulation for the Treatment of Major Depressive Disorder: An Open-Label Pilot Study". In: *American Journal of Psychiatry* 181.9 (Sept. 2024), pp. 842–845. DOI: 10.1176/appi.ajp.20230838.

[105] Tineke Grent-'t-Jong et al. "40-Hz Auditory Steady-State Responses in Schizophrenia: Toward a Mechanistic Biomarker for Circuit Dysfunctions and Early Detection and Diagnosis". In: *Biological Psychiatry* 94.7 (Oct. 2023), pp. 550–560. DOI: 10.1016/j.biopsych.2023.03.026.

[106] Sangtae Ahn et al. “Targeting reduced neural oscillations in patients with schizophrenia by transcranial alternating current stimulation”. In: *NeuroImage* 186 (Feb. 2019), pp. 126–136. DOI: 10.1016/j.neuroimage.2018.10.056.

[107] Juliann M. Mellin et al. “Randomized trial of transcranial alternating current stimulation for treatment of auditory hallucinations in schizophrenia”. In: *European Psychiatry* 51 (June 2018), pp. 25–33. DOI: 10.1016/j.eurpsy.2018.01.004.

[108] Da-Wei Zhang, Alexandros Moraidis, and Torkel Klingberg. “Individually tuned theta HD-tACS improves spatial performance”. In: *Brain Stimulation* 15.6 (Nov. 2022), pp. 1439–1447. DOI: 10.1016/j.brs.2022.10.009.

[109] Xiaojuan Wang et al. “Double-blind, randomized, placebo-controlled pilot clinical trial with gamma-band transcranial alternating current stimulation for the treatment of schizophrenia refractory auditory hallucinations”. In: *Translational Psychiatry* 15.1 (Jan. 2025). DOI: 10.1038/s41398-025-03256-z.

[110] Jacqueline A. Palmer et al. “Role of Interhemispheric Cortical Interactions in Poststroke Motor Function”. In: *Neurorehabilitation and Neural Repair* 33.9 (July 2019), pp. 762–774. DOI: 10.1177/1545968319862552.

[111] Elias Paolo Casula et al. “Evidence for interhemispheric imbalance in stroke patients as revealed by combining transcranial magnetic stimulation and electroencephalography”. In: *Human Brain Mapping* 42.5 (Jan. 2021), pp. 1343–1358. DOI: 10.1002/hbm.25297.

[112] Hoseok Choi et al. “Restoration of temporal separability between beta and movement ensemble co-firing with motor recovery”. In: *Neuron* 113.24 (Dec. 2025), 4263–4277.e9. DOI: 10.1016/j.neuron.2025.09.013.

[113] Marij Middag-van Spanje et al. “Alpha transcranial alternating current stimulation as add-on to neglect training: a randomized trial”. In: *Brain Communications* 6.5 (2024). DOI: 10.1093/braincomms/fcae287.

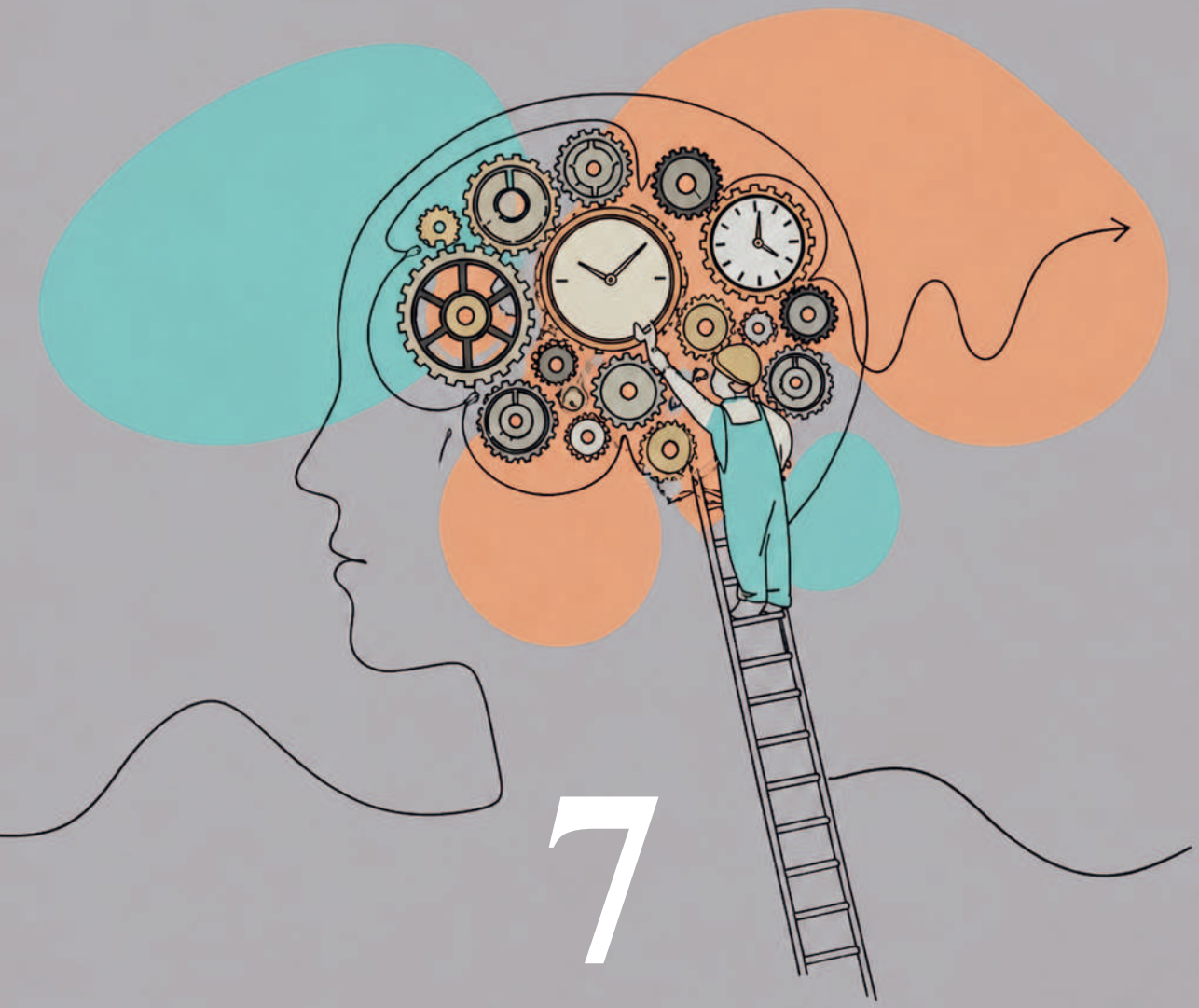
[114] Seoyon Yang, You Gyoung Yi, and Min Cheol Chang. “The effect of transcranial alternating current stimulation on functional recovery in patients with stroke: a narrative review”. In: *Frontiers in Neurology* 14 (Jan. 2024). DOI: 10.3389/fneur.2023.1327383.

[115] Ningjing Song et al. “Harnessing theta waves: tACS as a breakthrough in alleviating post-stroke chronic pain”. In: *Frontiers in Neuroscience* 19 (Apr. 2025). DOI: 10.3389/fnins.2025.1553862.

[116] Laura Bernardi et al. “Beyond physiotherapy and pharmacological treatment for fibromyalgia syndrome: tailored tACS as a new therapeutic tool”. In: *European Archives of Psychiatry and Clinical Neuroscience* 271.1 (Nov. 2020), pp. 199–210. DOI: 10.1007/s00406-020-01214-y.

[117] Robert J Barry, Adam R Clarke, and Stuart J Johnstone. “A review of electrophysiology in attention-deficit/hyperactivity disorder: I. Qualitative and quantitative electroencephalography”. In: *Clinical Neurophysiology* 114.2 (Feb. 2003), pp. 171–183. DOI: 10.1016/s1388-2457(02)00362-0.

[118] Adi Maron-Katz et al. “Individual Patterns of Abnormality in Resting-State Functional Connectivity Reveal Two Data-Driven PTSD Subgroups”. In: *American Journal of Psychiatry* 177.3 (Mar. 2020), pp. 244–253. DOI: 10.1176/appi.ajp.2019.19010060.



7

General discussion

Across the motor network, beta oscillations are associated with an anti-kinetic influence and systematic fluctuations in cortical excitability. The instantaneous phase of these oscillations has been proposed as a temporal reference frame that could regulate when control signals are most effective. Against this backdrop, this dissertation addressed two central questions: *Does the instantaneous beta phase gate motor inhibition?* And if so, *can we causally steer oscillations and inhibition by aligning or opposing stimulation to that phase?* Together, the five chapters converge on a consistent answer. First, stopping efficacy depends on the beta phase at the moment the stop process is engaged. Second, the supposedly "preferred" phase is not fixed: under rhythmic drive and changing brain state, it can shift adaptively, consistent with phase precession. Third, closing the loop with real-time phase-locking stimulation yields bidirectional, causal control of both beta synchronization and inhibitory performance. Fourth, the duration of phase-specific stimulation acts as a boundary condition, determining whether synchrony is disrupted or reinforced. Together, these results advance a mechanistic framework in which the beta phase is a control variable for human inhibitory function and a lever for phase-precise neuromodulation. Clinically, this framework motivates non-invasive, closed-loop, phase-locked transcranial alternating current stimulation as a principled route to normalize abnormal beta synchrony and improve motor control in Parkinson's disease. In the sections that follow, I bring together the core findings of this dissertation and situate them within broader perspectives on motor inhibition, oscillatory mechanisms, and closed-loop brain stimulation.

7.1 Summary of the main findings

Chapter 2 demonstrated that inhibitory efficacy varies sinusoidally with the phase of preSMA-centered beta entrained by 20 Hz transcranial

alternating current stimulation (tACS) during an anticipatory stop-signal task. Stop signals aligned to the trough yielded the strongest stopping, whereas those near the peak resulted in less efficient stopping. This finding is consistent with the communication-through-coherence theory, where inputs landing at high-excitability phases more strongly influence downstream nodes [1, 2]. Notably, the strength of the effect scaled with the match between each participant's intrinsic beta peak and the applied 20 Hz drive, highlighting an individual frequency-matching constraint for phase-sensitive control.

Chapter 3 tested whether this "best" inhibitory phase is rigid or returnable. During successful stops, the optimal phase remained stable, replicating the sinusoidal dependence. During failed stops, however, the phase associated with the strongest (yet insufficient) inhibitory attempt advanced across cycles, consistent with a behavioral signature of phase precession. A stimulation-free control reproduced phase dependence for successful stops but not reliable precession, pointing to an interaction between external rhythmic forcing and a stressed, error-prone inhibitory state in revealing precession.

Chapter 4 implemented a closed-loop tACS-EEG system that delivered stimulation at a prescribed phase offset from endogenous preSMA beta during stopping. Anti-phase stimulation ($\sim$180°) suppressed beta synchronization and slowed the covert stop process, whereas in-phase stimulation increased beta synchrony and stabilized ongoing motor output (reduced peak force rate and timing variability) without slowing stopping. These dissociations support destructive interference as the operative mechanism for anti-phase stimulation and stabilizing entrainment for in-phase stimulation.

Chapter 5 examined boundary conditions at the corticospinal interface during sustained isometric force. Brief anti-phase trains (1-2 s) reduced beta-band cortico-muscular coherence (CMC) after stimulation, whereas longer anti-phase trains (5 s) showed partial rebound. In contrast, in-phase trains increased CMC in a duration-dependent manner. Importantly, local EEG beta power and simple force metrics

were unchanged, indicating that aftereffects were expressed selectively in coupling rather than in local power or gross output.

Chapter 6 provided a practical guide for implementing an EEG-guided phase-dependent closed-loop tACS system. It specifies how to construct and validate an end-to-end phase targeting pipeline, including explicit measurement of acquisition, processing, short-horizon phase prediction to compensate for fixed delays, and stimulation control. The chapter then translates these engineering constraints into experimental design guidance that supports interpretable neural and behavioral inference, and it motivates clinical translation by highlighting how closed-loop strategies can reshape pathological rhythms more flexibly than conventional open-loop entrainment.

7.2 Beta oscillations and inhibitory control

Beta band activity within the fronto-basal ganglia circuit is well-established as a key mechanism supporting motor inhibition [3, 4, 5]. During action cancellation, successful stopping is consistently accompanied by a rapid increase in beta synchronization within basal ganglia and connected frontal regions, whereas movement execution is characterized by beta desynchronization followed by a post-movement be ta rebound once motor demands subside [6, 7].

Closely aligning with the established literature, the sham condition results in Chapter 4 replicated the natural beta dynamics that anchored the follow-up claims in baseline physiology. Specifically, successful stopping was accompanied by an increase in beta synchronization, consistent with the idea that motor inhibition is supported by a rapid recruitment of beta-mediated coordination during action cancellation [3, 4, 5]. Following task completion, post movement beta rebound was stronger after go and failed-stop trials than after successful stops, suggesting that beta rebound reflects the re-establishment of network stability once inhibitory demands subside [8, 9, 10, 11].

Together, the literature and our supplementary findings support a dual role for beta oscillations in inhibitory control. Transient beta synchronization accompanies the moment of reactive braking and appears to be part of the mechanism that implements cancellation, while the subsequent rebound helps re-stabilize the motor network and re-establish readiness for the next control demand.

Beyond confirming that beta power increases during stopping, the primary contribution of this dissertation is to show that *when*, within the beta cycle, inhibitory control is engaged critically shapes stopping performance. If beta implements a brake, then it matters whether control signals arrive at moments of relatively high versus low network receptivity. This is the conceptual move toward the beta phase as a causal variable.

7.2.1 Causal role of the beta phase in inhibitory control

Understanding how beta rhythms shape behavior requires attention not only to their amplitude but also to their phase, i.e., the moment-to-moment position within the beta cycle. This matters because beta oscillations organize neural excitability into rhythmic peaks and troughs, and the phase therefore specifies when synaptic inputs are most likely to drive downstream firing and when they are more likely to be ignored. In practical terms, this means that inhibition is not continuously available; instead, it fluctuates in short temporal windows defined by the beta cycle, so that the stop cue can be more or less effective depending on when it arrives relative to this internal timing.

Three main strategies have emerged to study this phase-dependent causal relationship. The first is the post-hoc phase analysis, in which EEG or MEG is normally used to estimate the instantaneous phase and relate it to trial-by-trial behavioral outcomes [12, 13]. The second strategy is closed-loop phase-triggered stimulation, where the timing of discrete stimulation events is locked to the phase of an ongoing rhythm estimated online. In the broader literature, this has been most

commonly implemented with TMS, visual or auditory stimuli [14, 15, 16]. The third strategy is externally imposed rhythmic stimulation, most commonly tACS, which provides a known oscillatory reference that can entrain endogenous activity. When behavioral events are aligned to specific phase angles of the tACS waveform, the stimulation cycle becomes an experimentally controllable phase reference for sampling phase-dependent behavior [17, 18, 19].

Across Chapters 2-4, the key finding is that stopping efficacy varies systematically with this oscillatory timing. When the stop cue coincides with phases associated with heightened cortical excitability, inhibitory signals propagate more effectively, resulting in successful stopping. When the cue lands in a low-excitability phase, inhibition is weaker, and failures are more likely. This sinusoidal modulation indicates that beta phase functions as a temporal gate for inhibitory control, with alternating ”open” and ”closed” windows for interrupting action.

In Chapter 2, this principle was tested by entraining beta oscillations through preSMA-targeted 20 Hz tACS and embedding stop cues at different points within the stimulation cycle. Stopping performance showed a robust sinusoidal dependence on phase, with the strongest inhibition when cues occurred near the trough of the driven beta cycle and the weakest inhibition near the opposite phase. This supports the interpretation that inhibitory control appears to be phase-gated, with alternating windows of high and low excitability [1]. Importantly, the effect size scaled with the match between each participant’s intrinsic beta peak and the 20 Hz drive. This specific scaling follows the principle of Arnold Tongues in non-linear oscillators, where entrainment is most effective when the external drive matches the system’s eigenfrequency [20, 21]. This strengthens the inference that the observed phase effect reflects a resonance interaction with endogenous dynamics rather than a random alignment.

This phase dependency was replicated in Chapters 3 and 4. Chapter 3 asked whether this phase dependence is expressed similarly across successful and failed inhibition. The normalized responding force

on successful stop trials showed significant phase-related modulation, while a modest phase effect was also observed on failed stop trials. Notably, the preferred phases for successful and failed trials diverged. This divergence suggests the recruitment of distinct neural subnetworks or excitability states, potentially reflecting a competition between a "Status Quo" maintenance state and an active inhibitory state [22, 23]. This issue will be further discussed in the following section. Complementary EEG analyses confirmed that even without external stimulation, the robust phase relationship in successful stop still held, underscoring that phase dependency is an endogenous feature of inhibitory control.

In Chapter 4, we tested whether perturbing the cortical oscillations could disrupt this phase relation. We implemented a closed-loop tACS paradigm, aligning the externally applied stimulation either in-phase or anti-phase with the participant's ongoing beta rhythm. In general, in-phase stimulation increased beta synchronization and stabilized aspects of motor output, whereas anti-phase stimulation reduced beta synchronization and slowed the covert stop process. Critically, the in-phase condition preserved the kind of phase-dependent modulation observed in earlier chapters. Conversely, anti-phase stimulation disrupted this alignment, diminishing both the strength and consistency of the phase-dependent modulation. Put differently, the findings support the interpretation that effective inhibitory control depends on maintaining an appropriate phase relationship within the control network. When that relationship is perturbed, both oscillatory coordination and stopping efficacy degrade [24, 25].

Phase-dependent modulation of neural processing has been demonstrated across motor [14, 26, 27, 28] and perceptual domains [12, 29, 30, 31, 32, 33, 34]. The present findings extend this principle to inhibitory control, demonstrating that the beta phase similarly constrains the efficacy of stopping. These converging observations motivate a common interpretation: rhythmic inhibition within local interneuron circuits creates phase-specific fluctuations in excitability that gate spiking probability and synaptic gain, while long-range communication is most effective when sending and receiving populations adopt a favorable

phase relationship. This alignment can transiently increase effective connectivity, a principle formalized as communication through coherence [1, 2]. Within this framework, the present results extend the general phase gating concept to reactive inhibitory control, suggesting that the motor stopping network is governed by a rhythmic excitability schedule in which the efficacy of a stop process depends on when it is launched relative to the ongoing beta cycle.

7.2.2 Phase effects depend on brain state

If inhibitory control is expressed through temporally specific "windows" within the beta cycle, then changes in arousal, conflict, task engagement, and ongoing motor preparation should alter which circuit configuration and, consequently, how inhibitory signals are timed relative to the beta cycle. In this view, phase effects reflect a dynamic relationship between oscillatory timing and the current operating mode, such that the phase associated with maximal inhibitory efficacy would shift when the brain transitions between distinct control states.

Consistent with this interpretation, Experiment 2 (no tACS) in Chapter 3 revealed a clear dissociation between successful and failed stopping with respect to beta phase sensitivity. Specifically, the phase of ongoing beta oscillations at the time of the stop signal significantly predicted behavioral outcome for successful stop trials, whereas no reliable phase modulation was observed for failed stops. This dissociation shows that the intrinsic beta phase constrains performance selectively when inhibitory control is effectively engaged. The idea underlying this observation is that distinct circuit configurations are engaged when inhibition succeeds versus fails. Neuroimaging and meta-analytic work convergently indicate that successful stopping preferentially recruits a relatively focused brake circuit centered on preSMA and subthalamic nucleus, commonly framed as engagement of the hyperdirect pathway. Failed stops, in contrast, tend to recruit a broader and less specific ensemble that includes anterior insula, dorsal anterior cingulate cortex, and distributed frontoparietal control networks [35, 36, 37, 38].

A phase-based interpretation follows directly. When a focused hyperdirect brake mode is engaged, inhibitory signals may propagate through a more temporally aligned pathway, allowing the beta phase to remain tightly organized and the effective inhibitory window to be expressed at a stable phase angle. When broader networks are co-activated, inputs into the stopping network are likely to become temporally more heterogeneous, with greater dispersion in conduction delays and mixed timing from parallel control processes. In such a regime, the phase at which inhibitory influence is maximal can be different because the network state has changed the timing of information flow relative to the beta cycle.

This pattern is well documented in the broader cognitive control literature. In decision and conflict tasks, midfrontal theta shows stronger phase alignment and inter-trial phase coherence when choices are accurate, while weaker or shifted alignment before and during errors [39, 40, 41, 42]. Similarly, in the stop-signal task, internal state determines how stable these phase relations are. The common interpretation is that successful control corresponds to a rhythmically organized network state, while lapses reflect a loss of temporal coordination.

Collective observations clarify how brain state shapes phase effects. State changes can shift the location of the preferred phase window, and they can also determine whether a stable phase relationship exists strongly enough for the phase to serve as a functional timing variable.

7.3 tACS interacts with the brain state

The effect of an external oscillatory drive is constrained by what the brain is doing at the moment, including how strong and stable the external rhythm is, and whether the relevant network is engaged in tasks. tACS delivers weak, subthreshold electric fields that do not force spiking but bias spike timing in neurons that are already near threshold, allowing phase shifts at the single neuron level to accumulate into population entrainment and, ultimately, changes in interregional phase

coherence and effective connectivity when task relevant circuits are engaged [43, 44, 45, 46, 47].

Indeed, tACS's impact on brain networks is likely shaped by the existing functional architecture and activity patterns [48, 49, 50]. Multiple studies show that tACS effects are amplified when the relevant network is engaged by learning, memory encoding, conflict, or error processing [51, 52, 53, 54, 55]. Similarly, state variables such as baseline oscillatory power and momentary attentional engagement can gate whether stimulation produces amplification or negligible effects [56, 57]. In this section, we ask how those interactions reshape phase organization and downstream inhibitory performance.

7.3.1 tACS promotes phase-realignment based on an error-prone state

A distinctive finding in Chapter 3 was the emergence of phase-precession-like dynamics specifically during error-prone stopping under tACS. Specifically, across the trials when unsuccessful stops occurred, the beta phase linked to the strongest inhibitory attempts shifted progressively forward across consecutive stimulation cycles. This pattern suggests that an externally applied oscillation can interact dynamically with intrinsic rhythms, such that the effective timing of control is not merely locked to a fixed phase angle but can advance systematically when the system is in an error-prone operating mode.

At a descriptive level, this observation relates to the broader phenomenon of phase precession, in which neural activity systematically advances to earlier phases of an ongoing oscillation. The phenomenon can be traced back to 1993, when O'Keefe and Recce discovered that hippocampal place cells do not fire at a fixed theta phase but instead shift their spikes to progressively earlier phases of the ongoing theta rhythm as an animal traverses the cell's place field [58]. John O'Keefe later shared the 2014 Nobel Prize in Physiology or Medicine. This phase

advance has since been observed across regions and species, including in humans, and it generalizes beyond spatial variables to include prospective and goal-related representations [59, 60, 61, 62]. In our case, the relevance of phase precession extends beyond the shift of oscillatory timing to how information is dynamically represented.

Several mechanistic accounts of phase precession converge on principles that are directly relevant to the present data. Precession can arise when oscillatory processes with slightly mismatched frequencies interact, producing gradual phase drift across cycles, or when intrinsic cellular and synaptic dynamics bias spiking toward earlier phases as excitation accumulates [63, 64]. These accounts differ in implementation, but they agree that phase advances are a natural consequence of oscillatory systems that integrate ongoing inputs while their internal frequency and excitability fluctuate. Indeed, previous studies have demonstrated that an external alternating electric field can interact with endogenous rhythms and bias the preferred spiking phase that constitutes precession [65, 66, 47], providing a plausible route by which tACS could shape phase relationships across cycles.

Within this broad picture, phase precession appeared primarily during error-prone stopping, suggesting that the brain's readiness to learn or adapt may determine how susceptible it is to weak electrical modulation. Such error states transiently engage mechanisms that promote synaptic updating and plasticity [67], providing an opportunity for external fields to interact with ongoing network adjustments. Pharmacological studies have demonstrated error-prone as a period of enhanced NMDA-receptor-dependent plasticity, where neural circuits are intrinsically more susceptible to modification [68, 69]. Consistent with this, direct human evidence has suggested that tACS itself can enhance NMDA-receptor-dependent plasticity [70], which has been linked to the emergence of phase precession by computational work [47]. In this view, the external electric field acts as a phase-aligning catalyst, reinforcing STDP-driven phase advancement across cycles when NMDA-dependent learning mechanisms are already mobilized, and spike-timing relationships are primed for adjustment. Direct evi-

dence for this specific interaction remains limited. Future work should, therefore, test whether precession metrics are systematically altered by pharmacological manipulation of NMDA receptor function in a placebo-controlled design.

7.3.2 Effects of tACS on offline electrophysiology are state-dependent

Electrophysiological measures such as EEG provide a direct readout of rhythmic population dynamics. However, when the EEG is recorded during tACS, the signal is confounded with a large stimulation artifact. Due to the lasting entrainment echoes after tACS, we treat post-stimulation EEG as the interpretable window onto stimulation-induced changes in beta dynamics [71].

In Chapter 4, we therefore implemented closed-loop tACS to either reinforce preSMA beta with in-phase alignment or disrupt it with an anti-phase offset, and then compared the ensuing offline beta signatures across go trials, stop failure trials, and successful stop trials. EEG results revealed a clear state-dependence: reductions in beta power following anti-phase tACS were most pronounced after go and stop-failure trials but attenuated after successful stops.

This pattern suggests that stimulation did not act in isolation but rather interacted with the brain's intrinsic beta rebound. These results evidence the principle that tACS effects are strongly state-dependent, varying as a function of ongoing neural activity and task engagement [48, 49, 50]. Another plausible account is that successful stopping is accompanied by an earlier beta re-synchrony due to the stop cue presenting earlier than the go cue. By the time the stimulation waned, few active beta dynamics remained to perturb, which relatively limited disruption during successful stops. Importantly, this interpretation also reinforces a broader principle that the impact of tACS is constrained by the intrinsic oscillatory activity that is present at the time of stimulation and in the immediate aftermath. If the post movement beta rebound is

reduced, there is less endogenous beta available for the external field to disturb. Alternatively, the system may have compensated through adaptive routing. As proposed by [72, 73, 74], cortical and subcortical systems can dynamically recruit parallel inhibitory pathways or alternative frequency bands when the dominant oscillatory rhythm is disturbed. Growing evidence also shows that the brain exhibits flexible network reorganization in response to external perturbations, particularly within the inhibitory control system [75].

Interestingly, the same protocol produced little change in local beta power in Chapter 5, instead producing lasting changes in connectivity measures such as cortico-muscular coherence (CMC). The discrepancy between Chapters 4 and 5 can be understood in terms of differences in how intrinsic neural oscillations interact with externally applied currents during stimulation, reflecting variations in entrainment strength and state dependence reported in the literature. In Chapter 4, post-stimulation EEG was recorded at rest, when endogenous activity had returned to baseline, and the system was free from task-related demands. Under these conditions, stimulation-induced plasticity could manifest as clear changes in local beta power because the resting brain provides a relatively stable and low-noise environment in which residual entrainment or homeostatic rebound can be detected. This interpretation aligns with prior work showing that tACS aftereffects are more readily observed in resting-state recordings, where spontaneous oscillations can express plastic changes without interference from task-related variability [76, 77, 78]. Studies have further demonstrated that resting-state conditions facilitate the consolidation of stimulation-induced phase alignment and amplitude modulation, supporting the notion that the absence of competing cognitive or motor demands allows for more robust expression of neural entrainment [79, 43]. In Chapter 5, however, EEG was recorded during an ongoing motor task that continuously engaged the same beta networks targeted by stimulation. The strong, task-locked beta synchronization and the presence of movement-related artifacts likely masked or counteracted subtle stimulation aftereffects. Moreover, active task performance may have triggered rapid homeo-

static mechanisms that restored oscillatory balance, thereby minimizing observable differences in local power. This is consistent with evidence that task engagement can suppress or override externally induced oscillatory changes, as the brain prioritizes task-relevant synchronization patterns [51, 80]. Thus, tACS effects appear more evident in resting data, where intrinsic rhythms can freely express stimulation-induced changes, than during task execution, where dynamic neural engagement constrains and potentially obscures these effects.

This comparison reinforces the interpretation that tACS interacts dynamically with the brain's oscillatory landscape. Integrating evidence from both studies, we suggest that rest-state readouts are well-suited to quantify local beta plasticity after stimulation, whereas task-state readouts should prioritize connectivity metrics to detect functionally meaningful changes [48, 49, 50].

7.4 A novel tACS strategy for adaptive modulation: EEG-guided phase-dependent closed-loop tACS

As we discussed in the previous chapter, tACS is an entraining drive: it tends to increase phase alignment and strengthen oscillatory expression [81]. This becomes a conceptual limitation in clinical contexts where the target rhythm is already excessive, as in Parkinsonian beta synchronization [82]. Such that amplifying an already dominant rhythm may be counterproductive. Advances in real-time electrophysiology and online signal processing now make it feasible to combine EEG with stimulation control, enabling closed-loop tACS strategies that track ongoing brain oscillations as the reference. In Chapters 4 and 5, we built a phase-dependent closed-loop tACS that continuously aligns stimulation phase to the brain's ongoing oscillations with a predefined phase lag and achieved bidirectional modulation on motor inhibition in real-time.

7.4.1 Offset phase effect of a closed-loop tACS

Chapters 4 and 5 provide converging evidence that the direction of the stimulation effect depends predictably on the relative phase offset. In the stop signal task in Chapter 4, anti-phase beta-tACS ($\sim$180° offset from endogenous phase) led to slower stopping, reflected by an increased central tendency of stop-signal reaction times (μ_{stop}). This pattern indicates impaired inhibitory control when stimulation cancels the intrinsic beta rhythm. In contrast, in-phase stimulation ($\sim$0° offset) maintained or even improved stopping efficiency, consistent with the idea that beta synchrony supports successful inhibition. During isometric contraction (Chapter 5), anti-phase stimulation again produced a disruptive effect, specifically, a reduction in CMC, which indexes synchronized activity between the motor cortex and peripheral effectors.

These results match a general physical and physiological logic: when the applied field is aligned with the ongoing rhythm, it reinforces phase locking and strengthens rhythmic communication; when the applied field is opposed, it promotes phase cancellation and reduces synchrony. This principle mirrors findings from Parkinsonian tremor studies, where phase-locked cortical tACS that tracked tremor phase produced polarity-contingent effects: stimulation aligned to cancel the tremor rhythm ($\sim$180° relative to the ongoing oscillation) suppressed tremor, whereas alignment that reinforced the rhythm increased tremor [83]. Similar double dissociations appear in closed-loop alpha-tACS paradigms targeting occipital cortex: in-phase (0°) bursts increase alpha power and enhance working-memory performance, whereas anti-phase (180°) bursts suppress alpha and impair performance [84, 85].

In this context, Chapters 4 and 5 extend the same principle into inhibitory control, showing that phase offset can be a meaningful control variable. Therefore, phase-dependent closed-loop tACS holds great clinical potential for precisely modulating pathological rhythms.

7.4.2 Duration effect of a closed-loop tACS

Chapter 5 further revealed a clear duration optimum for anti-phase stimulation. Brief bursts (1-2 s) maximally reduced beta-CMC, whereas longer trains (5 s) produced a partial rebound, suggesting re-entrainment rather than continued disruption. This temporal pattern implies a two-stage mechanism: (1) short anti-phase pulses create transient phase cancellation, weakening rhythmic synchrony and reducing CMC, while (2) with prolonged stimulation, the endogenous oscillator adapts and re-synchronizes with the external field, effectively flipping the effect from desynchronization back to entrainment [86].

Supporting this view, [87] demonstrated in a Parkinsonism model that weak electric fields initially disrupt beta-phase spiking, shifting neurons' preferred firing phase. Mechanistically, stronger or longer-lasting fields facilitate more cycles, providing more opportunities for adaptation, enabling the network to recover synchrony, subsequently re-establish entrainment. A practical inference from Chapters 4 and 5 is therefore that closed-loop tACS should be treated as a precise control policy. Effective desynchronization requires brief, strategically timed interventions, whereas longer stimulation may shift the regime toward re-entrainment.

7.4.3 Successful implementation of an EEG-guided closed-loop tACS system

In a phase-dependent closed-loop system, stimulation can be delivered in alignment with ongoing neural rhythms with a defined phase offset, enabling bidirectional modulation of neural dynamics and behavior. However, achieving this is technically challenging and demands precise coordination across hardware, software, and experimental design. In practice, acquisition delay, buffering, filtering, computation, and stimulator onset can shift the targeted phase by tens of degrees or more [88]. A credible closed-loop implementation, therefore, requires explicit end-to-end latency quantification, a principled compensation strategy that

includes short-horizon phase prediction when needed, and transparent reporting of realized performance in terms of hit rate and phase error distributions.

In Chapter 6, we provided a concrete guideline for implementing an EEG-based closed-loop tACS system that can genuinely target the phase. Hereby, the chapter aims to solve the main challenges:

1. Timing: phase targeting would collapse if loop latency and jitter are unknown. The solution is to treat acquisition delay, buffering, computation time, and stimulator onset as a single empirically measured latency budget, then to compensate that budget during triggering. In practice, this also implies selecting streaming protocols that preserve per-sample timestamps and make clock offsets auditable across devices, while keeping buffer sizes small enough to respect the oscillatory period and keeping computation bounded so that operating system scheduling does not introduce variable delay.

2. Data buffering: continuous streaming must avoid packet loss, overruns, and blocking calls, which is mediated by buffers. Smooth data streaming relies on countable buffer policies, such as timestamped ring buffers, double-buffered processing, small deterministic chunk sizes, and an analysis window that is long enough for stable processing but short enough to preserve temporal resolution.

3. Artifact handling: online EEG processing requires robust artifact handling with a tight time budget. Reliable solutions include source reduction: hardware control (low electrode impedances, rigorous grounding, and cable management), referencing, and rapid artifact detection and online removal.

4. Phase forecasting: accounting for system delays and filtering artifacts, precise phase targeting requires prediction to compensate for the mismatch. This real-time phase prediction. A principled implementation, therefore, treats phase forecasting as part of

the control problem: the algorithm estimates the current phase, projects that phase forward to the expected delivery time point, and triggers only when the forecasted phase matches the desired target within a predefined tolerance. Several strategies have been developed to forecast the instantaneous phase of an oscillatory neural signal.

5. Experimental setup: Closed-loop phase-dependent tACS benefits from paradigms that elicit a stable, high-amplitude target rhythm. Task engagement was reported to strengthen physiological relevance [51]. In this way, signal-to-noise for real-time tracking can be improved. Second, target selection and montage design should be relevant to the task. Stimulation amplitude, waveform, and duration should respect safety limits and be matched to the intended perturbation timescale.

Chapters 4 and 5 presented practical examples for successfully employing a phase-dependent closed-loop tACS system modulating cortical beta dynamics and motor control. In both studies, individual beta frequency was derived with a Laplacian at Fz and beta band filtering, followed by FFT-based peak picking in FieldTrip, thereby defining a participant-specific frequency target for online phase tracking. Online, a sliding 500 ms window updated with EEG segments was first dereferenced via Laplacian, band-pass filtered around individual beta frequency, trimmed to limit filter edge transients, then forward predicted using an autoregressive model before Hilbert-based phase extraction, enabling explicit compensation of a measured 16 ms end-to-end delay [89]. Finally, the digital trigger initiated the tACS sequence was shifted to coincide with the predicted current with an amplitude ramp-up.

7.4.4 Research Trends and Technological Advances

By precisely aligning stimulation to the ongoing oscillatory phase, closed-loop tACS enables clinicians to influence neural excitability and

inter-regional communication with high temporal specificity. Empirical and modeling work has shown that phase-locked stimulation can differentially enhance or suppress cortical excitability depending on the targeted phase of the endogenous rhythm [14, 90]. Recent advances in real-time phase estimation and prediction algorithms have further improved the feasibility of delivering stimulation at behaviorally and physiologically relevant phases despite neural delays and noise [91, 92, 47]. In parallel, progress in wearable and miniaturized stimulation hardware has enabled portable, closed-loop neuromodulation outside highly controlled laboratory environments [93, 94]. Finally, computational modeling and machine-learning approaches are increasingly being used to optimize phase targeting, adapt stimulation parameters online, and personalize control strategies at the level of individual cortical sites, collectively paving the way for precise, phase-specific neuromodulation with clinical relevance [95, 96, 97].

7.4.5 Clinical Trends and Translational Pathways

By precisely aligning stimulation to the ongoing oscillatory phase, closed-loop tACS enables clinicians to influence neural excitability and communication with unprecedented temporal specificity. Recent advances in real-time phase prediction, wearable and miniaturized hardware, computational modeling, and machine learning are paving the way for precise, phase-specific control of single cortical sites.

Parkinson's disease

Parkinson's disease is marked by pathological beta band synchronization within the cortico-basal ganglia loop and remains the clearest use case for a phase-locked stimulation [98]. Current treatments, such as pharmacotherapy and deep brain stimulation can suppress symptoms, yet remain constrained due to side effects and invasive nature.

Phase-dependent closed-loop tACS is attractive because it reframes treatment as rhythm control in a non-invasive way: stimulation can be delivered at phases predicted to disrupt synchrony when oscillations become excessive, or to stabilize physiological coupling when it is deficient. Invasive work has shown that phase-targeted stimulation can suppress tremor efficiently [99]. Noninvasively, rhythmic transcranial alternating current stimulation aligned to the tremor phase can reduce tremor amplitude [83]. The translational implication is that EEG-guided closed-loop tACS could use anti-phase beta current to counter pathological beta synchrony, particularly if triggers are restricted to windows of high rhythmicity or bursts in the beta band.

Other diseases

Beyond PD, closed-loop tACS also holds promise for other neurodegenerative conditions. In Alzheimer's disease and mild cognitive impairment, impaired cross-frequency coordination is increasingly viewed as a core pathophysiological feature, with reductions in theta gamma coupling tracking working memory deficits [100]. Existing treatments are largely symptomatic and rarely target temporal coordination as a primary mechanism. In this context, converging evidence that gamma tACS delivered at an optimal theta phase, often near the theta peak, can enhance memory encoding and retrieval while strengthening frontotemporal theta gamma coupling [101, 102, 103, 104, 105] motivates a phase-dependent closed-loop strategy. Conceptually, the controller would continuously estimate endogenous theta phase, deliver brief gamma bursts only within a narrow theta phase window during memory tasks, and adapt timing as theta frequency and coupling strength drift over time.

Extending from neurodegeneration to network-level dysfunction, mood and cognitive disorders represent a further translational frontier for phase-dependent closed-loop tACS. Major depressive disorder has been linked to abnormalities in rhythmic activity and network coordination,

motivating interventions that explicitly track and shape oscillatory state [106]. A recent clinical demonstration used closed-loop tACS to titrate stimulation to an endogenous target rhythm, reporting feasibility and symptomatic improvement in an open-label design [107]. Established treatments such as medication, psychotherapy, and rTMS remain first line, but they are not designed to enforce a desired phase relationship between distributed circuits. Phase-dependent closed-loop tACS offers a plausible next step: the controller could impose, or release phase lags between prefrontal nodes as a direct mechanism to normalize large-scale communication [24, 43].

Other disorders defined by network dysconnectivity and dysrhythmic cortical state regulation also offer a plausible translational pathway for the closed-loop tACS. Schizophrenia is marked by disrupted large-scale coordination, including reduced alpha band power and coupling and attenuated 40 Hz auditory steady state responses that reflect impaired gamma range synchronization [108]. 10 Hz tACS over dorsolateral prefrontal cortex and temporoparietal regions had attempted to strengthen deficient rhythms and relieve symptoms [109, 110, 111, 112]. More recent gamma band multi-site protocols, with early studies reporting physiological target engagement and symptom-relevant changes [113]. A closed-loop extension could be the next step that enforces a patient-specific phase relation between frontal and temporoparietal nodes. In ADHD, resting EEG differences are heterogeneous, but elevated theta power and increased theta beta ratios are among the most reproducible findings [114], suggesting a closed-loop theta or alpha tACS targeting DLPFC during attention tasks, with stimulation parameters adapted to real-time performance metrics. In PTSD, the alpha band is dysrhythmic across the visual cortex, and default mode regions [115], and clinical neurofeedback studies suggest that restoring alpha rhythm control can normalize default mode and salience network coupling [116], providing a plausible biomarker and control target for phase and power gated closed loop stimulation during therapy-relevant epochs.

The accelerating pace of innovation across academia and industry suggests that phase-locked tACS is poised to become a mainstream tool

in neurology, psychiatry, and cognitive neuroscience within the next decade. The work presented in this thesis contributes directly to this emerging landscape. By tracing beta-phase dynamics in motor inhibition from observation to causal closed-loop modulation, we demonstrated that real-time, phase-specific stimulation of a single cortical site can bidirectionally influence inhibitory control. In this sense, the oscillatory phase is not only a passive byproduct of neural activity but an active control parameter governing cortical excitability, network synchrony, and behavior. Looking forward, the insights and methodologies developed here offer a blueprint for next-generation interventions that normalize pathological oscillations from Parkinson's disease to a wider spectrum of disorders.

7.5 Considerations and limitations

This dissertation combines phase-resolved behavioral analyses, externally imposed rhythmic stimulation to test whether beta timing is functionally relevant for inhibitory control and whether that phase can be used to steer motor inhibition. The methodological issues discussed here are general constraints that set the limits of what can be concluded across the full set of chapters.

7.5.1 Inference about the phase requires care about which phase is measured

A central object in this thesis is the instantaneous phase of beta activity. In scalp EEG, the oscillatory phase reflects a weighted mixture of sources whose weights depend on anatomy, conductivity, and reference choice. Its estimation depends on referencing, spatial mixing, filter choices, and estimator design [117]. While the phase of the tACS waveform is defined at the stimulator output and reflects local field orientation and amplitude relative to cortical geometry [118, 119]. Its physiological meaning is mediated by the induced electric field in tissue.

Inference about phase-specific neural computations under tACS, therefore, requires care in distinguishing three phases: the device waveform phase, the local electric field phase in the cortex, and the phase of endogenous neural activity. This does not invalidate our phase-dependent results, but raises concern that interpretation should be constrained to a mechanistic hypothesis about what the sensor level phase is presumed to track.

Chapters 2 and 3 employed 20 Hz tACS as a controllable phase reference to sample behavior at different points in the stimulation cycle. This approach has the strength that the phase of the external waveform is known with high precision. The main limitation is that the measured behavioral phase relation is locked to the stimulation cycle rather than to a directly cortical phase. To this end, the frequency matching results support that the strongest phase-dependency is matched with the strongest coupling between internal and external oscillation.

7.5.2 Online electrophysiology data are obscured during stimulation

In Chapters 4 and 5, we used closed-loop phase-locked tACS in which a stimulation waveform is delivered with a specific phase lag to the endogenous rhythm's phase estimated from the EEG. The core concern here is that the precise online neural mechanism during stimulation is partially obscured by artifact. Mechanistically, it was well proven that weak alternating fields can rhythmically bias excitability and spike timing, yielding online phase locking when stimulation is near the intrinsic frequency [120, 21]. The same framework also supports disruptive style outcomes when the relative phase is chosen to reduce functional coupling. Finally, the observation of a short-lived post-stimulation 'echo' is a clear indicator of neural de-/synchronization.

7.5.3 Excluding peripheral confounds remains challenging

tACS can stimulate peripheral nerves and produce cutaneous sensations that vary with intensity, electrode placement, and time. These factors can alter arousal, attention, expectancy, or motor preparation. Chapters 4 and 5 used a designed sham session intended to minimize these confounds, but participants reported noticeably different sensations during active stimulation compared with sham. This is particularly important when interpreting behavioral effects during stimulation.

That said, our main conclusions are supported by the phase contrast within in- and anti-phase conditions, where participants did not report different sensations. Still, any sham-referenced comparisons should be interpreted cautiously, and future studies would benefit from an active sham that better matches the ongoing sensory experience without reproducing any cortical activity.

References

[1] Pascal Fries. "A mechanism for cognitive dynamics: neuronal communication through neuronal coherence". In: *Trends in Cognitive Sciences* 9.10 (2005), pp. 474–480. DOI: https://doi.org/10.1016/j.tics.2005.08.011.

[2] Pascal Fries. "Rhythms for Cognition: Communication through Coherence". In: *Neuron* 88.1 (2015), pp. 220–235. DOI: https://doi.org/10.1016/j.neuron.2015.09.034.

[3] Andrea A. Kühn et al. "Event-related beta desynchronization in human subthalamic nucleus correlates with motor performance". In: *Brain* 127.4 (Apr. 2004), pp. 735–746. DOI: 10.1093/brain/awh106.

[4] Nicole Swann et al. “Intracranial EEG Reveals a Time- and Frequency-Specific Role for the Right Inferior Frontal Gyrus and Primary Motor Cortex in Stopping Initiated Responses”. In: *The Journal of Neuroscience* 29.40 (Oct. 2009), pp. 12675–12685. DOI: 10.1523/jneurosci.3359-09.2009.

[5] Nicola J. Ray et al. “The role of the subthalamic nucleus in response inhibition: Evidence from local field potential recordings in the human subthalamic nucleus”. In: *NeuroImage* 60.1 (Mar. 2012), pp. 271–278. DOI: 10.1016/j.neuroimage.2011.12.035.

[6] G. Pfurtscheller and F.H. Lopes da Silva. “Event-related EEG/MEG synchronization and desynchronization: basic principles”. In: *Clinical Neurophysiology* 110.11 (Nov. 1999), pp. 1842–1857. DOI: 10.1016/s1388-2457(99)00141-8.

[7] Michael T. Jurkiewicz et al. “Post-movement beta rebound is generated in motor cortex: Evidence from neuromagnetic recordings”. In: *NeuroImage* 32.3 (Sept. 2006), pp. 1281–1289. DOI: 10.1016/j.neuroimage.2006.06.005.

[8] G. Pfurtscheller, A. Stancák, and C. Neuper. “Post-movement beta synchronization. A correlate of an idling motor area?” In: *Electroencephalography and Clinical Neurophysiology* 98.4 (Apr. 1996), pp. 281–293. DOI: 10.1016/0013-4694(95)00258-8.

[9] François Cassim et al. “Does post-movement beta synchronization reflect an idling motor cortex?” In: (Dec. 2001). DOI: 10.1097/00001756-200112040-00051.

[10] Teodoro Solis-Escalante et al. “Cue-induced beta rebound during withholding of overt and covert foot movement”. In: *Clinical Neurophysiology* 123.6 (June 2012), pp. 1182–1190. DOI: 10.1016/j.clinph.2012.01.013.

[11] Huiling Tan, Cian Wade, and Peter Brown. “Post-Movement Beta Activity in Sensorimotor Cortex Indexes Confidence in the Estimations from Internal Models”. In: *The Journal of Neuroscience*

36.5 (Feb. 2016), pp. 1516–1528. DOI: 10.1523/jneurosci.3204-15.2016.

[12] N. A. Busch, J. Dubois, and R. VanRullen. "The Phase of Ongoing EEG Oscillations Predicts Visual Perception". In: *Journal of Neuroscience* 29.24 (June 2009), pp. 7869–7876. DOI: 10.1523/jneurosci.0113-09.2009.

[13] Sanne ten Oever, Peter de Weerd, and Alexander T. Sack. "Phase-dependent amplification of working memory content and performance". In: *Nature Communications* 11.1 (2020), p. 1832. DOI: 10.1038/s41467-020-15629-7.

[14] Christoph Zrenner et al. "Real-time EEG-defined excitability states determine efficacy of TMS-induced plasticity in human motor cortex". In: *Brain Stimulation* 11.2 (Mar. 2018), pp. 374–389. DOI: 10.1016/j.brs.2017.11.016.

[15] Aqsa Shakeel et al. "Real-Time Implementation of EEG Oscillatory Phase-Informed Visual Stimulation Using a Least Mean Square-Based AR Model". In: *Journal of Personalized Medicine* 11.1 (Jan. 2021), p. 38. DOI: 10.3390/jpm11010038.

[16] Henry Hebron et al. "A closed-loop auditory stimulation approach selectively modulates alpha oscillations and sleep onset dynamics in humans". In: *PLOS Biology* 22.6 (June 2024). Ed. by Simon Hanslmayr, e3002651. DOI: 10.1371/journal.pbio.3002651.

[17] Christoph S. Herrmann et al. "Shaping Intrinsic Neural Oscillations with Periodic Stimulation". In: *The Journal of Neuroscience* 36.19 (May 2016), pp. 5328–5337. DOI: 10.1523/jneurosci.0236-16.2016.

[18] Sanne ten Oever et al. "Stimulus Presentation at Specific Neuronal Oscillatory Phases Experimentally Controlled with tACS: Implementation and Applications". In: *Frontiers in Cellular Neuroscience* 10 (Oct. 2016). DOI: 10.3389/fncel.2016.00240.

[19] Tom A. de Graaf et al. “Does alpha phase modulate visual target detection? Three experiments with tACS-phase-based stimulus presentation”. In: *European Journal of Neuroscience* 51.11 (2020), pp. 2299–2313. DOI: https://doi.org/10.1111/ejn.14677.

[20] Christoph S. Herrmann et al. “Transcranial alternating current stimulation: a review of the underlying mechanisms and modulation of cognitive processes”. In: *Frontiers in Human Neuroscience* 7 (2013). DOI: 10.3389/fnhum.2013.00279.

[21] M. M. Ali, K. K. Sellers, and F. Frohlich. “Transcranial Alternating Current Stimulation Modulates Large-Scale Cortical Network Activity by Network Resonance”. In: *Journal of Neuroscience* 33.27 (July 2013), pp. 11262–11275. DOI: 10.1523/jneurosci.5867-12.2013.

[22] Andreas K Engel and Pascal Fries. “Beta-band oscillations — signalling the status quo?” In: *Current Opinion in Neurobiology* 20.2 (Apr. 2010), pp. 156–165. DOI: 10.1016/j.conb.2010.02.015.

[23] Jan R. Wessel. “beta-Bursts Reveal the Trial-to-Trial Dynamics of Movement Initiation and Cancellation”. In: *The Journal of Neuroscience* 40.2 (Nov. 2019), pp. 411–423. DOI: 10.1523/jneurosci.1887-19.2019.

[24] Rafael Polanía et al. “The Importance of Timing in Segregated Theta Phase-Coupling for Cognitive Performance”. In: *Current Biology* 22.14 (July 2012), pp. 1314–1318. DOI: 10.1016/j.cub.2012.05.021.

[25] Gregor Thut, Philippe G. Schyns, and Joachim Gross. “Entrainment of Perceptually Relevant Brain Oscillations by Non-Invasive Rhythmic Stimulation of the Human Brain”. In: *Frontiers in Psychology* 2 (2011). DOI: 10.3389/fpsyg.2011.00170.

[26] Natalie Schaworonkow et al. "EEG-triggered TMS reveals stronger brain state-dependent modulation of motor evoked potentials at weaker stimulation intensities". In: *Brain Stimulation* 12.1 (Jan. 2019), pp. 110–118. DOI: 10.1016/j.brs.2018.09.009.

[27] Flavie Torrecillos et al. "Motor Cortex Inputs at the Optimum Phase of Beta Cortical Oscillations Undergo More Rapid and Less Variable Corticospinal Propagation". In: *Journal of Neuroscience* 40.2 (2020), pp. 369–381. DOI: https://doi.org/10.1523/JNEUROSCI.1953-19.2019.

[28] Miles Wischnewski et al. "The phase of sensorimotor mu and beta oscillations has the opposite effect on corticospinal excitability". In: *Brain Stimulation* 15.5 (Sept. 2022), pp. 1093–1100. DOI: 10.1016/j.brs.2022.08.005.

[29] Kyle E. Mathewson et al. "To See or Not to See: Prestimulus Alpha Phase Predicts Visual Awareness". In: *The Journal of Neuroscience* 29.9 (Mar. 2009), pp. 2725–2732. DOI: 10.1523/jneurosci.3963-08.2009.

[30] Molly J. Henry and Jonas Obleser. "Frequency modulation entrains slow neural oscillations and optimizes human listening behavior". In: *Proceedings of the National Academy of Sciences* 109.49 (Nov. 2012), pp. 20095–20100. DOI: 10.1073/pnas.1213390109.

[31] Alex Milton and Christopher W. Pleydell-Pearce. "The phase of pre-stimulus alpha oscillations influences the visual perception of stimulus timing". In: *NeuroImage* 133 (June 2016), pp. 53–61. DOI: 10.1016/j.neuroimage.2016.02.065.

[32] Stephanie J. Kayser, Steven W. McNair, and Christoph Kayser. "Prestimulus influences on auditory perception from sensory representations and decision processes". In: *Proceedings of the National Academy of Sciences* 113.17 (Apr. 2016), pp. 4842–4847. DOI: 10.1073/pnas.1524087113.

[33] Sanne ten Oever and Alexander T. Sack. “Oscillatory phase shapes syllable perception”. In: *Proceedings of the National Academy of Sciences* 112.52 (Dec. 2015), pp. 15833–15837. DOI: 10.1073/pnas.1517519112.

[34] Sanne Ten Oever et al. “Phase-dependent word perception emerges from region-specific sensitivity to the statistics of language”. In: *Proceedings of the National Academy of Sciences* 121.23 (May 2024). DOI: 10.1073/pnas.2320489121.

[35] Adam R. Aron et al. “Frontosubthalamic Circuits for Control of Action and Cognition”. In: *The Journal of Neuroscience* 36.45 (Nov. 2016), pp. 11489–11495. DOI: 10.1523/jneurosci.2348-16.2016.

[36] Ruibin Zhang, Xiujuan Geng, and Tatia M. C. Lee. “Large-scale functional neural network correlates of response inhibition: an fMRI meta-analysis”. In: *Brain Structure and Function* 222.9 (May 2017), pp. 3973–3990. DOI: 10.1007/s00429-017-1443-x.

[37] Witney Chen et al. “Prefrontal-Subthalamic Hyperdirect Pathway Modulates Movement Inhibition in Humans”. In: *Neuron* 106.4 (May 2020), 579–588.e3. DOI: 10.1016/j.neuron.2020.02.012.

[38] Jixin Long et al. “Distinct neural activation patterns of age in subcomponents of inhibitory control: A fMRI meta-analysis”. In: *Frontiers in Aging Neuroscience* 14 (Aug. 2022). DOI: 10.3389/fnagi.2022.938789.

[39] James F. Cavanagh, Michael X Cohen, and John J. B. Allen. “Prelude to and Resolution of an Error: EEG Phase Synchrony Reveals Cognitive Control Dynamics during Action Monitoring”. In: *The Journal of Neuroscience* 29.1 (Jan. 2009), pp. 98–105. DOI: 10.1523/jneurosci.4137-08.2009.

[40] Valentin Wyart et al. “Rhythmic Fluctuations in Evidence Accumulation during Decision Making in the Human Brain”. In: *Neuron* 76.4 (Nov. 2012), pp. 847–858. DOI: 10.1016/j.neuron.2012.09.015.

[41] Michael X Cohen and Tobias H. Donner. "Midfrontal conflict-related theta-band power reflects neural oscillations that predict behavior". In: *Journal of Neurophysiology* 110.12 (Dec. 2013), pp. 2752–2763. DOI: 10.1152/jn.00479.2013.

[42] Joan Duprez, Rasa Gulbinaite, and Michael X. Cohen. "Midfrontal theta phase coordinates behaviorally relevant brain computations during cognitive control". In: *NeuroImage* 207 (Feb. 2020), p. 116340. DOI: 10.1016/j.neuroimage.2019.116340.

[43] Randolph F. Helfrich et al. "Entrainment of Brain Oscillations by Transcranial Alternating Current Stimulation". In: *Current Biology* 24.3 (Feb. 2014), pp. 333–339. DOI: 10.1016/j.cub.2013.12.041.

[44] Yu Huang et al. "Measurements and models of electric fields in the in vivo human brain during transcranial electric stimulation". In: *eLife* 6 (Feb. 2017). DOI: 10.7554/elife.18834.

[45] Matthew R. Krause et al. "Transcranial alternating current stimulation entrains single-neuron activity in the primate brain". In: *Proceedings of the National Academy of Sciences* 116.12 (Mar. 2019), pp. 5747–5755. DOI: 10.1073/pnas.1815958116.

[46] Yao Wang et al. "The influence of different current-intensity transcranial alternating current stimulation on the eyes-open and eyes-closed resting-state electroencephalography". In: *Frontiers in Human Neuroscience* 16 (Aug. 2022). DOI: 10.3389/fnhum.2022.934382.

[47] Miles Wischnewski et al. "Induced neural phase precession through exogenous electric fields". In: *Nature Communications* 15.1 (Feb. 2024). DOI: 10.1038/s41467-024-45898-5.

[48] Ines R Violante et al. "Externally induced frontoparietal synchronization modulates network dynamics and enhances working memory performance". In: *eLife* 6 (Mar. 2017). DOI: 10.7554/elife.22001.

[49] Johannes Vosskuhl, Daniel Strüber, and Christoph S. Herrmann. "Non-invasive Brain Stimulation: A Paradigm Shift in Understanding Brain Oscillations". In: *Frontiers in Human Neuroscience* 12 (May 2018). DOI: 10.3389/fnhum.2018.00211.

[50] Kilian Abellaneda-Pérez et al. "Differential tDCS and tACS Effects on Working Memory-Related Neural Activity and Resting-State Connectivity". In: *Frontiers in Neuroscience* 13 (Jan. 2020). DOI: 10.3389/fnins.2019.01440.

[51] Matteo Feurra et al. "State-Dependent Effects of Transcranial Oscillatory Currents on the Motor System: What You Think Matters". In: *The Journal of Neuroscience* 33.44 (Oct. 2013), pp. 17483–17489. DOI: 10.1523/jneurosci.1414-13.2013.

[52] Yuranny Cabral-Calderin et al. "Transcranial alternating current stimulation affects the BOLD signal in a frequency and task-dependent manner". In: *Human Brain Mapping* 37.1 (Oct. 2015), pp. 94–121. DOI: 10.1002/hbm.23016.

[53] Aref Pariz et al. "Selective control of synaptic plasticity in heterogeneous networks through transcranial alternating current stimulation (tACS)". In: (Nov. 2022). DOI: 10.1101/2022.11.15.516556.

[54] Desmond Agboada, Zhihe Zhao, and Miles Wischnewski. "Neuroplastic effects of transcranial alternating current stimulation (tACS): from mechanisms to clinical trials". In: *Frontiers in Human Neuroscience* 19 (Mar. 2025). DOI: 10.3389/fnhum.2025.1548478.

[55] Aurimas Mockevičius, Jovana Bjekić, and Inga Griškova-Bulanova. "The modulation of steady-state responses by transcranial alternating current stimulation: a scoping review". In: *Frontiers in Systems Neuroscience* 19 (Oct. 2025). DOI: 10.3389/fnsys.2025.1661128.

[56] Sankaraleengam Alagapan et al. “Modulation of Cortical Oscillations by Low-Frequency Direct Cortical Stimulation Is State-Dependent”. In: *PLOS Biology* 14.3 (Mar. 2016). Ed. by Ole Jensen, e1002424. DOI: 10.1371/journal.pbio.1002424.

[57] Florian H. Kasten et al. “Integrating electric field modeling and neuroimaging to explain inter-individual variability of tACS effects”. In: *Nature Communications* 10.1 (Nov. 2019). DOI: 10.1038/s41467-019-13417-6.

[58] John O’Keefe and Michael L. Recce. “Phase relationship between hippocampal place units and the EEG theta rhythm”. In: *Hippocampus* 3.3 (1993), pp. 317–330. DOI: 10.1002/hipo.450030307.

[59] Matthew W. Jones and Matthew A. Wilson. “Phase precession of medial prefrontal cortical activity relative to the hippocampal theta rhythm”. In: *Hippocampus* 15.7 (2005), pp. 867–873. DOI: 10.1002/hipo.20119.

[60] Matthijs A. A. van der Meer and A. David Redish. “Theta phase precession in rat ventral striatum links place and reward information”. In: *Journal of Neuroscience* 31.8 (2011), pp. 2843–2854. DOI: 10.1523/JNEUROSCI.4869-10.2011.

[61] Salman E. Qasim, Itzhak Fried, and Joshua Jacobs. “Phase precession in the human hippocampus and entorhinal cortex”. In: *Cell* 184.12 (2021), 3242–3255.e10. DOI: 10.1016/j.cell.2021.04.017.

[62] Leila Reddy et al. “Theta-phase dependent neuronal coding during sequence learning in human single neurons”. In: *Nature Communications* 12.1 (2021), p. 4839. DOI: 10.1038/s41467-021-25150-0.

[63] Mayank R. Mehta, Carol A. Barnes, and Bruce L. McNaughton. “Experience-dependent, asymmetric expansion of hippocampal place fields”. In: *Proceedings of the National Academy of Sciences* 94.16 (Aug. 1997), pp. 8918–8921. DOI: 10.1073/pnas.94.16.8918.

[64] M. R. Mehta, A. K. Lee, and M. A. Wilson. “Role of experience and oscillations in transforming a rate code into a temporal code”. In: *Nature* 417.6890 (June 2002), pp. 741–746. DOI: 10.1038/nature00807.

[65] Jeffrey C. Magee. “Dendritic Mechanisms of Phase Precession in Hippocampal CA1 Pyramidal Neurons”. In: *Journal of Neurophysiology* 86.1 (July 2001), pp. 528–532. DOI: 10.1152/jn.2001.86.1.528.

[66] Rishikesh Narayanan and Daniel Johnston. “The h Channel Mediates Location Dependence and Plasticity of Intrinsic Phase Response in Rat Hippocampal Neurons”. In: *The Journal of Neuroscience* 28.22 (May 2008), pp. 5846–5860. DOI: 10.1523/jneurosci.0835-08.2008.

[67] Nicholas Cole et al. “Prediction-error signals in anterior cingulate cortex drive task-switching”. In: *Nature Communications* 15.1 (Aug. 2024). DOI: 10.1038/s41467-024-51368-9.

[68] Jennifer K. Forsyth et al. “Augmenting NMDA receptor signaling boosts experience-dependent neuroplasticity in the adult human brain”. In: *Proceedings of the National Academy of Sciences* 112.50 (Nov. 2015), pp. 15331–15336. DOI: 10.1073/pnas.1509262112.

[69] Lilian A. Weber et al. “Ketamine Affects Prediction Errors about Statistical Regularities: A Computational Single-Trial Analysis of the Mismatch Negativity”. In: *The Journal of Neuroscience* 40.29 (June 2020), pp. 5658–5668. DOI: 10.1523/jneurosci.3069-19.2020.

[70] Miles Wischnewski, Dennis J. L. G. Schutter, and Michael A. Nitsche. “Effects of beta-tACS on corticospinal excitability: A meta-analysis”. In: *Brain Stimulation* 12.6 (2019), pp. 1381–1389. DOI: 10.1016/j.brs.2019.07.023.

[71] Domenica Veniero et al. “Lasting EEG/MEG Aftereffects of Rhythmic Transcranial Brain Stimulation: Level of Control Over Oscillatory Network Activity”. In: *Frontiers in Cellular Neuroscience* 9 (Dec. 2015). DOI: 10.3389/fncel.2015.00477.

[72] Magdalena Nowak et al. “Driving Human Motor Cortical Oscillations Leads to Behaviorally Relevant Changes in Local GABAAInhibition: A tACS-TMS Study”. In: *The Journal of Neuroscience* 37.17 (Mar. 2017), pp. 4481–4492. DOI: 10.1523/jneurosci.0098-17.2017.

[73] Wing Ting To et al. “Changing Brain Networks Through Noninvasive Neuromodulation”. In: *Frontiers in Human Neuroscience* 12 (Apr. 2018). DOI: 10.3389/fnhum.2018.00128.

[74] Aref Pariz et al. “Selective control of synaptic plasticity in heterogeneous networks through transcranial alternating current stimulation (tACS)”. In: *PLOS Computational Biology* 19.4 (Apr. 2023). Ed. by Daniel Bush, e1010736. DOI: 10.1371/journal.pcbi.1010736.

[75] Terese L. Chmielewski et al. “Impaired motor control after sport-related concussion could increase risk for musculoskeletal injury: Implications for clinical management and rehabilitation”. In: *Journal of Sport and Health Science* 10.2 (Mar. 2021), pp. 154–161. DOI: 10.1016/j.jshs.2020.11.005.

[76] Toralf Neuling, Stefan Rach, and Christoph S. Herrmann. “Orchestrating neuronal networks: sustained after-effects of transcranial alternating current stimulation depend upon brain states”. In: *Frontiers in Human Neuroscience* 7 (2013). DOI: 10.3389/fnhum.2013.00161.

[77] Florian H. Kasten, James Dowsett, and Christoph S. Herrmann. “Sustained Aftereffect of α-tACS Lasts Up to 70 min after Stimulation”. In: *Frontiers in Human Neuroscience* 10 (May 2016). DOI: 10.3389/fnhum.2016.00245.

[78] Alexandra Vossen, Joachim Gross, and Gregor Thut. "Alpha Power Increase After Transcranial Alternating Current Stimulation at Alpha Frequency (alpha-tACS) Reflects Plastic Changes Rather Than Entrainment". In: *Brain Stimulation* 8.3 (May 2015), pp. 499–508. DOI: 10.1016/j.brs.2014.12.004.

[79] Tino Zaehle, Stefan Rach, and Christoph S. Herrmann. "Transcranial Alternating Current Stimulation Enhances Individual Alpha Activity in Human EEG". In: *PLoS ONE* 5.11 (Nov. 2010). Ed. by André Aleman, e13766. DOI: 10.1371/journal.pone.0013766.

[80] Philipp Ruhnau et al. "Eyes wide shut: Transcranial alternating current stimulation drives alpha rhythm in a state dependent manner". In: *Scientific Reports* 6.1 (June 2016). DOI: 10.1038/srep27138.

[81] Sreekari Vogeti, Cindy Boetzel, and Christoph S. Herrmann. "Entrainment and Spike-Timing Dependent Plasticity - A Review of Proposed Mechanisms of Transcranial Alternating Current Stimulation". In: *Frontiers in Systems Neuroscience* 16 (2022). DOI: https://doi.org/10.3389/fnsys.2022.827353.

[82] Robert Chen et al. "Clinical neurophysiology of Parkinson's disease and parkinsonism". In: *Clinical Neurophysiology Practice* 7 (2022), pp. 201–227. DOI: 10.1016/j.cnp.2022.06.002.

[83] John-Stuart Brittain et al. "Tremor Suppression by Rhythmic Transcranial Current Stimulation". In: *Current Biology* 23.5 (Mar. 2013), pp. 436–440. DOI: 10.1016/j.cub.2013.01.068.

[84] Xueli Chen et al. "Alpha oscillatory activity is causally linked to working memory retention". In: *PLOS Biology* 21.2 (Feb. 2023). Ed. by Simon Hanslmayr, e3001999. DOI: 10.1371/journal.pbio.3001999.

[85] David Haslacher et al. "Working memory enhancement using real-time phase-tuned transcranial alternating current stimulation". In: *Brain Stimulation* 17.4 (July 2024), pp. 850–859. DOI: 10.1016/j.brs.2024.07.007.

[86] Matthew R. Krause et al. “Brain stimulation competes with ongoing oscillations for control of spike timing in the primate brain”. In: *PLOS Biology* 20.5 (May 2022). Ed. by Huan Luo, e3001650. DOI: 10.1371/journal.pbio.3001650.

[87] Harry Tran et al. “Transcranial Alternating Current Stimulation can disrupt or reestablish neural entrainment in a primate model of Parkinson’s disease”. In: (Sept. 2025). DOI: 10.1101/2025.09.17.676896.

[88] Yu-Cheng Chang et al. “Delay Analysis in Closed-Loop EEG Phase-Triggered Transcranial Magnetic Stimulation”. In: *2023 45th Annual International Conference of the IEEE Engineering in Medicine & amp; Biology Society (EMBC)*. IEEE, July 2023, pp. 1–4. DOI: 10.1109/embc40787.2023.10340744.

[89] Sina Shirinpour et al. “Experimental evaluation of methods for real-time EEG phase-specific transcranial magnetic stimulation”. In: *Journal of Neural Engineering* 17.4 (July 2020), p. 046002. DOI: 10.1088/1741-2552/ab9dba.

[90] Anke Ninija Karabanov et al. “Can Transcranial Electrical Stimulation Localize Brain Function?” In: *Frontiers in Psychology* 10 (Feb. 2019). DOI: 10.3389/fpsyg.2019.00213.

[91] Christoph Zrenner et al. “Closed-Loop Neuroscience and Non-Invasive Brain Stimulation: A Tale of Two Loops”. In: *Frontiers in Cellular Neuroscience* 10 (Apr. 2016). DOI: 10.3389/fncel.2016.00092.

[92] Reza Sameni and Esmaeil Seraj. “A robust statistical framework for instantaneous electroencephalogram phase and frequency estimation and analysis”. In: *Physiological Measurement* 38.12 (Nov. 2017), pp. 2141–2163. DOI: 10.1088/1361-6579/aa93a1.

[93] Gregor Thut et al. “Guiding transcranial brain stimulation by EEG/MEG to interact with ongoing brain activity and associated functions: A position paper”. In: *Clinical Neurophysiology* 128.5 (May 2017), pp. 843–857. DOI: 10.1016/j.clinph.2017.01.003.

[94] Andrea Antal and Christoph S. Herrmann. "Transcranial Alternating Current and Random Noise Stimulation: Possible Mechanisms". In: *Neural Plasticity* 2016 (2016), pp. 1–12. DOI: 10.1155/2016/3616807.

[95] Flavio Fröhlich. "Experiments and models of cortical oscillations as a target for noninvasive brain stimulation". In: *Computational Neurostimulation*. Elsevier, 2015, pp. 41–73. DOI: 10.1016/bs.pbr.2015.07.025.

[96] Randolph F Helfrich, Assaf Breska, and Robert T Knight. "Neural entrainment and network resonance in support of top-down guided attention". In: *Current Opinion in Psychology* 29 (Oct. 2019), pp. 82–89. DOI: 10.1016/j.copsyc.2018.12.016.

[97] Nicholas Ketz et al. "Closed-Loop Slow-Wave tACS Improves Sleep-Dependent Long-Term Memory Generalization by Modulating Endogenous Oscillations". In: *The Journal of Neuroscience* 38.33 (July 2018), pp. 7314–7326. DOI: 10.1523/jneurosci.0273-18.2018.

[98] Andrea A. Kühn et al. "Pathological synchronisation in the subthalamic nucleus of patients with Parkinson's disease relates to both bradykinesia and rigidity". In: *Experimental Neurology* 215.2 (Feb. 2009), pp. 380–387. DOI: 10.1016/j.expneurol.2008.11.008.

[99] Abbey B. Holt et al. "Phase-Dependent Suppression of Beta Oscillations in Parkinson's Disease Patients". In: *Journal of Neuroscience* 39.6 (2019), pp. 1119–1134. DOI: https://doi.org/10.1523/JNEUROSCI.1913-18.2018.

[100] Valerio Manippa et al. "Cognitive and Neuropathophysiological Outcomes of Gamma-tACS in Dementia: A Systematic Review". In: *Neuropsychology Review* 34.1 (Mar. 2023), pp. 338–361. DOI: 10.1007/s11065-023-09589-0.

[101] Ivan Alekseichuk et al. “Spatial Working Memory in Humans Depends on Theta and High Gamma Synchronization in the Prefrontal Cortex”. In: *Current Biology* 26.12 (June 2016), pp. 1513–1521. DOI: 10.1016/j.cub.2016.04.035.

[102] Robert M. G. Reinhart and John A. Nguyen. “Working memory revived in older adults by synchronizing rhythmic brain circuits”. In: *Nature Neuroscience* 22.5 (Apr. 2019), pp. 820–827. DOI: 10.1038/s41593-019-0371-x.

[103] Wiam Al Qasem et al. “Improving working memory by electrical stimulation and cross-frequency coupling”. In: *Molecular Brain* 17.1 (Oct. 2024). DOI: 10.1186/s13041-024-01142-1.

[104] Mohammed Abubaker et al. “Theta-gamma-coupling as predictor of working memory performance in young and elderly healthy people”. In: *Molecular Brain* 17.1 (Oct. 2024). DOI: 10.1186/s13041-024-01149-8.

[105] Lukas Diedrich et al. “Boosting working memory in the elderly: driving prefrontal theta-gamma coupling via repeated neuromodulation”. In: *GeroScience* 47.2 (July 2024), pp. 1425–1440. DOI: 10.1007/s11357-024-01272-3.

[106] Alexander A. Fingelkurts and Andrew A. Fingelkurts. “Altered Structure of Dynamic Electroencephalogram Oscillatory Pattern in Major Depression”. In: *Biological Psychiatry* 77.12 (June 2015), pp. 1050–1060. DOI: 10.1016/j.biopsych.2014.12.011.

[107] Tobias Schwippel et al. “Closed-Loop Transcranial Alternating Current Stimulation for the Treatment of Major Depressive Disorder: An Open-Label Pilot Study”. In: *American Journal of Psychiatry* 181.9 (Sept. 2024), pp. 842–845. DOI: 10.1176/appi.ajp.20230838.

[108] Tineke Grent-’t-Jong et al. “40-Hz Auditory Steady-State Responses in Schizophrenia: Toward a Mechanistic Biomarker for Circuit Dysfunctions and Early Detection and Diagnosis”. In: *Biological Psychiatry* 94.7 (Oct. 2023), pp. 550–560. DOI: 10.1016/j.biopsych.2023.03.026.

[109] Sangtae Ahn et al. “Targeting reduced neural oscillations in patients with schizophrenia by transcranial alternating current stimulation”. In: *NeuroImage* 186 (Feb. 2019), pp. 126–136. DOI: 10.1016/j.neuroimage.2018.10.056.

[110] Juliann M. Mellin et al. “Randomized trial of transcranial alternating current stimulation for treatment of auditory hallucinations in schizophrenia”. In: *European Psychiatry* 51 (June 2018), pp. 25–33. DOI: 10.1016/j.eurpsy.2018.01.004.

[111] Da-Wei Zhang, Alexandros Moraidis, and Torkel Klingberg. “Individually tuned theta HD-tACS improves spatial performance”. In: *Brain Stimulation* 15.6 (Nov. 2022), pp. 1439–1447. DOI: 10.1016/j.brs.2022.10.009.

[112] Jinwen Wei et al. “State-Dependent tACS Effects Reveal the Potential Causal Role of Prestimulus Alpha Traveling Waves in Visual Contrast Detection”. In: *The Journal of Neuroscience* 44.27 (May 2024), e2023232024. DOI: 10.1523/jneurosci.2023-23.2024.

[113] Xiaojuan Wang et al. “Double-blind, randomized, placebo-controlled pilot clinical trial with gamma-band transcranial alternating current stimulation for the treatment of schizophrenia refractory auditory hallucinations”. In: *Translational Psychiatry* 15.1 (Jan. 2025). DOI: 10.1038/s41398-025-03256-z.

[114] Robert J Barry, Adam R Clarke, and Stuart J Johnstone. “A review of electrophysiology in attention-deficit/hyperactivity disorder: I. Qualitative and quantitative electroencephalography”. In: *Clinical Neurophysiology* 114.2 (Feb. 2003), pp. 171–183. DOI: 10.1016/s1388-2457(02)00362-0.

[115] Adi Maron-Katz et al. “Individual Patterns of Abnormality in Resting-State Functional Connectivity Reveal Two Data-Driven PTSD Subgroups”. In: *American Journal of Psychiatry* 177.3 (Mar. 2020), pp. 244–253. DOI: 10.1176/appi.ajp.2019.19010060.

[116] Andrew A. Nicholson et al. "A randomized, controlled trial of alpha-rhythm EEG neurofeedback in posttraumatic stress disorder: A preliminary investigation showing evidence of decreased PTSD symptoms and restored default mode and salience network connectivity using fMRI". In: *NeuroImage: Clinical* 28 (2020), p. 102490. DOI: 10.1016/j.nicl.2020.102490.

[117] Brigitte Zrenner et al. "Brain oscillation-synchronized stimulation of the left dorsolateral prefrontal cortex in depression using real-time EEG-triggered TMS". In: *Brain Stimulation* 13.1 (Jan. 2020), pp. 197–205. DOI: 10.1016/j.brs.2019.10.007.

[118] Alexander Opitz et al. "Spatiotemporal structure of intracranial electric fields induced by transcranial electric stimulation in humans and nonhuman primates". In: *Scientific Reports* 6.1 (Aug. 2016). DOI: 10.1038/srep31236.

[119] Mihály Vöröslakos et al. "Direct effects of transcranial electric stimulation on brain circuits in rats and humans". In: *Nature Communications* 9.1 (Feb. 2018). DOI: 10.1038/s41467-018-02928-3.

[120] Davide Reato et al. "Effects of weak transcranial alternating current stimulation on brain activity—a review of known mechanisms from animal studies". In: *Frontiers in Human Neuroscience* 7 (2013). DOI: 10.3389/fnhum.2013.00687.

Valorisation

This dissertation asked the question: when the brain is preparing to stop an action, does the timing of beta activity matter, and can we use that timing to steer inhibition? In doing so, the work delivers impact at three levels: (1) it sharpens a mechanistic account of inhibitory control, (2) it demonstrates a feasible route toward precision stimulation that can either reinforce or disrupt rhythmic coupling, and (3) it provides practical guidance for building closed-loop stimulation systems that are technically credible and reproducible.

Scientific impact

A key scientific contribution is the empirical validation of the ”Communication through Coherence” (CTC) hypothesis in the context of human motor control. In Chapter 2, we moved beyond the focus on oscillatory power to demonstrate that the phase beta oscillations causally modulate stopping performance. We showed that inhibitory performance is not static but fluctuates sinusoidally with the beta cycle. This provides the first causal evidence that the effectiveness of a ”stop” signal depends on the precise millisecond-level timing of its arrival relative to the ongoing beta phase of the cortex.

In Chapter 3, this work extends the concept of phase precession to human cognitive control. We observed that during failed attempts to stop, the ”preferred phase” (the optimal timing for inhibition) shifted systematically. This discovery suggests that the brain attempts to adapt to rhythmic stimulation by sliding the temporal window of susceptibility according to the task demands. Importantly, tACS seems to promote this process. In practical terms, it suggests that the brain’s inhibitory network may be most susceptible to intervention when it is already in a state of adjustment, and tACS could, in principle, be used to facilitate

structured experience gaining, in which the brain is nudged toward a temporally optimal regime and repeatedly pairing specific network states with successful control demands.

Chapters 4 and 5 provide the most direct evidence that the beta phase is not merely a readout of inhibition, but a controllable handle that can mediate it in a bidirectional way. While in-phase stimulation stabilizes motor states and enhances synchronization (consistent with entrainment), anti-phase stimulation (delivered 180 degrees offset) successfully disrupts beta oscillations and impairs stopping behavior. Together, these chapters strengthen the thesis level claim that beta timing is part of the functional control architecture for motor inhibition and motor output, and that manipulating phase relations can systematically bias the efficacy of inhibitory signalling.

Methodological impact

This dissertation challenges the conventional open-loop tACS that only serves to ”entrain” or amplify brain rhythms. In Chapter 4, we tested a closed-loop system that tracked the beta phase and delivered stimulation either aligned to the endogenous rhythm or opposed to it. Furthermore, Chapter 5 provides critical parameters for optimization, showing that the duration of stimulation acts as a boundary condition for efficacy. We found that brief pulses of anti-phase stimulation (1–2 seconds) are more effective at desynchronizing networks than longer trains, which may inadvertently trigger homeostatic entrainment mechanisms. Chapter 6 establishes a rigorous set of methodological guidelines for closed-loop design, translating the conceptual promise of phase-dependent stimulation into an implementable and reproducible engineering program. These works provide the technical foundation for a phase-dependent closed-loop tACS that can be used to drive neural dynamics in opposite directions depending on phase alignment, enabling bidirectional behaviour modulation. In this sense, the contributions support both causal tests of oscillatory timing hypotheses and

the practical implementation of neuromodulation protocols that can stabilize or suppress rhythmic coupling when needed.

Clinical and societal impact

The dissertation helps reposition tACS as a practical clinical tool by directly addressing one-directional effects as a long-standing barrier. The most immediate clinical relevance of this work is for Parkinson's disease. In Parkinson's, beta activity can become overly synchronized, which is often described as an excessive braking mode that contributes to rigidity and slowness of movement. Deep Brain Stimulation can relieve symptoms very effectively, but it requires neurosurgery and is not an option everyone wants or can receive. Noninvasive tACS is attractive in principle, yet standard open-loop stimulation tends to entrain rhythms, which could be counterproductive for PD. This dissertation offered a closed-loop, phase-specific stimulation strategy that delivers stimulation to oppose the ongoing beta rhythm with anti-phase. The findings in Chapter 4 support this approach: anti-phase stimulation suppresses beta synchronization and shifts behavior in the predicted direction. The main gap before clinical translation is not the basic idea, but the reliability of delivering it in patient settings, meaning patient-grade robustness of the closed-loop pipeline, clear benchmarks for target engagement, and outcome measures that connect neurophysiology to clinically meaningful motor readouts. If these pieces can be demonstrated, the work points to a plausible noninvasive therapy that targets a core pathophysiological marker, potentially as an add-on that reduces medication burden and the side effects that come with higher doses. In the near term, the most realistic promise is session-based use to transiently reduce pathological beta and improve motor state. The next question for longer-term trials is whether repeated application can produce durable changes in beta dynamics and, importantly, sustained symptom improvement. Beyond Parkinson's disease, the impact of this work is a conceptual and technical foundation for precision neuromodulation, where oscillatory timing becomes a controllable variable for

oriented intervention policies.

Summary

Motor inhibition is a core executive control function that allows rapid cancellation or suppression of intended actions in response to a dynamic environment. Neurophysiological research has established that inhibitory processes are governed by the fronto-basal ganglia network, in which beta-band oscillations (13-30 Hz) have been consistently correlated with tuning this ”braking” mechanism. Elevated beta power is associated with the maintenance of the status quo and the suppression of movement, while a drop in beta power is necessary to initiate movement.

Yet beta oscillations are not simply a tonic marker of inhibition. The theoretical framework of communication through coherence proposes that excitability and effective communication fluctuate across the oscillatory cycle. This raises the mechanistic possibility that motivates the first part of the dissertation: inhibition may depend not only on the magnitude of beta activity, but also on when, within the beta cycle, control signals arrive and propagate through the network. This dissertation tests this idea by combining phase-resolved behavioral analysis with transcranial alternating current stimulation to causally probe whether beta phase is functionally relevant for motor inhibition.

When beta oscillations become pathological, the inhibitory system malfunctions by locking behavior into a persistent brake state. Parkinson’s disease provides a clear clinical example of this failure mode: exaggerated beta synchronization in cortico-basal ganglia loops is linked to bradykinesia and rigidity. Treatments that reduce this pathological beta activity, such as dopaminergic medication and deep brain stimulation (DBS), often relieve symptoms. At the same time, both approaches have obvious downsides. Medication can bring unwanted side effects, such as emotional changes, and lose effectiveness for some patients over time, while DBS, although effective, is highly invasive and requires surgery.

Transcranial alternating current stimulation (tACS), in contrast, is a noninvasive brain stimulation technology delivering weak oscillating current through scalp electrodes that can bias membrane potentials and influence spike timing, allowing it to interact with ongoing cortical rhythms. A limitation arises from the nature of tACS entrainment, meaning that with long stimulation, it can reinforce rhythms rather than interrupt them. In Parkinson's disease, where the goal would be to relieve excessive beta synchrony, entraining the rhythm could be the opposite of what is needed. This motivates a different strategy: neurostimulation that adapts to the brain in real time, timing anti-phase perturbations to the instantaneous beta rhythms to cancel excessive beta oscillations. This idea sets up the second part of the dissertation, which develops and tests a closed-loop, phase-adaptive tACS system that tracks ongoing rhythms and delivers stimulation dynamically to reshape neural synchronization and motor inhibition.

Chapter 2

Chapter 2 provides the first causal probe of whether inhibitory efficacy depends on when, within the beta cycle, a stop signal is presented. We applied 20 Hz tACS over the pre-supplementary motor area (preSMA) to entrain endogenous beta rhythms, creating a predictable temporal structure. Stop signals were then presented at specific, equidistant phases of this entrained cycle (e.g., peak, trough, rising flank, falling flank).

Consistent with the "Communication through Coherence" hypothesis, the results revealed that inhibitory performance is not static but fluctuates sinusoidally. Participants were significantly faster and more successful at inhibiting their movements when the stop signal occurred at the trough of the entrained beta oscillation. Conversely, performance degraded when the signal arrived at the peak. This provides the causal evidence that the efficacy of a "stop" command depends on the timing of its arrival relative to the brain's excitability cycle in the beta

band. Importantly, the magnitude of this phase dependence is strongest when stimulation is well matched to each participant's individual beta frequency, further supporting the conclusion that the phase of beta oscillations is causally involved in successful motor inhibition.

Chapter 3

Having established that a "preferred phase" for inhibition exists, Chapter 3 explored the dynamic nature of this gating mechanism. In biological systems, such as the rodent hippocampus during navigation, neural firing often shifts systematically relative to the oscillatory cycle—a phenomenon known as phase precession.

We questioned whether similar dynamics exist in human cognitive control, particularly when the system is under pressure. By analyzing the single-trial relationship between the beta phase and behavioral outcomes, we discovered a dissociation between successful and failed inhibition. During successful stops, the optimal phase remained stable. However, during failed stop attempts, the preferred phase exhibited a precession. Interestingly, by applying a 20 Hz tACS, the preferred phase of failed-stop shifted continuously across the cycle, while it stays stable for the successful-stop trials.

The impact of this result is twofold. First, it suggests that the inhibitory network does not operate with a single static optimal phase but can exert a phase precession in a state dependent manner. During an error-prone stage, the neural network attempts to adapt by sliding its temporal window of excitability. Second, it supports the idea that rhythmic stimulation can participate in driving these systematic dynamic shifts and reshape temporal coding. In a broader interpretation, repeatedly biasing the system toward specific phase states could support structured experience gain, where temporally favorable network configurations are reinforced through repeated pairing with inhibitory demands.

Chapter 4

Transitioning to the second motivation of this dissertation, the development of therapeutic interventions for pathological synchrony, Chapter 4 implemented a closed-loop strategy. To test whether we could non-invasively modulate the ”braking” mechanism, we developed a real-time system that traces the ongoing cortical beta phase by electroencephalography (EEG), triggering tACS with precise timing. We tested in-phase stimulation (aimed at enhancing the rhythm) against anti-phase stimulation (aimed at cancelling the rhythm via destructive interference).

Our results revealed that anti-phase stimulation successfully suppressed beta synchronization and, critically, impaired behavioral inhibition (slowing down the stopping process). In contrast, in-phase stimulation stabilized motor outputs. This chapter provides the strongest evidence to date that we can bidirectionally modulate human inhibitory executive control by targeting endogenous oscillatory beta phase. This strategy offers a mechanistic blueprint for noninvasively treating conditions characterized by excessive beta, such as Parkinson’s disease.

Chapter 5

Chapter 5 addressed a crucial boundary condition for the phase-dependent closed-loop tACS: the duration of stimulation. As noted, prolonged open-loop stimulation risks entraining the very rhythm that it seeks to disrupt. Here, we systematically varied the duration of stimulation trains while measuring cortico-muscular coherence (CMC) over the primary motor cortex.

We found that brief pulses (1–2 seconds) of anti-phase stimulation were significantly more effective at suppressing neural synchrony than longer durations. When anti-phase stimulation was applied for 5 seconds, the suppressive effect diminished, suggesting that entrainment

eventually overrides the phase cancellation. This finding establishes the duration as a vital parameter for clinical device design to effectively desynchronize a pathological network.

Chapter 6

The transition from theoretical possibility to experimental reality requires overcoming substantial technical hurdles. Chapter 6 serves as a methodological guideline, detailing the engineering principles required for a phase-dependent closed-loop tACS system. The chapter lays out the sources of delay and variability across the full pipeline, including signal acquisition, causal filtering, computation, and stimulator onset. In this work, we also review concrete approaches for real-time phase estimation and prediction. In doing so, Chapter 6 ensures that the experimental results of this dissertation are robust and replicable, laying the groundwork for the next generation of adaptive neuromodulation devices.

Discussion and conclusion

Across the dissertation, the findings converge on a coherent account of how beta phase contributes to inhibitory executive control. First, inhibitory efficacy varies across the beta cycle, consistent with the communication through coherence theory in which control signals are more likely to propagate effectively through fronto-basal ganglia circuitry at specific phases. Second, under error-prone conditions, rhythmic stimulation can help drive the optimal phase advancing across the beta circles, pointing to a mechanism through which repeated phase biasing could support sequential learning and experience-dependent tuning. Third, closed-loop tACS can be precisely timed to reinforce or disrupt beta synchrony by tracking its ongoing phase, enabling bidirectional modulation of both, neural dynamics and inhibition performances. Fourth, the impact of disruption from anti-phase tACS is bounded by practical

constraints, including stimulation duration. Finally, phase-dependent closed-loop tACS requires rigorous engineering and explicit validation that the intended phase is precisely delivered.

In sum, the dissertation provides mechanistic and technical evidence that phase-specific closed-loop tACS can serve both as a tool for causal inference in experimental brain research and as a route toward non-invasive precision neurostimulation intervention. This advances the translational promise of tACS by outlining a path toward clinically credible neuromodulation that is personalized, non-invasive, and adaptive to the patient's neural state, with particular relevance for disorders such as Parkinson's disease.

Samenvatting

Motorische inhibitie is een kernfunctie van executieve controle die het mogelijk maakt om voorgenomen handelingen snel te annuleren of te onderdrukken, zodat gedrag zich kan aanpassen aan een dynamische omgeving. Neurofysiologisch onderzoek heeft aangetoond dat inhibitoire processen worden aangestuurd door het fronto basale ganglia netwerk, waarin beta band oscillaties (13-30 Hz) consistent in verband zijn gebracht met het afstemmen van dit "remmende" mechanisme. Verhoogde beta power hangt samen met het handhaven van de status quo en het onderdrukken van beweging, terwijl een daling in beta power nodig is om beweging te initiëren.

Toch zijn beta oscillaties niet louter een tonische marker van inhibitie. Het theoretische kader van communication through coherence stelt dat prikkelbaarheid en effectieve communicatie fluctueren over de oscillatoire cyclus. Dit leidt tot een mechanistische mogelijkheid die het eerste deel van het proefschrift motiveert: inhibitie kan niet alleen afhangen van de omvang van beta activiteit, maar ook van wanneer, binnen de beta cyclus, controlesignalen aankomen en zich door het netwerk voortplanten. Dit proefschrift test deze hypothese door fase opgeloste gedragsanalyses te combineren met transcraniële wisselstroomstimulatie (tACS) om causaal te onderzoeken of de fase van beta-oscillaties functioneel relevant is voor motorische inhibitie.

Wanneer beta-oscillaties pathologisch worden, faalt het inhibitoire systeem door gedrag vast te zetten in een aanhoudende remtoestand. De ziekte van Parkinson vormt een duidelijk klinisch voorbeeld van deze faalmodus: overdreven beta-synchronisatie in cortico-basale-ganglia-lussen is geassocieerd met bradykinesie en rigiditeit. Behandelingen die deze pathologische beta-activiteit verminderen, zoals dopaminerge medicatie en diepe hersenstimulatie (DBS), verlichten vaak de symptomen. Tegelijkertijd kennen beide benaderingen duidelijke nadelen.

Medicatie kan ongewenste bijwerkingen veroorzaken, zoals emotionele veranderingen, en verliest bij sommige patiënten na verloop van tijd effectiviteit, terwijl DBS, hoewel effectief, sterk invasief is en een chirurgische ingreep vereist.

Transcraniële wisselstroomstimulatie (tACS) vormt daarentegen een niet-invasieve neurostimulatiemethode, waarbij een zwakke oscillerende stroom via elektroden op de hoofdhuid wordt toegediend. Deze stroom kan membraanpotentialen beïnvloeden en spike-timing moduleren, waardoor tACS kan interageren met lopende corticale ritmes. Een beperking volgt echter uit de aard van tACS-entrainment: bij langdurige stimulatie kan tACS ritmes juist versterken in plaats van onderbreken. Bij de ziekte van Parkinson, waar het doel is om overmatige beta-synchronie te verminderen, kan het entrainen van het ritme dus het tegenovergestelde zijn van wat nodig is. Dit motiveert een andere strategie: neurostimulatie die zich in real time aanpast aan de hersentoestand, waarbij anti-fase-perturbaties precies worden getimed op de actuele beta-ritmes om overmatige beta-oscillaties te dempen. Deze gedachte vormt de basis voor het tweede deel van dit proefschrift, waarin gesloten-lus, fase-adaptieve tACS-systemen worden ontwikkeld en getest die lopende ritmes volgen en stimulatie dynamisch toedienen om neurale synchronisatie en motorische inhibitie te hervormen.

Hoofdstuk 2

Hoofdstuk 2 levert de eerste causale test van de vraag of inhibitoire effectiviteit afhangt van het tijdstip waarop, binnen de beta-cyclus, een stop-signaal wordt aangeboden. We dienden 20 Hz tACS toe over de pre-supplementaire motorische area (preSMA) om endogene beta-ritmes te entrainen en zo een voorspelbare temporele structuur te creëren. Vervolgens werden stop-signalen aangeboden op specifieke, gelijkmatig verdeelde fasen van deze ge-entrainde cyclus (bijvoorbeeld piek, dal, stijgende flank, dalende flank).

In lijn met de communication through coherence-hypothese lieten de resultaten zien dat inhibitoire prestaties niet statisch zijn, maar sinusvormig fluctueren. Deelnemers konden hun beweging significant sneller en succesvoller inhiberen wanneer het stop-signaal viel op de dalfase van de ge-entrainde beta-oscillatie. Daarentegen verslechterde de prestatie wanneer het signaal op de piek arriveerde. Dit levert causale evidentie dat de effectiviteit van een "stop"-commando afhangt van het tijdstip waarop het aankomt ten opzichte van de prikkelbaarheidscyclus van het brein in de beta-band. Belangrijk is dat de grootte van deze fase-afhankelijkheid het sterkst was wanneer de stimulatie goed overeenkwam met de individuele beta-frequentie van de deelnemer, wat de conclusie ondersteunt dat de fase van beta-oscillaties causaal betrokken is bij succesvolle motorische inhibitie.

Hoofdstuk 3

Na het aantonen dat er een "voorkeursfase" voor inhibitie bestaat, onderzoekt Hoofdstuk 3 de dynamische aard van dit poortmechanisme. In biologische systemen, zoals de hippocampus van knaagdieren tijdens navigatie, verschuift neurale firing vaak systematisch ten opzichte van de oscillatoire cyclus, een fenomeen dat bekendstaat als fase-precessie.

Wij onderzochten of vergelijkbare dynamiek bestaat in menselijke cognitieve controle, met name wanneer het systeem onder druk staat. Door de relatie tussen beta-fase en gedragsuitkomsten op single-trial-niveau te analyseren, vonden we een duidelijke dissociatie tussen succesvolle en mislukte inhibitie. Tijdens succesvolle stops bleef de optimale fase stabiel. Tijdens mislukte stoppogingen vertoonde de voorkeursfase een fase-precessie. Opvallend was dat bij toepassing van 20 Hz tACS de voorkeursfase bij mislukte stops continu door de cyclus verschoof, terwijl zij bij succesvolle stop-trials stabiel bleef.

De betekenis van dit resultaat is tweeledig. Ten eerste suggereert het dat het inhibitoire netwerk niet opereert met één statische optimale

fase, maar in een toestandafhankelijke manier fase-precessie kan vertonen. Tijdens foutgevoelige toestanden lijkt het neurale netwerk te proberen zich aan te passen door zijn temporele prikkelbaarheidsvenster te verschuiven. Ten tweede ondersteunt dit de gedachte dat ritmische stimulatie kan bijdragen aan het aansturen van deze dynamische verschuivingen en zo temporele codering kan herstructureren. In een bredere interpretatie zou herhaaldelijk het systeem biasen naar specifieke fase-toestanden kunnen bijdragen aan gestructureerde ervaringsopbouw, waarbij temporeel gunstige netwerkconfiguraties worden versterkt door herhaalde koppeling aan inhibitoire eisen.

Hoofdstuk 4

Met de overgang naar de tweede motivatie van dit proefschrift, de ontwikkeling van therapeutische interventies voor pathologische synchronie, implementeert Hoofdstuk 4 de gesloten lus strategie. Om te testen of we het "remmende" mechanisme niet invasief kunnen moduleren, ontwikkelden we een real time systeem dat de lopende corticale beta fase met elektro encefalografie (EEG) volgt en tACS met precieze timing triggert. We vergeleken in fase stimulatie (gericht op het versterken van het ritme) met anti fase stimulatie (gericht op het onderdrukken van het ritme via destructieve interferentie).

Onze resultaten lieten zien dat anti-fase-stimulatie beta-synchronisatie succesvol onderdrukte en, cruciaal, de gedragsmatige inhibitie verslechterde door het stopproces te vertragen. In-fase-stimulatie stabiliseerde daarentegen motorische output. Dit hoofdstuk levert sterke evidentie dat menselijke inhibitoire executieve controle bidirectioneel kan worden gemoduleerd door de endogene beta-fase te targeten. Daarmee biedt deze strategie een mechanistisch blueprint voor niet-invasieve behandeling van aandoeningen die worden gekenmerkt door excessieve beta-activiteit, zoals de ziekte van Parkinson.

Hoofdstuk 5

Hoofdstuk 5 onderzoekt een cruciale randvoorwaarde voor fase afhankelijke gesloten lus tACS, namelijk de duur van stimulatie. Zoals hierboven beschreven, bestaat bij langdurige open loop stimulatie het risico dat juist het ritme wordt geentrained dat men wil verstoren. In dit hoofdstuk varieerden we systematisch de duur van stimulatietreinen, terwijl we cortico musculaire coherentie (CMC) boven de primaire motorische cortex maten.

We vonden dat korte pulsen (1-2 seconden) van anti-fase-stimulatie significant effectiever waren in het onderdrukken van neurale synchronie dan langere duurcondities. Wanneer anti-fase-stimulatie 5 seconden werd toegepast, nam het onderdrukkende effect af, wat suggereert dat entrainment uiteindelijk de fase-cancellatie kan overnemen. Deze bevinding maakt duidelijk dat duur een vitale parameter is voor klinisch device-ontwerp wanneer het doel is om een pathologisch netwerk effectief te desynchroniseren.

Hoofdstuk 6

De stap van theoretische mogelijkheid naar experimentele realiteit vereist het overwinnen van substantiële technische barrières. Hoofdstuk 6 fungeert daarom als methodologische richtlijn en beschrijft de engineeringsprincipes die nodig zijn voor een fase afhankelijke gesloten lus tACS systeem. Het hoofdstuk inventariseert de bronnen van vertraging en variabiliteit in de volledige pijplijn, waaronder signaalacquisitie, causale filtering, berekening, en stimulator onset. Daarnaast bespreken we concrete benaderingen voor real time fase schatting en voorspelling. Daarmee waarborgt Hoofdstuk 6 dat de experimentele resultaten van dit proefschrift robuust en reproduceerbaar zijn, en legt het de basis voor een volgende generatie adaptieve neuromodulatie-devices.

Discussie en conclusie

Over het hele proefschrift convergeren de bevindingen naar een samenhangend model van hoe beta-fase bijdraagt aan inhibitoire executieve controle. Ten eerste varieert inhibitoire effectiviteit over de beta-cyclus, in lijn met communication through coherence, waarin controlesignalen met grotere kans effectief door fronto-basale-ganglia-circuits propagëren op specifieke fasen. Ten tweede kan ritmische stimulatie onder foutgevoelige omstandigheden bijdragen aan het systematisch voortschrijden van de optimale fase over beta-cycli, wat wijst op een mechanisme waarmee herhaalde fase-biasing sequentieel leren en ervaring-afhankelijke afstemming kan ondersteunen. Ten derde kan gesloten-lus-tACS, door de lopende fase te volgen, precies worden getimed om beta-synchronie te versterken of te verstoren, wat bidirectionele modulatie van zowel neurale dynamiek als inhibitieprestaties mogelijk maakt. Ten vierde is de mate van verstoring door anti-fase-tACS begrensd door praktische factoren, waaronder stimulatieduur. Ten slotte vereist fase-afhankelijke gesloten-lus-tACS rigoureuze engineering en expliciete validatie dat de beoogde fase daadwerkelijk met hoge precisie wordt afgeleverd.

Samengevat levert dit proefschrift mechanistische en technische evidentie dat fase-specifieke gesloten-lus-tACS zowel kan dienen als instrument voor causale inferentie in experimenteel hersenonderzoek als een route richting niet-invasieve precisie-neurostimulatie. Daarmee wordt de translationele belofte van tACS versterkt door een pad te schetsen naar klinisch geloofwaardige neuromodulatie die gepersonaliseerd, niet-invasief en adaptief is aan de neurale toestand van de patiënt, met bijzondere relevantie voor aandoeningen zoals de ziekte van Parkinson.

About the author



Zhou Fang was born on 11 April 1995 in Inner Mongolia, China. In 2014, Zhou entered Southeast University in Nanjing as a sports student and began her Bachelor's degree in Biomedical Engineering. During this period, she first encountered cognitive neuroscience and became fascinated by the possibility that invisible patterns of brain activity could explain visible changes in human behavior.
In 2018, she continued with a Master's degree in Biomedical Engineering at Nanjing University of Aeronautics and Astronautics. She was involved in the development of EEG visualization software for detecting motion sickness and fatigue in pilots, a project that brought neural signal processing closer to real-world human performance monitoring.
In 2021, Zhou moved to the Netherlands to begin her PhD in Cognitive Neuroscience at Maastricht University, under the supervision of Prof. Alexander Sack and Dr. Inge Leunissen. Throughout her PhD, she combined neuroscience, engineering, and computation to study how the brain's ongoing state can influence the ability to act, stop, and adapt.
Long before she entered the laboratory, she entered the badminton court at the age of five and started training at the age of ten. Badminton is one of the most cognitively demanding sports. Through years of training and tournaments, she became familiar with the phenomenon that, performance is not constant. Even with the same preparation, some moments feel effortless, while in others, the body seems to fall just slightly out of synchrony with intention. It seems that performance depends on more than memories and muscles alone, but also the 'brain state'. Her PhD allowed her to investigate this intuition through neuroscience.
Her research reflects a long-standing fascination with the dynamic relationship between brain activity and human movement, and a commitment to developing neuromodulation technologies that can respond

to the brain as an active, changing system.

List of publications and work in progress

- **Z. Fang**, A.T. Sack, I. Leunissen (2024). The phase of tACS-entrained pre-SMA beta oscillations modulates motor inhibition. *NeuroImage*, 290, 120572. DOI: 10.1016/j.neuroimage.2024.120572
- **Z. Fang**, A.T. Sack, I. Leunissen (2025). Closed-loop anti-phase tACS over preSMA reduced oscillatory beta synchronization and modulated motor inhibition performance *(Preprint)*. DOI: 10.1101/2025.11.25.690566
- **Z. Fang**, S. ten Oever, A.T. Sack, I. Leunissen (2025). tACS induces state-dependent shifts in inhibitory phase preference consistent with phase precession *(Preprint)*.DOI: 10.64898/2025.11.28.691215
- **Z. Fang**, A.T. Sack, I. Leunissen. Anti-phase closed-loop tACS disrupts cortico-muscular coherence during isometric contraction. *(In Prep)*
- **Z. Fang**, A.T. Sack, I. Leunissen. Online EEG phase tracking for adaptive tACS: Practical engineering and methodological considerations. *(In Prep)*
- **Z. Fang**, L. Yao, Z. Qian (2019). Research on Multi-parameter Visualization Technology of Brain Function Based on EEG. *ICMIPE 2019*. DOI: 10.1109/ICMIPE47306.2019.9098189

Talks

- **Closed-loop tACS-EEG modulation of motor inhibition.**
  5th Int. Brain Stimulation Conference, Lisbon (2023).
- **Phase-dependent tACS modulates motor inhibition.**
  BeNe Brain Stimulation Symposium, Hasselt (2022).
- **Real-time visualization technology for EEG brain function.**
  ICMIPE, Shenzhen (2019).

Acknowledgments

Before I quite realised it, my doctoral journey had reached its final chapter. This dissertation is the culmination of my PhD work, but the story behind it reaches far beyond the pages of this thesis. I would like to express my heartfelt gratitude to everyone who has been part of it.

I would like to express my deepest appreciation to my daily supervisor, **Inge**. Your name has probably appeared more often than anyone else's in my email inbox, which is a sign of excellent supervision and my very high number of questions. Thank you for giving me such a fascinating research topic and for helping me find my own area within it. You were always incredibly responsive, no matter when I reached out, and you were always there to answer questions, discuss ideas, and provide support. Your kindness, guidance, and encouragement made a great difference throughout my PhD. I feel very lucky to have received the hereditary wine cap from you when my first paper was accepted. I hope this bottle cap will continue its mission.

Alex, thank you for leading a team that provides not only professional support but also a joyful working environment. Although your schedule is always full, you always manage to reply, sign documents, and revise drafts with miraculous speed and high quality. Your support was always present and reliable.

Sanne, thank you for supporting my projects with your strong expertise. You always provided ideas that could immediately be turned into action. I was always impressed by how much work you put into revising my drafts.

I would like to thank all the seniors in the BSC group. **Felix**, thank you for offering insightful perspectives and comments from a broader view of my project. I always appreciated that you came to say hi when passing by my office. Somehow, my memories of Oxfordlaan

55 are closely connected with your presence. **Teresa**, thank you for your energy, leadership, and thoughtful contributions to the team. I always felt that you understood my ideas quickly, even when I was still trying to understand how to explain them myself. **Vincent**, whenever I saw you, there was a smile on your face. I learned a lot from the way you presented your work and shared your thoughts in the group. **Jelena**, thank you for always contributing valuable input in the group meetings. I enjoyed all the meetings and discussions that included you, and I always looked forward to your comments.

I am also very grateful to all my colleagues in the BSC group. **Tingting**, we have accompanied each other through the entire PhD journey. I liked sharing the same office with you. You are energetic and impressively hardworking. I have to say that your discipline motivated me a lot, even on days when my own discipline was temporarily unavailable. **Jasmina**, it has been a pleasure to share an office with you over the past four years. You are a fantastic and inspiring person, not only at work, but also in daily life. The bracelet you gave me indeed brought me good luck, and I am very grateful for it. **Tuba**, from watching your PhD defence to seeing you work as a brilliant scientist, I have learned a lot from you. I was deeply inspired by your working aesthetics. **Zhen**, thank you for your company over the past four years. You are always energetic and always a wonderful host for dinners at your place. **Qiannong**, thank you for your company through the journey. I enjoy all the events that you presented. **Ting**, thank you for your cooking and help during my early PhD years. **Rick**, thank you for your help in preparing the EEG and collecting data. Many thanks also to all members of the team, including **Tara**, **Yuejuan**, **Thomas**, **Antonia**, **Oscar**, **Melanie**, **Michelle**, **Laurie**, **Salil**, **Leia**, **Dominik**, **Max**, **Hatice**, and all the students. Together, you created such a vivid, warm, and inspiring working environment. It was a privilege to be part of it.

I would like to especially thank all the interns who have contributed to my PhD projects, **Hilde**, **Christina**, **Elne**, **Aine**, **Daan**, **Issac**, and **Charles**. Each of you did a great job recruiting participants, helping with data collection, working on analyses, and putting tremendous

effort into the projects. Without your dedication and hard work, the projects would not have run as smoothly as they did.

I am also very grateful to the departmental teams, especially **Christl**, **Andra**, and **Shirley**. Your assistance was never late, and your support always arrived exactly when it was needed. I would also like to thank our department head, **Peter**, for organising wonderful events and for helping create such a pleasant working environment. Thank you also for serving as the chair of my thesis reading committee. I am grateful as well to colleagues from other teams. It was always nice to have a warm conversation whenever we met in the building.

To the people that I have met in Maastricht, thank you for being part of my journey. Special thanks to **Wouter** for your care and for always being there for me. Your support has meant a great deal to me. **Mo**, from the days when we were repeatedly paired together for badminton doubles until now, you have become my best friend. Thank you for all your advice on work and life, although perhaps not always on badminton. **Nora**, from Italy to Greece, Spain, and Turkey, we somehow managed to talk about the brain while being surrounded by sunshine, good food, and unforgettable views. To the badminton mates from UM, **Tim,** thank you for the good moments, especially when we won the gold medal in the Limburg game, and thank you for participating in my pilot study twice. **Jinzhe**, thank you for always being willing to help. **Justin** and **Ziyang**, thank you for the court time we share and for also being part of my study. To my friends I met at the Rally, **Jonah**, I enjoyed our morning gym sessions very much. I would also like to thank all my teammates at the Rally. The moment we lifted the national championship trophy in the fifth division is still vivid in my mind. Thank you to all my teammates in Trilan, with whom I challenged myself in the first division competition in 2023, and to all my teammates in Roosteren, with whom I pushed myself again in the second division games in 2024. I am also grateful to my badminton coaches, **Rolf** and **Indra**, who pushed me to my physical limits and, in doing so, helped me build persistence that extended far beyond the badminton court.

Finally, and most importantly, I am deeply grateful to my parents. You have always supported me quietly and firmly from behind. You never pressured me to be the most successful person. Instead, you always wished for me to be healthy and happy. Thanks to Tailang and Yibu. Although you may not understand what a PhD is, you certainly understand when I need company, distraction, or unconditional love. Thanks to all my family members, because of you, I was raised with both mental and physical strength. For all of this, and for much more than I can express here, thank you.

I am grateful to everyone who crossed my path during these years and contributed, in small or large ways, to making this journey possible and memorable.

Zhou Fang
Maastricht
June 10, 2026

